

Visible Light Mediated Oxidative Halogenation Reactions and Reductive Liberation of Fluorophosgene

Dissertation

Zur Erlangung des Doktorgrades der Naturwissenschaften

(Dr. rer. nat.)

an der Fakultät für Chemie und Pharmazie

der Universität Regensburg



vorgelegt von
Daniel Petzold
aus Düren
2019

The experimental work was carried out between November 2016 and January 2019 at the University of Regensburg, Institute of Organic Chemistry under the supervision of Prof. Dr. Burkhard König.

Date of submission: 14.02.2019

Date of colloquium: 29.03.2019

Board of examiners:

Prof. Dr. Julia Rehbein	(Chair)
Prof. Dr. Burkhard König	(1st Referee)
Prof. Dr. Martin Breugst	(2nd Referee)
Prof. Dr. Antje Bäumner	(Examiner)



Universität Regensburg

To my family

&

Katharina

Table of Contents

1. Retrosynthetic Applications in Visible Light Photoredox Catalysis.....	1
1.1 Introduction.....	1
1.2 C-F bond:.....	3
1.2.1 Generation of aliphatic C-F bonds.....	4
1.3 C-Cl/Br/I bond:.....	7
1.3.1 Generation of aliphatic C-Cl bonds.....	8
1.3.2 Generation of aromatic C-Cl bonds.....	11
1.3.3 Generation of aliphatic C-Br bonds.....	12
1.3.4 Generation of aromatic C-Br bonds.....	16
1.3.5 Generation of aliphatic C-I bonds.....	17
1.3.6 Generation of aromatic C-I bonds.....	19
1.4 References.....	20
2. Photocatalytic Oxidative Bromination of Electron-Rich Arenes and Heteroarenes by Anthraquinone.....	23
2.1 Introduction.....	24
2.2 Results and Discussion.....	24
2.2.1 Synthesis.....	24
2.2.2 Mechanistic Investigations.....	27
2.3 Conclusion.....	29
2.4 Experimental Part.....	30
2.4.1 General Information.....	30
2.4.2 Mechanistic Investigations.....	32
2.5 Product Characterizations.....	36
2.6 References.....	45
3. Visible Light Mediated Synthesis of β Chloro Ketones from Aryl Cyclopropanes.....	47
3.1 Introduction.....	48
3.2 Results and Discussion.....	49
3.2.1 Synthesis.....	49
3.2.2 Mechanistic Investigations.....	51
3.3 Conclusion.....	53
3.4 Experimental Part.....	54
3.4.1 General Information.....	54
3.4.2 Mechanistic Investigations.....	55
3.4.3 Starting Material Synthesis and Characterizations.....	58
3.4.4 Product Characterizations.....	69
3.5 References.....	80
4. Visible Light Mediated Liberation and <i>in situ</i> Conversion of Fluorophosgene.....	83
4.1 Introduction.....	84
4.2 Results and Discussion.....	85

4.2.1 Synthesis	85
4.2.2 Mechanistic Investigations.....	88
4.3 Conclusion	91
4.4 Experimental Part.....	92
4.4.1 General Information.....	92
4.4.2 Mechanistic Investigations.....	93
4.5 Product Characterizations	118
4.6 References	128
5. Summary	130
6. Zusammenfassung	131
7. Curriculum Vitae	132
8. Abbreviations	135
9. Danksagung	138

1. Retrosynthetic Applications in Visible Light Photoredox Catalysis

1.1 Introduction

Visible light mediated chemical reactions received a significant boost in popularity within the past 15-20 years. Photons which were already predicted to play a vital part in the future of chemistry in the beginning of the 20th century, were rediscovered and accepted as traceless and easily accessible reagents by organic chemists.^[1] The reason for this is not only the availability of selective and intensive light sources but also the broad range of newly developed photocatalysts that enable a manifold of formerly unknown chemical transformations.^[2] With these powerful tools in hand, photocatalysis is not a merely academic field of research anymore but slowly find its way into applications in the chemical and pharmaceutical industry like e.g. transition metal catalysis in the past.^[3]

However, despite their popularity photochemistry and photo(redox) catalysis rarely constitute a significant part of the basic chemical education during bachelor and master studies retarding the overall perception and broader application of the field. As a consequence, a chemist who was taught to perform retrosynthetic disconnections exclusively with intuitive polar strategies, might be skeptical to integrate the less intuitive radical disconnections into his/her lab routine.^[4]

To facilitate the general entry into the field, many reviews try to give an overview of the hardly countable number of publications about photochemistry and photocatalysis.^[5] For almost all traditional / thermal reactions a photocatalytic counterpart was developed and many new disconnections were discovered. However, since not all visible light mediated reactions can be discussed in this thesis, the introduction focuses on providing a summary of different photochemical and photocatalytic halogenation strategies due to their importance in organic synthesis and their thematic connection to this work. Instead of a recapitulation of the basic principles of photocatalysis and the individual reaction mechanism, retrosynthetic disconnections for each halide are provided as a condensed excerpt of the overall published literature (Table 1). These solutions are always displayed in a similar style including the target structure, the corresponding retrosynthetic synthon and the required starting materials as published in the reference. Next, the functional group tolerance as well as a few selected example structures are displayed to illustrate the scope. Additionally, the reaction conditions, additives, photocatalyst and light source are provided to give an overview of the required equipment and chemicals. Finally, the scheme is discussed concisely in text form (e.g. commercial availability of important reagents/catalysts). If multiple procedures for the same/ or very similar disconnection exist, those are listed after the main text with short notes about their differences to the method highlighted in the scheme.

Table 1-1. Top table: Overview of photocatalytically accessible, retrosynthetic C-C / C-X bond disconnections. Bottom Table: Condensed excerpt that will be elucidated in this thesis.

	C-sp ³	C-sp ²	C-sp [*]	F	Cl	Br	I	B	N	O	P	S
C-sp ³	✓	✓	n.c.	✓	(✓)	✓	(✓)	(✓)	✓	✓	✓	✓
C-sp ²	✓	✓	(✓)	X	(✓)	(✓)	(✓)	✓	✓	✓	✓	✓



	F	Cl	Br	I
C-sp ³	✓	(✓)	✓	(✓)
C-sp ²	X	(✓)	(✓)	(✓)

✓: well exploited, (✓): limited number of examples, X: no / very few, limited examples, n.c. not covered in this survey. *: C-sp centered disconnections will not be discussed due to the overall low number of examples.

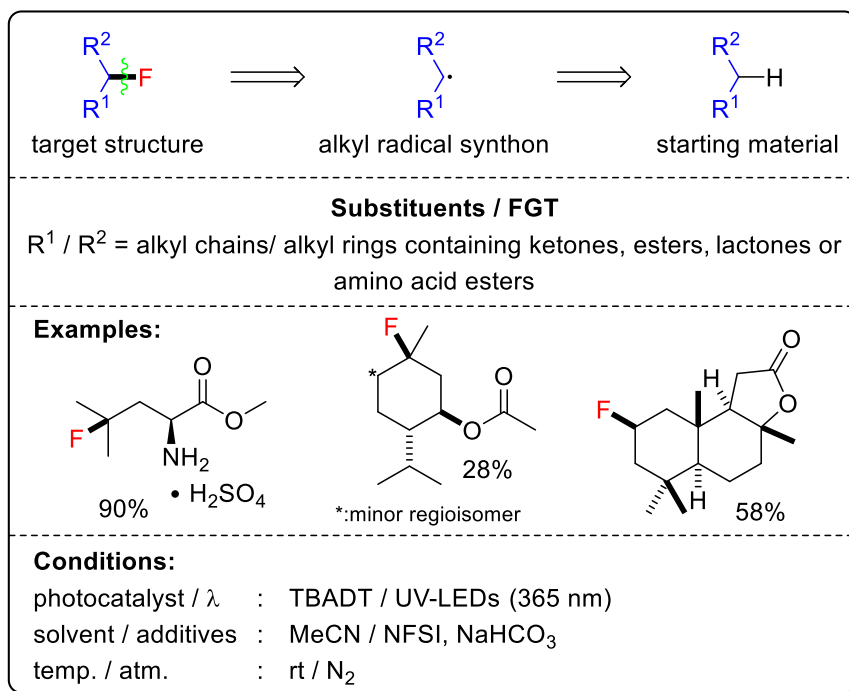
To summarize the published literature on visible light mediated halogenation reactions it can be stated that many different methods including direct C-H activations, the use of prefunctionalized substrates (e.g. carboxylic acids) and atom transfer radical addition (ATRA) reactions were reported. Especially the fluorination and the bromination of sp³ centered carbon atoms were explored in detail due to the high synthetic value of those intermediates. On the other hand, the photocatalytic fluorination of arenes is severely underexploited and remains a challenge to be tackled in the future. This leads to the conclusion that although chlorination, bromination and iodination reactions are well established text-book transformations in organic chemistry, light driven halogenations do not only complement the existing methods, but also enable access to new, unknown or challenging C-X bond disconnections. The versatility and utility of these new reactions might be the key for a successful transition from academic research to application in the chemical or pharmaceutical industry.

1.2 C-F bond:

Fluorinated organic molecules play an important role in bioactive compounds e.g. pharmaceuticals and pesticides.^[6] Currently, more than 25% of all candidates in the pharmaceutical pipeline contain at least a single fluorine atom due to its influence on drug metabolism and protein stabilizing effects.^[6a] Further applications of fluorine containing molecules include medicinal diagnostics with ¹⁸F labeled PET tracers and polyfluorination of organic compounds.^[7] Many methods for the introduction of fluorine atoms into small molecules on both lab and industrial scale have been developed, relying mainly on the use of extremely reactive elemental F₂, highly toxic HF or unreactive fluoride salts.^[7] Therefore, there is still a demand for new, selective and mild procedures facilitating especially late-stage modifications of bioactive compounds.^[8] In this respect, photocatalysis adds a significant amount of retrosynthetic synthons to the toolbox of the organic chemist by supplying both new methods for direct C-H fluorinations and for directed decarboxylative fluorinations.

1.2.1 Generation of aliphatic C-F bonds

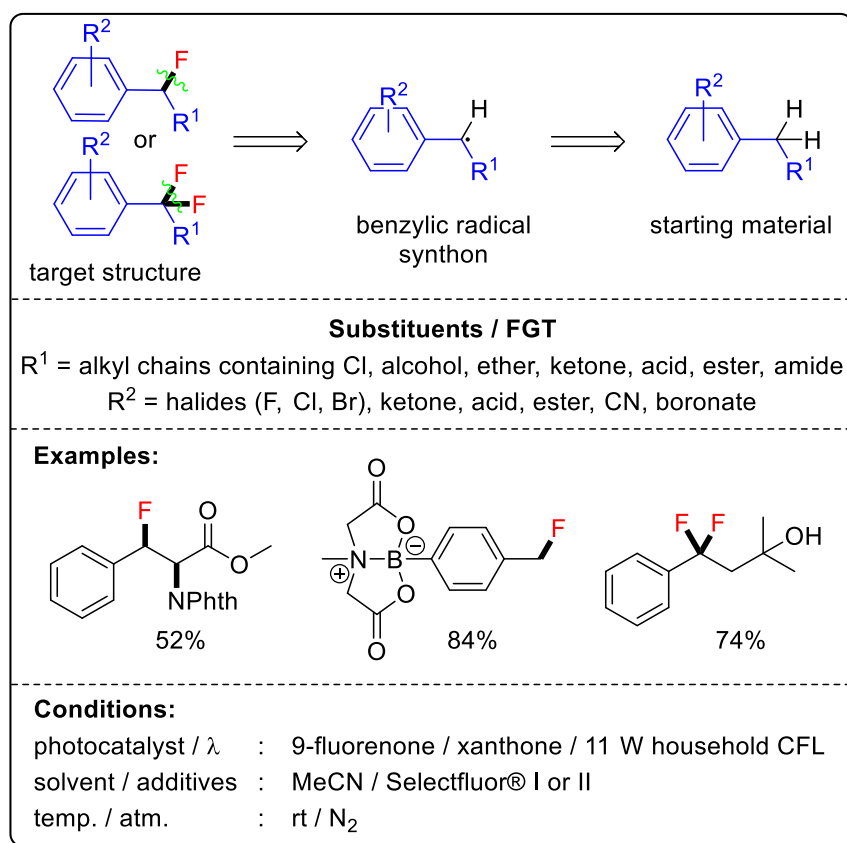
Strategy 1 – C-H fluorination



Scheme 1-1. Direct fluorination of sec. and tert. aliphatic C-H bonds.^[9]

The selective fluorination of aliphatic C-H bonds is a big challenge of modern organic chemistry and it is still desirable to find new and simple methods for this kind of disconnection. One solution was provided by the group of Britton who developed a strategy for the fluorination of simple molecules (Scheme 1-1).^[9] The photocatalyst, tetrabutylammonium decatungstate (TBADT), and the fluorination reagent *N*-fluorobenzenesulfonimide (NFSI) are commercially available and the reaction mixture was irradiated with 365 nm LEDs for 16 h. Although the isolated yields were generally moderate (40-60%) and the functional group tolerance was rather low, since mostly only ketones, esters, lactones and protonated amino acid esters worked, this work was adopted by Merck & Co for the remote fluorination of leucine methyl ester which was a precursor for the (now ceased) anti-cancer agent odanacatib.^[10] After transfer of the reaction into flow and another optimization cycle, the yield could be increased to 90% in a 45 g scale reaction which illustrated the utility of this method for the selective fluorination of tertiary C-H bonds. Alternative strategies for this disconnection employed either tetracyanobenzene^[11] or anthraquinone^[12] as photosensitizers and provided a similar substrate scope. Further alternative methods used ketones as directing groups recommending these strategies particularly for the fluorination of steroids.^[13] Hamashima and coworkers demonstrated that not only ketones but also phthalimides could act as directing group for selective C-H bond fluorinations.^[14] Finally, even an uranium and visible light mediated method was described by Sorensen and coworkers.^[15]

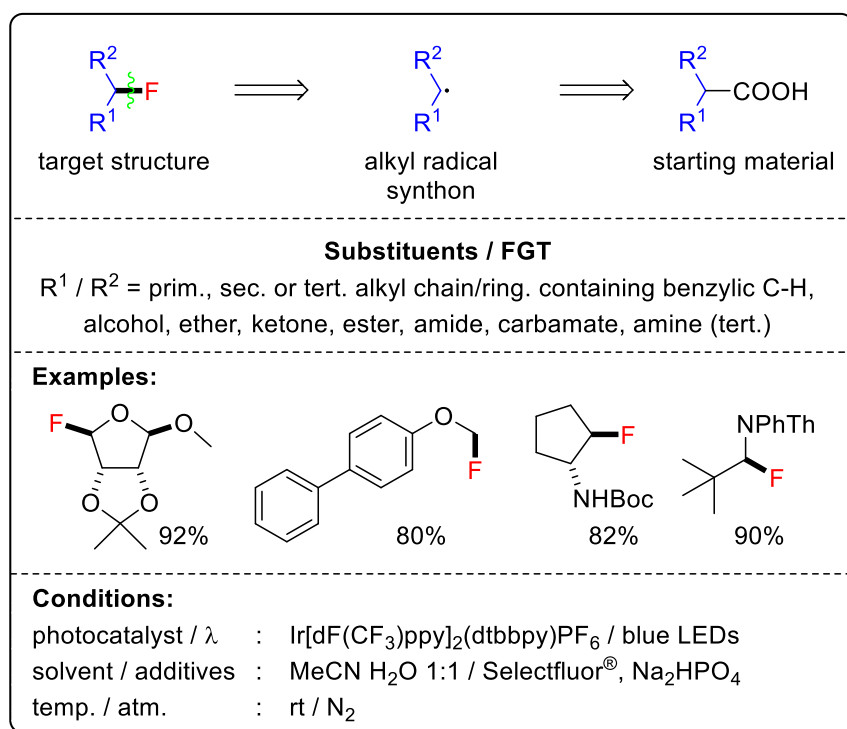
Strategy 2 – C-H fluorination of benzylic C-H bonds



Scheme 1-2. Direct mono or double fluorination of benzylic C-H bonds.^[16]

Since the benzylic position is typically a weak spot in metabolism of biomolecules, Chen and coworkers developed a specialized method for mono or double fluorination of benzylic C-H bonds depending on the catalyst and fluorination reagent used (Scheme 1-2).^[16] Both catalysts, 9-fluorenone and xanthone are cheap and commercially available, as are the fluorination reagents Selectfluor® I and II. The reaction mixture was irradiated for 6 h to 96 h with a simple 11 W fluorescent light bulb. The yields ranged typically from 60% to 80% and the functional group tolerance of the method was moderate including aromatic halides (F, Cl, Br), ketones, esters, aromatic carboxylic acids and protected amino groups. Alternative strategies for the monofluorination of benzylic C-H bonds were reported by Lectka and coworkers who employed tetracyanobenzene as photocatalyst and by Wu and coworkers who used Fukuzumi's catalyst.^[17]

Strategy 3 – Decarboxylative fluorination



Scheme 1-3. Decarboxylative fluorination of aliphatic carboxylic acids.^[18]

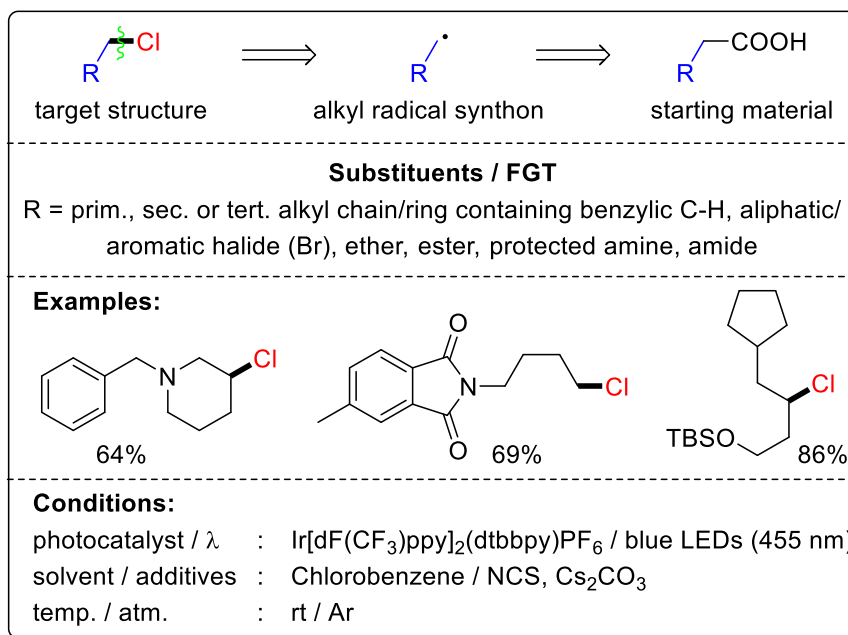
Carboxylic acids are among the most abundant functional groups in both natural products and fine chemicals. Therefore, the MacMillan group developed a viable, photoredox-catalytic strategy for the decarboxylative fluorination of aliphatic carboxylic acids (Scheme 1-3).^[18] The method employed commercially available [Ir{dF(CF₃)ppy}₂(dtbbpy)]PF₆ as the photocatalyst, Selectfluor[®] as the fluorine source and Na₂HPO₄ as base. The reaction mixture was irradiated with blue LEDs for 1 h to 15 h leading to the fluorinated products in generally very good yields (70-90%). The shown functional group tolerance was moderate including alcohols, ethers, ketones, esters and protected amines. Many alternative decarboxylative fluorination procedures were published complementing the substrate scope of MacMillan's method e.g. by Paquin and coworkers who used α-oxo carboxylic acids as starting materials and the cheaper Ru(bpy)₃Cl₂ as photosensitizer or by Ye and coworkers who used an organic dye instead of transition metals.^[19] Another recent, but regarding the scope more limited alternative was published by Hammond using a heterogeneous photosensitizer.^[20] Moreover, a new strategy for the decarboxylative fluorination of heteroarenes was realized by Tang and coworkers.^[21] However, the method is limited to electron-rich heteroarenes and suffers from dimerization of the heteroaryl radical intermediate which lowered the overall yield. Finally, Jamison and coworkers developed a SF₆ and visible light mediated strategy for aliphatic fluorination starting from allylic alcohols rather than carboxylic acids.^[22]

1.3 C-Cl/Br/I bond:

Aliphatic and aromatic halides (Cl, Br, I) are valuable synthetic intermediates in organic synthesis which are accessible by many standard text book reactions.^[23] However, the field for the development of novel halogenation strategies is still active. The main goal is to find milder and more selective conditions, to enable stereoselective halogenation or to perform late-stage functional group interconversions turning bioactive molecules into complex building blocks.^[24] The contributions of visible light mediated methods to this field are numerous offering both radical and polar reactivity as well as ATRA reactions leading to diverse substrate scopes. The versatility of these protocols recommends photocatalysis as a powerful tool for aliphatic and aromatic halogenation reactions.

1.3.1 Generation of aliphatic C-Cl bonds

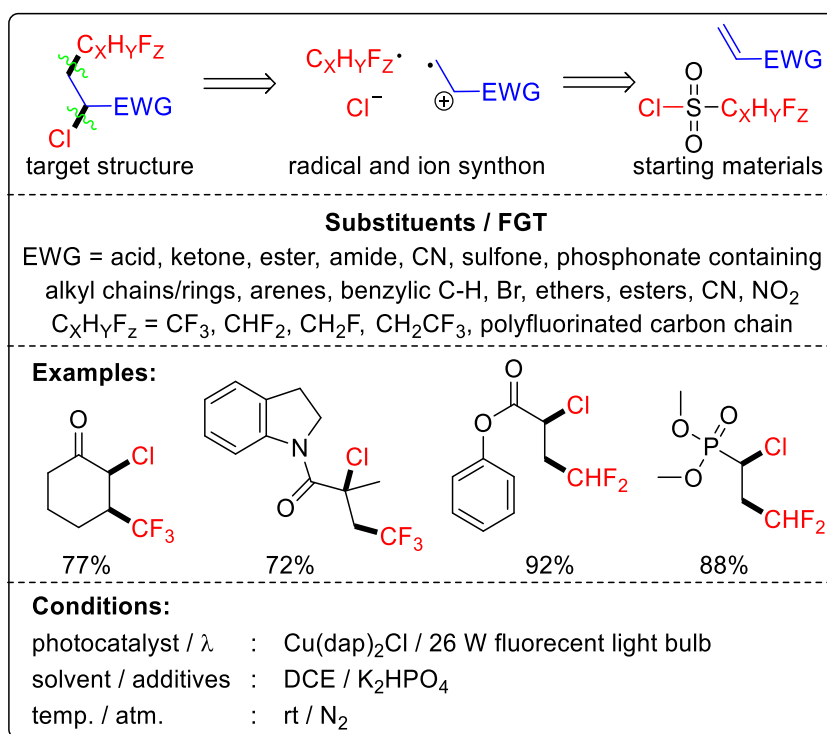
Strategy 1 – Decarboxylative chlorination



Scheme 1-4. Decarboxylative chlorination of aliphatic carboxylic acids.^[25]

For example, Glorius and coworkers published a silver-free procedure for a Hunsdiecker-type decarboxylative halogenation of the readily available feedstock of aliphatic carboxylic acids (Scheme 1-4).^[25] The method employed [Ir{dF(CF₃)ppy}₂(dtbbpy)]PF₆ as photocatalyst and the common lab chemicals *N*-chloro succinimide (NCS) as chlorine source and cesium carbonate as base. The reaction mixture was irradiated with blue LEDs (455 nm) for 14 h providing the corresponding chlorinated products in generally very good yields (70-90%). However, the reported functional group tolerance was limited to bromides, ethers, esters, protected amines and amides. Noteworthy, the method could not only be applied for decarboxylative chlorinations but also for brominations and iodinations if either diethyl bromomalonate or *N*-iodo succinimide (NIS), were used as halide sources. A direct, photocatalytic chlorination of aliphatic C-H bonds was developed by Chen and coworkers who employed benzo- or acetophenone as photocatalysts and NCS as chlorine source providing a broader functional group tolerance but limited to benzylic C-H bonds or low selectivity if molecules without benzylic C-H bonds were used.^[26]

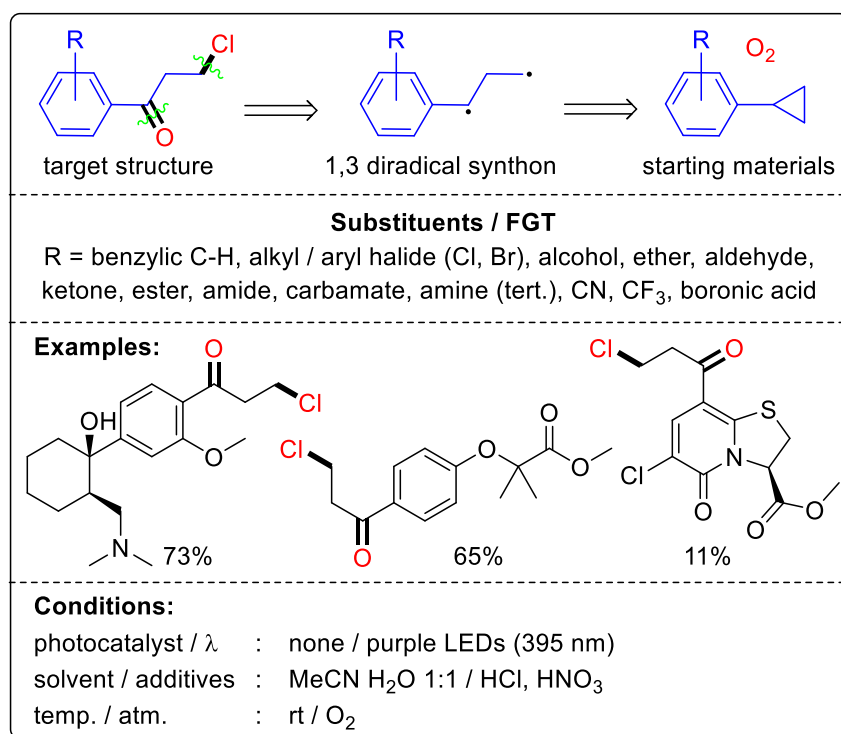
Strategy 2 – ATRA reactions generating chlorinated products



Scheme 1-5. ATRA reaction of fluorinated sulfonyl chlorides with Michael acceptors.^[27]

The group of Dolbier developed a strategy for an atom transfer radical addition (ATRA) of fluorinated sulfonyl chlorides to Michael acceptors (Scheme 1-5).^[27] The method employed Cu(dap)₂Cl as photocatalyst, the fluorinated sulfonyl chloride as ATRA precursor and K₂HPO₄ as base. The reaction mixture was irradiated with a 26 W fluorescent light bulb for 12-24 h giving the ATRA products in generally excellent yields (70-90%). The functional group tolerance was broad including many different electron withdrawing groups (EWG) as well as many different fluorinated sulfonyl chlorides. An alternative ATRA chlorotrifluoromethylation was developed by Han and coworkers using Ru(phen)₃Cl₂ as photocatalyst providing similar yields and functional group tolerance.^[28] Reiser and coworkers reported an ATRA chlorination with sulfonyl chlorides and managed to preserve the SO₂ in the product leading to chlorinated sulfones.^[29] Noteworthy, this method is not limited to Michael acceptors but both electron rich and poor double as well as triple bonds are tolerated. Finally, the Magnier group managed to perform this ATRA reaction with *N*-chlorinated sulfoximines adding both the sulfoximine and Cl to the double bond.^[30]

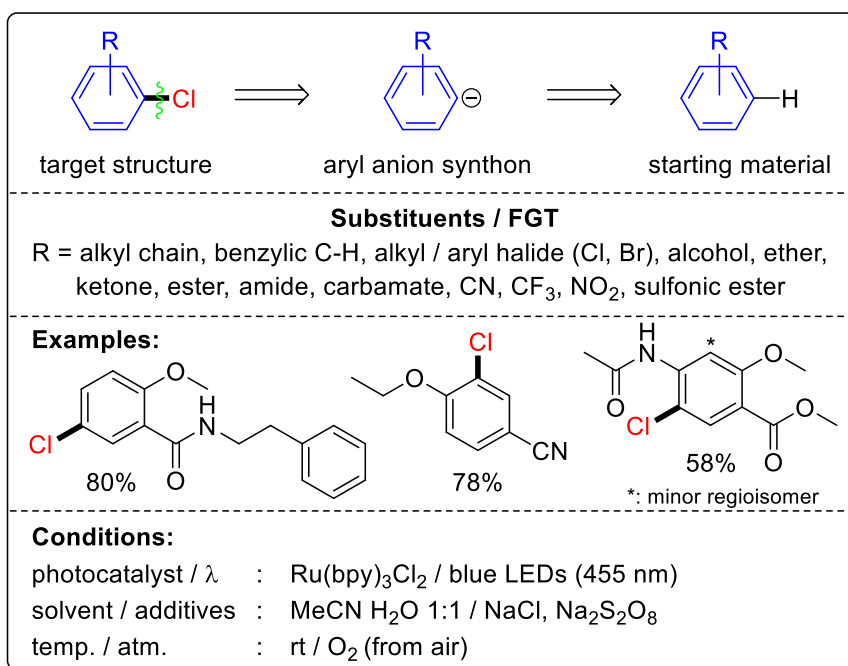
Strategy 3 – Generation of β -chloro ketones



Scheme 1-6. Oxochlorination of aryl cyclopropanes.^[31]

Very recently, our group developed a visible light mediated oxochlorination of aryl cyclopropanes (Scheme 1-6).^[31] No photocatalyst but only diluted HCl and HNO₃ as well as irradiation with a high power 395 nm LED for 2 h were required to promote the reaction giving the corresponding β -chloro ketones in generally good yields (50-70%). The functional group tolerance was broad including many common functionalities (e.g. halides (F, Cl, Br), alcohols, ethers, aldehydes, esters, amides, CN, CF₃ and boronic acids) although electron rich starting materials generally gave better yields than electron deficient ones. Noteworthy, if sodium anthraquinone-2-sulfonate (SAS) was used as a photosensitizer, other nucleophiles than chloride could be used (e.g. bromide, H₂O or MeOH) expanding the utility of the method.

1.3.2 Generation of aromatic C-Cl bonds

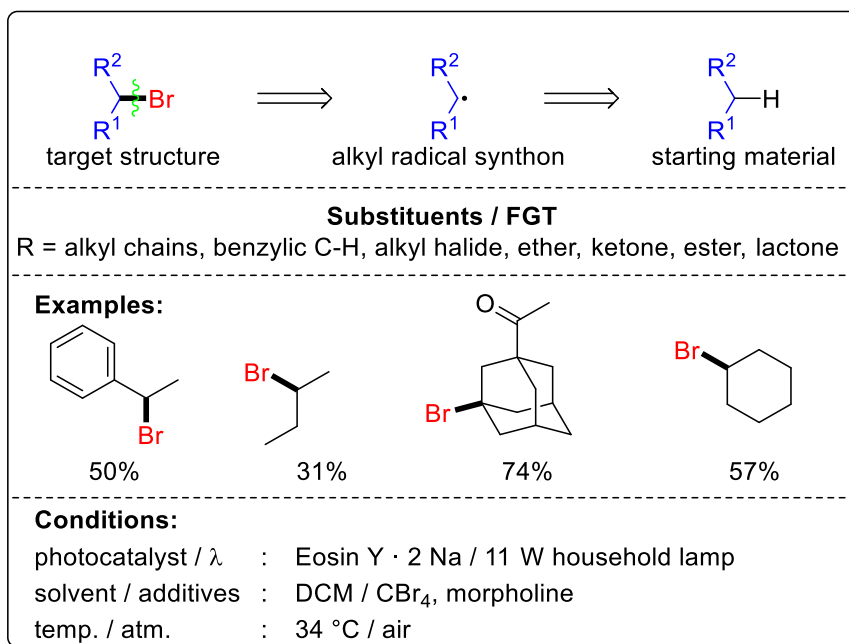


Scheme 1-7. Direct chlorination of aromatic C-H bonds of electron rich arenes.^[32]

An electrophilic aromatic substitution relying on simple NaCl rather than Cl₂/AlCl₃ as the chlorine source for a Cl⁺ synthon was realized. This strategy was reported by Hu and coworkers in 2017 as a method for the photocatalytic chlorination of electron rich arenes (Scheme 1-7).^[32] Utilization of NaCl and sodium persulfate as well as ruthenium trisbipyridine (Ru(bpy)₃Cl₂) as commercially available photosensitizer and irradiation with blue LEDs for 24 h led to the corresponding chlorinated arenes in excellent yields (60-90%) albeit only moderate ortho/para regio-selectivity, which was to be expected from the Cl⁺ reactivity. Many functional groups were tolerated including halides (Cl, Br), alcohols, esters, amides, CN, CF₃ and NO₂ groups but the method failed to chlorinate very electron deficient arenes e.g. nitrobenzene or trifluoromethoxybenzene. Alternatively, a transition metal free, photocatalytic chlorination method was developed by our group giving similar yields and showing the same functional group tolerance.^[33]

1.3.3 Generation of aliphatic C-Br bonds

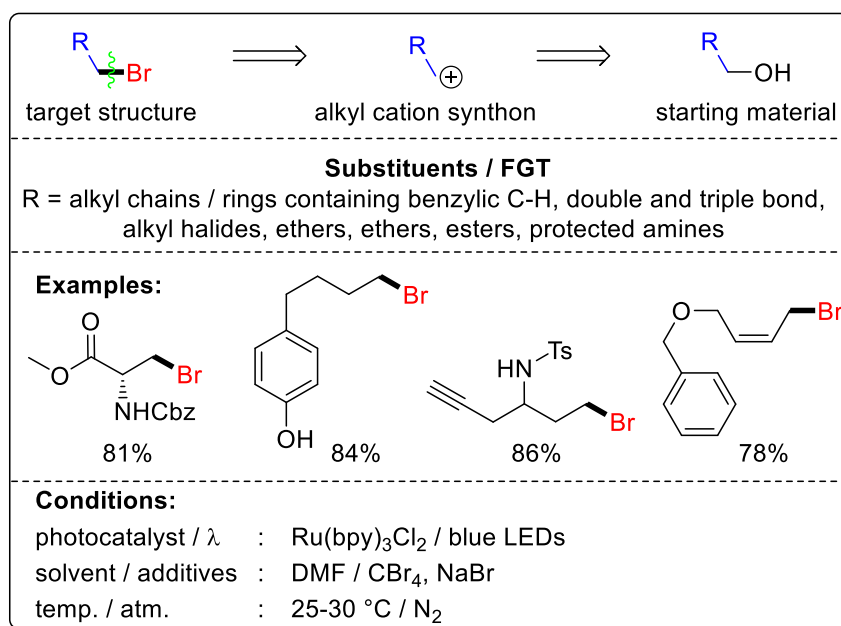
Strategy 1 – C-H bromination



Scheme 1-8. Direct bromination of sec. or tert. aliphatic C-H bonds.^[34]

In addition to the chlorination, several photocatalytic strategies for bromination of aliphatic C-H bonds were published. Tan and coworkers employed the commercially available disodium salt of Eosin Y as photocatalyst and CBr₄ as bromine source, as well as morpholine as sacrificial electron donor (Scheme 1-8).^[34] The reaction mixture was irradiated with a simple 11 W household lamp for 24 h providing the corresponding brominated products in generally good yields (50-70%). The reported functional group tolerance was low including only alkyl halides (Cl, Br), ethers, ketones and esters. An alternative procedure with a similar substrate scope was published by Lu and coworkers using KBr and NaNO₂ as bromination system.^[35] Another strategy was published by Franzén and coworkers employing NBS as the bromine source.^[36] The authors proposed that a trityl-cation as Lewis acid together with simple hood light promoted an efficient bromination of the benzylic position of electron rich arenes.

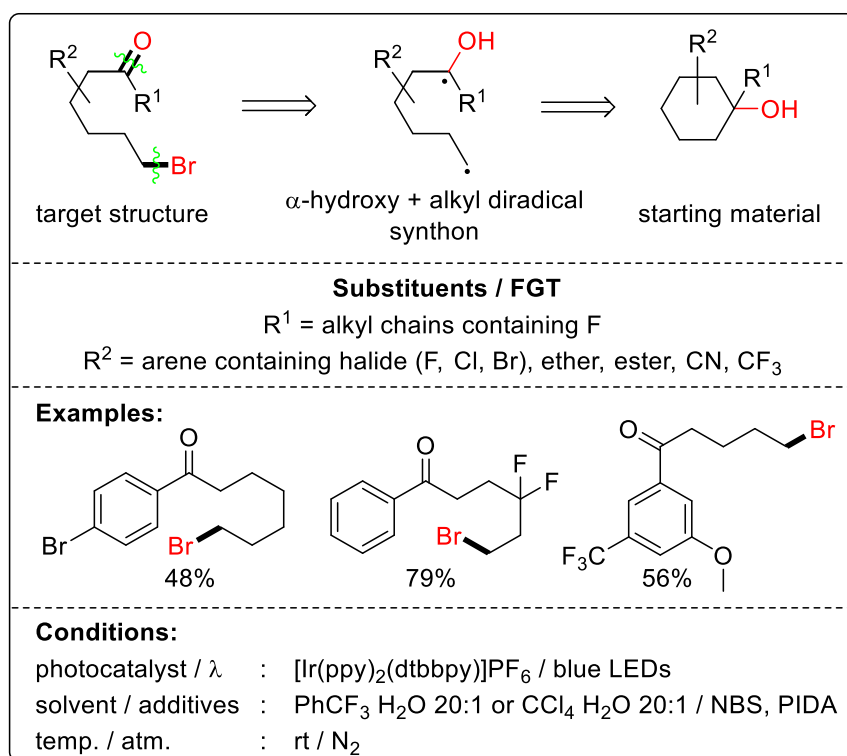
Strategy 2 – Deoxygenative bromination



Scheme 1-9. Deoxygenative bromination of aliphatic alcohols.^[37]

Another text book bromination is the Appel reaction which turns aliphatic alcohols into the corresponding halides.^[38] However, its significant disadvantage is the generation of stoichiometric amounts of triphenylphosphin oxide as side product which is often hard to separate.^[37] Therefore, Stephenson and coworkers developed an elegant method for a photocatalytic Appel reaction which completely avoids the generation of triphenylphosphin oxide (Scheme 1-9).^[39] The strategy required Ru(bpy)₃Cl₂ as photocatalyst, a mixture of CBr₄ and NaBr as bromine sources as well as DMF as the solvent. The reaction mixture was illuminated with blue LEDs for 5-15 h giving the corresponding deoxobrominated products in generally very good yields (70-90%). The reported functional group tolerance was moderate including double and triple bonds, ethers, esters and protected amines. Noteworthy, also iodinations could be performed if iodoform and NaI instead of CBr₄ and NaBr were used.

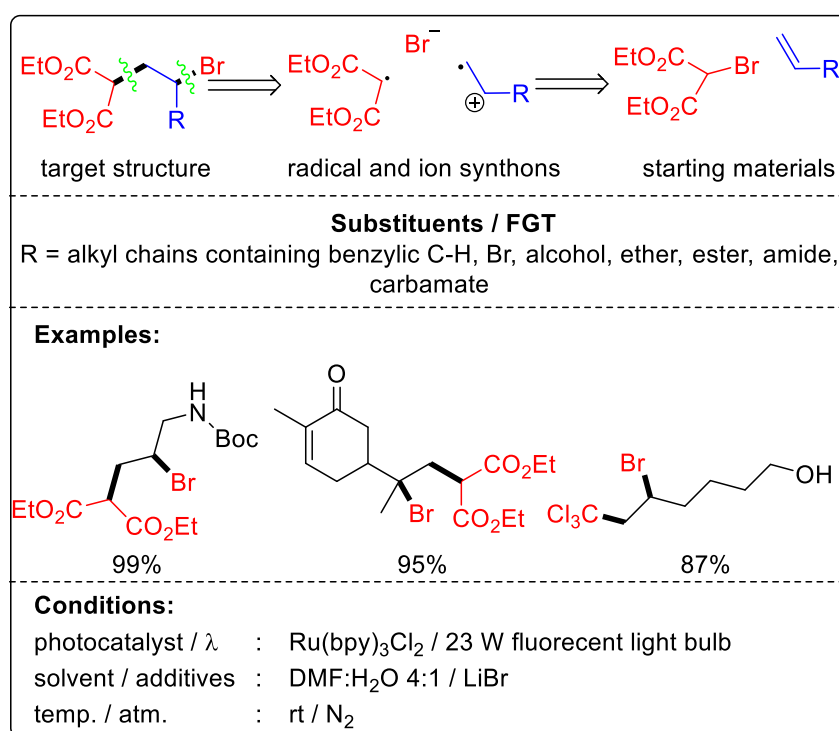
Strategy 3 – Remote oxidative bromination



Scheme 1-10. Remote oxidative bromination of cyclic, aliphatic alcohols.^[40]

Zhu and coworkers developed a photocatalytic, oxidative ring opening bromination of unstrained, cyclic, benzylic, tertiary alcohols (Scheme 1-10).^[40] The procedure used [Ir(ppy)₂(dtbbpy)]PF₆ as photocatalyst, NBS as bromine source and phenyliodine(III) diacetate (PIDA) as hypervalent iodine species. The reaction mixture was irradiated with blue LEDs giving the corresponding remotely brominated ketones in generally good yields (50-70%). The functional group tolerance was moderate including aromatic halides (F, Cl, Br), ethers, esters, CN and CF₃ groups. Noteworthy, the reaction times were very long ranging from 12 h to 100 h.

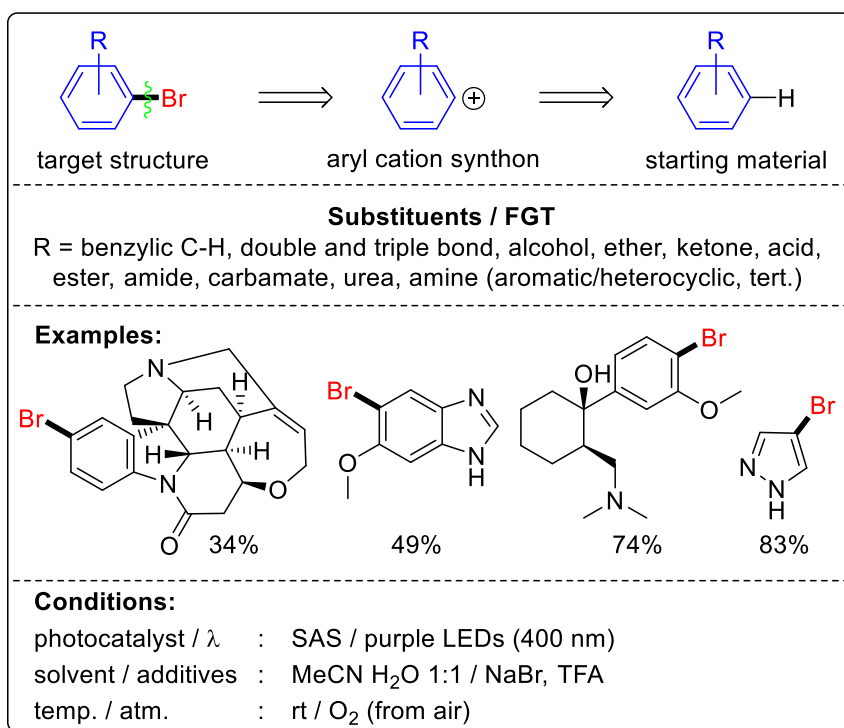
Strategy 3 – ATRA reactions generating brominated products



Scheme 1-11. ATRA reaction between diethyl bromomalonate and alkenes.^[41]

Stephenson and coworkers published a visible light mediated ATRA reaction of diethyl bromomalonate with alkenes (Scheme 1-11).^[41] The method employed Ru(bpy)₃Cl₂ as photocatalyst, diethyl bromomalonate as ATRA precursor and LiBr. The reaction mixture was irradiated with a fluorescent light bulb for 24 h giving the ATRA reaction products in generally excellent yields (70-90%). The functional group tolerance was moderate including alcohols, ethers, esters, amides and carbamates. However, the authors demonstrated that also many other ATRA precursors instead of just diethyl bromomalonate could be used e.g. CF₂BrCO₂Et or CCl₃Br providing the corresponding products also in excellent yields. Many alternative methods for this transformation were published e.g. by Pericàs using Bi₂O₃ as heterogeneous photocatalyst^[42] or by Reiser using Cu(dap)₂Cl instead of Ru(bpy)₃Cl₂.^[43]

1.3.4 Generation of aromatic C-Br bonds

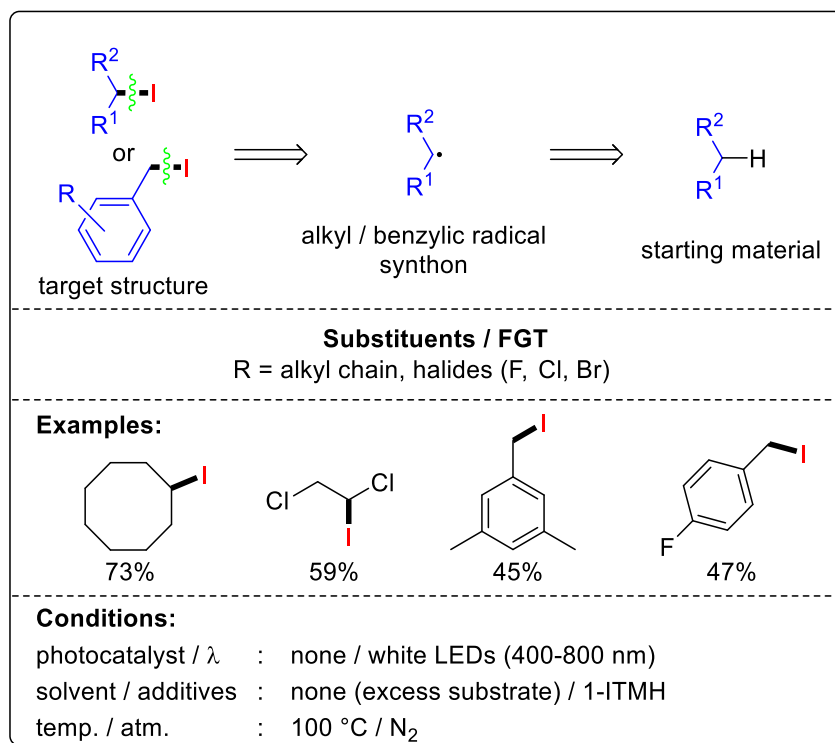


Scheme 1-12. Direct bromination of aromatic C-H bonds of electron rich arenes.^[44]

Our group published a method for the direct bromination of electron rich arenes and heteroarenes using sodium anthraquinone-2-sulfonate (SAS) as an inexpensive and commercially available photocatalyst as well as NaBr and TFA as common lab reagents (Scheme 1-12).^[44] The reaction mixture was irradiated with a 400 nm LED for 4 h giving the brominated products in generally very good yields (60-80%). The functional group tolerance was broad including double and triple bonds, halides, alcohols, acids, esters and free amines but the procedure failed to brominate electron deficient arenes e.g. chlorobenzene. An alternative method published by Lamar uses NBS as bromine source extending the substrate scope by phenols and free amine groups.^[45] The groups of Fukuzumi and Zhang also published visible light mediated methods for the oxidative bromination of arenes however with more limited substrate scopes.^[46]

1.3.5 Generation of aliphatic C-I bonds

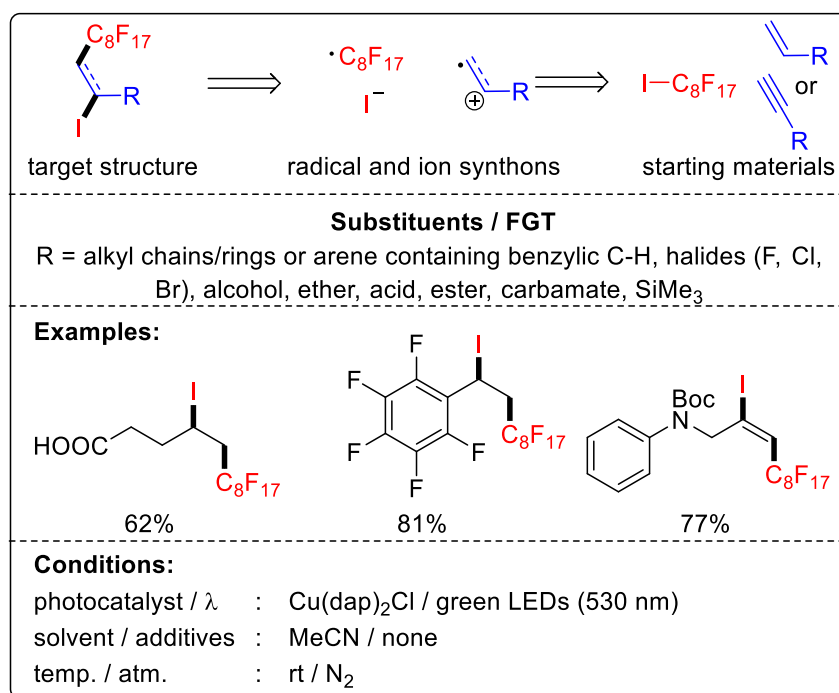
Strategy 1 – C-H iodination



Scheme 1-13. Direct iodination of sec. or benzylic aliphatic C-H bonds.^[47]

The direct, visible light mediated iodination of benzylic and secondary C-H bonds was realized by Gandelmann and coworkers (Scheme 1-13).^[47] The method did not require a photocatalyst and used 1-iodo-3,5,5-trimethylhydantoin (1-ITMH) which was activated by white light (400-800 nm) and high temperatures (100 °C). The yields of the iodinated products were moderate (40-60%) and the reaction was unselective towards alkyl chains. The functional group tolerance was low (only chloride and fluoride were shown) but the reaction time was short (0.5-2 h). Additional methods for the generation of aliphatic iodides were developed by Glorius and coworkers focusing on the decarboxylative iodination of aliphatic carboxylic acids^[25] (see 1.3.1, Strategy 1 for details) and by Stephenson and coworkers enabling the deoxygenative iodination of aliphatic alcohols (see 1.3.3, Strategy 2 for details).^[39]

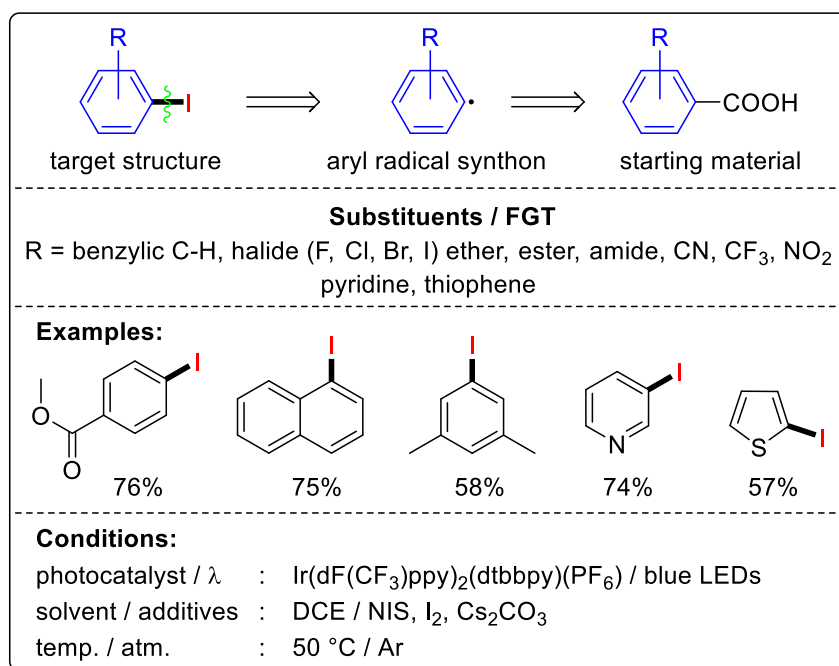
Strategy 2 – ATRA reactions generating iodinated products



Scheme 1-14. ATRA reaction between perfluoroalkyl iodides and alkenes/alkynes.^[48]

Reiser and coworkers developed a visible light mediated ATRA reaction between perfluoroalkyl iodides and alkenes or alkynes (Scheme 1-14).^[48] The method employed Cu(dap)₂Cl as photocatalyst as well as perfluorinated octyl iodide as ATRA reagent and did not require any other additives. The reaction mixture was irradiated with green LEDs for 12-42 h giving the ATRA products in generally very good yields (60-80%). The functional group tolerance was good including halides, alcohols, ethers, esters, acids, carbamates and silanes. Alternative methods focusing on other fluorinated alkyl iodides were published by Stephenson^[41] (e.g. CF₃I) and Guo^[49] (CF₃CH₂I) providing similar yields and functional group tolerance.

1.3.6 Generation of aromatic C-I bonds



Scheme 1-15. Decarboxylative iodination of aromatic carboxylic acids.^[50]

Fu and coworkers published a procedure for the decarboxylative aromatic iodination (Scheme 1-15).^[50] They used [Ir{dF(CF₃)ppy}₂(dtbbpy)]PF₆ as commercially available photocatalyst, *N*-iodosuccinimide (NIS) in combination with I₂ as iodine source and cesium carbonate as base. The reaction mixture was illuminated with blue LEDs for 24-36 h giving the products in generally good yields (60-80%). The functional group tolerance was broad including both electron donating and electron withdrawing substituents (halides, ethers, CN and NO₂ group) as well as pyridine and thiophene as heterocycles. Another method which did not require a photocatalyst, was published by Li and coworkers and started from aryl triflates instead of carboxylic acids providing similar yields and functional group tolerance.^[51]

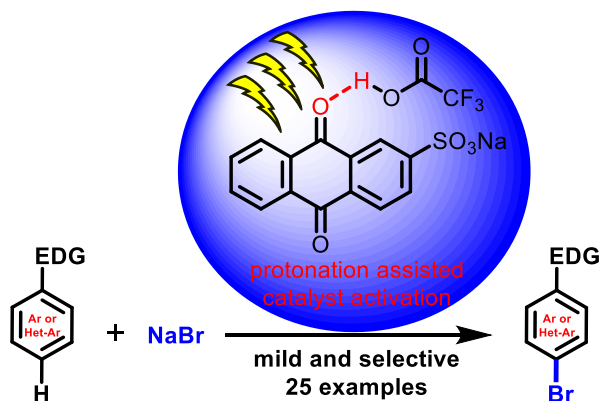
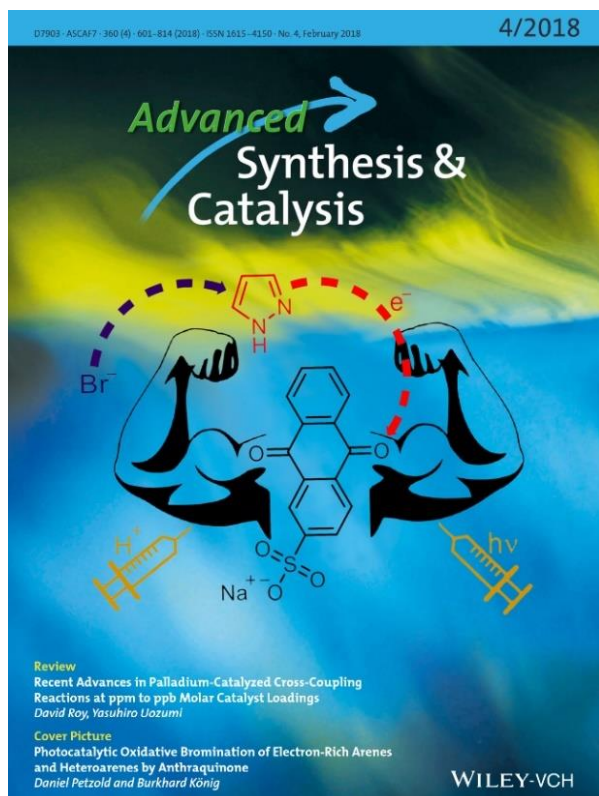
1.4 References

- [1] a) G. Ciamician, *Science* **1912**, 36, 385-394; b) N. Hoffmann, *Photochem. Photobiol. Sci.* **2012**, 11, 1613-1641; c) N. J. Turro, *J. Org. Chem.* **2011**, 76, 9863-9890.
- [2] a) W.-K. Jo, R. J. Tayade, *Ind. Eng. Chem. Res.* **2014**, 53, 2073-2084; b) L. Marzo, S. K. Pagire, O. Reiser, B. König, *Angew. Chem. Int. Ed.* **2018**, 57, 10034-10072.
- [3] a) D. C. Blakemore, L. Castro, I. Churcher, D. C. Rees, A. W. Thomas, D. M. Wilson, A. Wood, *Nat. Chem.* **2018**, 10, 383-394; b) I. W. Davies, C. J. Welch, *Science* **2009**, 325, 701-704; c) J. J. Douglas, M. J. Sevrin, C. R. J. Stephenson, *Org. Proc. Res. Dev.* **2016**, 20, 1134-1147; d) M. L. Crawley, B. M. Trost, *Applications of Transition Metal Catalysis in Drug Discovery and Development: An Industrial Perspective*, John Wiley & Sons, Hoboken, **2012**.
- [4] J. M. Smith, S. J. Harwood, P. S. Baran, *Acc. Chem. Res.* **2018**, 51, 1807-1817.
- [5] a) M. Silvi, P. Melchiorre, *Nature* **2018**, 554, 41; b) L. Buzzetti, G. E. M. Crisenza, P. Melchiorre *Angew. Chem. Int. Ed.* <https://doi.org/10.1002/anie.201809984>; c) J. Twilton, C. Le, P. Zhang, M. H. Shaw, R. W. Evans, D. W. C. MacMillan, *Nat. Rev. Chem.* **2017**, 1, 0052; d) F. Strieth-Kalthoff, M. J. James, M. Teders, L. Pitzer, F. Glorius, *Chem. Soc. Rev.* **2018**, 47, 7190-7202; e) K. L. Skubi, T. R. Blum, T. P. Yoon, *Chem. Rev.* **2016**, 116, 10035-10074; f) Y.-Q. Zou, F. M. Hörmann, T. Bach, *Chem. Soc. Rev.* **2018**, 47, 278-290; g) T. Courant, G. Masson, *J. Org. Chem.* **2016**, 81, 6945-6952.
- [6] a) C. Isanbor, D. O'Hagan, *J. Fluor. Chem.* **2006**, 127, 303-319; b) P. Jeschke, *Pest Manag. Sci.* **2017**, 73, 1053-1066.
- [7] C. N. Neumann, T. Ritter, *Angew. Chem. Int. Ed.* **2015**, 54, 3216-3221.
- [8] a) T. Liang, C. N. Neumann, T. Ritter, *Angew. Chem. Int. Ed.* **2013**, 52, 8214-8264; b) X. Yang, T. Wu, R. J. Phipps, F. D. Toste, *Chem. Rev.* **2015**, 115, 826-870; c) P. A. Champagne, J. Desroches, J.-D. Hamel, M. Vandamme, J.-F. Paquin, *Chem. Rev.* **2015**, 115, 9073-9174.
- [9] S. D. Halperin, H. Fan, S. Chang, R. E. Martin, R. Britton, *Angew. Chem. Int. Ed.* **2014**, 53, 4690-4693.
- [10] S. D. Halperin, D. Kwon, M. Holmes, E. L. Regalado, L.-C. Campeau, D. A. DiRocco, R. Britton, *Org. Lett.* **2015**, 17, 5200-5203.
- [11] S. Bloom, J. L. Knippel, T. Lectka, *Chem. Sci.* **2014**, 5, 1175-1178.
- [12] C. W. Kee, K. F. Chin, M. W. Wong, C.-H. Tan, *Chem. Commun.* **2014**, 50, 8211-8214.
- [13] a) D. D. Bume, C. R. Pitts, F. Ghorbani, S. A. Harry, J. N. Capilato, M. A. Siegler, T. Lectka, *Chem. Sci.* **2017**, 8, 6918-6923; b) D. D. Bume, S. A. Harry, C. R. Pitts, T. Lectka, *J. Org. Chem.* **2018**, 83, 1565-1575.
- [14] H. Egami, S. Masuda, Y. Kawato, Y. Hamashima, *Org. Lett.* **2018**, 20, 1367-1370.
- [15] J. G. West, T. A. Bedell, E. J. Sorensen, *Angew. Chem. Int. Ed.* **2016**, 55, 8923-8927.
- [16] J.-B. Xia, C. Zhu, C. Chen, *J. Am. Chem. Soc.* **2013**, 135, 17494-17500.
- [17] a) S. Bloom, M. McCann, T. Lectka, *Org. Lett.* **2014**, 16, 6338-6341; b) M. Xiang, Z.-K. Xin, B. Chen, C.-H. Tung, L.-Z. Wu, *Org. Lett.* **2017**, 19, 3009-3012; c) D. D. Bume, C. R. Pitts, R. T. Jokhai, T. Lectka, *Tetrahedron* **2016**, 72, 6031-6036.
- [18] S. Ventre, F. R. Petronijevic, D. W. C. MacMillan, *J. Am. Chem. Soc.* **2015**, 137, 5654-5657.

- [19] a) M. Rueda-Becerril, O. Mahé, M. Drouin, M. B. Majewski, J. G. West, M. O. Wolf, G. M. Sammis, J.-F. Paquin, *J. Am. Chem. Soc.* **2014**, *136*, 2637-2641; b) X. Wu, C. Meng, X. Yuan, X. Jia, X. Qian, J. Ye, *Chem. Commun.* **2015**, *51*, 11864-11867.
- [20] G. Tarantino, C. Hammond, *ACS Catal.* **2018**, *8*, 10321-10330.
- [21] X. Yuan, J.-F. Yao, Z.-Y. Tang, *Org. Lett.* **2017**, *19*, 1410-1413.
- [22] T. A. McTeague, T. F. Jamison, *Angew. Chem. Int. Ed.* **2016**, *55*, 15072-15075.
- [23] J. Clayden, N. Greeves, S. G. Warren, *Organic Chemistry*, Oxford University Press, Oxford; New York, **2012**.
- [24] a) Z. Wang, L. Zhu, F. Yin, Z. Su, Z. Li, C. Li, *J. Am. Chem. Soc.* **2012**, *134*, 4258-4263; b) X. Tan, T. Song, Z. Wang, H. Chen, L. Cui, C. Li, *Org. Lett.* **2017**, *19*, 1634-1637; c) K. Shibatomi, K. Kitahara, N. Sasaki, Y. Kawasaki, I. Fujisawa, S. Iwasa, *Nat. Commun.* **2017**, *8*, 15600; d) R. Ben-Daniel, S. P. de Visser, S. Shaik, R. Neumann, *J. Am. Chem. Soc.* **2003**, *125*, 12116-12117.
- [25] L. Candish, E. A. Standley, A. Gómez-Suárez, S. Mukherjee, F. Glorius, *Chem. Eur. J.* **2016**, *22*, 9971-9974.
- [26] L. Han, J.-B. Xia, L. You, C. Chen, *Tetrahedron* **2017**, *73*, 3696-3701.
- [27] X.-J. Tang, W. R. Dolbier Jr., *Angew. Chem. Int. Ed.* **2015**, *54*, 4246-4249.
- [28] S. H. Oh, Y. R. Malpani, N. Ha, Y.-S. Jung, S. B. Han, *Org. Lett.* **2014**, *16*, 1310-1313.
- [29] A. Hossain, S. Engl, E. Lutsker, O. Reiser, *ACS Catal.* **2019**, *9*, 1103-1109.
- [30] A. Prieto, P. Diter, M. Toffano, J. Hannedouche, E. Magnier, *Adv. Syn. Catal.* <https://doi.org/10.1002/adsc.201801207>.
- [31] D. Petzold, P. Singh, F. Almqvist, B. König, **2019**
- [32] L. Zhang, X. Hu, *Chem. Sci.* **2017**, *8*, 7009-7013.
- [33] T. Hering, B. Mühldorf, R. Wolf, B. König, *Angew. Chem. Int. Ed.* **2016**, *55*, 5342-5345.
- [34] C. W. Kee, K. M. Chan, M. W. Wong, C.-H. Tan, *Asian J. Org. Chem.* **2014**, *3*, 536-544.
- [35] M. Zhao, W. Lu, *Org. Lett.* **2018**, *20*, 5264-5267.
- [36] S. Ni, M. A. E. A. A. El Remaily, J. Franzén, *Adv. Syn. Catal.* **2018**, *360*, 4197-4204.
- [37] D. C. Batesky, M. J. Goldfogel, D. J. Weix, *J. Org. Chem.* **2017**, *82*, 9931-9936.
- [38] R. Appel, *Angew. Chem. Int. Ed.* **1975**, *14*, 801-811.
- [39] C. Dai, J. M. R. Narayanam, C. R. J. Stephenson, *Nat. Chem.* **2011**, *3*, 140.
- [40] D. Wang, J. Mao, C. Zhu, *Chem. Sci.* **2018**, *9*, 5805-5809.
- [41] a) J. D. Nguyen, J. W. Tucker, M. D. Konieczynska, C. R. J. Stephenson, *J. Am. Chem. Soc.* **2011**, *133*, 4160-4163; b) C.-J. Wallentin, J. D. Nguyen, P. Finkbeiner, C. R. J. Stephenson, *J. Am. Chem. Soc.* **2012**, *134*, 8875-8884.
- [42] P. Riente, M. A. Pericàs, *ChemSusChem* **2015**, *8*, 1841-1844.
- [43] a) M. Pirtsch, S. Paria, T. Matsuno, H. Isobe, O. Reiser, *Chem. Eur. J.* **2012**, *18*, 7336-7340; b) K. Matsuo, E. Yamaguchi, A. Itoh, *Asian J. Org. Chem.* **2018**, *7*, 2435-2438.
- [44] D. Petzold, B. König, *Adv. Syn. Catal.* **2018**, *360*, 626-630.
- [45] D. A. Rogers, R. G. Brown, Z. C. Brandeburg, E. Y. Ko, M. D. Hopkins, G. LeBlanc, A. A. Lamar, *ACS Omega* **2018**, *3*, 12868-12877.

- [46] a) K. Ohkubo, K. Mizushima, R. Iwata, S. Fukuzumi, *Chem. Sci.* **2011**, 2, 715-722; b) R. Li, Z. J. Wang, L. Wang, B. C. Ma, S. Ghasimi, H. Lu, K. Landfester, K. A. I. Zhang, *ACS Catal.* **2016**, 6, 1113-1121.
- [47] A. Artaryan, A. Mardyukov, K. Kulbitski, I. Avigdori, G. A. Nisnevich, P. R. Schreiner, M. Gandelman, *J. Org. Chem.* **2017**, 82, 7093-7100.
- [48] T. Rawner, E. Lutsker, C. A. Kaiser, O. Reiser, *ACS Catal.* **2018**, 8, 3950-3956.
- [49] M. Huang, L. Li, Z.-G. Zhao, Q.-Y. Chen, Y. Guo, *Synthesis* **2015**, 47, 3891-3900.
- [50] M. Jiang, H. Yang, Y. Jin, L. Ou, H. Fu, *Synlett* **2018**, 29, 1572-1577.
- [51] W. Liu, X. Yang, Y. Gao, C.-J. Li, *J. Am. Chem. Soc.* **2017**, 139, 8621-8627.

2. Photocatalytic Oxidative Bromination of Electron-Rich Arenes and Heteroarenes by Anthraquinone



The estimated excited oxidation potential of sodium anthraquinone-2-sulfonate (SAS) increases from 1.8 V to about 2.3 V vs SCE by protonation with Brønsted acids. This increased photooxidation power of protonated anthraquinone was used for the regio-selective oxidative bromination of electron rich (hetero)arenes and drugs in good yield. The mild reaction conditions are compatible with many functional groups, such as double and triple bonds, ketones, amides and amines, hydroxyl groups, carboxylic acids and carbamates. Mechanistic investigations indicate the photooxidation of the arene followed by nucleophilic bromide addition as the likely pathway.

This chapter has been published in:

D. Petzold, B. König *Adv. Syn. Catal.* **2018**, 360, 626–630. (Communication) – Reproduced with permission from John Wiley and Sons.

Author Contributions:

DP discovered the reaction, performed the optimization, synthesized the scope, carried out all the mechanistic investigations and wrote the manuscript. BK supervised the project and is the corresponding author.

2.1 Introduction

The development of novel, photocatalytic transformations received tremendous attention in the past decade due to the versatile reactivity of radical intermediates.^[1] To form radicals, a single electron transfer step is necessary.^[1] However, direct single electron oxidation or reduction of many substrates is thermodynamically not feasible by the currently available photocatalysts. Proton coupled electron transfer (PCET) extends the accessible range, as the interaction with acids or bases alters the oxidation or reduction potential of carbonyl compounds, amides and other substances up to 500 mV.^[2]

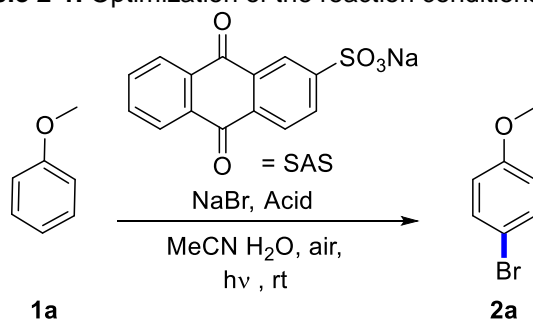
However, PCET activation of aromatic C-H bonds is difficult to realize, because they cannot be polarized by simple bases. Thus, the direct photocatalytic activation of aromatic C-H bonds is still challenging and requires photocatalysts with a high oxidation potential. Commonly used photocatalysts for these processes are $[\text{Ir}\{\text{dF}(\text{CF}_3)\text{ppy}\}_2(\text{dtbpy})]\text{PF}_6$ ($E_{\text{Ox}} \sim +1.2\text{-}1.7$ V) and acridinium based dyes ($E_{\text{Ox}} \sim +2.0$ V).^[1] Photocatalysts offering a significantly higher oxidation potential have not been developed yet or require multistep syntheses.^[3]

To enable the photo-oxidation of arenes and heteroarenes with easily available photocatalysts, we envisioned enhancing the oxidative power of anthraquinones by protonation.^[2] The applicability of this approach was demonstrated by the photocatalytic bromination of electron-rich arenes.^[4] Employing sodium anthraquinone sulfonate (SAS) as the photocatalyst, sodium bromide as bromine source and oxygen as terminal oxidant allows an efficient and selective bromination of aromatic substrates with oxidation potentials up to 2.3 V vs. SCE.^[5] The excited state oxidation potential of SAS was estimated from electrochemical and spectroscopic data.^[6] The interaction of arenes with the SAS excited state was confirmed by fluorescence quenching studies.^[7] Furthermore, the viability of this method for late-stage functionalization of complex, bioactive molecules was demonstrated.^[8]

2.2 Results and Discussion

2.2.1 Synthesis

We started our investigations using anisole (**1a**) as a model substrate, sodium anthraquinone sulfonate as the catalyst, two equivalents of acetic acid ($\text{pK}_a = 4.76$) to activate the anthraquinone derivative and five equivalents of sodium bromide in a mixture of acetonitrile and demineralized water (4:1) under air atmosphere. Irradiation at 445 nm by a single LED for 18 h gave 43% conversion to the corresponding brominated anisole derivative (**2a**) (Table 2-1, entry 1). As an increase of the amount of the acid did not improve the yield significantly (entry 2), different acids were tested (entries 3-4). The amount of converted starting material increased with the strength of the corresponding acid. Employing KHSO_4 ($\text{pK}_a = 2.1$) gave 80% conversion and changing to TFA ($\text{pK}_a = 0.2$) lead to full conversion. After more optimization steps, the best conditions were identified, using 2 equiv. of NaBr, 2 equiv. of TFA and 5 mol% of catalyst in a mixture of MeCN H₂O 1:1 at 400 nm irradiation, giving full conversion of the starting material within 4 h (entry 5). Especially the change of the light source from 445 nm to 400 nm greatly accelerated the reaction due to the greater extinction coefficient of the catalyst at shorter wavelengths (see Chapter 2.4.2 for details). Moreover, control experiments revealed that in absence of acid, catalyst, light and/or air no reaction took place (entries 6-8).

Table 2-1. Optimization of the reaction conditions.

Entry	SAS [mol%]	Acid [equiv.]	NaBr [equiv.]	Yield of 2a ^[a]
1	20	AcOH [2]	5	43%
2	20	AcOH [5]	5	50%
3	20	KHSO ₄ [2]	5	80%
4	20	TFA [2]	5	100%
5 ^[b]	5	TFA [2]	2	100%
6 ^[b]	5	-	2	n.r.
7 ^[b]	-	TFA [2]	2	n.r.
8 ^[c]	5	TFA [2]	2	n.r.
9 ^[d]	5	TFA [2]	2	traces

General conditions: 0.1 mmol of **1a**, indicated amount of SAS, acid and NaBr in 1 mL of MeCN H₂O 4:1, 18 h irradiation at 445 nm. [a] Yield determined by GC-FID using naphthalene as internal standard. [b] MeCN H₂O 1:1 and 400 nm irradiation was used. [c] MeCN H₂O 1:1 but no light. [d] MeCN H₂O 1:1, 400 nm irradiation under nitrogen atmosphere. n.r. no reaction.

In the next step, the synthetic scope of the photocatalytic oxidative bromination was explored (Fig. 2-1). All tested methoxy arenes showed full conversion and good isolated yields (**2a-2i**). Moreover, despite the acidic environment, Boc-protected amine **2k** was isolated in good yield. On the other hand, the electron withdrawing substituent in compound **2l** reduces its reactivity in the reaction significantly. Interestingly, amide **2m** gave only the displayed brominated product despite the presence of two electron-donating groups at the second aromatic ring. This indicates that also steric factors influence the selectivity of the bromination. Electron-deficient indole derivative **2o** gave a moderate yield, as well as the electron-rich benzimidazole derivative **2p**. Notably, SAS could oxidize pyrazole **2q** and its derivatives **2r** and **2s** to give the brominated compounds in excellent yields. This extends recent observations, in which pyrazole ($E_{ox} = 2.21$ V vs SCE)^[5] was shown to be inert towards the oxidation by acridinium dyes and used as a nucleophile in amination reactions instead.^[3, 9] Finally, also bioactive compounds were brominated. The painkillers phenazone (**2t**) and tramadol (**2u**) gave excellent yields of only a single brominated product and the complex alkaloid strychnine (**2v**) could be selectively brominated in moderate yield. The hypolipidemic agent gemfibrozil (**2w**) and the anesthetic lidocaine (**2x**) gave moderate yields due to a competing oxidation of the benzylic position to the aldehyde.^[10] The reaction of the benzylic position was exploited for toluene (**1ac**) ($E_{ox} = 2.2$ V vs SCE)^[4a] if persulfate was used as oxidant under inert atmosphere (scheme 2-1). In this case, it was possible to achieve exclusive bromination of the benzylic position in good yield. Unfortunately, benzene (**1y**) and electron-poor benzene derivatives **1z-1ab** did not give any brominated products due to their high oxidation potentials.^[5]

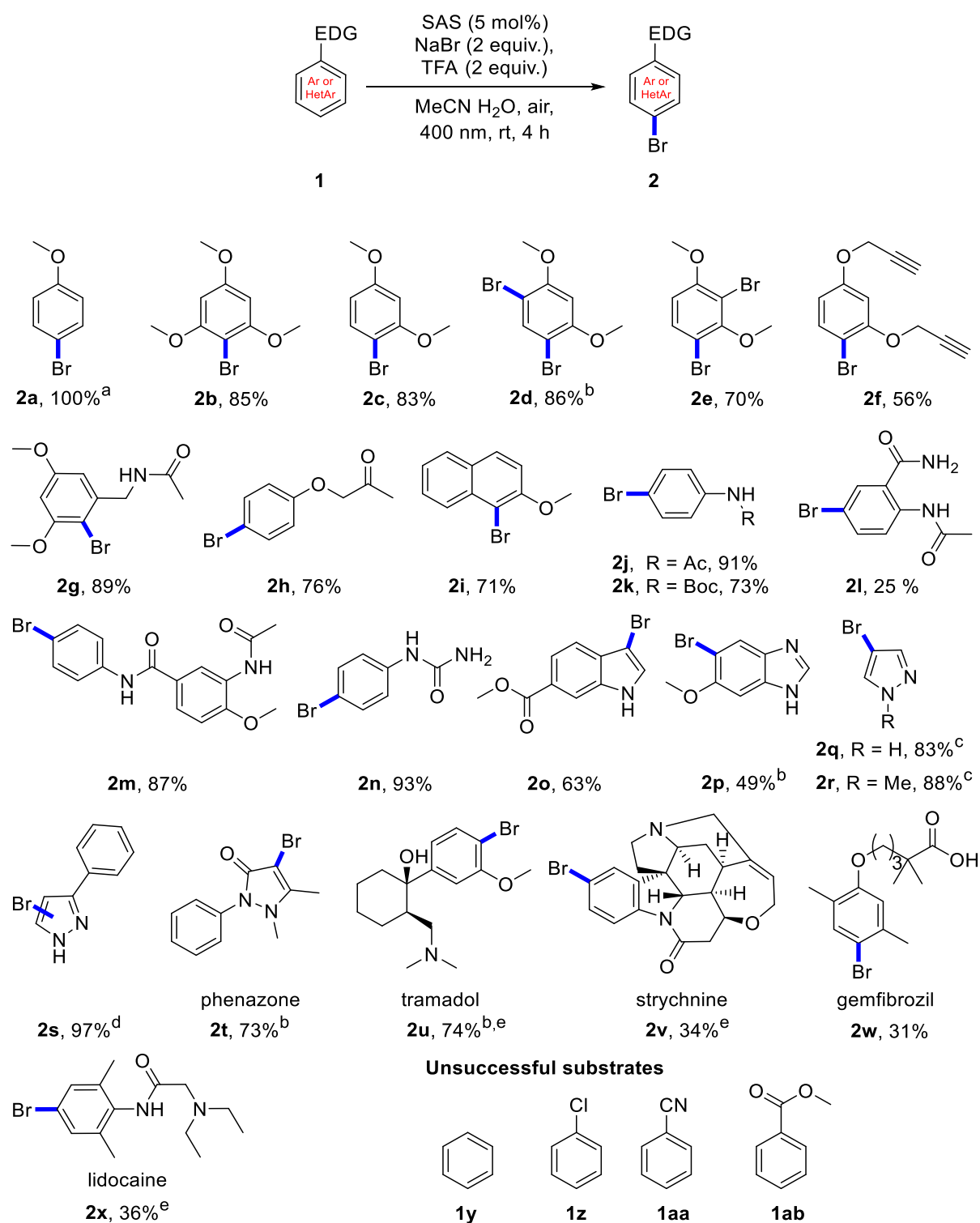
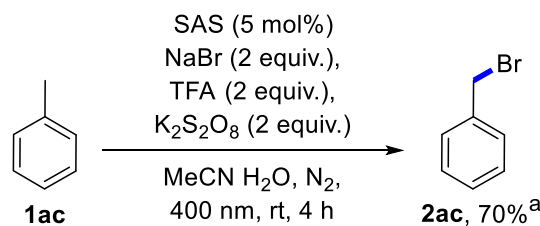


Figure 2-1. General conditions: 0.1 mmol of substrate, 5 mol% of SAS, 2 equiv. of TFA and 2 equiv. of NaBr were dissolved in 1 mL of MeCN H₂O 1:1 and irradiated at 400 nm for 4 h. Given yields are isolated yields. **a:** Yield determined by GC-FID calibration using naphthalene as internal standard. **b:** An oxygen balloon was connected to the vial through the septum. **c:** Yield determined by ¹H-NMR using dimethyl sulfone as internal standard. **d:** mixture of isomers at pyrazole position 4 and 5, ratio C4:C5 6:4. **e:** 4 equiv. of TFA were used.



Scheme 2-1. Benzylic bromination of toluene. Conditions: 0.1 mmol of **1ac**, 5 mol% of SAS, 2 equiv. of TFA, $\text{K}_2\text{S}_2\text{O}_8$ and NaBr respectively were dissolved in 1 mL of MeCN H_2O 1:1 and irradiated at 400 nm for 4 h. **a:** Yield determined by $^1\text{H-NMR}$ using dimethyl sulfone as internal standard.

2.2.2 Mechanistic Investigations

To get insight into the mechanism, cyclovoltammetric and spectroscopic investigations were performed. Cyclovoltammetry revealed a ground state reduction potential of -0.56 V vs. SCE for SAS in MeCN H_2O 1:1 (see Chapter 2.4.2 for details). Addition of TFA to this solution showed a tremendous impact by lowering the required potential by 0.55 V to merely -0.01 V vs. SCE. We propose that the reduction is facilitated by protonation in the presence of TFA (see Chapter 2.4.2 for details).^[11] This shift of the ground state reduction potential leads to a significant increase of the excited state oxidation potential by approximately the same voltage from 1.76 V to 2.3 V vs SCE (see Chapter 2.4.2 for details) and explains why TFA is required to successfully oxidize anisole ($E_{\text{Ox}} = 1.81$ V vs. SCE). To support this hypothesis, control experiments using substrates with a low oxidation potential were performed. These experiments revealed that the photocatalytic bromination was also possible without TFA. 1,3,5-Trimethoxy-benzene ($E_{\text{Ox}} = 1.4$ V vs. SCE)^[4a] and 2-methoxynaphthalene ($E_{\text{Ox}} = 1.5$ V vs. SCE)^[4a] gave the corresponding brominated products, but at a much slower rate and in lower yield indicating that the PCET increases the driving force of the reaction. To investigate the interaction between the excited photocatalyst and the substrate, emission quenching experiments were performed. We found that anisole and the more electron rich 1,3-dimethoxybenzene (1,3-DMB) are efficient quenchers, whereas *N*-methylpyrazole is a moderate quencher of the delayed fluorescence of SAS (Fig. 2-2 A).^[12] Notably, all three compounds showed non-linear quenching, which might indicate a ground state pre-orientation *via* π -stacking between the substrates and SAS. On the other hand, TFA showed no significant quenching at all as well as benzene, which has an oxidation potential of 2.48 V vs SCE.^[13] This observation is in good agreement with the estimated oxidation potential of SAS and the experimental findings, because benzene did not react under our bromination conditions. Moreover, sodium bromide showed similar quenching compared to anisole and 1,3-DMB at low quencher concentrations (Fig. 2-2 A). However, the formation of elemental bromine was not observed during the reaction or without substrate present (*vide infra*). This indicates that bromide is not oxidized by SAS and only engages in intermolecular heavy atom fluorescence quenching.^[14] Next, we investigated the ground state interaction between the catalyst and the other reaction components by UV-VIS spectroscopy. No significant change of the spectrum was observed by addition of NaBr or TFA (not shown). However, a small, concentration dependent change of the SAS spectrum could be observed after addition of 1,3-DMB to the catalyst (Fig. 2-2 B).^[15] The reason for the shift might be π -stacking of the non-polar anthraquinone core and 1,3-DMB in the polar solvent mixture rather than the formation of a charge transfer complex. This potential pre-orientation of substrate and catalyst might also play a role in the selectivity of the reaction.^[16]

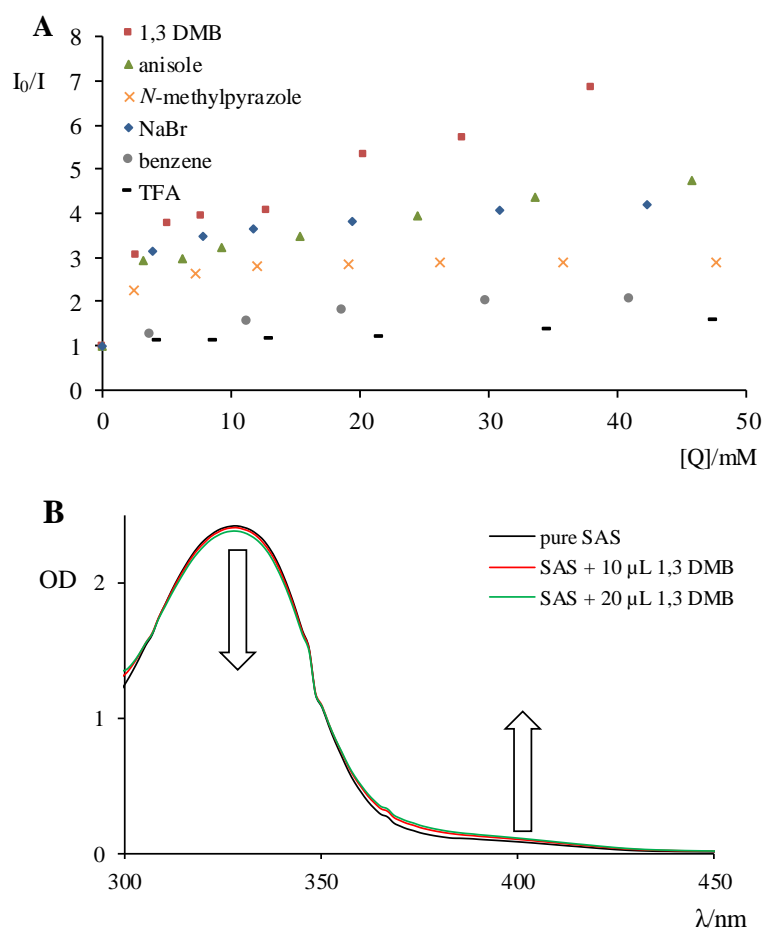
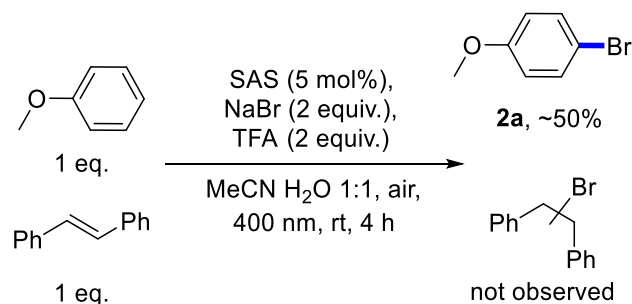


Figure 2-2. A: Stern-Volmer quenching plot of different substrates and additives. The oxidation potentials of TFA and benzene are too high to quench the catalyst whereas 1,3-DMB, anisole and *N*-methylpyrazole are good/moderate quenchers. Sodium bromide also shows moderate quenching of the catalyst, which can be attributed to the intermolecular heavy atom quenching effect.^[14] **B:** UV-VIS absorption spectra of pure SAS and after addition of different amounts of 1,3-DMB.^[15]

Thus, the oxidation of the arene is proposed as the key step of the mechanism (Fig. 2-3). To demonstrate that this step is exergonic, the ΔG value for the oxidation of pyrazole, which had the highest investigated oxidation potential, was estimated to be -2.1 kcal. Therefore, the catalytic cycle commences by protonation of SAS by TFA to give the SAS-H⁺ cation, which is excited by 400 nm and transitions into the long-lived triplet state SAS-H⁺*. This intermediate oxidizes the arene and the resulting radical cation is subsequently attacked by a bromide anion. Hydrogen abstraction by a hydroperoxyl radical yields the product and hydrogen peroxide.^[17] The formation of hydrogen peroxide enables a second mechanistic pathway *via* electrophilic bromination by hypobromous acid.^[18] However, control experiments indicated that this process is much slower than the photocatalytic pathway under the investigated conditions. The reason for this is the slow reaction rate of the bromide anion with H₂O₂.^[19] Moreover, compounds **7** and **9** showed neither addition of bromine to the triple bond nor α -bromination of the ketone indicating that electrophilic bromine species do not contribute significantly to the conversion of the substrates. To clarify the role of H₂O₂, a competition experiment between anisole and trans-stilbene was performed, because *in situ* formed HOBr or Br₂ should react several orders of magnitude faster with trans-stilbene than with anisole (Scheme 2-2). However, no brominated stilbene was observed supporting the subordinate role of electrophilic bromine species in the reaction mixture.



Scheme 2-2. Competition experiment between aromatic and olefinic bromination to elucidate the role of H₂O₂ in the reaction mixture.

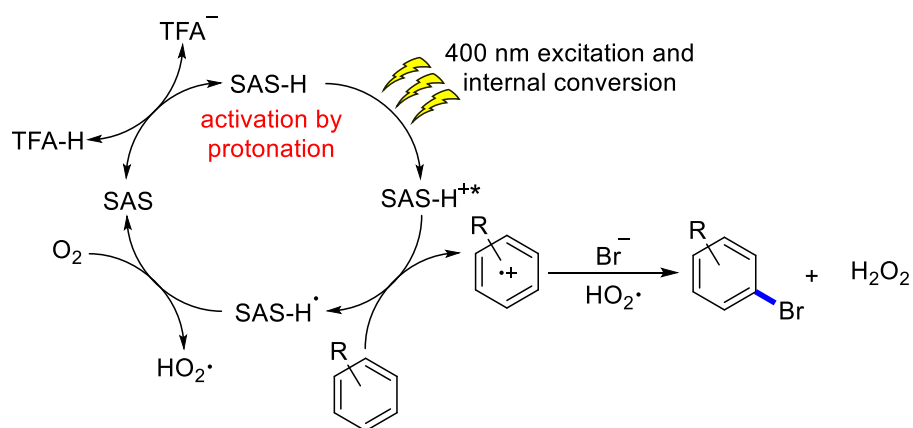


Figure 2-3. Proposed mechanism for the photocatalytic bromination of arenes and heteroarenes yielding exclusively mono-brominated compounds.

2.3 Conclusion

In summary, we have developed a new, photocatalytic bromination method using protonated anthraquinone as a strongly oxidizing photocatalyst. The procedure extends previously reported methods and shows good regio-selectivity and functional group tolerance including double and triple bonds, ketones, amides and amines, hydroxyl groups, carboxylic acids and carbamates. The proton activation of anthraquinone was shown using cyclic voltammetry. An interaction between the aromatic substrates and SAS in the ground as well as in the excited state was confirmed by UV-VIS spectrometry and emission quenching experiments. The readily available photocatalyst, very simple reaction conditions and a good substrate scope recommend the procedure for the mild oxidative bromination of arenes and heteroarenes.

2.4 Experimental Part

2.4.1 General Information

Starting materials and reagents were purchased from commercial suppliers (Sigma Aldrich, Alfa Aesar, Acros, Fluka or abcr) and were used without further purification. Solvents were used as *p.a.* grade. Industrial grade of solvents was used for automated flash column chromatography. Dry nitrogen was used as inert gas atmosphere. Liquids were added *via* syringe, needle and septum technique unless stated differently.

Nuclear magnetic resonance spectroscopy

All NMR spectra were measured at room temperature using a Bruker Avance 300 (300 MHz for ^1H , 75 MHz for ^{13}C) or a Bruker Avance 400 (400 MHz for ^1H , 101 MHz for ^{13}C) NMR spectrometer. All chemical shifts are reported in δ -scale as parts per million [ppm] (multiplicity, coupling constant J , number of protons) relative to the solvent residual peaks as the internal standard.^[20] The spectra were analyzed by first order and coupling constants J are given in Hertz [Hz]. Abbreviations used for signal multiplicity: ^1H -NMR: br = broad, s = singlet, d = doublet, t = triplet, q = quartet, dd = doublet of doublets, ddd = doublet of doublet of doublet, dt = doublet of triplets and m = multiplet.

Gas chromatography and gas chromatography coupled with mass spectrometry

GC measurements were performed on a GC 7890 from Agilent Technologies. Data acquisition and evaluation was done with Agilent ChemStation Rev.C.01.04.

GC-MS measurements were performed on a 7890A GC system from Agilent Technologies with an Agilent 5975 MSD Detector. Data acquisition and evaluation was done with MSD ChemStation E.02.02.1431.

A capillary column HP-5MS/30 m x 0.25 mm/0.25 μM film and helium as carrier gas (flow rate of 1 mL/min) were used. The injector temperature (split injection: 40:1 split) was 300 °C and the detection temperature was 300 °C for the flame ionization detector (FID). GC measurements were performed and investigated *via* integration of the signals obtained. The GC oven temperature program was adjusted as follows: initial temperature 40 °C was kept for 3 min, the temperature was increased at a rate of 25 °C/min over a period of 10.4 min until 300 °C was reached and kept for 5 min.

Mass spectrometry

The mass spectrometric measurements were performed at the Central Analytical Laboratory of the University of Regensburg. All mass spectra were recorded on a Finnigan MAT 95, ThermoQuest Finnigan TSQ 7000, Finnigan MAT SSQ 710 A or an Agilent Q-TOF 6540 UHD instrument.

Thin layer chromatography

Analytical TLC was performed on silica gel coated alumina plates (MN TLC sheets ALUGRAM® Xtra SIL G/UV254). Visualization was done by UV light (254 or 366 nm). If necessary, potassium permanganate was used for chemical staining.

Automated flash column chromatography

Purification by column chromatography was performed with silica gel 60 M (40–63 μm , 230–440 mesh, Merck) on a Biotage® Isolera™ Spektra One device.

UV-VIS / fluorescence spectroscopy

Absorption spectra were measured on an Agilent Cary 100 UV/VIS spectrometer in a quartz cuvette at 25.0 °C. Fluorescence spectra were measured on a Horiba Scientific Fluoromax-4 spectrometer at room temperature in a quartz cuvette.

Cyclic voltammetry measurements

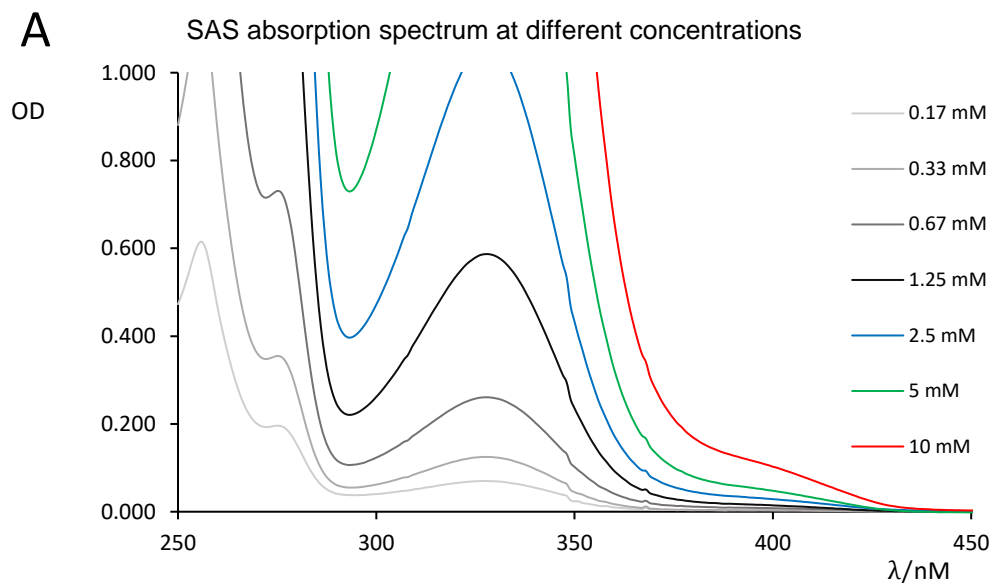
CV measurements were performed with the three-electrode potentiostat galvanostat PGSTAT302N from Metrohm Autolab using a glassy carbon working electrode, a platinum wire counter electrode, a silver wire as a reference electrode and tetrabutylammonium tetrafluoroborate (TBATFB) 0.1 M as supporting electrolyte. The potentials are given relative to the Fc/Fc⁺ redox couple with ferrocene as internal standard. The control of the measurement instrument, the acquisition and processing of the cyclic voltammetric data were performed with the software Metrohm Autolab NOVA 1.10.4. The measurements were carried out as follows: a 0.1 M solution of TBATFB in acetonitrile was added to the measuring cell and the solution was degassed by argon purge for 5 min. After recording the baseline, the electroactive compound was added (0.01 M) and the solution was again degassed by a stream of argon for 5 min. The cyclic voltammogram was recorded with one to three scans. Afterwards ferrocene (2.20 mg, 12.0 μmol) was added to the solution which was again degassed by argon purge for 5 min and the final measurement was performed with three scans.

General Procedure for the photocatalytic bromination

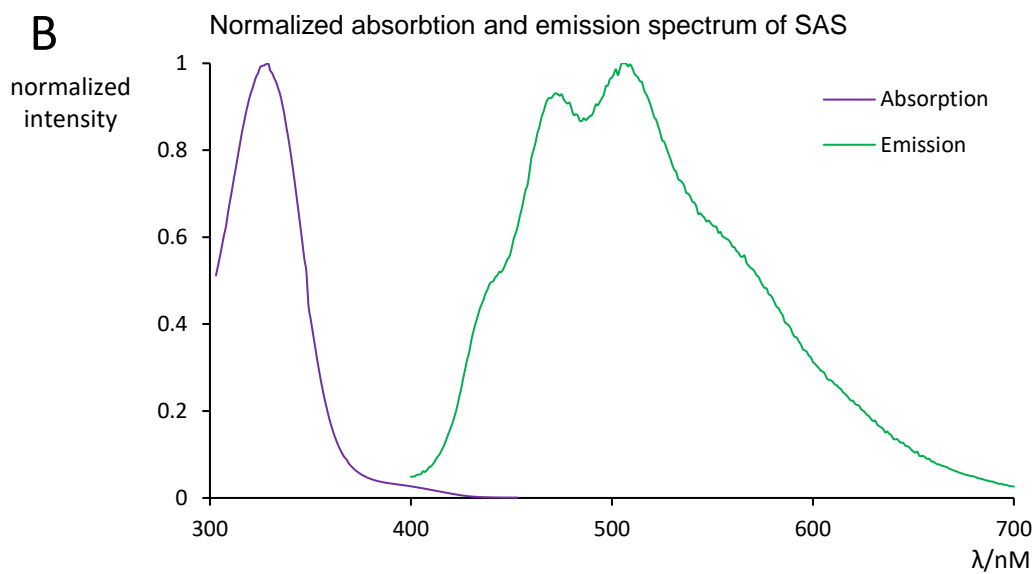
Sodium anthraquinone sulfonate (1.6 mg, 0.005 mmol, 0.05 equiv.), NaBr (20.6 mg, 0.2 mmol, 2 equiv.) and the substrate (0.1 mmol) were weight into a 5 mL crimp cap vial. A stirring bar and 1 mL of a mixture of MeCN and H₂O 1:1 were added and the vial was sealed with a crimp cap with septum under air atmosphere. Trifluoroacetic acid (15.4 μL , 0.2 mmol, 2 equiv.) was added *via* syringe through the septum and the vial was shaken briefly. The vial was placed approximately 2 cm above a 455 nm or 400 nm LED and stirred under irradiation for 4 h. After completion of the reaction, the reaction mixture was poured into a 50 mL round bottom flask and diluted with DCM. Silica was added, the solvent was evaporated from the suspension and the residue was used as dry load for column chromatography on a Biotage® Isolera™ Spektra One using a petrol ether and ethyl acetate (and/or methanol) mixture as the mobile phase. For compounds containing a free amine or a carboxylic acid functional group 1% v/v triethylamine or trifluoroacetic acid were added to the ethyl acetate. A 10 g column was employed with silica gel of type 60 M (40-63 μm , 230-440 mesh) by Merck as stationary phase.

2.4.2 Mechanistic Investigations

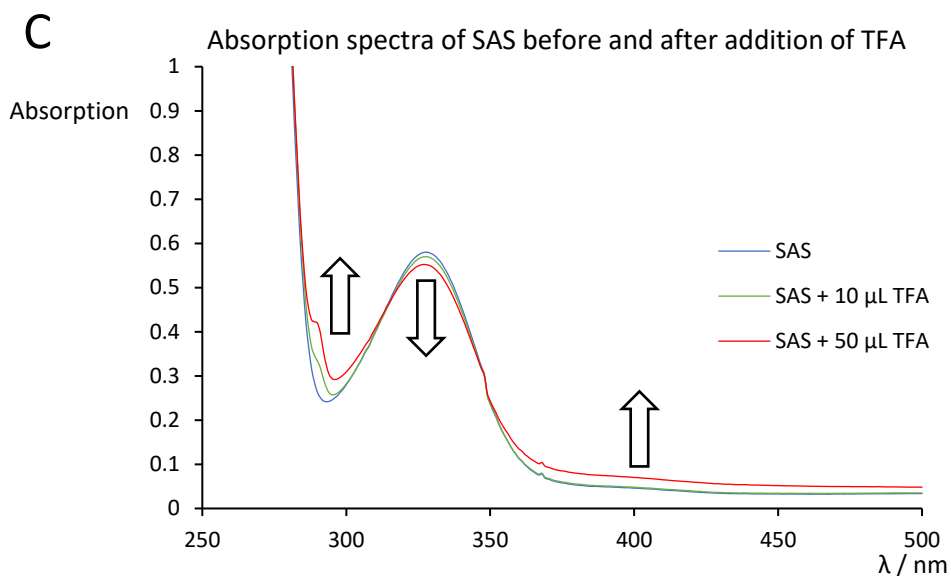
Catalyst absorption and LED Emission Spectra



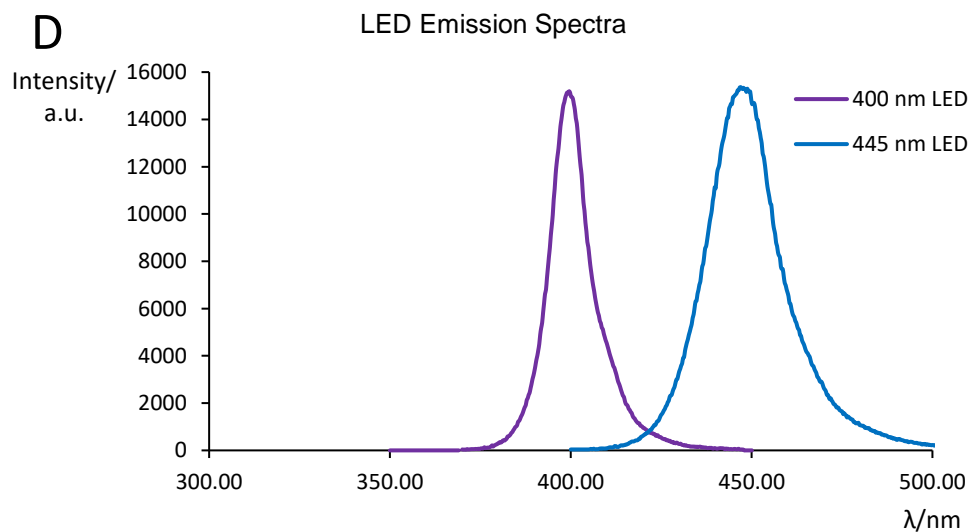
A: Absorption spectra of different concentrations of SAS in MeCN H₂O 1:1 detected at 25.0 °C in a 10x0.1 mm quartz cuvette.



B: Normalized absorption and emission spectrum of SAS in MeCN H₂O 1:1 detected at 25.0 °C in a 10x10 mm quartz cuvette.



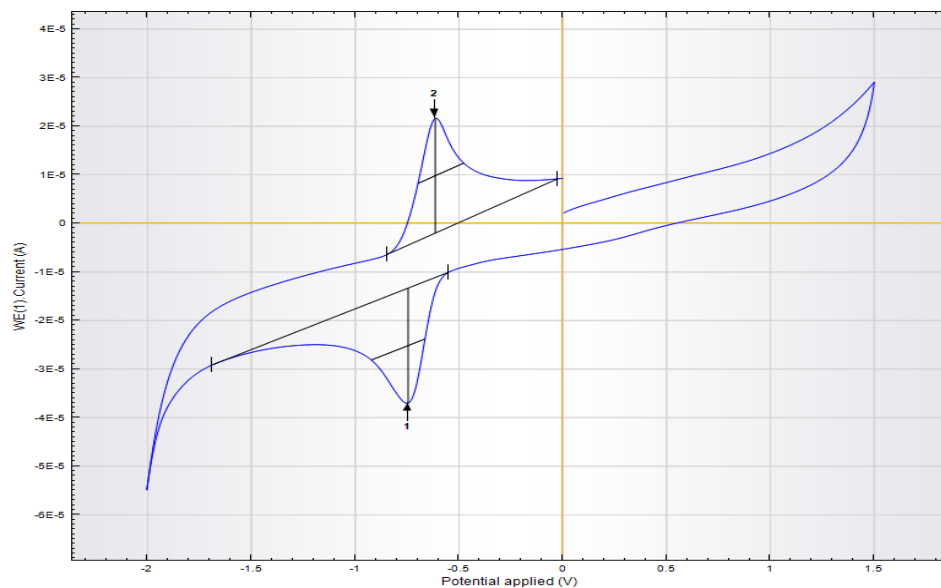
C: Absorption spectrum of SAS in MeCN H₂O 1:1 before and after addition of different amounts of TFA detected at 25.0 °C in a 10x0.1 mm quartz cuvette. Addition of TFA leads to a minor increase of the absorption at ~400 nm and 300 nm however the absorption maximum at 350 nm decreases. The change of the absorption spectrum might indicate a ground state interaction between SAS and TFA.



D: Emission spectra of the employed LEDs recorded by an OceanOptics HR4000CG-UV-NIR spectrometer. In combination, the spectra explain, why the initial reaction of anisole proceeded slowly at 445 nm irradiation considering the broad emission peak of the LED. The type of the 400 nm LED was “Ultraviolet Edixeon” by “Edison Opto Corporation” with an irradiation intensity of about 20 mW/cm² and the type of the 445 nm LED was “OSLON SLL LD CQ7P” by “Osram Opto Semiconductors” with an irradiation intensity of about 80 mW/cm².

Cyclo Voltammetry of SAS

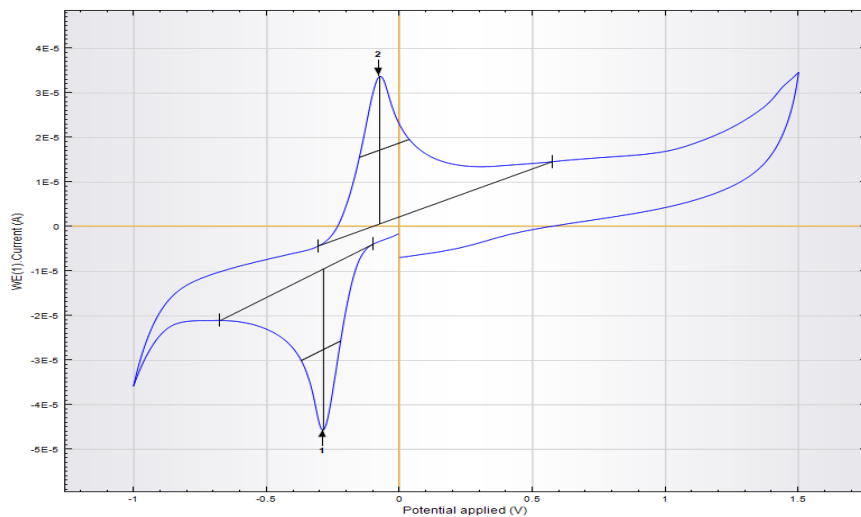
Pure SAS



Index Peak position

1	-0.750 V
2	-0.612 V

SAS with 40 equiv. TFA

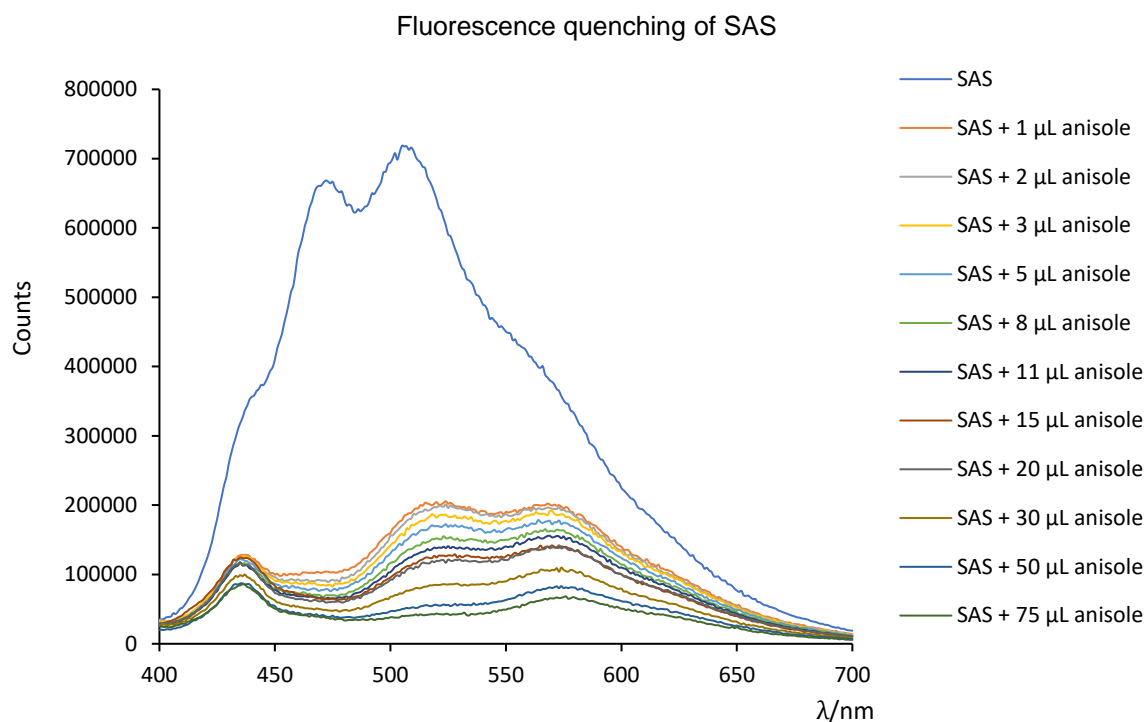


Index Peak position

1	-0.287 V
2	-0.075 V

Comparison of the potentials of SAS with and without TFA indicates a significant difference of 0.5 V. Explaining the increased excited state oxidation potential. Values were determined against ferrocene (not shown) and then calculated against SCE.^[21]

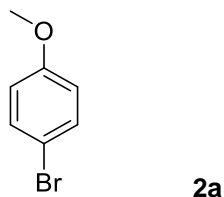
Fluorescence quenching of SAS with anisole



Stern-Volmer quenching was performed with 1.6 mg (5 μmol) sodium anthraquinone sulfonate (SAS) in 3 mL MeCN H₂O 1:1 at 25 °C in a 10x10 mm quartz cuvette. The indicated amounts of anisole were added stepwise *via* syringe. The fluorescence count at 527 nm was used for the creation of the Stern-Volmer Plot because it showed the highest intensity after addition of the first μL of anisole. The energy of this wavelength (2.35 eV) was used to estimate the excited state oxidation potential of the catalyst according to the Rehm-Weller equation.^[6]

2.5 Product Characterizations

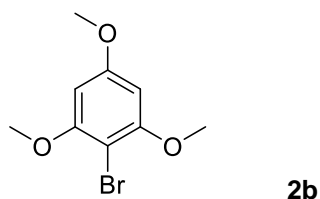
1-Bromo-4-methoxybenzene^[22]



GC-Yield: 100%.

LR-MS (EI): (M)⁺: calc.: 185.9680, found: 185.9672. **MF:** C₇H₇BrO. **MW:** 187.04 g/mol.

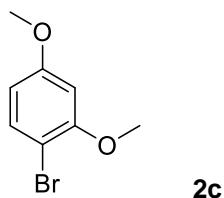
2-Bromo-1,3,5-trimethoxybenzene^[23]



Yield: 20.0 mg, 0.081 mmol, 81%, colorless liquid.

¹H NMR (400 MHz, DMSO-d₆); δ 6.33 (s, 2H); 3.81 (s, 6H); 3.79 (s, 3H). **¹³C NMR** (101 MHz; DMSO-d₆); δ 160.3; 156.9; 92.0; 90.6; 56.3; 55.5. **LR-MS (EI):** (M)⁺: calc.: 245.9892, found: 245.9909. **MF:** C₈H₁₁BrO₃. **MW:** 247.09 g/mol.

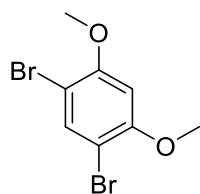
1-Bromo-2,4-dimethoxybenzene^[24]



Yield: 18.5 mg, 0.085 mmol, 85%, colorless oil.

¹H NMR (400 MHz, DMSO-d₆); δ 7.46-7.40 (d, *J* = 8.7 Hz, 1H); 6.68-6.64 (d, *J* = 2.9 Hz, 1H); 6.53-6.46 (dd, *J* = 11.4 Hz, 2.7 Hz, 1H); 3.82 (s, 3H); 3.76 (s, 3H). **¹³C NMR** (101 MHz; DMSO-d₆); δ 160.1; 156.1; 132.8; 106.7; 101.2; 100.0; 56.1; 55.5. **LR-MS (EI):** (M)⁺: calc.: 215.9786, found: 216.080. **MF:** C₈H₉BrO₂. **MW:** 217.06 g/mol.

1,5-Dibromo-2,4-dimethoxybenzene^[25]



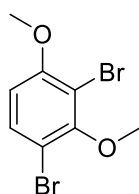
2d

Yield: 25.4 mg, 0.086 mmol, 86%, white solid.

¹H NMR (400 MHz, CDCl₃); δ 7.65 (s, 1H); 6.48 (s, 1H); 3.90 (s, 3H) **¹³C NMR** (101 MHz; CDCl₃); δ 156.3; 136.0; 102.5; 97.5; 56.7. **LR-MS (EI):** (M)⁺: calc.: 295.8871, found: 295.8951. **MF:** C₈H₈Br₂O₂. **MW:** 217.06 g/mol.

Reaction conditions: An O₂ balloon was used in addition to the air in the vial.

1,3-Dibromo-2,4-dimethoxybenzene^[26]

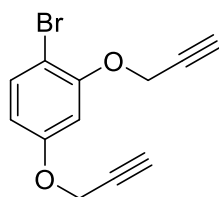


2e

Yield: 20.7 mg, 0.07 mmol, 70%, white solid.

¹H NMR (300 MHz, CDCl₃); δ 7.48-7.40 (d, *J* = 9.3 Hz, 2H); 6.63-6.57 (d, *J* = 9.3 Hz, 2H); 3.88 (s, 3H). **¹³C NMR** (75 MHz; CDCl₃); δ 156.9; 155.2; 131.8; 108.9; 108.8; 108.5; 60.7; 56.8. **LR-MS (EI):** (M)⁺: calc.: 295.8871, found: 295.8891. **MF:** C₈H₈Br₂O₂. **MW:** 295.96 g/mol.

1-Bromo-2,4-bis(prop-2-yn-1-yloxy)benzene

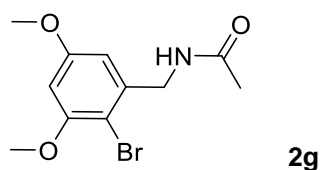


2f

Yield: 14.8 mg, 0.056 mmol, 56%, yellowish oil.

¹H NMR (400 MHz, CDCl₃); δ 7.47-7.42 (d, *J* = 8.8 Hz, 1H); 6.76-6.72 (d, *J* = 2.7 Hz, 1H); 6.56-6.51 (dd, *J* = 11.5, 2.9 Hz, 1H); 4.76-4.74 (d, *J* = 2.5 Hz, 2H); 4.69-4.67 (d, *J* = 2.5 Hz, 2H); 2.58-2.52 (m, 2H). **¹³C NMR** (101 MHz; CDCl₃); δ 158.0; 154.8; 133.5; 108.4; 104.2; 102.9; 78.2; 77.9; 76.5; 76.1; 57.0; 56.3. **HR-MS (EI):** (M+H)⁺: calc.: 264.9859, found: 264.9860. **MF:** C₁₂H₉BrO₂. **MW:** 265.11 g/mol.

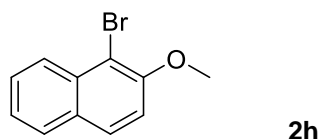
***N*-(2-Bromo-3,5-dimethoxybenzyl)acetamide**



Yield: 25.7 mg, 0.089 mmol, 89%, yellowish solid.

¹H NMR (400 MHz, CDCl₃); δ 6.58-6.54 (d, *J* = 2.8 Hz 1H); 6.42-6.39 (d, *J* = 2.8 Hz 1H); 6.07 (brs, 1H); 4.49-4.44 (d, *J* = 6.1 Hz 2H); 3.85 (s, 3H); 3.78 (s, 3H); 2.00 (s, 3H). **¹³C NMR** (101 MHz; CDCl₃); δ 170.1; 160.0; 156.9; 139.3; 106.8; 104.1; 99.1; 56.5; 55.7; 44.4; 23.4. **LR-MS (ESI):** (M+H)⁺: calc.: 288.0230, found: 288.0219. **MF:** C₁₁H₁₄BrNO₃. **MW:** 288.14 g/mol.

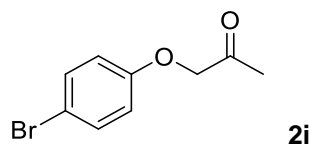
1-Bromo-2-methoxynaphthalene^[27]



Yield: 16.8 mg, 0.071 mmol, 71%, white solid.

¹H NMR (400 MHz, DMSO-d₆); δ 8.11-8.05 (d, *J* = 8.4 Hz 1H); 8.04-7.98 (d, *J* = 9.1 Hz 1H); 7.97-7.91 (d, *J* = 8.4 Hz 1H); 7.66-7.59 (m, 1H); 7.56-7.51 (d, *J* = 9.1 Hz, 1H); 7.48-7.42 (m, 1H); 3.99 (s, 3H). **¹³C NMR** (101 MHz; DMSO-d₆); δ 153.6; 132.2; 129.4; 129.3; 128.3; 128.1; 125.1; 124.3; 114.3; 106.9; 56.9. **LR-MS (EI):** (M)⁺: calc.: 235.9837, found: 236.0177. **MF:** C₁₁H₉BrO. **MW:** 237.10 g/mol.

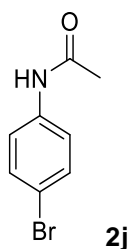
1-(4-Bromophenoxy)propan-2-one



Yield: 17.4 mg, 0.076 mmol, 76%, white solid.

¹H NMR (400 MHz, CDCl₃); δ 7.42-7.37 (m, 2H); 6.80-6.74 (m, 2H); 4.51 (s, 2H); 2.27 (s, 3H). **¹³C NMR** (101 MHz; CDCl₃); δ 205.1; 156.9; 132.7; 116.5; 114.2; 73.2; 26.7. **LR-MS (EI):** (M)⁺: calc.: 227.9786, found: 227.9781. **MF:** C₉H₉BrO₂. **MW:** 229.07 g/mol.

***N*-(4-Bromophenyl)acetamide^[28]**

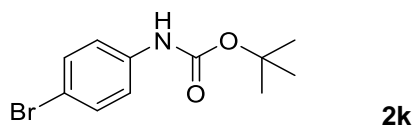


Yield: 19.4 mg, 0.091 mmol, 91%, white solid.

¹H NMR (400 MHz, CDCl₃); δ 7.41 (brs, 4H); 2.13 (s, 3H). **¹³C NMR** (101 MHz; CDCl₃); δ 168.5; 137.1; 132.1; 121.5; 117.0; 24.7. **LR-MS (EI):** (M)⁺: calc.: 212.9789, found: 212.9773.

MF: C₈H₈BrNO. **MW:** 214.06 g/mol.

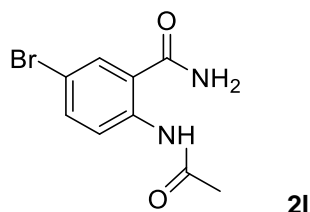
***tert*-Butyl (4-bromophenyl)carbamate^[29]**



Yield: 19.8 mg, 0.073 mmol, 73%, white solid.

¹H NMR (400 MHz, CDCl₃); δ 7.41-7.33 (m, 2H); 7.31-7.22 (m, 2H); 6.51 (brs, 1H); 1.51 (s, 9H). **¹³C NMR** (101 MHz; CDCl₃); δ 152.6; 137.6; 132.0; 120.2; 115.5; 81.0; 28.4. **LR-MS (ESI):** (M+Na)⁺: calc.: 294.0100, found: 294.0102. **MF:** C₁₁H₁₄BrNO₂. **MW:** 272.14 g/mol.

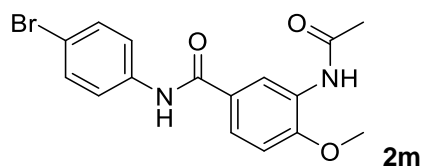
2-Acetamide-5-bromobenzamide^[30]



Yield: 6.5 mg, 0.007 mmol, 25%, yellowish solid.

¹H NMR (400 MHz, CDCl₃); δ 11.21 (s, 1H); 8.53-8.44 (d, *J* = 8.9 Hz, 1H); 7.86-7.81 (d, *J* = 2.6 Hz, 1H) (s, 4H); 7.63-7.57 (dd, *J* = 11.2 Hz, 2.4 Hz, 1H); 6.98 (brs, 1H); 6.30 (brs, 1H); 2.09 (s, 3H). **¹³C NMR** (101 MHz; CDCl₃); δ 170.8; 169.8; 140.4; 136.1; 131.9; 123.2; 121.9; 111.0; 25.4. **LR-MS (ESI):** (M+H)⁺: calc.: 256.9920, found: 256.9920. **MF:** C₉H₉BrN₂O₂. **MW:** 257.09 g/mol.

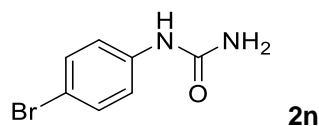
3-Acetamido-N-(4-bromophenyl)-4-methoxybenzamide



Yield: 31.6 mg, 0.087 mmol, 87%, yellowish solid.

¹H NMR (400 MHz, CDCl₃); δ 10.22 (s, 1H); 9.31 (s, 1H); 8.50 (s, 1H); 7.78-7.72 (m, 3H); 7.55-7.49 (m, 2H); 7.18-7.13 (d, *J* = 9.1 Hz, 1H); 3.91 (s, 3H); 2.11 (s, 3H). **¹³C NMR** (101 MHz; CDCl₃); δ 168.7; 165.2; 152.5; 138.8; 131.4; 127.1; 126.5; 124.3; 122.2; 120.3; 115.1; 110.5; 56.0; 23.8. **HR-MS (ESI):** (M+H)⁺: calc.: 363.0339, found: 363.0340. **MF:** C₁₆H₁₅BrN₂O₃. **MW:** 363.21 g/mol.

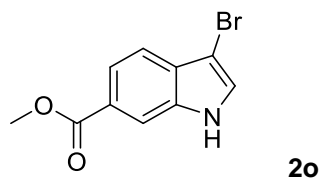
1-(4-Bromophenyl)urea^[31]



Yield: 20.0 mg, 0.093 mmol, 93%, white solid.

¹H NMR (400 MHz, DMSO-d₆); δ 8.67 (s, 1H); 7.37 (s, 4H); 5.91 (s, 2H). **¹³C NMR** (101 MHz; DMSO-d₆); δ 155.8; 140.0; 131.3; 119.6; 112.3. **LR-MS (ESI):** (M+H)⁺: calc.: 214.9815, found: 214.9813. **MF:** C₇H₇BrN₂O. **MW:** 215.05 g/mol.

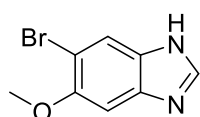
Methyl-3-bromo-1H-indole-6-carboxylate



Yield: 16.1 mg, 0.063 mmol, 63%, yellowish oil.

¹H NMR (400 MHz, CDCl₃); δ 11.88 (brs, 1H); 8.09 (s, 1H); 7.84-7.80 (d, *J* = 2.7 Hz, 1H); 7.74-7.70 (m, 1H); 7.53-7.49 (d, *J* = 8.3 Hz, 1H); 3.86 (s, 3H). **¹³C NMR** (101 MHz; CDCl₃); δ 166.9; 134.6; 129.5; 128.8; 123.3; 120.4; 118.0; 114.1; 89.0; 52.0. **HR-MS (EI):** (M)⁺: calc.: 252.9738, found: 252.9737. **MF:** C₁₀H₈BrNO₂. **MW:** 254.08 g/mol.

6-Bromo-5-methoxy-1H-benzo[d]imidazole



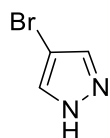
2p

Yield: 11.1 mg, 0.049 mmol, 49%, yellowish solid.

¹H NMR (400 MHz, DMSO-d₆); δ 9.15 (brs, 1H); 8.36 (s, 1H); 7.60-7.54 (d, *J* = 8.8 Hz, 1H); 7.13-7.08 (d, *J* = 8.8 Hz, 1H); 3.88 (s, 3H). **¹³C NMR** (101 MHz; DMSO-d₆); δ 151.3; 143.4; 142.3; 138.2; 118.5; 110.8; 109.6; 57.3. **HR-MS (EI):** (M)⁺: calc.: 225.9742, found: 225.9740. **MF:** C₈H₇BrN₂O. **MW:** 227.06 g/mol.

Reaction conditions: An O₂ balloon was used in addition to the air in the vial.

4-Bromo-1H-pyrazole^[32]



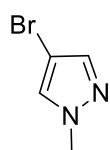
2q

NMR-Yield: 83%.

¹H NMR (400 MHz, CD₃CN); δ 7.65 (s, 2H). **HR-MS (ESI):** (M+H)⁺: calc.: 146.9552, found: 146.9553. **MF:** C₃H₃BrN₂. **MW:** 146.98 g/mol.

Reaction conditions: The sample was prepared and reacted according to the general procedure but a mixture of CD₃CN D₂O 1:1 was used as a solvent. After 4 h of irradiation the vial was opened and 9.5 mg dimethyl sulfone as internal standard for H-NMR were added. The mixture was then transferred into an NMR tube and quantitated with respect to the H-atom integrals.

4-Bromo-1-methyl-1H-pyrazole^[33]



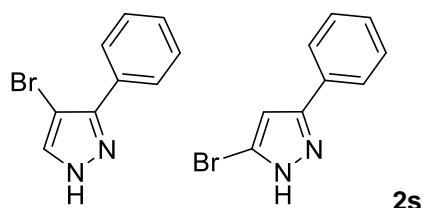
2r

NMR-Yield: 88%.

¹H NMR (400 MHz, CD₃CN); δ 7.57 (s, 1H); 7.39 (s, 1H); 3.76 (s, 3H). **HR-MS (ESI):** (M+H)⁺: calc.: 160.9709, found: 160.9708. **MF:** C₄H₅BrN₂. **MW:** 161.00 g/mol.

Reaction conditions: The sample was prepared and reacted according to the general procedure but a mixture of CD₃CN D₂O 1:1 was used as a solvent. After 4 h of irradiation the vial was opened and 10.0 mg dimethyl sulfone as internal standard for H-NMR were added. The mixture was then transferred into an NMR tube and quantitated with respect to the H-atom integrals.

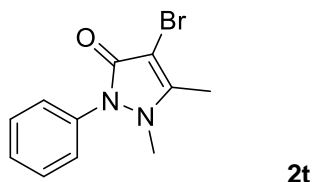
4-Bromo-3-phenyl-1H-pyrazole / 5-bromo-3-phenyl-1H-pyrazole^[34]



Yield: 21.6 mg, 0.097 mmol, 97%, yellowish solid.

¹H NMR (400 MHz, DMSO-d₆); δ 13.58 (s, 0.4H); 13.36 (s, 0.6H); 8.09 (s, 0.6H); 7.87-7.66 (m, 2.4H); 7.56-7.35 (m, 3H). **¹³C NMR** (101 MHz; DMSO-d₆); δ 147.0; 141.0; 132.3; 131.2; 128.9; 127.9; 127.1; 90.4. **LR-MS (EI):** (M)⁺⁺: calc.: 221.9793, found: 221.9958. **MF:** C₉H₇BrN₂. **MW:** 223.07 g/mol.

4-Bromo-1,5-dimethyl-2-phenyl-1,2-dihydro-3H-pyrazol-3-one^[35]

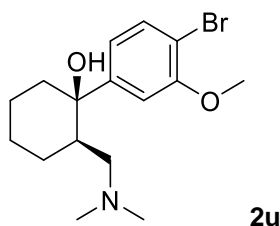


Yield: 19.4 mg, 0.041 mmol, 41%, yellowish solid.

¹H NMR (400 MHz, CD₃CN); δ 7.53-7.47 (m, 2H); 7.39-7.32 (m, 3H); 3.09 (s, 3H); 2.28 (s, 3H). **¹³C NMR** (101 MHz; CD₃CN); δ 163.1; 155.7; 136.2; 130.1; 128.1; 126.6; 88.8; 36.7; 12.7. **HR-MS (EI):** (M)⁺⁺: calc.: 266.0055, found: 266.0054. **MF:** C₈H₇BrN₂O. **MW:** 267.13 g/mol.

Reaction conditions: An O₂ balloon was used in addition to the air in the vial.

(1R, 2R)-1-(4-Bromo-3-methoxyphenyl)-2-((dimethylamino)methyl)cyclohexan-1-ol

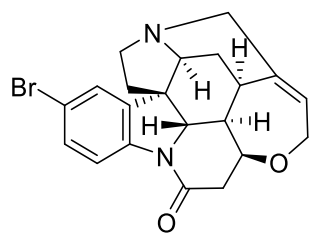


Yield: 25.2 mg, 0.074 mmol, 74% yellowish oil.

¹H NMR (400 MHz, DMSO-d₆); δ 7.48-7.41 (d, J = 8.4 Hz, 1H); 7.22-7.16 (m, 1H); 7.01-6.95 (m, 1H); 5.04 (brs, 1H); 3.83 (s, 3H); 2.14-2.07 (m, 1H); 1.95-1.87 (m, 6H); 1.86-1.21 (m, 10H). **¹³C NMR** (101 MHz; DMSO-d₆); δ 156.5; 153.0; 133.3; 119.6; 110.6; 109.0; 77.3; 62.1; 56.8; 47.5; 44.8; 42.1; 28.3; 27.1; 23.0. **HR-MS (ESI):** (M+H)⁺: calc.: 342.1063, found: 342.1062. **MF:** C₁₆H₂₄BrNO₂. **MW:** 342.28 g/mol.

Reaction conditions: An O₂ balloon was used in addition to the air in the vial. 4 equiv. of TFA were used to keep the tertiary amine protonated to prevent it from transferring an electron to the excited photocatalyst.

(4aR,4a1R,5aS,8aR,8a1S,15aS)-10-Bromo-2,4a,4a1,5,5a,7,8,8a1,15,15a-decahydro-14H-4,6-methanoindolo[3,2,1-ij]oxepino[2,3,4-de]pyrrolo[2,3-h]quinolin-14-one



2v

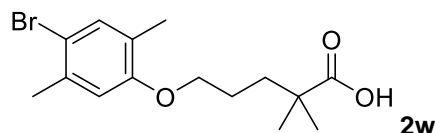
Yield: 13.5 mg, 0.035 mmol, 35% yellowish solid.

¹H NMR (400 MHz, CDCl₃); δ 8.00-7.93 (d, *J* = 8.7 Hz, 1H); 7.38-7.32 (dd, *J* = 6.6 Hz, 2.1 Hz, 1H); 7.25-7.23 (m, 1H); 5.96-5.87 (m, 1H); 4.31-4.25 (dt, *J* = 3.2 Hz, *J* = 8.5 Hz, 1H); 4.19-4.00 (m, 2H) 3.93-3.83 (m, 2H); 3.75-3.66 (m, 1H); 3.28-3.19 (m, 1H); 3.18-3.07 (m, 2H); 2.93-2.82 (m, 1H); 2.77-2.70 (d, *J* = 15.0 Hz, 1H); 2.69-2.60 (dd, *J* = 3.2 Hz; 14.2 Hz; 1H); 2.41-2.32 (dt, *J* = 4.4 Hz; 14.4 Hz, 1H); 1.94-1.84 (m, 2H); 1.50-1.42 (d, *J* = 14.6 Hz, 1H); 1.29-1.25 (m, 1H). **¹³C NMR** (101 MHz; CDCl₃); δ 169.5; 141.4; 140.0; 135.1; 131.7; 128.0; 125.7; 117.8; 116.7; 77.6; 64.7; 60.5; 60.4; 52.7; 52.0; 50.4; 48.2; 42.8; 42.5; 31.6; 26.9. **HR-MS (ESI):** (M+H)⁺: calc.: 413.0859, found: 413.0863.

MF: C₂₁H₂₁BrN₂O₂. **MW:** 413.32 g/mol.

Reaction conditions 4 equiv. of TFA were used to keep the tertiary amine protonated to prevent it from transferring an electron to the excited photocatalyst.

5-(4-Bromo-2,5-dimethylphenoxy)-2,2-dimethylpentanoic acid

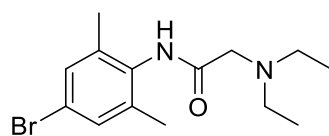


2w

Yield: 10.1 mg, 0.031 mmol, 31%, yellowish solid.

¹H NMR (400 MHz, DMSO-d₆); δ 12.13 (brs, 1H); 7.30 (s, 1H); 6.90 (s, 1H); 3.96-3.86 (m, 2H); 2.28 (s, 3H); 2.09 (s, 3H); 1.70-1.56 (m, 4H); 1.11 (s, 6H). **¹³C NMR** (101 MHz; DMSO-d₆); δ 178.7; 156.0; 135.2; 133.0; 125.8 114.1; 113.7; 68.0; 41.0; 36.5; 25.0; 24.7; 22.4; 15.1. **HR-MS (-ESI):** (M-H)⁻: calc.: 327.0601, found: 327.0603. **MF:** C₁₅H₂₁BrO₃. **MW:** 329.23 g/mol.

N-(4-Bromo-2,6-dimethylphenyl)-2-(diethylamino)acetamide



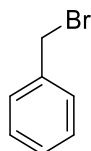
2x

Yield: 11.3 mg, 0.036 mmol, 36%, yellowish oil.

¹H NMR (300 MHz, DMSO-d₆); δ 9.25 (brs, 1H); 7.29 (s, 2H); 3.22-3.15 (m, 2H); 2.69-2.58 (m, 4H); 2.13 (s, 6H); 1.11-1.03 (m, 6H). **¹³C NMR** (75 MHz; DMSO-d₆); δ 169.5; 138.0; 134.8; 130.0; 118.9; 56.6; 48.1; 17.9; 12.0. **HR-MS (ESI):** (M+H)⁺: calc.: 313.0910, found: 313.0916. **MF:** C₁₄H₂₁BrN₂O. **MW:** 313.24 g/mol.

Reaction conditions 4 equiv. of TFA were used to keep the tertiary amine protonated to prevent it from transferring an electron to the excited photocatalyst.

Bromomethyl-benzene^[36]



2ac

NMR-Yield: 70%.

¹H NMR (400 MHz, CD₃CN); δ 4.50 (s, 2H). **LR-MS (EI):** (M)⁺: calc.: 169.9731, found: 169.9736. **MF:** C₇H₇Br. **MW:** 171.04 g/mol.

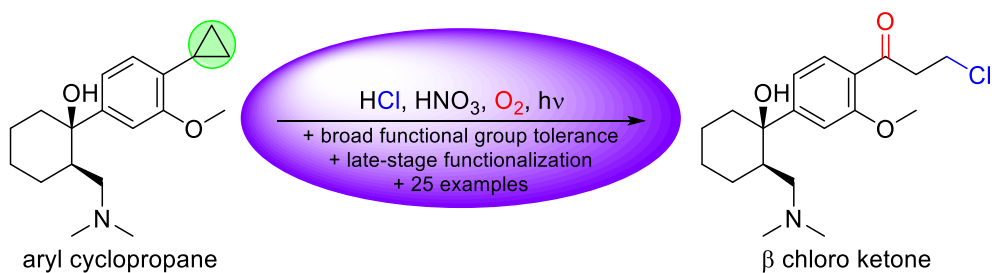
Reaction conditions: The sample was prepared and reacted according to the general procedure but a mixture of CD₃CN D₂O 1:1 was used as a solvent and 54 mg (0.2 mmol, 2 equiv.) K₂S₂O₈ were added. Then the reaction mixture was degassed by three consecutive freeze-pump-thaw cycles using dry nitrogen as inert gas. After 4 h of irradiation the vial was opened and 9.9 mg dimethyl sulfone as internal standard for H-NMR were added. The mixture was then transferred into an NMR tube and quantitated with respect to the H-atom integrals.

2.6 References

- [1] a) N. A. Romero, D. A. Nicewicz, *Chem. Rev.* **2016**, 116, 10075-10166; b) C. K. Prier, D. A. Rankic, D. W. C. MacMillan, *Chem. Rev.* **2013**, 113, 5322-5363; c) J. P. Goddard, C. Ollivier, L. Fensterbank, *Acc. Chem. Res.* **2016**, 49, 1924-1936.
- [2] N. Hoffmann, *Eur. J. Org. Chem.* **2017**, 1982-1992.
- [3] N. A. Romero, K. A. Margrey, N. E. Tay, D. A. Nicewicz, *Science* **2015**, 349, 1326-1330.
- [4] a) K. Ohkubo, K. Mizushima, R. Iwataa, S. Fukuzumi, *Chem. Sci.* **2011**, 2, 715-722; b) R. Li; Z. J. Wang, L. Wang, B. C. Ma, S. Ghasimi, H. Lu, K. Landfester, K. A. I. Zhang, *ACS Catal.* **2016**, 6, 1113-1221.
- [5] H. G. Roth, N. A. Romero, D. A. Nicewicz, *Synlett* **2016**, 27, 714-723.
- [6] D. Rehm, A. Weller, *Isr. J. Chem.* **1970**, 8, 259-271.
- [7] O. Stern, M. Volmer, *Phys. Z.* **1919**, 20, 183-188.
- [8] a) P. Ruiz-Castillo, S. L. Buchwald, *Chem. Rev.* **2016**, 116, 12564-12649; b) N. Miyaura, A. Suzuki, *Chem. Rev.* **1995**, 95, 2475-2483.
- [9] L. Niu, H. Yi, S. Wang, T. Liu, J. Liu, A. Lei, *Nat. Commun.* **2017**, 8:14226, DOI:10.1038/ncomms14226.
- [10] W. Zhang, J. Gacs, I. W. C. E. Arends, F. Hollmann, *ChemCatChem* **2017**, 9, 3821-3826.
- [11] M. H. V. Huynh, T. J. Meyer, *Chem. Rev.* **2007**, 107, 5004-5064.
- [12] S. A. Carlson, D. M. Hercules, *J. Am. Chem. Soc.* **1971**, 93, 5611-5616.
- [13] K. Ohkubo, A. Fujimoto, S. Fukuzumi, *J. Am. Chem. Soc.* **2013**, 135, 5368-5371.
- [14] a) J. Najbar, M. Mac, *J. Chem. Soc. Farad. Trans.* **1991**, 87, 1523-1529; b) M. Rae, F. Perez-Balderas, C. Baleizao, A. Fedorov, J. A. S. Cavaleiro, A. C. Tomé, M. N. Berberan-Santos, *J. Phys. Chem. B* **2006**, 110, 12809-12814.
- [15] Addition of more 1,3 DMB lead to phase separation of the MeCN H₂O mixture.
- [16] Pre-orientation and spatial proximity of substrate and catalyst, e.g. like in enzymes or other templated reactions, is known to be a prerequisite for selectivity. See also: a) J. Svoboda, B. König, *Chem. Rev.* **2006**; 106; 5413-5430; b) S. Poplata, A. Tröster, Y. Q. Zou, T. Bach, *Chem. Rev.* **2016**; 116; 9748-9815.
- [17] The presence of oxidants, potentially H₂O₂, in the reaction mixture after the reaction was completed has been confirmed by a commercially available KI-starch test.
- [18] a) A. Podgorsek, S. Stavber, M. Zupana, J. Iskraa, *Tetrahedron Lett.* **2006**, 47, 7245-7247; b) K. V. V. Krishna Mohan, N. Narender, P. Srinivasu, S. J. Kulkarni, K. V. Raghavan, *Synth. Commun.* **2004**, 34, 2143-2152.
- [19] A. Mohammad, H. A. Liebafsky, *J. Am. Chem. Soc.* **1934**, 56, 1680-1685.
- [20] a) G. R. Fulmer, A. J. M. Miller, N. H. Sherden, H. E. Gottlieb, A. Nudelman, B. M. Stoltz, J. E. Bercaw, K. I. Goldberg, *Organometallics* **2010**, 29, 2176-2179; b) V. Kotlyar., H. E. Gottlieb, A. Nudelman, *J. Org. Chem.* **1997**, 62, 7512-7515.
- [21] V. V. Pavlishchuk, A. W. Addison, *Inorg. Chim. Acta* **2000**, 298, 97-102.
- [22] C. D. Braddock, G. Cansell, S. A. Hermitage, *Synlett* **2004**, 3, 461-464.
- [23] S. Kawamorita, H. Ohmiya, T. Iwai, M. Sawamura, *Angew. Chem. Int. Ed.* **2011**, 50, 8363-8366.

- [24] P. Wawrzyniak, M. K. Kindermann, J. W. Heinicke, P. G. Jones, *Eur. J. Org. Chem.* **2011**, 3, 593-606.
- [25] N. Kishi, Z. Li, K. Yoza, M. Akita, M. Yoshizawa, *J. Am. Chem. Soc.* **2011**, 133, 11438-11441.
- [26] M. Sauer, C. Yeung, J. H. Chong, B. O. Patrick, M. J. MacLachlan, *J. Org. Chem.* **2006**, 71, 775-788.
- [27] L. S. de Almeida, P. M. Esteves, M. C. S. de Mattos, *Synthesis* **2006**, 221-223.
- [28] J.-M. Chretien, F. Zammattio, E. Le Grogneq, M. Paris, B. Cahingt, G. Montavon, J.-P. Quintard, *J. Org. Chem* **2005**, 70, 2870-2873.
- [29] F. Jahani, M. Tajbakhsh, H. Golchoubian, S. Khaksar, *Tetrahedron Lett.* **2011**, 52, 1260-1264.
- [30] A. V. Dolzhenko-Podchezertseva, L. M. Korkodinova, M. V. Vasilyuk, V. P. Kotegov, *Pharm. Chem. J.* **2002**, 36, 647-648.
- [31] S. P. Bew, R. A. Brimage, G. Hiatt-Gipson, S. V. Sharma, S. Thurston, *Org. Lett.* **2009**, 11, 2483-2486.
- [32] G. Li, R. Kakarla, S. W. Gerritz, *Tetrahedron Lett.* **2007**, 48, 4595-4599.
- [33] P. R. Mullens, *Tetrahedron Lett.* **2009**, 50, 6783-6786.
- [34] P. Cabildo, R. M. Claramunt, *Organ. Magnet. Res.* **1984**, 22, 603-607.
- [35] R. C. Mease, S. J. Gatley, A. M. Friedman, *J. Label. Compd. Rad.* **1991**, 29, 393-403.
- [36] J. M. Dougherty, M. Jimenez, P. R. Hanson, *Tetrahedron* **2005**, 61, 6218-6230.

3. Visible Light Mediated Synthesis of β Chloro Ketones from Aryl Cyclopropanes



We report the visible light mediated synthesis of β chloro ketones from aryl cyclopropanes, oxygen, hydrochloric acid and nitric acid. The operationally simple and catalyst free method uses cheap standard lab reagents and displays a broad functional group tolerance. Moreover, scale up of the reaction and late stage functionalization of bioactive compounds is possible, providing the opportunity to utilize the cyclopropane ring as a masked β chloro ketone in a reaction sequence. We propose a light-driven radical chain reaction initiated by the reaction of diluted hydrochloric and nitric acid producing small quantities of molecular chlorine. The mechanistic hypothesis is supported by ^{18}O labelling and UV-VIS experiments, cyclovoltammetry and several control reactions.

This chapter has been published in:

D. Petzold, P. Singh, F. Almqvist, B. König *Angew. Chem. Int. Ed.* **2019**, <https://doi.org/10.1002/ange.201902473>. (Communication) – Reproduced with permission from John Wiley and Sons.

Author Contributions:

DP discovered the reaction, performed the optimization, synthesized the scope, carried out all the mechanistic investigations and wrote the manuscript. PS contributed to the scope of the reaction. FA and BK supervised the project. BK is the corresponding author.

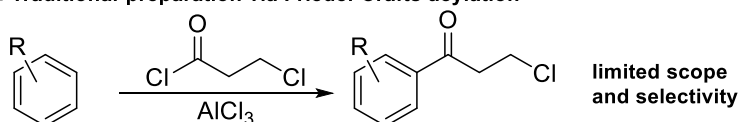
3.1 Introduction

The cyclopropane ring offers many synthetic opportunities in organic and total synthesis, medicinal chemistry and crop science due to its versatile reactivity originating from a high ring strain.^[1] Moreover, different activation modes are possible by thermal or catalytic methods depending on the ring substitution pattern.^[2] Since the cyclopropane ring reacts also well with radicals, it is especially useful in photocatalytic and photochemical reactions which often proceed *via* radical intermediates.^[3] This phenomenon was already exploited in the 1970s by the group of Hixson. They found that electron rich cyclopropyl arenes could be oxidized by excited 1,4-dicyanobenzene leading to ring opening *via* an anti Markownikow addition of methanol.^[4] The aryl cyclopropane radical cation was proposed as key intermediate and its formation could be confirmed in several studies.^[5] However, despite the intensive research on aryl cyclopropanes and their behavior in light driven reactions, the addition of a nucleophile and subsequent trapping of the benzylic radical by oxygen has not been reported yet.

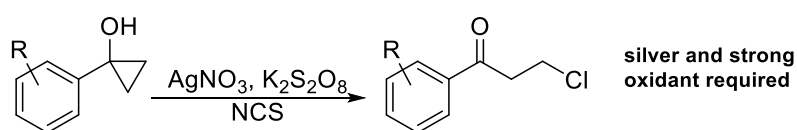
Therefore, we envisioned to develop a visible light mediated method for the synthesis of beta substituted ketones from aryl cyclopropanes. We focused on the preparation of β chloro ketones, which are useful building blocks for many chemical transformations e.g. the synthesis of heterocycles, cross coupling, alkylation reactions or chemical probes in bioassays.^[6] Thereby, the aryl cyclopropane could act as synthon in a reaction sequence over several steps for the much more reactive β chloro ketone. Traditionally, aromatic β chloro ketones are prepared *via* Friedel-Crafts acylation which suffers from a limited substrate scope and regioselectivity issues (Scheme 3-1).^[7] Moreover, Zhu and coworkers reported a ring-opening chlorination of prefunctionalized cyclopropanes which requires a silver salt as catalyst, a strong stoichiometric oxidant and NCS as a source for Cl radicals.^[8]

Previous work:

A. Traditional preparation via Friedel-Crafts acylation

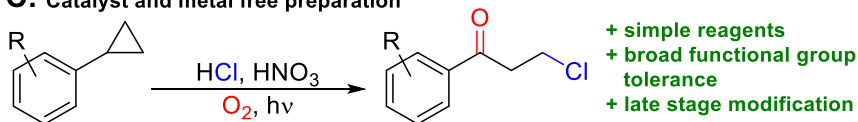


B. Silver mediated preparation



This work:

C. Catalyst and metal free preparation



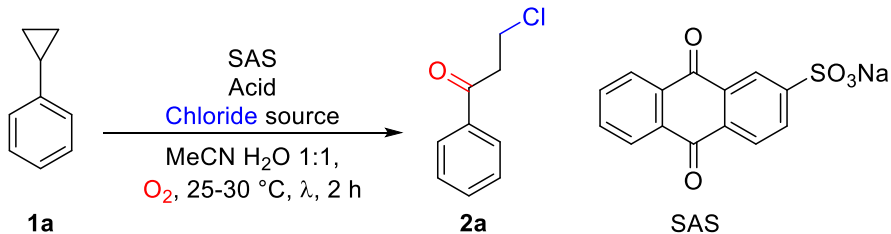
Scheme 3-1. Overview of preparation methods for chlorinated ketones. **A:** Traditional preparation *via* Friedel-Crafts acylation. **B:** Silver mediated ring-opening chlorination of hydroxy-cyclopropanes. **C:** Catalyst and metal free ring-opening chlorination of unfunctionalized aryl cyclopropanes.

3.2 Results and Discussion

3.2.1 Synthesis

We intended to avoid super stoichiometric amounts of strong Lewis acids, the use of precious metals and pre-functionalized aryl cyclopropanes by employing photoredox catalysis. Therefore, we started our investigations using simple cyclopropyl benzene (**1a**) as model substrate, sodium chloride as chloride source, sodium anthraquinone-2-sulfonate (SAS) as strongly oxidizing photosensitizer and trifluoroacetic acid (TFA) to activate the photocatalyst.^[9] Under these conditions we observed 53% of the desired β chloro ketone **2a** (Table 3-1, entry 1). The use of sulfuric acid instead of TFA or a combination of HCl and HNO₃ did not alter the yield significantly (entries 2-3). Surprisingly, the control reaction without photocatalyst using HCl and HNO₃ gave **2a** in 80% ¹H-NMR and 77% isolated yield, while all other control reactions did not show significant product formation (entries 4-8, see Chapter 3.4.2 for more control reactions and see the mechanistic section for more details on this observation).

Table 3-1. Optimization of the reaction conditions^[a]



Entry	Photocatalyst / λ	Chloride source, Acid	Yield of 2a ^[b]
1	SAS (10%) / 395 nm	NaCl (5 equiv.), TFA (2.5 equiv.)	53%
2	SAS (10%) / 395 nm	NaCl (5 equiv.), H ₂ SO ₄ (2.5 equiv.)	45%
3	SAS (10%) / 395 nm	HCl (5 equiv.), HNO ₃ (10 mol%)	51%
4	- / 395 nm	HCl (5 equiv.), HNO ₃ (10 mol%)	80% (77%)
5 ^[c]	- / -	HCl (5 equiv.), HNO ₃ (10 mol%)	0%
6	- / 395 nm	NaCl (5 equiv.), TFA (2.5 equiv.)	0%
7	- / 395 nm	HCl (5 equiv.)	0%
8 ^[d]	- / 455 nm or 400 nm	HCl (5 equiv.), HNO ₃ (10 mol%)	<10%

[a] General conditions: Cyclopropylbenzene (0.1 mmol) and the indicated amount of SAS, chloride source and acid were dissolved in 2 mL of MeCN H₂O 1:1, set under oxygen atmosphere and irradiated with one high intensity 395 nm LED for 2 h. [b] Yield determined by ¹H-NMR using benzene as internal standard, isolated yield in brackets. [c] Either no light for 24 h at rt or no light for 24 h at 80 °C. [d] Either two 455 nm high power or one low intensity 400 nm LED were used (see Chapter 3.4.2 for details about the light sources).

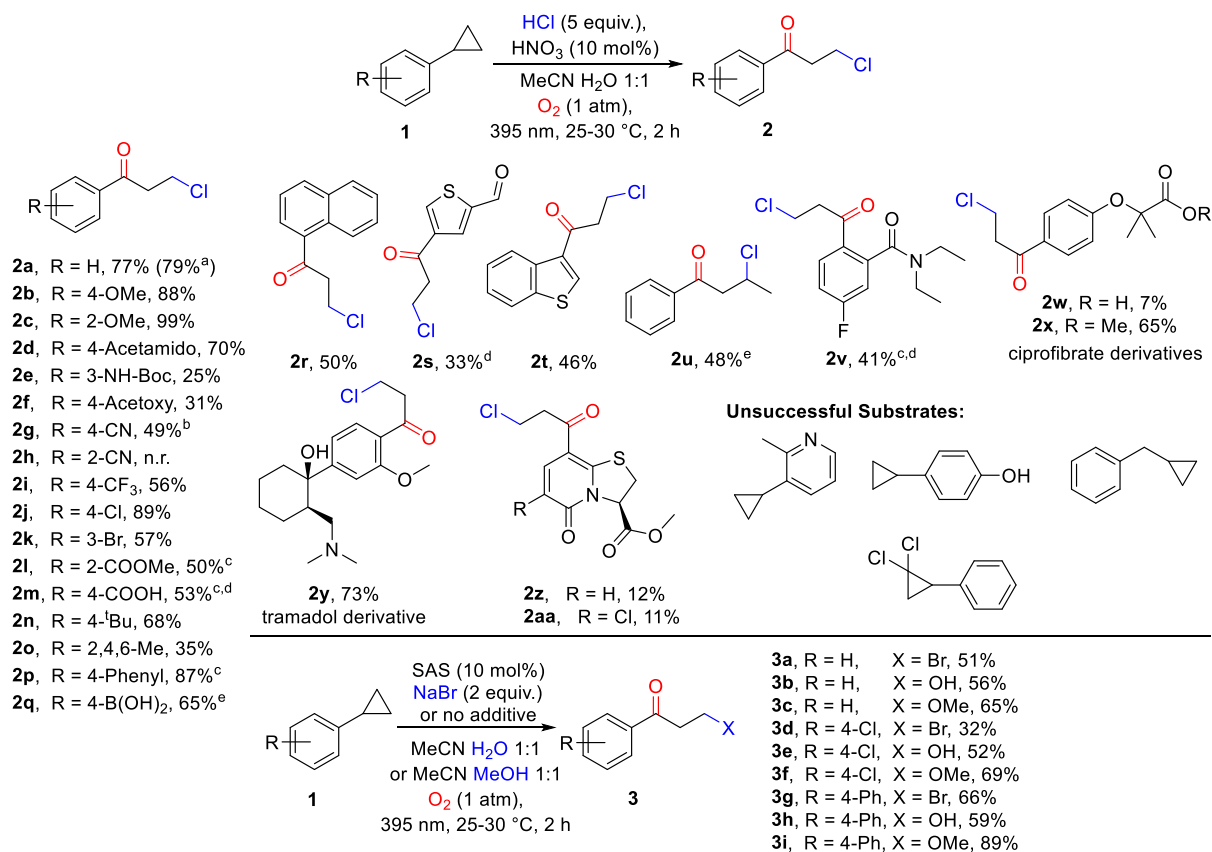


Figure 3-1. Substrate scope or the reaction. **a:** Gram scale reaction with 10 mmol of **1a** as substrate (see Chapter 3.4.1 for details). **b:** Mixture of product and elimination product, ratio: 1.5:1. **c:** 4 h reaction time. **d:** Oxygen overpressure (~2 bar) was used. **e:** Yield determined with ¹H-NMR using benzene as internal standard.

With the best conditions in hand, we explored the substrate scope of the reaction (Fig. 3-1). Electron donating substituents in 4 or 2 position increased the yield of the corresponding product (**2b-2d**), while electron withdrawing substituents in 2,3 or 4 position gave lower yields or suppressed the reaction completely, except in case of 4-chloro substitution (**2e-2m**). In addition, different alkyl or aryl substituents gave moderate to excellent yields (**2n-2p**, **2r**) and even a boronic acid substituent was well tolerated under the reaction conditions (**2q**). In case of **2o** the yield might be lower due to the many oxidizable benzylic C-H bonds which could have led to side reactions. However, to our delight, also an electron deficient thiophene derivative as well as a benzothiophene gave low to moderate yields (**2s**, **2t**). While the methyl substituted cyclopropane derivative **1u** gave only a single product in moderate yield, also a double substituted aromatic ring was well tolerated giving the corresponding product (**2v**) in moderate yield. Finally, we submitted bioactive compounds like derivatives of ciprofibrate, tramadol and antibacterially active ring-fused 2-pyridones^[10] to our reaction conditions leading to mixed results. The free aliphatic carboxylic acid of the ciprofibrate derivative was probably easily decarboxylated under the reaction conditions giving **2w** only in low yield. On the other hand, the ciprofibrate methyl ester as well as the tramadol derivative gave the products in high yields (**2x-2y**). Since 2-pyridones are known to react with oxygen under irradiation, only low yields were obtained in case of ring-fused 2-pyridones under optimized conditions (**2z-2aa**).^[11] To illustrate the utility of the method, a gram scale reaction (10 mmol scale) was performed giving **2a** in 79% isolated yield. In addition, if SAS was used as

photosensitizer, it was possible to add other nucleophiles, e.g. bromide, water or methanol, to the cyclopropyl arene in moderate to excellent yields (**3a-3i**).

Finally, we explored the utility of the β chloro ketones in further synthetic transformations (Fig. 3-2). The synthesis of 2-isoxazoline derivative **4a** or 2-pyrazoline derivative **4b** proceeded in moderate yield. In addition, the formation of the phosphonium chloride **4c** proceeded smoothly and in high yield generating a valuable precursor for a Wittig type reaction.^[12] Finally, we believe that β chloro ketones generated from bioactive compounds might be interesting precursors for bioconjugation of pharmacophores to antibodies and/or biological probes for the exploration of receptor functions (**4d**).^[13]

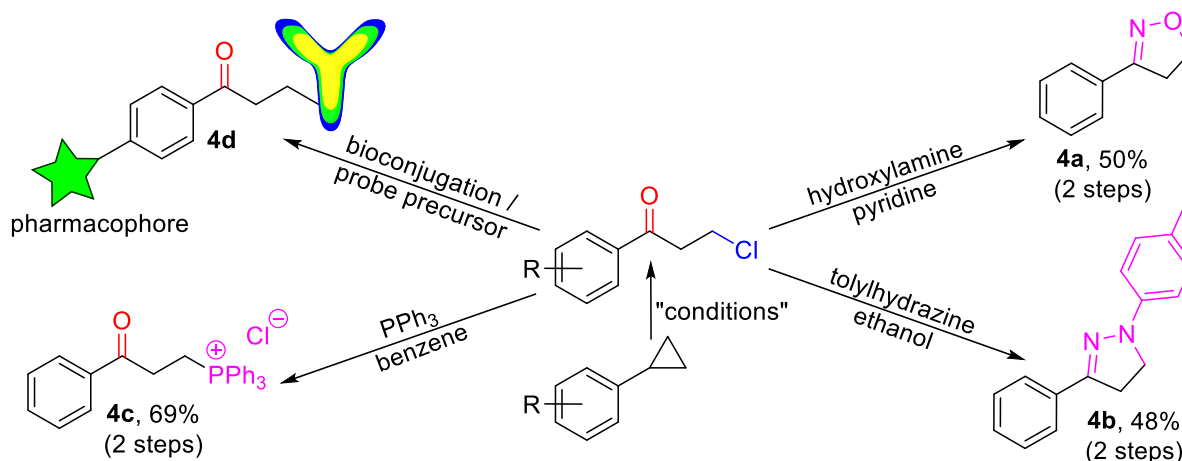


Figure 3-2. Illustration of different applications for β chloro ketones synthesized from aryl cyclopropanes. For “conditions” see Fig. 3-1.

3.2.2 Mechanistic Investigations

To investigate the reaction mechanism, we performed ^{18}O labelling experiments, as well as UV-VIS measurements, cyclovoltammetric investigations and control reactions. The ^{18}O labelling experiments showed that the ketone oxygen atom originates from molecular oxygen and not from a nucleophilic attack by water (see Chapter 3.4.2 for details). The UV-VIS measurements of elemental chlorine dissolved in an acetonitrile water mixture showed, that it absorbs reasonably well at 395 nm supporting the light induced initiation (see Chapter 3.4.2 for details). On the other hand, also the cyclovoltammetric measurements of several substrates (**1a**, **1b**, **1h**, **1i**, **1n**) in an acetonitrile water mixture revealed that their oxidation by a chlorine radical ($E_{\text{ox}}(\text{Cl}\cdot)$ in MeCN $\sim +1.84$ V vs. SCE^[5a], in H_2O $\sim +2.2$ V vs SCE^[14]) is feasible (see Chapter 3.4.2 for oxidation potentials of the substrates). In combination, UV-VIS and cyclovoltammetric experiments provide good evidence for a $\text{Cl}\cdot$ initiated reaction. To get further insight into the mechanism, several control experiments were performed. To demonstrate that the reaction is initiated by the light driven cleavage of Cl_2 , we performed reactions with super stoichiometric and catalytic amounts of chlorine gas (Fig. 3-3 A). Only polychlorinated side products could be observed if an excess of chlorine gas and HCl were used to promote the reaction. If catalytic amounts of Cl_2 and excess of HCl were used, the desired product was obtained in 50% yield and the amount of side products was reduced. Since the opening of cyclopropyl rings by chloride radicals is well known to proceed *via* oxidation of the cyclopropyl arene and since other nucleophiles could only be used in the presence of a

photosensitizer, we assume the presence of an aryl cyclopropyl radical cation intermediate.^[5a] The presence of this radical cation could be observed in the reaction of 4-bromocyclopropyl-benzene (**1ab**), because the para-bromo substituent was replaced partially by chloride giving a mixture of p-brominated and p-chlorinated product (Fig. 3-3 B).^[15] Furthermore, if the substituted starting materials **1ac** or **1ad** were used, only **1ac** gave the decarboxylated product **2a**, whereas **1ad** was completely recovered. This indicates that either a positively charged leaving group or an oxidizable/hydrogen atom donor is required in the benzylic position (Fig. 3-3 C, see Chapter 3.4.2 for more mechanistic investigations).

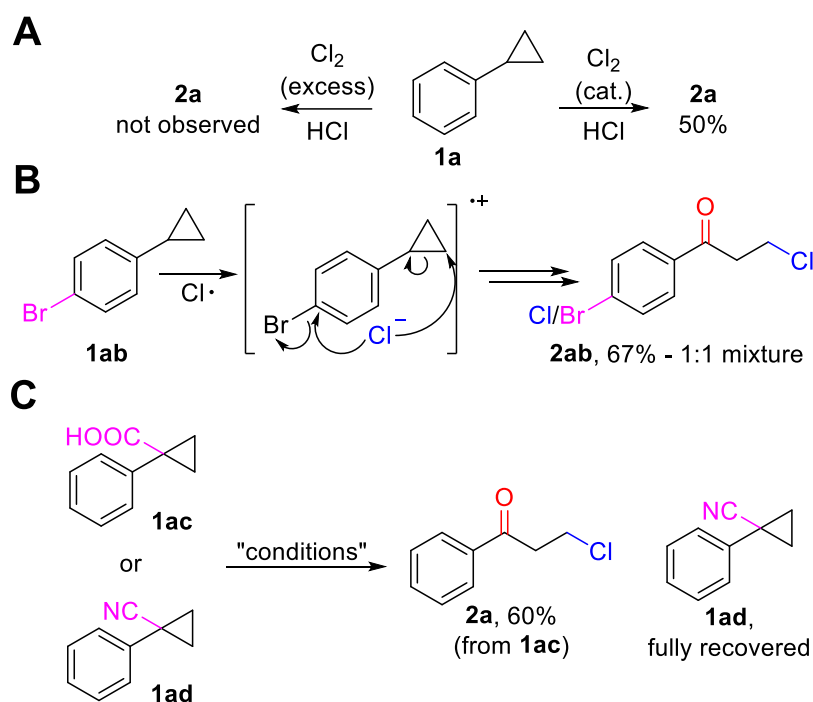


Figure 3-3. Overview of control reactions that support the mechanistic proposal. **A:** Experiments with elemental chlorine. **B:** Evidence for the intermediary of a cyclopropyl arene radical cation. **C:** Evidence that a positively charged or good radical leaving group is required. For “conditions” see Fig. 3-1.

As a summary of the mechanistic investigations, we propose the following mechanism (Fig. 3-4). We propose that Cl_2 is generated from the reaction between the diluted hydrochloric and nitric acid mixture.^[16] The generated molecular chlorine is cleaved by light into chlorine radicals, which can oxidize the aryl cyclopropane (**A**) and initiates a radical chain reaction. The so formed cyclopropyl radical cation (**B**) can be opened by Cl^- to give a transient benzylic radical (**C**) which can be trapped by the persistent triplet oxygen diradical to give a benzylic peroxy radical (**D**). This species can react rapidly with a second chlorine molecule which releases another $\text{Cl}\cdot$ to continue the radical chain.^[17] The formed hydroperoxyl chloride (**E**) can undergo a heterolytic fragmentation to give the desired ketone (**F**).^[18] Upon this fragmentation, hypochlorous acid is released which can react with HCl to give molecular chlorine which continues the chain reaction.^[19]

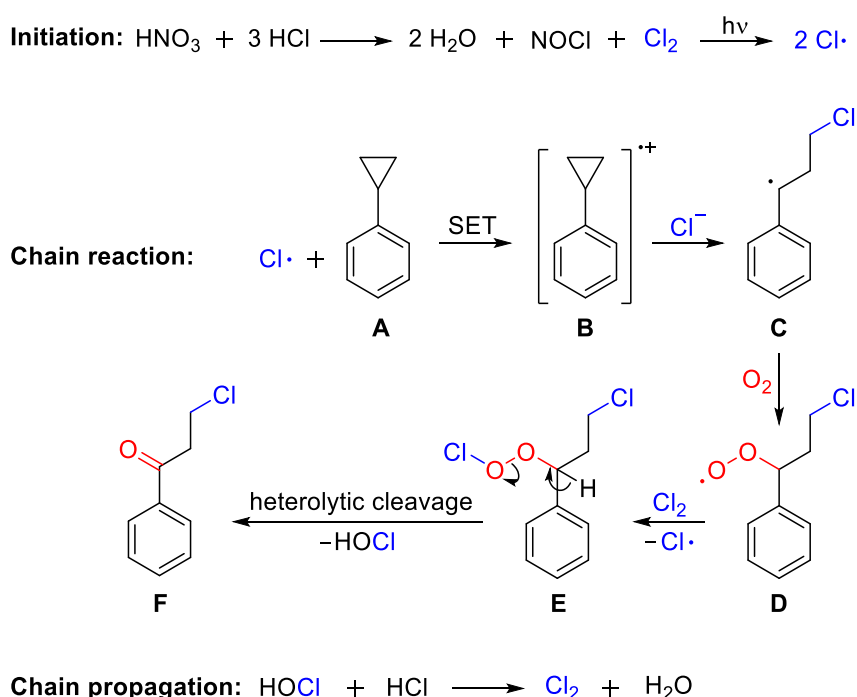


Figure 3-4. Conclusive mechanism for the generation of β chloro ketones from aryl cyclopropanes.

3.3 Conclusion

In summary, we developed a light mediated procedure for the oxidative ring opening of aryl cyclopropanes yielding β chloro ketones in low to excellent yields. The method uses cheap standard lab chemicals and leads to an increased molecular complexity and synthetic utility comparing the product and the starting material. The substrate scope exhibits a broad functional group tolerance and a scale up of the reaction could be performed. The products are valuable precursors for heterocycles, further synthetic transformations and might find application in biochemistry. We assume that HCl and HNO_3 react, despite the dilution, like in *aqua regia* leading to traces of Cl_2 that start an efficient chain reaction upon light-induced homolytic cleavage. The mechanistic proposal is supported by several control reactions, ^{18}O labelling and UV-VIS experiments as well as cyclovoltammetry. Moreover, other nucleophiles than chloride could be used in presence of a simple, anthraquinone based photosensitizer recommending the reaction for many applications.

3.4 Experimental Part

3.4.1 General Information

See Chapter 2.4.1 for General Information.^[20]

General ring opening procedure A

The aryl cyclopropane (0.1 mmol, 1 equiv.) was weight into a 5 mL crimp cap vial, 1 mL of acetonitrile and 1 mL of 0.5M aqueous HCl (0.5 mmol, 5 equiv.), 0.5 μ L (0.01 mmol, 0.1 equiv.) fuming HNO₃ and a stirring bar were added, the vial was closed with a crimp cap with septum, shaken briefly and purged with oxygen from a balloon for 1 minute. The reaction mixture was irradiated with one 395 nm LED for 2 h. Upon completion, three equal reaction mixtures were combined, diluted with 10 mL of DCM and 10 mL of water and the phases were separated. The aqueous phase was extracted with an additional 10 mL of DCM and the combined organic phases were dried with MgSO₄, concentrated and the residue was purified by column chromatography to give the title compound.

Gram scale reaction

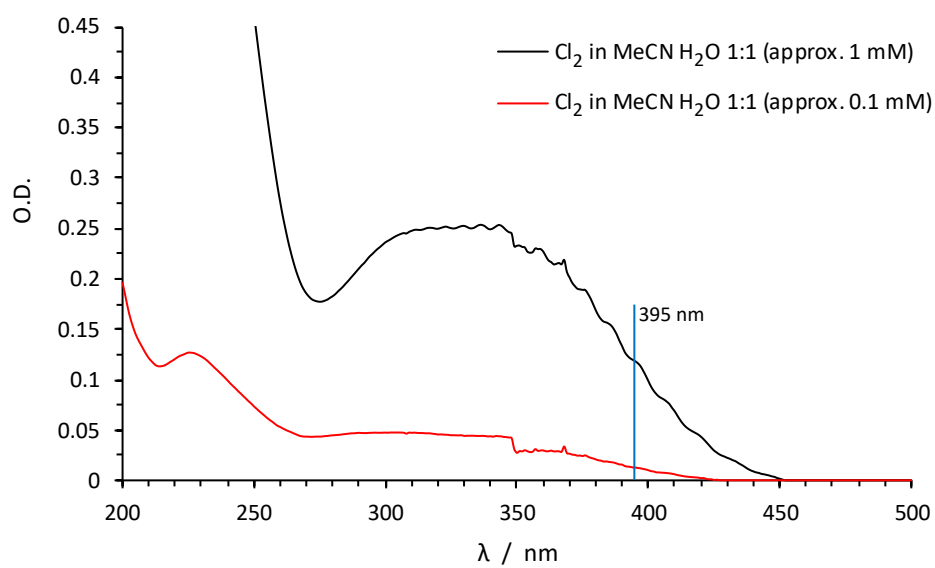
1.3 mL (10 mmol, 1 equiv.) cyclopropylbenzene was added into a 500 mL round bottom Schlenk flask under oxygen atmosphere, 100 mL of acetonitrile and 100 mL of 0.5M aqueous HCl (50 mmol, 5 equiv.), 48 μ L (1.0 mmol, 0.1 equiv.) fuming HNO₃ and a stirring bar were added. The reaction mixture was irradiated with four 395 nm LEDs for 16 h. Upon completion, the reaction mixture was diluted with 150 mL of DCM and 100 mL of water and the phases were separated. The aqueous phase was extracted with an additional 50 mL of DCM and the combined organic phases were dried with MgSO₄, concentrated and the residue was purified by column chromatography.

General ring opening procedure B

The aryl cyclopropane (0.1 mmol, 1 equiv.), (only for the bromination: 21 mg (0.2 mmol, 2 equiv.) NaBr and 3.2 mg (0.01 mmol, 0.1 equiv.) sodium anthraquinone-2-sulfonate were weight into a 5 mL crimp cap vial, 1 mL of acetonitrile and 1 mL water (or 1 mL of methanol for the methoxylation) and a stirring bar were added, the vial was closed with a crimp cap with septum and purged with oxygen from a balloon for 1 minute. Oxygen overpressure was applied by adding an additional 12 mL of oxygen *via* syringe into the vial. The reaction mixture was irradiated with one 395 nm LED for 2 h. Upon completion, three equal reaction mixtures were combined, diluted with 10 mL of DCM and 10 mL of water and the phases were separated. The aqueous phase was extracted with an additional 10 mL of DCM and the combined organic phases were dried with MgSO₄, concentrated and the residue was purified by column chromatography to give the title compound.

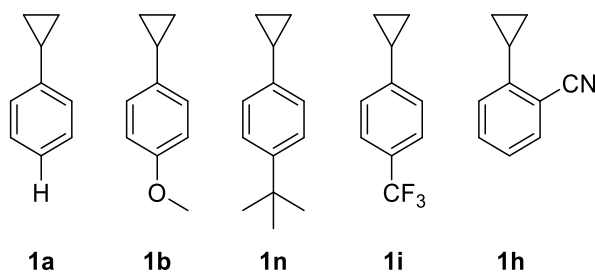
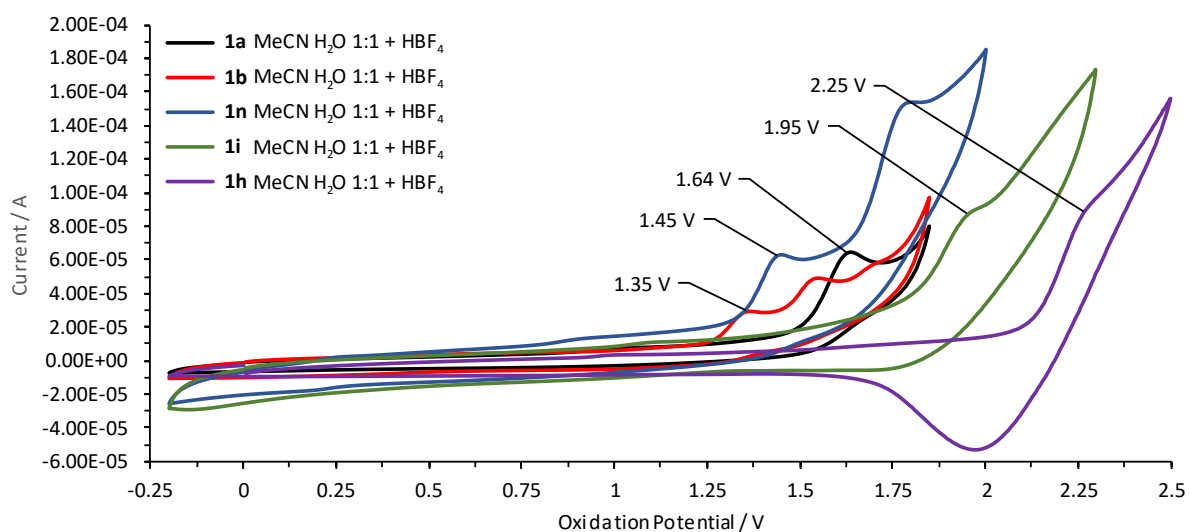
3.4.2 Mechanistic Investigations

UV-VIS spectroscopy



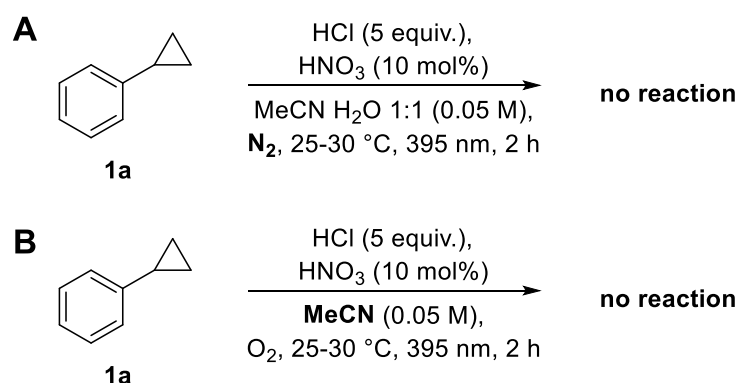
The UV-VIS spectra of diluted solutions of molecular chlorine in MeCN H₂O 1:1 show that excitation of small chlorine quantities is possible by the employed 395 nm LEDs.

Cyclovoltammetry



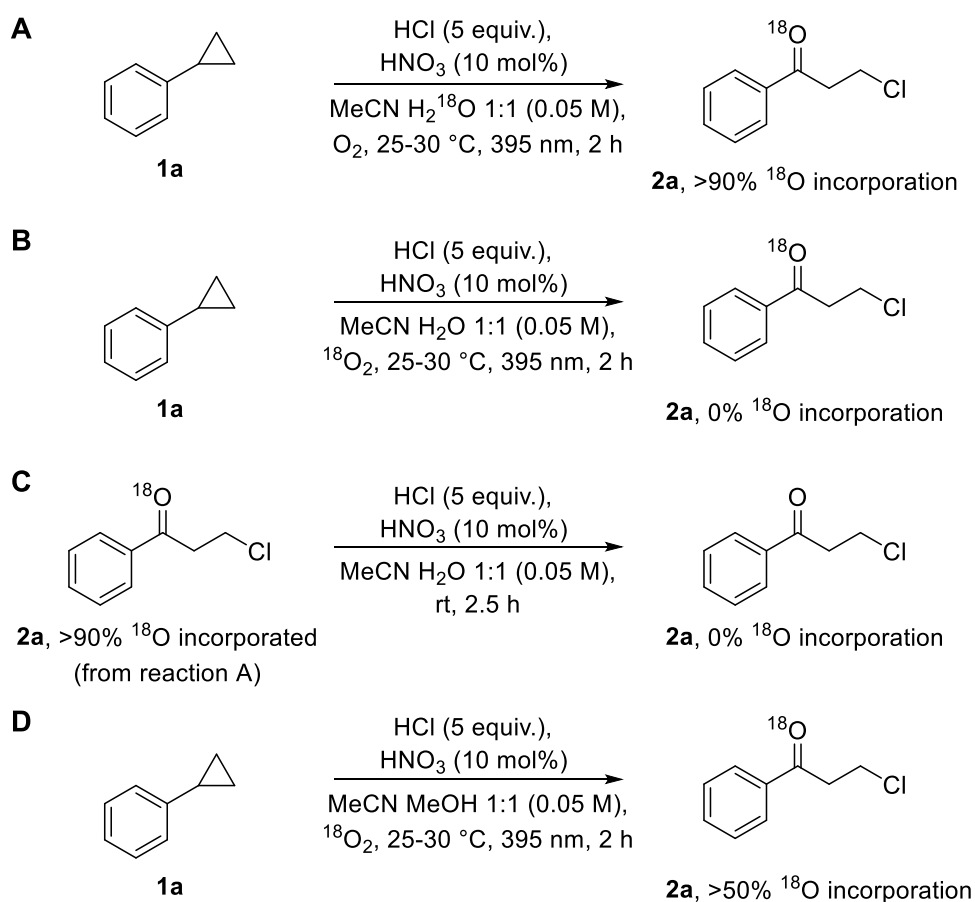
The cyclovoltammometric data show that single electron oxidation of substrates **1a**, **1b**, **1n** and **1i** by a chlorine radical is possible in an acetonitrile water mixture under acidic conditions (HBF₄ was used instead of HCl as proton source because it cannot be degraded under the applied electrochemical conditions). The required oxidation potential of **1h** is too high to be oxidized by Cl[•], which is in good agreement with the reported literature potentials for Cl[•] and the experimental observations.

Control experiments



No reaction to the desired product occurred under N₂ atmosphere and if the reaction was performed in pure MeCN (no water).

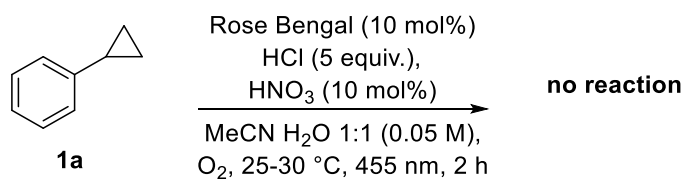
¹⁸O labeling experiments



The labeling experiments showed that if H₂¹⁸O is used more than 90% ¹⁸O is incorporated into the product (**A**), while if ¹⁸O₂ is used no incorporated ¹⁸O could be detected by mass spectrometry (**B**). However, if the labeled compound is stirred for 2.5 h in acidic, unlabeled water, full exchange to the non-labeled oxygen was detected (**C**). We assume that the ketone was protonated and exchanged with the labeled/unlabeled solvent to bias the results.

Therefore, we repeated the reaction using unlabeled methanol as solvent (**D**), which did not give a clean reaction but was supposed to exchange less with the ketone. Indeed, we found a significant ¹⁸O incorporation being good evidence that the oxygen in the product originates from O₂.

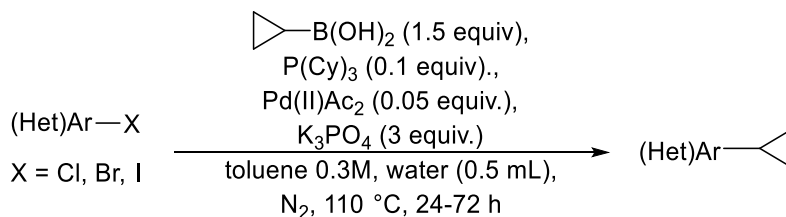
Exclusion of a singlet oxygen mediated ring opening pathway



If Rose Bengal, a common singlet oxygen sensitizer, was employed as photocatalyst no reaction occurred, excluding a singlet oxygen mediated ring opening pathway.

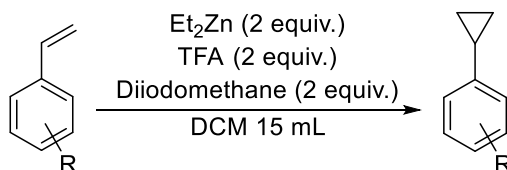
3.4.3 Starting Material Synthesis and Characterizations

General procedure A: Suzuki-Coupling Reaction^[21]



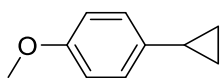
Into a 20 mL microwave vial were weighed the aryl halide (1.5-3 mmol, 1 equiv.), tricyclohexylphosphine (0.1 equiv.), palladium(II) acetate (0.05 equiv.), potassium phosphate (3 equiv.) and cyclopropylboronic acid (1.5 equiv.). A magnetic stirring bar, toluene (0.3M) and 0.5 mL of water were added, and the vial was closed. The reaction mixture was shaken briefly and set under inert atmosphere by bubbling nitrogen gas through the vial for 5 minutes. Afterwards, the vial was placed into an oil bath and stirred at 110 °C for 24-72 h. The reaction was monitored by LCMS or GC-FID. Upon completion, the reaction mixture was poured into a separatory funnel, diluted with ethyl acetate and washed with 15 mL water twice (sat. NaHCO₃ in case of pyridines). The organic layer was dried with Na₂SO₄, concentrated in vacuo and purified by column chromatography to give the title compound.

General procedure B: Simmons-Smith Cyclopropanation^[22]



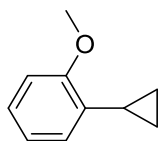
To 15 mL distilled DCM was added 10 mL (10.0 mmol, 2 equiv.) Et₂Zn (1.0 M in hexanes) under N₂ atmosphere. The solution was cooled in an ice bath and a solution of trifluoroacetic acid (0.8 mL, 10.0 mmol, 2 equiv.) in 5 mL DCM was then dripped very slowly into the reaction mixture *via* syringe. Upon stirring for 20 min, a solution of CH₂I₂ (0.8 mL, 10.0 mmol, 2 equiv.) in 5 mL DCM was added. After an additional 20 min of stirring, a solution of the respective styrene derivative (5.0 mmol, 1 equiv.) in 5 mL DCM was added, and the ice bath was removed. After an additional 3 h of stirring, the reaction mixture was quenched with 1M HCl (10 mL) and the phases were separated. The aqueous layer was extracted with DCM. The combined organic layers were washed with saturated NaHCO₃, and brine and then dried with Na₂SO₄, filtered and concentrated. The residue was purified by column chromatography to give the title compound.

Starting Material Characterizations



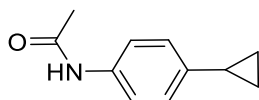
1b

1-Cyclopropyl-4-methoxybenzene was prepared on 1.5 mmol scale following general procedure A using 4-bromoanisole as starting material (reaction time 72 h) and isolated as a colorless oil (178 mg, 1.2 mmol, 80%). **¹H NMR** (400 MHz, CDCl₃): δ 7.06-7.00 (m, 2H), 6.85-6.80 (m, 2H), 3.79 (s, 3H), 1.91-1.83 (m, 1H), 0.94-0.88 (m, 2H), 0.66-0.61 (m, 2H). **¹³C NMR** (101 MHz, CDCl₃): δ 157.7, 136.0, 127.0, 113.9, 55.4, 14.7, 8.6. NMR data matches literature reference.^[23] **HRMS**: calcd. for C₁₀H₁₂O⁺, (M)⁺: 148.0883; found: 148.0878. **MF**: C₁₀H₁₂O. **MW**: 148.21.



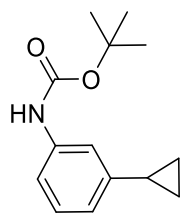
1c

1-Cyclopropyl-2-methoxybenzene was prepared on 3 mmol scale following general procedure A using 2-bromoanisole as starting material (reaction time 24 h) and isolated as a colorless oil (164 mg, 1.1 mmol, 74%). **¹H NMR** (400 MHz, CDCl₃): δ 7.34-7.27 (m, 1H), 7.08-6.96 (m, 3H), 4.00 (s, 3H), 2.45-2.32 (m, 1H), 1.14-1.06 (m, 2H), 0.88-0.80 (m, 2H). **¹³C NMR** (101 MHz, CDCl₃): δ 158.3, 131.9, 126.3, 124.7, 120.5, 110.1, 55.4, 9.4, 7.8. NMR data matches literature reference.^[24] C₁₀H₁₂O⁺, (M)⁺: 148.0883; found: 148.0879. **MF**: C₁₀H₁₂O. **MW**: 148.21.

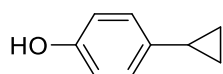


1d

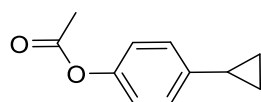
N-(4-Cyclopropylphenyl)acetamide was prepared on 2 mmol scale following general procedure A using 4-bromoacetanilide as starting material (reaction time 24 h) and isolated as a white/yellowish solid (250 mg, 1.43 mmol, 71%). **¹H NMR** (600 MHz, CDCl₃): δ 7.36 (d, *J* = 8.2 Hz, 2H), 7.00 (d, *J* = 8.2 Hz, 2H), 2.13 (s, 3H), 1.89-1.83 (m, 1H), 0.95-0.89 (m, 2H), 0.66-0.61 (m, 2H). **¹³C NMR** (151 MHz, CDCl₃): δ 168.6, 140.2, 135.4, 126.3, 120.3, 24.5, 15.05, 9.1. NMR data matches literature reference.^[23] **HRMS**: calcd. for C₁₁H₁₃NO⁺, (M+H)⁺: 176.1070; found: 176.1090. **MF**: C₁₁H₁₃NO. **MW**: 175.23.

**1e**

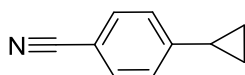
Tert-butyl (3-cyclopropylphenyl)carbamate was prepared on 2 mmol scale following general procedure A using tert-butyl (3-bromophenyl)carbamate as starting material (reaction time 24 h) and isolated as a yellowish crystals (392 mg, 1.68 mmol, 84%). **¹H NMR** (400 MHz, CDCl₃) δ 7.19-7.05 (m, 3H), 6.79-6.68 (m, 1H), 6.44 (s, 1H), 1.93-1.81 (m, 1H), 1.52 (s, 9H), 0.96-0.88 (m, 2H), 0.73-0.65 (m, 2H). **¹³C NMR** (101 MHz, CDCl₃): δ 152.9, 145.2, 138.5, 128.9, 120.5, 116.1, 115.8, 80.5, 28.5, 15.6, 9.3. **HRMS**: calcd. for C₁₄H₂₀NO₂⁺, (M+H)⁺: 234.1489; found: 234.1489. **MF**: C₁₄H₁₉NO₂. **MW**: 233.31.

**1fp**

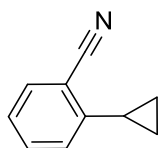
4-Cyclopropylphenol was prepared on 1.5 mmol scale by demethylation of **1b**.^[25] 229 μL (1.5 mmol, 1.0 equiv.) **1b** were dissolved in 5 mL of dry DCM in a dried 100 mL round bottom flask under inert atmosphere and cooled with an ice bath. 1.65 mL (1.65 mmol, 1.1 equiv.) BBr₃ (1M in DCM) was added dropwise *via* syringe through the septum and the reaction was stirred at 0 °C for 3 h. The reaction mixture was diluted with 5 mL of DCM and 10 mL of 1M aqueous NaOH were added and the phases were separated. The organic phase was extracted with another 10 mL of 1M NaOH. The combined aqueous phases were acidified with conc. HCl and extracted with DCM twice. The organic phase was concentrated, and the residue was purified by column chromatography to give the title compound as white crystal (90 mg, 0.67 mmol, 45%). **¹H NMR** (400 MHz, CDCl₃): δ 7.00-6.92 (m, 1H), 6.76-6.69 (m, 1H), 4.64 (brs, 1H), 1.90-1.77 (m, 1H), 0.99-0.79 (m, 1H), 0.68-0.52 (m, 1H). **¹³C NMR** (101 MHz, CDCl₃): δ 153.4, 136.2, 129.8, 127.2, 115.2, 14.8, 8.7. NMR data matches literature reference.^[26] **HRMS**: calcd. for C₉H₁₀O⁺, (M)⁺: 134.0726; found: 134.0730. **MF**: C₉H₁₀O. **MW**: 134.18.

**1f**

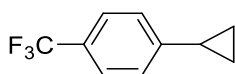
4-cyclopropylphenyl acetate was prepared on 0.3 mmol scale by acetylation of **1fp**. 55 mg (0.4 mmol, 1 equiv.) **1fp**, 113 μL (0.8 mmol, 2 equiv.) triethylamine and a few mg of DMAP were dissolved in 5 mL of DCM. 37 μL (0.5 mmol, 1.25 equiv.) acetyl chloride were added dropwise *via* syringe and the reaction mixture was stirred for 5 h at room temperature. Upon completion, the reaction mixture was diluted with 10 mL of DCM, 10 mL of 1M aqueous HCl were added and the phases were separated. The aqueous phase was extracted with another 10 mL of DCM and the combined organic phases were dried with MgSO₄, concentrated and the residue was purified by column chromatography giving the product as colorless oil (62 mg, 0.35 mmol, 88%). **¹H NMR** (300 MHz, CDCl₃): δ 7.12-7.05 (m, 2H), 7.00-6.94 (m, 2H), 2.29 (s, 3H), 196-184 (m, 1H), 1.01-0.91 (m, 2H), 0.72-0.62 (m, 2H). **¹³C NMR** (75 MHz, CDCl₃): δ 169.8, 148.5, 141.6, 129.6, 126.7, 121.3, 21.2, 15.0, 9.2. NMR data matches literature reference.^[27] **HRMS**: calcd. for C₁₁H₁₂O₂⁺, (M)⁺: 176.0832; found: 176.0827. **MF**: C₁₁H₁₂O₂. **MW**: 176.22.

**1g**

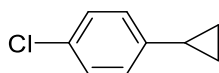
4-Cyclopropylbenzonitrile was prepared on 1.5 mmol scale following general procedure A using 4-bromobenzonitrile as starting material (reaction time 24 h) and isolated as a colorless oil (212 mg, 1.5 mmol, 99%). **¹H NMR** (400 MHz, CDCl₃): δ 7.51 (d, *J* = 8.4 Hz, 2H), 7.11 (d, *J* = 8.3 Hz, 2H), 1.97-1.88 (m, 1H), 1.11-1.05 (m, 2H), 0.79-0.73 (m, 2H). **¹³C NMR** (101 MHz, CDCl₃): δ 150.3, 132.2, 126.2, 119.3, 108.9, 16.0, 10.7. NMR data matches literature reference.^[28] **HRMS**: calcd. for C₁₀H₉N⁺, (M)⁺: 143.0730; found: 143.0722. **MF**: C₁₀H₉N. **MW**: 143.19.

**1h**

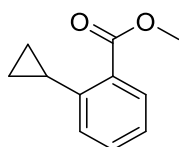
2-Cyclopropylbenzonitrile was prepared on 3 mmol scale following the general procedure A using 2-iodobenzonitrile as starting material (reaction time 24 h) and isolated as a yellowish oil (400 mg, 2.8 mmol, 93%). **¹H NMR** (400 MHz, CDCl₃): δ 7.61-7.55 (m, 1H), 7.50-7.42 (m, 1H), 7.25-7.18 (m, 1H), 6.96-6.90 (m, 1H), 2.33-2.23 (m, 1H), 1.18-1.10 (m, 2H), 0.82-0.76 (m, 2H). **¹³C NMR** (101 MHz, CDCl₃): δ 148.0, 132.9, 132.7, 125.9, 124.4, 118.5, 113.1, 14.2, 9.7. NMR data matches literature reference.^[29] **HRMS**: calcd. for C₁₀H₉N⁺, (M)⁺: 143.0730; found: 143.0731. **MF**: C₁₀H₉N. **MW**: 143.19.

**1i**

1-Cyclopropyl-4-(trifluoromethyl)benzene was prepared on 2 mmol scale following general procedure A using 1-bromo-4-(trifluoromethyl)benzene as starting material (reaction time 24 h) and isolated as a colorless oil (225 mg, 1.2 mmol, 60%). **¹H NMR** (600 MHz, CDCl₃): δ 7.49 (d, *J* = 8.0 Hz, 2H), 7.15 (d, *J* = 8.0 Hz, 2H), 1.98-1.90 (m, 1H), 1.07-1.00 (m, 2H), 0.77-0.72 (m, 2H). **¹³C NMR** (151 MHz, CDCl₃): δ 148.5 (s), 127.7 (q, *J* = 32.3 Hz), 125.9 (s), 125.3 (q, *J* = 3.8 Hz), 124.55 (q, *J* = 271.5 Hz), 15.6 (s), 10.1 (s). **¹⁹F NMR** (600 MHz, CDCl₃): -62.2. NMR data matches literature reference.^[30] **HRMS**: calcd. for C₁₀H₉F₃⁺, (M)⁺: 186.0651; found: 186.0644. **MF**: C₁₀H₉F₃. **MW**: 186.18.

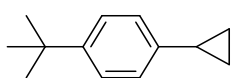
**1j**

1-Chloro-4-cyclopropylbenzene was prepared on 5 mmol scale following general procedure B using 4-chlorostyrene as starting material and isolated as a colorless oil (750 mg, 4.91 mmol, 98%). **¹H NMR** (400 MHz, CDCl₃): δ 7.24-7.19 (m, 2H), 7.03-6.96 (m, 2H), 1.92-1.81 (m, 1H), 1.00-0.93 (m, 2H), 0.70-0.63 (m, 2H). **¹³C NMR** (101 MHz, CDCl₃): δ 142.6, 131.0, 128.4, 127.2, 15.1, 9.4. NMR data matches literature reference.^[27] **HRMS**: calcd. for C₉H₉Cl⁺, (M)⁺: 152.0387; found: 152.0383. **MF**: C₉H₉Cl. **MW**: 152.62.



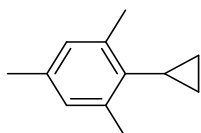
1l

Methyl 2-cyclopropylbenzoate was prepared on 2 mmol scale following the general procedure A using methyl 2-iodobenzoate as starting material (reaction time 24 h) and isolated as a brownish oil (300 mg, 1.70 mmol, 85%). **¹H NMR** (400 MHz, CDCl₃): δ 7.79 (dd, *J* = 7.8, 1.5 Hz, 1H), 7.19 (td, *J* = 7.6, 1.1 Hz, 2H), 7.01 (d, *J* = 7.9 Hz, 1H), 3.91 (m, 1H), 2.69-2.60 (m, 1H), 1.03-0.95 (m, 2H), 0.72-0.64 (m, 2H). **¹³C NMR** (101 MHz, CDCl₃): δ 168.8, 144.8, 131.9, 131.3, 130.1, 125.7, 125.3, 52.1, 13.6, 8.9. NMR data matches literature reference.^[31] **HRMS**: calcd. for C₁₁H₁₃O₂⁺, (M+H)⁺: 177.0910; found: 177.0913. **MF**: C₁₁H₁₂O₂. **MW**: 176.22.



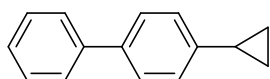
1n

1-(Tert-butyl)-4-cyclopropylbenzene was prepared on 2 mmol scale following the general procedure A using 1-bromo-4-(tert-butyl)benzene as starting material (reaction time 24 h) and isolated as a colorless oil (325 mg, 1.9 mmol, 93%). **¹H NMR** (400 MHz, CDCl₃): δ 7.29 (d, *J* = 8.4 Hz, 2H), 7.03 (d, *J* = 8.3 Hz, 2H), 1.92-1.82 (m, 1H), 1.31 (s, 9H), 0.96-0.90 (m, 2H), 0.71-0.65 (m, 2H). **¹³C NMR** (101 MHz, CDCl₃): δ 148.4, 141.0, 125.5, 125.3, 34.5, 31.6, 15.0, 9.1. NMR data matches literature reference.^[32] **HRMS**: calcd. for C₁₃H₁₈⁺, (M)⁺: 174.1403; found: 174.1402. **MF**: C₁₃H₁₈. **MW**: 174.29.



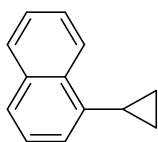
1o

2-Cyclopropyl-1,3,5-trimethylbenzene was prepared on 3 mmol scale following general procedure A using 2-bromo-1,3,5-trimethylbenzene as starting material (reaction time 24 h) and isolated as a colorless oil (450 mg, 2.81 mmol, 94%). **¹H NMR** (400 MHz, CDCl₃): δ 6.90 (s, 2H), 2.47 (s, 6H), 2.33 (s, 3H), 1.80-1.67 (m, 1H), 1.10-1.01 (m, 2H), 0.63-0.55 (m, 2H). **¹³C NMR** (101 MHz, CDCl₃): δ 139.0, 136.2, 135.7, 128.7, 20.9, 20.7, 11.9, 8.2. NMR data matches literature reference.^[33] **HRMS**: calcd. for C₁₂H₁₆⁺, (M)⁺: 160.1252; found: 160.1245. **MF**: C₁₂H₁₆. **MW**: 160.26.

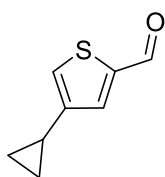


1p

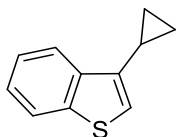
4-Cyclopropyl-1,1'-biphenyl was prepared on 3 mmol scale following the general procedure A using 4-bromo-1,1'-biphenyl as starting material (reaction time 24 h) and isolated as white crystals (550 mg, 2.83 mmol, 94%). **¹H NMR** (400 MHz, CDCl₃): δ 7.63-7.58 (m, 2H), 7.55-7.50 (m, 2H), 7.48-7.42 (m, 2H), 7.38-7.32 (m, 1H), 7.21-7.15 (m, 2H), 2.01-1.92 (m, 1H), 1.06-0.99 (m, 2H), 0.80-0.74 (m, 2H). **¹³C NMR** (101 MHz, CDCl₃): δ 143.3, 141.2, 138.5, 128.8, 127.1, 127.1, 127.1, 126.2, 15.3, 9.5. NMR data matches literature reference.^[34] **HRMS**: calcd. for C₁₅H₁₄⁺, (M)⁺: 194.1096; found: 194.1094. **MF**: C₁₅H₁₄. **MW**: 194.28.

**1r**

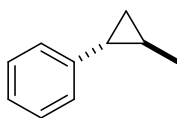
1-Cyclopropylnaphthalene was prepared on 1.5 mmol scale following the general procedure A using 1-bromonaphthalene as starting material (reaction time 24 h) and isolated as a colorless oil (226 mg, 1.34 mmol, 90%). **¹H NMR** (400 MHz, CDCl₃): δ 8.45 (d, *J* = 8.7 Hz, 1H), 7.89 (d, *J* = 8.1 Hz, 1H), 7.62-7.50 (m, 2H), 7.51-7.48 (m, 1H), 7.45-7.39 (m, 1H), 7.33-7.29 (m, 1H), 2.43-2.34 (m, 1H), 1.14-1.07 (m, 2H), 0.84-0.78 (m, 2H). **¹³C NMR** (101 MHz, CDCl₃): δ 139.3, 133.66, 133.65, 128.6, 126.7, 125.8, 125.7, 125.6, 124.6, 123.9, 13.4, 6.6. NMR data matches literature reference.^[34] **HRMS**: calcd. for C₁₃H₁₂⁺, (M)⁺: 168.0934; found: 168.0923. **MF**: C₁₃H₁₂. **MW**: 168.24.

**1s**

4-Cyclopropylthiophene-2-carbaldehyde was prepared on 2 mmol scale following general procedure A using 4-iodothiophene-2-carbaldehyde as starting material (reaction time 18 h) and isolated as a yellow/brownish oil (220 mg, 1.83 mmol, 92%) **¹H NMR** (600 MHz, CDCl₃): δ 9.84 (s, 1H), 7.49 (s, 1H), 7.30 (s, 1H), 1.97-1.89 (m, 1H), 0.99-0.93 (m, 2H), 0.69-0.63 (m, 2H). **¹³C NMR** (151 MHz, CDCl₃): δ 183.0, 146.8, 143.7, 135.0, 128.5, 11.2, 8.8. **HRMS**: calcd. for C₈H₈OS⁺, (M)⁺: 152.0290; found: 152.0282. **MF**: C₈H₈OS. **MW**: 152.21.

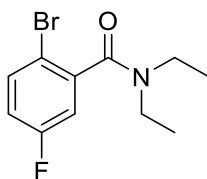
**1t**

3-Cyclopropylbenzo[b]thiophene was prepared on 3 mmol scale following general procedure A using 3-bromobenzo[b]thiophene as starting material (reaction time 18 h) and isolated as a yellow oil (450 mg, 2.58 mmol, 86%) **¹H NMR** (400 MHz, CDCl₃): δ 7.98 (d, *J* = 8.1 Hz, 1H), 7.85 (d, *J* = 7.8 Hz, 1H), 7.46-7.34 (m, 2H), 6.96 (d, *J* = 0.9 Hz, 1H), 2.11-2.02 (m, 1H), 1.02-0.95 (m, 2H), 0.74-0.69 (m, 2H). **¹³C NMR** (101 MHz, CDCl₃): δ 140.6, 140.0, 138.9, 124.5, 124.0, 122.9, 122.2, 119.9, 9.3, 6.3. **HRMS**: calcd. for C₁₁H₁₀S⁺, (M)⁺: 174.0498; found: 174.0497. **MF**: C₁₁H₁₀S. **MW**: 174.26.



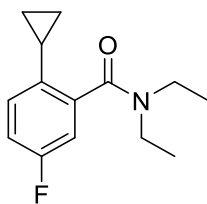
2u

2-Methylcyclopropylbenzene was prepared on 5 mmol scale following general procedure B using (E)-prop-1-en-1-ylbenzene as starting material and isolated as a colorless oil (410 mg, 3.10 mmol, 62%) **¹H NMR** (400 MHz, CDCl₃): δ 7.28-7.22 (m, 2H), 7.17-7.11 (m, 1H), 7.07-7.02 (m, 2H), 1.58 (dt, *J* = 8.9, 4.7 Hz, 1H), 1.20 (d, *J* = 5.9 Hz, 3H), 1.12-1.02 (m, 1H), 0.93-0.87 (m, 1H), 0.78-0.72 (m, 1H). **¹³C NMR** (101 MHz, CDCl₃): δ 144.2, 128.4, 125.6, 125.3, 24.5, 19.2, 18.1, 17.8. NMR data matches literature reference.^[27] **HRMS**: calcd. for C₁₀H₁₂⁺, (*M*)⁺: 132.0934; found: 132.0936. **MF**: C₁₀H₁₂. **MW**: 132.21.



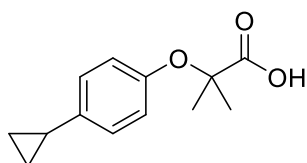
1vp

2-Bromo-N,N-diethyl-5-fluorobenzamide was prepared on 2.3 mmol scale by coupling of 2-bromo-4-fluorobenzoic acid with diethylamine. 500 mg (2.3 mmol, 1 equiv.) 2-bromo-4-fluorobenzoic was suspended in 5 mL DCM and stirred at 0°C. 217 μL (2.53 mmol, 1.1 equiv.) oxalylchloride was added dropwise over 5 minutes. After 1 h of additional stirring an excess of diethylamine (2 mL, 20 mmol, 8.7 equiv.) was added slowly at 0°C and stirred for 30 min. The reaction mixture was diluted with 10 mL DCM, poured into a separatory funnel, washed with 10 mL 1M HCl and 10 mL sat. NaHCO₃, dried with Na₂SO₄ and concentrated *in vacuo*. The residue was loaded onto silica and purified by column chromatography to give the product as a yellowish oily liquid (490 mg, 1.79 mmol, 78%). **¹H NMR** (400 MHz, CDCl₃): δ 7.56-7.45 (m, 1H), 7.03-6.90 (m, 2H), 3.87-3.74 (m, 1H), 3.39-3.27 (m, 1H), 3.22-3.08 (m, 2H), 1.26 (t, *J* = 7.1 Hz, 3H), 1.08 (t, *J* = 7.1 Hz, 3H). **¹³C NMR** (101 MHz, CDCl₃): δ 167.1 (d, *J* = 1.7 Hz), 161.8 (d, *J* = 249.4 Hz), 140.3 (d, *J* = 6.9 Hz), 134.4 (d, *J* = 8.0 Hz), 117.3 (d, *J* = 22.5 Hz), 114.8 (d, *J* = 24.0 Hz), 113.5 (d, *J* = 3.4 Hz), 42.7, 39.0, 13.9, 12.5. **¹⁹F NMR** (400 MHz, CDCl₃): -114.1. **HRMS**: calcd. for C₁₁H₁₄BrFNO⁺, (*M*+H)⁺: 274.0237; found: 274.0273. **MF**: C₁₁H₁₃BrFNO. **MW**: 274.13.



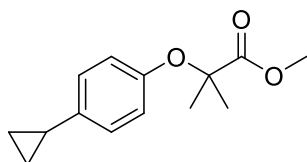
1v

2-Cyclopropyl-N,N-diethyl-5-fluorobenzamide was prepared on 2 mmol scale following general procedure A using **2vp** as starting material (reaction time 24 h) and isolated as a yellowish oil (154 mg, 0.65 mmol, 33%) **¹H NMR** (600 MHz, CDCl₃): δ 6.97-6.92 (m, 1H), 6.89-6.84 (m, 2H), 3.87-3.73 (m, 1H), 3.42-3.31 (m, 1H), 3.16 (q, *J* = 7.1 Hz, 1H), 1.90-1.81 (m, 1H), 1.25 (t, *J* = 7.1 Hz, 2H), 1.07 (t, *J* = 7.1 Hz, 1H), 0.97-0.85 (m, 2H), 0.82-0.73 (m, 1H), 0.58-0.49 (m, 1H). **¹³C NMR** (151 MHz, CDCl₃): δ 169.5, 160.8 (d, *J* = 245.5 Hz), 139.2 (d, *J* = 6.6 Hz), 135.2 (d, *J* = 3.2 Hz), 126.8 (d, *J* = 8.0 Hz), 115.7 (d, *J* = 21.1 Hz), 112.6 (d, *J* = 22.7 Hz), 42.9, 38.8, 14.1, 12.9, 12.2, 9.0, 8.1. **HRMS**: calcd. for C₁₄H₁₉FNO⁺, (M+H)⁺: 236.1445; found: 236.1448. **MF**: C₁₄H₁₈FNO. **MW**: 235.30.



1w

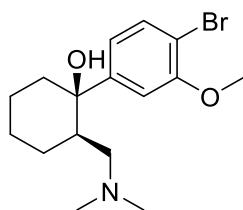
2-(4-Cyclopropylphenoxy)-2-methylpropanoic acid was prepared 1.5 mmol scale by dehalogenation of Ciprofibrate. 443 mg (1.5 mmol, 1 equiv.) Ciprofibrate was dissolved in 15 mL of ethanol and cooled with an ice bath. 700 mg (30 mmol, 20 equiv.) finely cut sodium pieces were added piece by piece and the reaction mixture was stirred for 5 h until all solid sodium disappeared. 1M aqueous HCl was added dropwise (very slowly) until pH 1. The aqueous phase was extracted 3x with 20 mL ethyl acetate and the combined organic phases were dried with MgSO₄, concentrated and purified by reversed phase column chromatography (H₂O (0.5% formic acid) / MeCN) giving the title compound as a white solid after freeze-drying. (90 mg, 0.41 mmol, 27%) **¹H NMR** (400 MHz, CDCl₃): δ 10.91 (s, 1H), 7.03-6.94 (m, 2H), 6.89-6.81 (m, 2H), 1.92-1.79 (m, 1H), 1.59 (s, 6H), 0.99-0.88 (m, 2H), 0.67-0.60 (m, 2H). **¹³C NMR** (101 MHz, CDCl₃): δ 179.7, 152.4, 138.9, 126.6, 120.8, 79.6, 25.2, 14.9, 9.0. **HRMS**: calcd. for C₁₃H₁₅O₃⁻, (M-H)⁻: 219.1027; found: 217.1033. **MF**: C₁₃H₁₆O₃. **MW**: 220.27.



1x

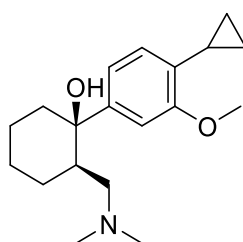
Methyl 2-(4-cyclopropylphenoxy)-2-methylpropanoate was prepared 0.75 mmol scale by etherification of methyl α-bromoisobutyrate with **1fp**. 101 mg (0.75 mmol, 1 equiv.) **1fp** and 311 mg (2.25 mmol, 3 equiv.) K₂CO₃ were dissolved in 4 mL of DMF and stirred for 10 min at rt. Then, 96 μL (0.75 mmol, 1 equiv.) methyl α-bromoisobutyrate was added and the reaction mixture was stirred for 16 h at rt. 15 mL of ethyl acetate were added and the organic layer was washed with 10 mL of 1M NaOH, 10 mL of water and 10 mL of brine subsequently. The organic phase was dried with MgSO₄, concentrated

and purified by column chromatography giving the title compound as colorless oil. (70 mg, 0.3 mmol, 40%) **¹H NMR** (400 MHz, CDCl₃): δ 6.98-6.90 (m, 2H), 6.77-6.70 (m, 2H), 3.76 (s, 3H), 1.88-1.78 (m, 1H), 1.56 (s, 6H), 0.93-0.85 (m, 2H), 0.65-0.57 (m, 2H). **¹³C NMR** (101 MHz, CDCl₃) δ 175.0, 153.2, 137.9, 126.5, 119.6, 79.3, 52.5, 25.4, 14.8, 8.9. **HRMS**: calcd. for C₁₄H₁₉O₃⁺, (M+H)⁺: 235.1329; found: 235.1333. **MF**: C₁₄H₁₈O₃. **MW**: 234.30.



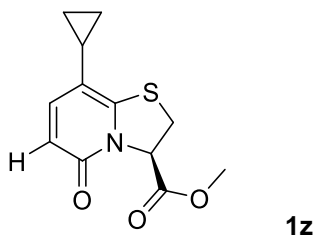
1yp

(1R,2R)-1-(4-Bromo-3-methoxyphenyl)-2-((dimethylamino)methyl)cyclohexan-1-ol was prepared on 0.9 mmol scale by photocatalytic bromination of Tramadol hydrochloride.^[44] Into a 5 mL crimp vial were weight 45 mg (0.15 mmol, 1 equiv.) Tramadol hydrochloride, 31.5 mg (3 mmol, 2 equiv.) NaBr, and 2.4 mg (0.075 mmol, 0.05 equiv.) sodium anthraquinone-2-sulfonate and 1.5 mL of MeCN and 1.5 mL of water were added. 46 μL (0.6 mmol, 4 equiv.) of trifluoroacetic acid and a stirring bar were added, the vial was closed and purged with oxygen for 1 minute. The reaction mixture was irradiated with a single 400 nm LED for 6 h. Upon completion, 6 equal reaction mixtures were combined and diluted with 20 mL of ethyl acetate and 20 mL of saturated, aqueous Na₂CO₃. The phases were separated and the aqueous phase was extracted with another 20 mL of ethyl acetate. The combined organic phases were dried with MgSO₄ and concentrated. The residue was purified by column chromatography giving the title compound as viscous oil. (195 mg, 0.57 mmol, 63%). **¹H NMR** (400 MHz, CD₃CN): δ 7.48-7.41 (d, *J* = 8.4 Hz, 1H), 7.22-7.16 (m, 1H), 7.01-6.95 (m, 1H), 5.04 (brs, 1H), 3.83 (s, 3H), 2.14-2.07 (m, 1H), 1.95-1.87 (m, 6H), 1.86-1.21 (m, 10H). **¹³C NMR** (101 MHz, CDCl₃): δ 156.5, 153.0, 133.3, 119.6, 110.6, 109.0, 77.3, 62.1, 56.8, 47.5, 44.8, 42.1, 28.3, 27.1, 23.0. NMR data matches literature reference.^[35] **HRMS**: calc. for C₁₆H₂₅BrNO₂⁺, (M+H)⁺: 342.1063, found: 342.1062. **MF**: C₁₆H₂₄BrNO₂. **MW**: 342.28.

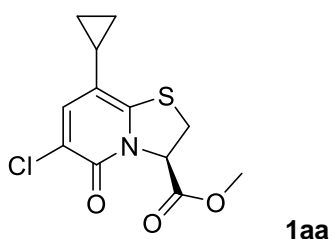


1y

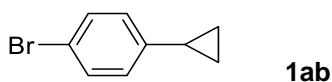
(1R,2R)-1-(4-Cyclopropyl-3-methoxyphenyl)-2-((dimethylamino)methyl)cyclohexan-1-ol was prepared on 0.57 mmol scale following general procedure A using **1yp** as starting material (reaction time 18h), purified by reversed phase column chromatography and isolated as a white solid (70 mg, 0.23 mmol, 42%). **¹H NMR** (400 MHz, Methanol-d₄): δ 7.09 (s, 1H), 6.97 (d, *J* = 8.0 Hz, 1H), 6.84 (d, *J* = 8.0 Hz, 1H), 3.88 (s, 3H), 2.97 (dd, *J* = 13.3, 9.3 Hz, 1H), 2.78-2.57 (m, 7H), 2.27-2.19 (m, 1H), 2.16-2.07 (m, 1H), 2.00-1.46 (m, 9H), 0.93-0.82 (m, 2H), 0.65-0.55 (m, 2H). **¹³C NMR** (101 MHz, Methanol-d₄) δ 159.8, 147.2, 131.8, 125.8, 117.9, 108.4, 75.9, 62.0, 56.1, 46.1, 43.0, 42.7, 41.7, 27.1, 26.1, 22.5, 10.0, 8.1, 8.0. **HRMS**: calc. for C₁₉H₃₀NO₂⁺, (M+H)⁺: 304.2271, found: 304.2275. **MF**: C₁₉H₂₉NO₂. **MW**: 303.45.



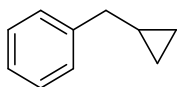
Methyl (R)-8-cyclopropyl-5-oxo-2,3-dihydro-5H-thiazolo[3,2-a]pyridine-3-carboxylate was prepared 27.6 mmol scale following literature known methods and isolated as a dark red, viscous oil (2.25 g, 8.95 mmol, 32%).^[36] **¹H NMR** (400 MHz, CDCl₃): δ 7.07 (d, *J* = 9.3 Hz, 1H), 6.23 (d, *J* = 9.3 Hz, 1H), 5.61 (dd, *J* = 8.5, 2.3 Hz, 1H), 3.80 (s, 3H), 3.73-3.66 (m, 1H), 3.54 (dd, *J* = 11.7, 2.3 Hz, 1H), 1.61-1.50 (m, 1H), 0.87-0.80 (m, 2H), 0.59-0.53 (m, 2H). **¹³C NMR** (101 MHz, CDCl₃): δ 166.7, 161.6, 146.6, 141.1, 115.3, 114.5, 63.4, 53.4, 31.8, 12.5, 6.3, 6.1. **HRMS**: calcd. for C₁₂H₁₃NO₃S⁺, (M+H)⁺: 252.0724; found: 252.0724. **MF**: C₁₂H₁₃NO₃S. **MW**: 251.30.



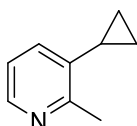
Methyl (R)-6-chloro-8-cyclopropyl-5-oxo-2,3-dihydro-5H-thiazolo[3,2-a]pyridine-3-carboxylate was prepared on 0.6 mmol scale by chlorination of compound **1z**. 150 mg (0.6 mmol, 1.0 equiv.) **1z** was dissolved in 5 mL of DCM and cooled to 0°C. 88 mg (0.66 mmol, 1.1 equiv.) *N*-Chlorosuccinimide was added and the reaction mixture was stirred overnight, diluted with DCM, washed with 10 mL of sat. NaHCO₃ twice, dried with Na₂SO₄, concentrated *in vacuo* and purified by column chromatography. The title compound was isolated as a dark brownish viscous oil (116 mg, 0.41 mmol, 77%) **¹H NMR** (400 MHz, CDCl₃): δ 7.22 (s, 1H), 5.60 (dd, *J* = 8.5, 2.0 Hz, 1H), 3.77 (s, 3H), 3.77-3.70 (m, 1H), 3.54 (dd, *J* = 11.8, 2.0 Hz, 1H), 1.58-1.49 (m, 1H), 0.87-0.79 (m, 2H), 0.59-0.50 (m, 2H). **¹³C NMR** (101 MHz, CDCl₃): δ 168.1, 157.5, 145.7, 139.1, 120.4, 114.0, 64.0, 53.5, 32.2, 12.4, 6.5, 6.2. **HRMS**: calcd. for C₁₂H₁₃ClNO₃S⁺, (M+H)⁺: 286.0299; found: 286.0301. **MF**: C₁₂H₁₂ClNO₃S. **MW**: 285.74.



1-Bromo-4-cyclopropylbenzene was prepared on 5 mmol scale following general procedure B using 4-bromostyrene as starting material and isolated as a colorless oil (800 mg, 4.06 mmol, 81%). **¹H NMR** (400 MHz, CDCl₃): δ 7.38-7.33 (m, 2H), 6.97-6.90 (m, 2H), 1.89-1.80 (m, 1H), 1.00-0.92 (m, 2H), 0.69-0.62 (m, 2H). **¹³C NMR** (101 MHz, CDCl₃): δ 143.2, 131.4, 127.6, 118.9, 15.1, 9.5. NMR data matches literature reference.^[27] **HRMS**: calcd. for C₉H₉Br⁺, (M)⁺: 195.9885; found: 195.9882. **MF**: C₉H₉Br. **MW**: 197.08.

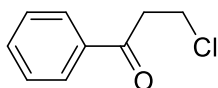


(Cyclopropylmethyl)benzene was prepared on 5 mmol scale following general procedure B using allyl benzene as starting material and isolated as a colorless oil (422 mg, 3.19 mmol, 64%) **¹H NMR** (400 MHz, CDCl₃): δ 7.38-7.24 (m, 4H), 7.23-7.17 (m, 1H), 2.57 (d, *J* = 6,9 Hz, 2H), 1.06-0.95 (m, 1H), 0.60-0.47 (m, 2H), 0.24-0.18 (m, 2H). **¹³C NMR** (101 MHz, CDCl₃): δ 142.3, 128.5, 128.4, 126.0, 40.5, 12.0, 4.8. NMR data matches literature reference.^[27] **HRMS**: calcd. for C₁₀H₁₂⁺, (M)⁺: 132.0934; found: 132.0925. **MF**: C₁₀H₁₂. **MW**: 132.21.



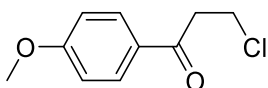
3-Cyclopropyl-2-methylpyridine was prepared on 1.5 mmol scale following general procedure A using 3-bromo-2-methylpyridine as starting material (reaction time 24 h) and isolated as a yellowish oil (226 mg, 1.34 mmol, 90%) **¹H NMR** (400 MHz, CDCl₃): δ 8.28-8.18 (m, 1H), 7.34-7.22 (m, 1H), 6.86 (dd, *J* = 7.5, 4.8 Hz, 1H), 2.34 (s, 3H), 2.07-1.96 (m, 1H), 1.07-1.01 (m, 2H), 0.94-0.87 (m, 2H). **¹³C NMR** (101 MHz, CDCl₃): δ 160.4, 146.5, 136.7, 128.6, 130.9, 120.0, 18.8, 13.5, 8.8. **HRMS**: calcd. for C₉H₁₁N⁺, (M)⁺: 133.0886; found: 133.0885. **MF**: C₉H₁₁N. **MW**: 133.19.

3.4.4 Product Characterizations



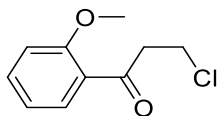
2a

3-Chloro-1-phenylpropan-1-one was prepared following the general ring opening procedure A using cyclopropylbenzene as starting material and isolated as yellowish crystals (39 mg, 0.23 mmol, 77%). **¹H NMR** (400 MHz, CDCl₃): δ 7.99-7.93 (m, 2H), 7.63-7.56 (m, 1H), 7.52-7.45 (m, 2H), 3.93 (t, *J* = 6.8 Hz, 2H), 3.46 (t, *J* = 6.8 Hz, 2H). **¹³C NMR** (101 MHz, CDCl₃): δ 196.8, 136.5, 133.7, 128.9, 128.2, 41.4, 38.8. **HRMS**: calcd. for C₉H₁₀ClO⁺, (M+H)⁺: 169.0415; found: 169.0425. **MF**: C₉H₉ClO. **MW**: 168.62.



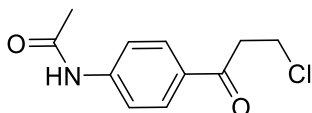
2b

3-Chloro-1-(4-methoxyphenyl)propan-1-one was prepared following the general ring opening procedure A using **1b** as starting material and isolated as a colorless solid (53 mg, 0.26 mmol, 88%). **¹H NMR** (400 MHz, CDCl₃): δ 7.94 (d, *J* = 8.9 Hz, 2H), 6.95 (d, *J* = 8.9 Hz, 2H), 3.92 (t, *J* = 6.9 Hz, 2H), 3.88 (s, 3H), 3.41 (t, *J* = 6.9 Hz, 2H). **¹³C NMR** (101 MHz, CDCl₃): δ 195.4, 164.0, 130.5, 129.7, 114.0, 55.7, 41.1, 39.1. NMR data matches literature reference.^[37] **HRMS**: calcd. for C₁₀H₁₂ClO₂⁺, (M+H)⁺: 199.0520; found: 199.0536. **MF**: C₁₀H₁₁ClO₂. **MW**: 198.65.



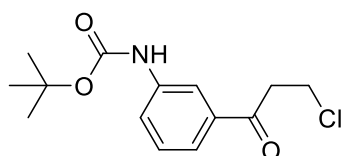
2c

3-Chloro-1-(2-methoxyphenyl)propan-1-one was prepared following the general ring opening procedure A using **1c** as starting material and isolated as a yellow oil (59 mg, 0.3 mmol, 99%). **¹H NMR** (300 MHz, CDCl₃): δ 7.76 (dd, *J* = 7.7, 1.8 Hz, 1H), 7.48 (ddd, *J* = 8.4, 7.3, 1.8 Hz, 1H), 7.06–6.93 (m, 3H), 3.92 (s, 3H), 3.87 (t, *J* = 6.8 Hz, 2H), 3.48 (t, *J* = 6.8 Hz, 2H). **¹³C NMR** (75 MHz, CDCl₃): δ 198.5, 159.0, 134.3, 130.7, 127.2, 120.9, 111.7, 55.6, 46.7, 39.3. **HRMS**: calcd. for C₁₀H₁₂ClO₂⁺, (M+H)⁺: 199.0520; found: 199.0524. **MF**: C₁₀H₁₁ClO₂. **MW**: 198.65.



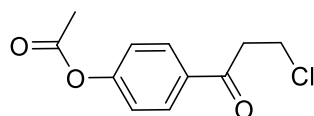
2d

N-(4-(3-Chloropropanoyl)phenyl)acetamide was prepared following the general ring opening procedure A using **1d** as starting material and isolated as a white solid (47 mg, 0.21 mmol, 70%). **¹H NMR** (400 MHz, DMSO-d₆) δ 10.29 (s, 1H), 7.94 (d, *J* = 8.8 Hz, 2H), 7.72 (d, *J* = 8.8 Hz, 2H), 3.91 (t, *J* = 6.3 Hz, 2H), 3.48 (t, *J* = 6.3 Hz, 2H), 2.09 (s, 3H). **¹³C NMR** (101 MHz, DMSO-d₆): δ 195.8, 169.4, 144.4, 131.3, 129.8, 118.7, 40.8, 40.1, 24.7. **HRMS**: calcd. for C₁₁H₁₃ClNO₂⁺, (M+H)⁺: 226.0629; found: 226.0630. **MF**: C₁₁H₁₂ClNO₂. **MW**: 225.67.



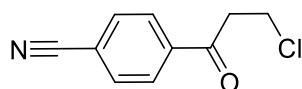
2e

Tert-butyl (3-(3-chloropropanoyl)phenyl)carbamate was prepared following the general ring opening procedure A using **1e** as starting material and isolated as a beige solid (21 mg, 0.07 mmol, 25%). **¹H NMR** (400 MHz, CDCl₃) δ 8.00-7.91 (m, 1H), 7.70-7.57 (m, 2H), 7.40 (t, *J* = 7.9 Hz, 1H), 6.68 (s, 1H), 3.91 (t, *J* = 6.8 Hz, 2H), 3.45 (t, *J* = 6.8 Hz, 2H), 1.53 (s, 9H). **¹³C NMR** (101 MHz, CDCl₃): δ 196.6 152.7, 139.2, 137.2, 129.6, 123.5, 122.7, 117.9, 81.2, 41.5, 38.8, 28.5. **HRMS**: calcd. for (C₁₄H₂₂ClN₂O₃, (M+NH₄)⁺): 301.1313; found: 301.1319. **MF**: C₁₄H₁₈ClNO₃. **MW**: 283.75.



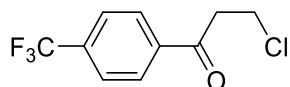
2f

4-(3-Chloropropanoyl)phenyl acetate was prepared following the general ring opening procedure A using **1f** as starting material and isolated as a yellow solid (21 mg, 0.09 mmol, 31%). **¹H NMR** (400 MHz, CDCl₃) δ 8.04-7.96 (m, 2H), 7.25-7.19 (m, 2H), 3.92 (t, *J* = 6.8 Hz, 2H), 3.44 (t, *J* = 6.8 Hz, 2H), 2.33 (s, 3H). **¹³C NMR** (101 MHz, CDCl₃): δ 195.6, 168.9, 154.8, 134.1, 129.8, 122.1, 41.4, 38.7, 21.3. **HRMS**: calcd. for C₁₁H₁₂ClO₃⁺, (M+H)⁺: 227.0496; found: 227.0494. **MF**: C₁₁H₁₁ClO₃. **MW**: 226.66.



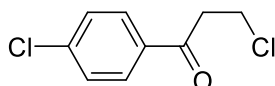
2g

4-(3-Chloropropanoyl)benzonitrile was prepared following the general ring opening procedure A using **1g** as starting material and isolated as yellowish oil (28,5 mg, 0.15 mmol, 49%). **¹H NMR** (400 MHz, CDCl₃) δ 8.09-8.03 (m, 2H), 7.82-7.77 (m, 2H), 3.92 (t, *J* = 6.6 Hz, 2H), 3.47 (t, *J* = 6.6 Hz, 2H). **¹³C NMR** (101 MHz, CDCl₃): δ 195.5, 139.3, 132.8, 131.9, 128.6, 117.0, 41.6, 38.2. **HRMS**: calcd. for C₁₀H₈ClNO⁺, (M+H)⁺: 193.0289; found: 193.0286. **MF**: C₁₀H₈ClNO. **MW**: 193.63.



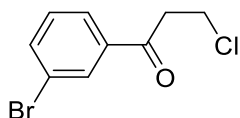
2h

3-Chloro-1-(4-(trifluoromethyl)phenyl)propan-1-one was prepared following the general ring opening procedure A using **1i** as starting material and isolated as yellowish solid (40 mg, 0.17 mmol, 56%). **¹H NMR** (400 MHz, CDCl₃) δ 8.07 (d, *J* = 8.2 Hz, 2H), 7.76 (d, *J* = 8.2 Hz, 2H), 3.93 (t, *J* = 6.7 Hz, 2H), 3.49 (t, *J* = 6.7 Hz, 2H). **¹³C NMR** (101 MHz, CDCl₃) δ 195.9, 139.1, 135.0 (q, *J* = 32.8 Hz), 128.6, 126.0 (q, *J* = 3.7 Hz), 123.63 (q, *J* = 272.8 Hz), 41.7, 38.4. **¹⁹F NMR** (400 MHz, CDCl₃): -63.7. **HRMS**: calcd. for C₁₀H₈ClF₃O⁺, (M)⁺: 236.0216; found: 236.0214. **MF**: C₁₀H₈ClF₃O. **MW**: 236.62.



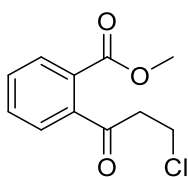
2j

3-Chloro-1-(4-chlorophenyl)propan-1-one was prepared following the general ring opening procedure A using **1j** as starting material and isolated as yellowish oil (54 mg, 0.27 mmol, 89%). **¹H NMR** (400 MHz, CDCl₃) 1H NMR δ 7.83-7.74 (m, 2H), 7.39-7.31 (m, 2H), 3.81 (t, *J* = 6.8 Hz, 3H), 3.32 (t, *J* = 6.8 Hz, 2H). **¹³C NMR** (101 MHz, CDCl₃) δ 195.6, 140.2, 134.8, 129.6, 129.2, 41.3, 38.6. **HRMS**: calcd. for C₉H₈Cl₂O⁺, (M)⁺: 203.0025, found: 203.0019. **MF**: C₉H₈Cl₂O. **MW**: 203.06.



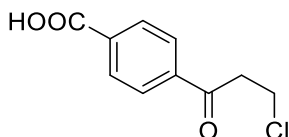
2k

1-(3-Bromophenyl)-3-chloropropan-1-one was prepared following the general ring opening procedure A using 3-bromocyclopropylbenzene as starting material and isolated as colorless solid (42 mg, 0.17 mmol, 57%). **¹H NMR** (300 MHz, CDCl₃) 1H NMR δ 8.08 (t, *J* = 1.7 Hz, 1H), 7.88 (ddd, *J* = 7.8, 1.6, 1.1 Hz, 1H), 7.72 (ddd, *J* = 8.0, 2.0, 1.0 Hz, 1H), 7.37 (t, *J* = 7.9 Hz, 1H), 3.91 (t, *J* = 6.7 Hz, 2H), 3.43 (t, *J* = 6.7 Hz, 1H). **¹³C NMR** (101 MHz, CDCl₃) δ 13C NMR (75 MHz, CDCl₃) δ 195.5, 138.2, 136.6, 131.3, 130.5, 126.7, 123.3, 41.5, 38.5. **HRMS**: calcd. for C₉H₈BrClO⁺, (M)⁺: 245.9442, found: 245.9436. **MF**: C₉H₈BrClO. **MW**: 247.52.



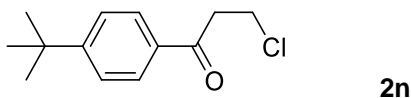
2l

Methyl 2-(3-chloropropanoyl)benzoate was prepared following the general ring opening procedure A using **1l** as starting material and isolated as yellowish oil (34 mg, 0.15 mmol, 50%). **¹H NMR** (400 MHz, CDCl₃): δ 7.93 (dd, *J* = 7.8, 0.9 Hz, 1H), 7.59 (td, *J* = 7.5, 1.3 Hz, 1H), 7.51 (td, *J* = 7.6, 1.3 Hz, 1H), 7.36 (dd, *J* = 7.5, 0.9 Hz, 1H), 3.91 (t, *J* = 6.9 Hz, 2H), 3.90 (s, 3H), 3.28 (t, *J* = 6.9 Hz, 2H). **¹³C NMR** (101 MHz, CDCl₃): δ 202.6, 167.0, 142.8, 132.6, 130.2, 130.2, 128.3, 126.3, 52.8, 45.6, 38.7. **HRMS**: calcd. for C₁₁H₁₂ClO₃⁺, (M+H)⁺: 227.0469; found: 227.0490. **MF**: C₁₁H₁₁ClO₃. **MW**: 226.66.

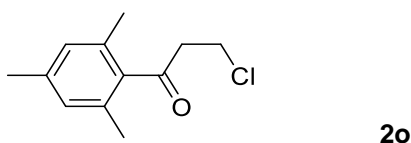


2m

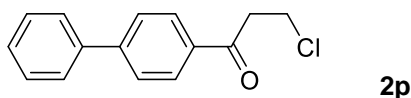
4-(3-Chloropropanoyl)benzoic acid was prepared following the general ring opening procedure A using 4-cyclopropyl benzoic acid as starting material and isolated as white solid (34 mg, 0.16 mmol, 53%). **¹H NMR** (¹H NMR (400 MHz, DMSO-d₆) δ 13.31 (brs, 1H), 8.07 (s, 4H), 3.93 (t, *J* = 6.3 Hz, 2H), 3.60 (t, *J* = 6.3 Hz, 2H). **¹³C NMR** (101 MHz, DMSO-d₆) δ 196.8, 166.6, 139.3, 134.8, 129.6, 128.2, 41.1, 39.5. **HRMS**: calcd. for C₁₀H₈ClO₃⁻, (M-H)⁻: 211.0167; found: 211.0172. **MF**: C₁₀H₉ClO₃. **MW**: 212.63.



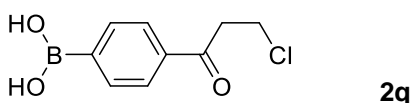
1-(4-(Tert-butyl)phenyl)-3-chloropropan-1-one was prepared following the general ring opening procedure A using **1n** as starting material and isolated as colorless oil (46 mg, 0.21 mmol, 68%). **¹H NMR** (300 MHz, CDCl₃): δ 7.90 (d, *J* = 8.7 Hz, 2H), 7.49 (d, *J* = 8.7 Hz, 2H), 3.92 (t, *J* = 6.9 Hz, 2H), 3.44 (t, *J* = 6.9 Hz, 2H), 1.34 (s, 9H). **¹³C NMR** (75 MHz, CDCl₃) δ 196.5, 157.5, 133.9, 128.2, 125.8, 41.3, 39.0, 35.3, 31.2. **HRMS**: calcd. for C₁₃H₁₈ClO⁺, (M+H)⁺: 225.1041; found: 225.1090. **MF**: C₁₃H₁₇ClO. **MW**: 224.73.



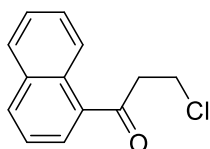
3-Chloro-1-mesitylpropan-1-one was prepared following the general ring opening procedure A using **1o** as starting material and isolated as colorless oil (22 mg, 0.10 mmol, 35%). **¹H NMR** (300 MHz, CDCl₃): δ 7.90 (d, *J* = 8.7 Hz, 2H), 7.49 (d, *J* = 8.7 Hz, 2H), 3.92 (t, *J* = 6.9 Hz, 2H), 3.44 (t, *J* = 6.9 Hz, 2H), 1.34 (s, 9H). **¹³C NMR** (75 MHz, CDCl₃) δ 206.9, 139.0, 138.6, 132.9, 128.8, 47.2, 37.9, 21.2, 19.3. **HRMS**: calcd. for C₁₂H₁₆ClO⁺, (M+H)⁺: 211.0884; found: 211.0887. **MF**: C₁₂H₁₅ClO. **MW**: 210.70.



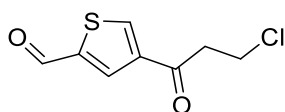
1-([1,1'-Biphenyl]-4-yl)-3-chloropropan-1-one was prepared following the general ring opening procedure A using **1p** as starting material and isolated as white crystals (64 mg, 0.26 mmol, 87%). **¹H NMR** (400 MHz, CDCl₃): δ 8.06-8.01 (m, 2H), 7.73-7.68 (m, 2H), 7.66-7.61 (m, 2H), 7.51-7.45 (m, 2H), 7.44-7.39 (m, 1H), 3.95 (t, *J* = 6.8 Hz, 2H), 3.49 (t, *J* = 6.8 Hz, 2H). **¹³C NMR** (101 MHz, CDCl₃): δ 196.4, 146.3, 139.8, 135.2, 129.1, 128.8, 128.5, 127.5, 127.4, 41.4, 38.9. **HRMS**: calcd. for C₁₅H₁₃ClO⁺, (M)⁺: 244.0655; found: 244.0649. **MF**: C₁₅H₁₃ClO. **MW**: 244.72.



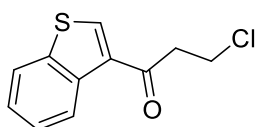
(4-(3-Chloropropanoyl)phenyl)boronic acid was prepared following the general ring opening procedure A using 4-cyclopropylbenzene boronic acid as starting material. The yield was determined using ¹H-NMR with benzene as internal standard (65%). **¹H NMR** (300 MHz, D₂O) δ 8.29-8.14 (m, 4H), 4.21 (t, *J* = 6.2 Hz, 2H), 3.82 (t, *J* = 6.2 Hz, 2H). **¹³C NMR** (101 MHz, Acetone-d₆) δ 197.4, 138.8, 135.1, 127.6, 41.9, 39.8. **HRMS**: calcd. for C₉H₉BClO₃⁻, (M-H)⁻: 211.0339; found: 211.0339. **MF**: C₉H₁₀BClO₃. **MW**: 212.44.

**2r**

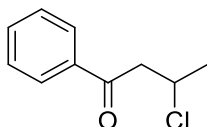
3-Chloro-1-(naphthalen-1-yl)propan-1-one was prepared following the general ring opening procedure A using **1r** as starting material and isolated as yellowish oil (33 mg, 0.15 mmol, 50%). **¹H NMR** (400 MHz, CDCl₃): δ 8.67 (d, *J* = 9.0 Hz, 1H), 8.02 (d, *J* = 8.2 Hz, 1H), 7.92-7.87 (m, 2H), 7.64-7.50 (m, 3H), 3.99 (t, *J* = 6.6 Hz, 2H), 3.54 (t, *J* = 6.6 Hz, 2H). **¹³C NMR** (101 MHz, CDCl₃) δ 200.6, 135.1, 134.1, 133.4, 130.2, 128.6, 128.4, 128.1, 126.8, 125.9, 124.5, 44.4, 39.3. **HRMS**: calcd. for C₁₃H₁₁ClO⁺, (*M*)⁺: 218.0493; found: 218.0487. **MF**: C₁₃H₁₁ClO. **MW**: 218.68.

**2s**

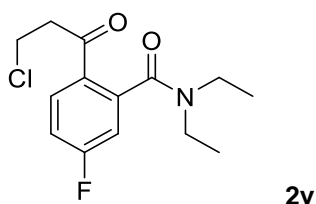
4-(3-Chloropropanoyl)thiophene-2-carbaldehyde was prepared following the general ring opening procedure A using **1s** as starting material and isolated as yellow crystalline solid (19 mg, 0.09 mmol, 31%). **¹H NMR** (400 MHz, CDCl₃): δ 9.96 (s, 1H), 8.41 (s, 1H), 8.19 (s, 1H), 3.91 (t, *J* = 6.6 Hz, 2H), 3.38 (t, *J* = 6.6 Hz, 2H). **¹³C NMR** (101 MHz, CDCl₃): δ 190.4, 182.9, 144.9, 142.4, 139.7, 135.0, 42.4, 38.2, 29.8. **HRMS**: calcd. for C₈H₈ClO₂S⁺, (*M*+H)⁺: 202.9928; found: 202.9931. **MF**: C₈H₇ClO₂S. **MW**: 202.65.

**2t**

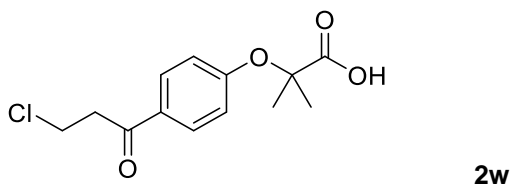
41-(Benzo[b]thiophen-3-yl)-3-chloropropan-1-one was prepared following the general ring opening procedure A using **1t** as starting material and isolated as colorless oil (31 mg, 0.14 mmol, 46%). **¹H NMR** (400 MHz, CDCl₃): δ 8.77 (d, *J* = 8.5 Hz, 1H), 8.31 (s, 1H), 7.87 (d, *J* = 8.1 Hz, 1H), 7.54-7.48 (m, 1H), 7.47-7.41 (m, 1H), 3.96 (t, *J* = 6.7 Hz, 2H), 3.47 (t, *J* = 6.7 Hz, 2H). **¹³C NMR** (101 MHz, CDCl₃): δ 191.7, 139.9, 137.49, 136.51, 135.0, 126.2, 125.8, 125.8, 122.4, 42.7, 38.9. NMR data matches literature reference.^[38] **HRMS**: calcd. for C₁₁H₉ClOS⁺, (*M*)⁺: 224.0057; found: 224.0052. **MF**: C₁₁H₉ClOS. **MW**: 224.70.

**2u**

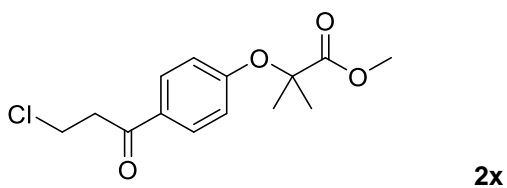
3-Chloro-1-phenylbutan-1-one was prepared following the general ring opening procedure A using **1u** as starting material and isolated as colorless solid (26 mg, 0.14 mmol, 47%). **¹H NMR** (400 MHz, CDCl₃): δ 7.98-7.93 (m, 2H); 7.62-7.56 (m, 1H), 7.52-7.45 (m, 2H), 4.67 (h, *J* = 6.6 Hz, 1H), 3.59 (dd, *J* = 17.1, 6.8 Hz, 1H), 3.26 (dd, *J* = 17.1, 6.5 Hz, 1H), 1.64 (d, *J* = 6.6 Hz, 3H). **¹³C NMR** (101 MHz, CDCl₃): δ 196.8, 136.7, 133.6, 128.9, 128.3, 52.9, 48.8, 25.5. NMR matches literature reference.^[39] **HRMS**: calcd. for C₁₀H₁₁ClO⁺, (*M*)⁺: 182.0493; found: 182.0488. **MF**: C₁₀H₁₁ClO. **MW**: 182.65.



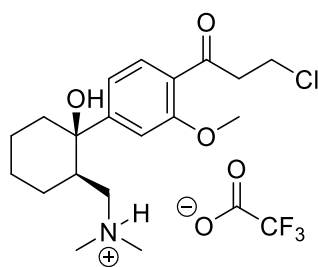
2-(3-Chloropropanoyl)-N,N-diethyl-5-fluorobenzamide was prepared following the general ring opening procedure A using **1v** as starting material and isolated as colorless oil (35 mg, 0.12 mmol, 41%). **¹H NMR** (400 MHz, CDCl₃): δ 7.84 (dd, *J* = 8.7, 5.2 Hz, 1H), 7.14 (td, *J* = 8.3, 2.6 Hz, 1H), 6.98 (dd, *J* = 8.4, 2.6 Hz, 1H), 3.85 (t, *J* = 6.8 Hz, 2H), 3.55 (q, *J* = 7.2 Hz, 2H), 3.37 (t, *J* = 6.8 Hz, 2H), 3.09 (q, *J* = 7.1 Hz, 2H), 1.29 (t, *J* = 7.1 Hz, 3H), 1.05 (t, *J* = 7.2 Hz, 3H). **¹³C NMR** (101 MHz, CDCl₃): 196.0, 169.1 (d, *J* = 1.6 Hz), 164.9 (d, *J* = 257.2 Hz), 141.3 (d, *J* = 7.7 Hz), 131.8 (d, *J* = 9.3 Hz), 131.0 (d, *J* = 3.3 Hz), 115.7 (d, *J* = 21.7 Hz), 115.0 (d, *J* = 23.1 Hz), 42.9, 42.5, 39.0, 38.6, 13.6, 12.3. **¹⁹F NMR** (400 MHz, CDCl₃): -104.9. **HRMS**: calcd. for C₁₄H₁₈ClFNO₂⁺, (M+H)⁺: 286.1005; found: 286.1025. **MF**: C₁₄H₁₇ClFNO₂. **MW**: 285.74.



2-(4-(3-Chloropropanoyl)phenoxy)-2-methylpropanoic acid was prepared following the general ring opening procedure A using **1w** as starting material and isolated as colorless solid (6 mg, 0.02 mmol, 7%). **¹H NMR** (400 MHz, CDCl₃): δ 7.95-7.89 (m, 2H), 6.96-6.91 (m, 2H), 3.91 (t, *J* = 6.8 Hz, 2H), 3.40 (t, *J* = 6.8 Hz, 2H), 1.70 (s, 6H). **HRMS**: calcd. for C₁₃H₁₄ClO₄⁻, (M-H)⁻: 269.0586; found: 269.0593. **MF**: C₁₃H₁₅ClO₄. **MW**: 270.71.



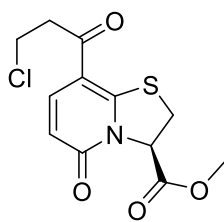
Methyl 2-(4-(3-chloropropanoyl)phenoxy)-2-methylpropanoate was prepared following the general ring opening procedure A using **1x** as starting material and isolated as colorless oil (59 mg, 0.20 mmol, 65%). **¹H NMR** (400 MHz, CDCl₃): δ 7.92-7.83 (m, 2H), 6.87-6.79 (m, 2H), 3.90 (t, *J* = 6.9 Hz, 2H), 3.76 (s, 3H), 3.39 (t, *J* = 6.9 Hz, 2H), 1.66 (s, 6H). **¹³C NMR** (101 MHz, CDCl₃): δ 195.3, 174.3, 160.2, 130.2, 117.6, 79.5, 52.9, 41.1, 39.0, 25.5. **HRMS**: calcd. for C₁₃H₁₄ClO₄⁺, (M+H)⁺: 285.0888; found: 285.0891. **MF**: C₁₄H₁₇ClO₄. **MW**: 284.74.



2y

3-Chloro-1-(4-((1R,2R)-2-((dimethylamino)methyl)-1-hydroxycyclohexyl)-2-

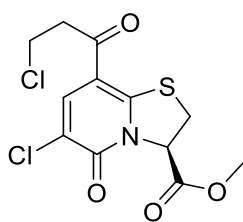
methoxyphenyl)propan-1-one was prepared following the general ring opening procedure A (but only on 0.15 mmol scale) using **1y** as starting material and isolated as white solid (TFA salt) after reverse phase column chromatography and lyophilization (51 mg, 0.11 mmol, 73%). **¹H NMR** (400 MHz, DMSO-d₆) δ 9.34 (s, 1H), 7.64 (d, *J* = 8.1 Hz, 1H), 7.30 (s, 1H), 7.20 (d, *J* = 8.1 Hz, 1H), 3.93 (s, 3H), 3.89 (t, *J* = 6.3 Hz, 2H), 3.44 (t, *J* = 6.3 Hz, 2H), 2.89 (t, *J* = 11.7 Hz, 1H), 2.66 (d, *J* = 4.3 Hz, 3H), 2.53 (d, *J* = 4.5 Hz, 3H), 2.43-2.29 (m, 2H), 1.93-1.34 (m, 9H). **¹³C NMR** (101 MHz, DMSO-d₆) δ 197.1, 158.8, 155.4, 129.8, 124.9, 117.3, 109.4, 74.2, 59.3, 55.9, 45.8, 44.9, 40.8, 40.1, 39.9, 39.6, 25.3, 24.2, 21.0. **HRMS**: calcd. for C₁₉H₂₉ClNO₃⁺, (M+H)⁺: 354.1830; found: 354.1845. **MF**: C₂₁H₂₉ClF₃NO₅. **MW**: 467.91.



2z

Methyl (R)-8-(3-chloropropanoyl)-5-oxo-2,3-dihydro-5H-thiazolo[3,2-a]pyridine-3-carboxylate

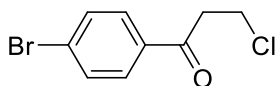
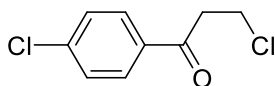
was prepared following the general ring opening procedure A using **1z** as starting material and isolated as yellowish solid (9 mg, 0.03 mmol, 10%). **¹H NMR** (400 MHz, CDCl₃) δ 7.78 (d, *J* = 9.6 Hz, 1H), 6.32 (d, *J* = 9.6 Hz, 1H), 5.61 (dd, *J* = 9.6, 2.6 Hz, 1H), 3.89 (t, *J* = 6.9 Hz, 2H), 3.81 (s, 3H), 3.64 (dd, *J* = 12.1, 9.6 Hz, 1H), 3.49 (dd, *J* = 12.1, 2.6 Hz, 1H), 3.26 (t, *J* = 6.7 Hz, 2H). **HRMS**: calcd. for C₁₂H₁₃ClNO₄S⁺, (M+H)⁺: 302.0248; found: 302.0250. **MF**: C₁₂H₁₂ClNO₄S. **MW**: 301.74.



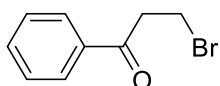
2aa

Methyl (R)-6-chloro-8-(3-chloropropanoyl)-5-oxo-2,3-dihydro-5H-thiazolo[3,2-a]pyridine-3-carboxylate

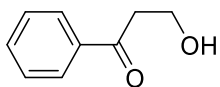
was prepared following the general ring opening procedure A using **1aa** as starting material and isolated as yellowish solid (11 mg, 0.03 mmol, 11%). **¹H NMR** (400 MHz, CDCl₃) δ 7.95 (s, 1H), 5.64 (dd, *J* = 9.6, 2.4 Hz, 1H), 3.89 (t, *J* = 6.7 Hz, 1H), 3.81 (s, 3H), 3.68 (dd, *J* = 12.2, 9.6 Hz, 1H), 3.52 (dd, *J* = 12.2, 2.5 Hz, 1H), 3.26 (t, *J* = 6.6 Hz, 1H). **¹³C NMR** (101 MHz, CDCl₃) δ 191.1, 167.8, 157.6, 156.7, 136.7, 120.1, 111.4, 62.8, 53.8, 40.8, 38.3, 31.9. **HRMS**: calcd. for C₁₂H₁₁Cl₂NO₄S⁺, (M+H)⁺: 335.9859; found: 335.9864. **MF**: C₁₂H₁₁Cl₂NO₄S. **MW**: 336.18.

**2ad****2j**

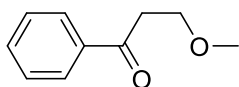
1-(4-Bromophenyl)-3-chloropropan-1-one was prepared following the general ring opening procedure A using **1ad** as starting material and isolated as yellow solid as a 1:1 mixture with **2j** (27 mg, 0.11 mmol, 36% + 22 mg, 0.11 mmol **2j**). **¹H NMR** (300 MHz, CDCl₃) δ 7.84-7.79 (m, 2H), 7.65-7.60 (m, 2H), 3.91 (t, *J* = 6.7 Hz, 2H), 3.43 (t, *J* = 6.8 Hz, 1H). **¹³C NMR** (75 MHz, CDCl₃) δ 195.9, 135.2, 132.2, 129.7, 128.7, 41.3, 38.6. NMR data matches literature reference.^[40] **HRMS**: calcd. for C₉H₈BrClO⁺, (M)⁺: 245.9442; found: 245.9440. **MF**: C₉H₈BrClO. **MW**: 247.52.

**3a**

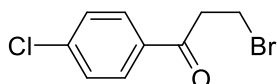
3-Bromo-1-phenylpropan-1-one was prepared following general ring opening procedure B using **1a** as starting material and isolated as white crystals (23 mg, 0.15 mmol, 51%). **¹H NMR** (400 MHz, CDCl₃) δ 7.99-7.92 (m, 2H), 7.62-7.57 (m, 1H), 7.52-7.45 (m, 2H), 3.75 (t, *J* = 7.1 Hz, 2H), 3.58 (t, *J* = 7.0 Hz, 2H). **¹³C NMR** (101 MHz, CDCl₃) δ 197.1, 136.4, 133.7, 128.9, 128.2, 41.7, 25.9. NMR data matches literature reference.^[41] **HRMS**: calcd. for C₉H₁₀BrO⁺, (M+H)⁺: 212.9910; found: 212.9912. **MF**: C₉H₉BrO. **MW**: 213.07.

**3b**

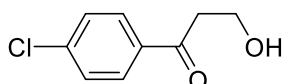
3-Hydroxy-1-phenylpropan-1-one was prepared following general ring opening procedure B using **1a** as starting material and isolated as yellow oil (25 mg, 0.17 mmol, 56%). **¹H NMR** (400 MHz, CDCl₃): δ 7.99-7.93 (m, 2H), 7.63-7.55 (m, 1H), 7.52-7.44 (m, 2H), 4.04 (t, *J* = 5.3 Hz, 2H), 3.23 (t, *J* = 5.3 Hz, 2H), 2.80 (brs, 1H). **¹³C NMR** (101 MHz, CDCl₃) δ 200.6, 136.8, 133.7, 128.8, 128.2, 58.2, 40.5. NMR matches literature reference.^[42] **HRMS**: calcd. for C₉H₁₁O₂⁺, (M+H)⁺: 151.0754; found: 151.0763. **MF**: C₉H₁₀O₂. **MW**: 150.18.

**3c**

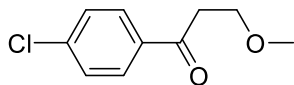
3-Methoxy-1-phenylpropan-1-one was prepared following general ring opening procedure B using **1a** as starting material and isolated as colorless oil (32 mg, 0.19 mmol, 65%). **¹H NMR** (400 MHz, CDCl₃): δ 7.99-7.93 (m, 2H), 7.59-7.53 (m, 1H), 7.49-7.43 (m, 2H), 3.83 (t, *J* = 6.5 Hz, 2H), 3.38 (s, 3H), 3.25 (t, *J* = 6.5 Hz, 2H). **¹³C NMR** (101 MHz, CDCl₃) δ 198.5, 137.1, 133.3, 128.7, 128.3, 68.0, 59.1, 38.8. NMR matches literature reference.^[43] **HRMS**: calcd. for C₁₀H₁₃O₂⁺, (M+H)⁺: 165.0910; found: 165.0927. **MF**: C₁₀H₁₂O₂. **MW**: 164.20.

**3d**

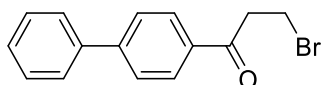
3-Bromo-1-(4-chlorophenyl)propan-1-one was prepared following general ring opening procedure B using **1j** as starting material and isolated as colorless oil (24 mg, 0.10 mmol, 32%). **¹H NMR** (400 MHz, CDCl₃) δ 7.93-7.84 (m, 2H), 7.50-7.41 (m, 2H), 3.73 (t, *J* = 6.8 Hz, 2H), 3.54 (t, *J* = 6.8 Hz, 2H). **¹³C NMR** (101 MHz, CDCl₃) δ 195.9, 140.2, 134.7, 129.6, 129.2, 41.6, 25.6. NMR data matches literature reference.^[41] **HRMS**: calcd. for C₉H₉BrClO⁺, (M+H)⁺: 246.9520; found: 246.9522. **MF**: C₉H₈BrClO. **MW**: 247.52.

**3e**

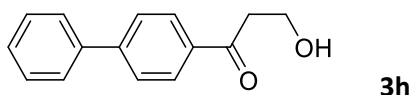
1-(4-Chlorophenyl)-3-hydroxypropan-1-one was prepared following general ring opening procedure B using **1j** as starting material and isolated as colorless oil (29 mg, 0.16 mmol, 52%). **¹H NMR** (400 MHz, CDCl₃): δ 7.95-7.85 (m, 2H), 7.49-7.39 (m, 2H), 4.03 (t, *J* = 5.3 Hz, 2H), 3.20 (t, *J* = 5.3 Hz, 2H), 2.29 (brs, 1H). **¹³C NMR** (101 MHz, CDCl₃) δ 199.3, 140.2, 135.1, 129.6, 129.2, 58.1, 40.5. NMR data matches literature reference.^[42] **HRMS**: calcd. for C₉H₁₀ClO₂⁺, (M+H)⁺: 185.0364; found: 185.0364. **MF**: C₉H₉ClO₂. **MW**: 184.62.

**3f**

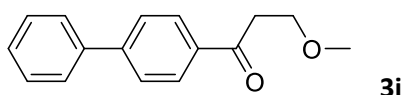
1-(4-Chlorophenyl)-3-methoxypropan-1-one was prepared following general ring opening procedure B using **1j** as starting material and isolated as colorless oil (32 mg, 0.19 mmol, 65%). **¹H NMR** (400 MHz, CDCl₃): δ 7.93-7.86 (m, 2H), 7.46-7.40 (m, 2H), 3.81 (t, *J* = 6.4 Hz, 2H), 3.37 (s, 3H), 3.20 (t, *J* = 6.4 Hz, 2H). **¹³C NMR** (101 MHz, CDCl₃) δ 197.3, 139.8, 135.5, 129.7, 129.1, 67.9, 59.1, 38.8. NMR matches literature reference.^[43] **HRMS**: calcd. for C₁₀H₁₂ClO₂⁺, (M+H)⁺: 199.0520; found: 199.0521. **MF**: C₁₀H₁₁ClO₂. **MW**: 198.65.

**3g**

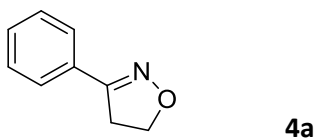
1-([1,1'-Biphenyl]-4-yl)-3-bromopropan-1-one was prepared following general ring opening procedure B using **1p** as starting material and isolated as white crystals (57 mg, 0.20 mmol, 66%). **¹H NMR** (400 MHz, CDCl₃): δ 8.07-7.99 (m, 2H), 7.74-7.68 (m, 2H), 7.66-7.61 (m, 2H), 7.52-7.45 (m, 2H), 7.44-7.39 (m, 1H), 3.77 (t, *J* = 7.0 Hz, 2H), 3.61 (t, *J* = 6.8 Hz, 2H). **¹³C NMR** (101 MHz, CDCl₃) δ 196.7, 146.4, 139.8, 135.1, 129.1, 128.8, 128.5, 127.5, 127.4, 41.7, 26.0. **HRMS**: calcd. for C₁₅H₁₄BrO⁺, (M)⁺: 289.0223; found: 289.0221. **MF**: C₁₅H₁₃BrO. **MW**: 289.17.



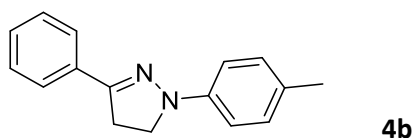
1-([1,1'-Biphenyl]-4-yl)-3-hydroxypropan-1-one was prepared following general ring opening procedure B using **1p** as starting material and isolated as white crystals (40 mg, 0.18 mmol, 59%). **¹H NMR** (400 MHz, CDCl₃): δ 8.00-7.92 (m, 2H), 7.63-7.55 (m, 1H), 7.52-7.43 (m, 2H), 4.48 (brs, 1H), 4.06 (t, *J* = 5.3 Hz, 2H), 3.25 (t, *J* = 5.3 Hz, 2H). **¹³C NMR** (101 MHz, CDCl₃) δ 200.8, 136.6, 133.8, 128.9, 128.2, 58.3, 40.3. **HRMS**: calcd. for C₁₅H₁₅O₂⁺, (M+H)⁺: 227.1067; found: 227.1067. **MF**: C₁₅H₁₄O₂. **MW**: 226.28.



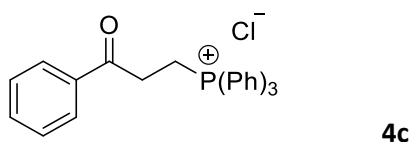
1-([1,1'-Biphenyl]-4-yl)-3-methoxypropan-1-one was prepared following general ring opening procedure B using **1p** as starting material and isolated as colorless/yellowish crystals (64 mg, 0.27 mmol, 89%). **¹H NMR** (400 MHz, CDCl₃): δ 8.08-8.02 (m, 2H), 7.72-7.66 (m, 2H), 7.65-7.60 (m, 2H), 7.50-7.43 (m, 2H), 7.43-7.36 (m, 1H), 3.86 (t, *J* = 6.5 Hz, 2H), 3.40 (s, 3H), 3.28 (t, *J* = 6.5 Hz, 2H). **¹³C NMR** (101 MHz, CDCl₃) δ 198.0, 145.9, 139.9, 135.8, 129.1, 128.9, 128.3, 127.4, 127.4, 68.1, 59.1, 38.8. NMR matches literature reference.^[43] **HRMS**: calcd. for C₁₆H₁₇O₂⁺, (M+H)⁺: 241.1223; found: 241.1219. **MF**: C₁₆H₁₆O₂. **MW**: 240.30.



3-Phenyl-4,5-dihydroisoxazole was prepared on 0.3 mmol scale using **2a** as starting material. **2a** from step 1 was dissolved in pyridine (1 mL) and hydroxylamine hydrochloride (192 mg, 1.8 mmol, 6 equiv.) was added. Additional pyridine (5 mL) was added, and the reaction was stirred for 24 hours at room temperature before heating the reaction to 120 °C. After two hours at 120 °C, the reaction was concentrated *via* rotary evaporation, then purified by column chromatography yielding a white solid (22 mg, 0.15 mmol, 50% over 2 steps). **¹H NMR** (400 MHz, CDCl₃): δ 7.75-7.64 (m, 1H), 7.46-7.37 (m, 1H), 4.48 (t, *J* = 10.1 Hz, 1H), 3.34 (t, *J* = 10.1 Hz, 1H). **¹³C NMR** (101 MHz, CDCl₃): δ 156.9, 130.2, 129.6, 128.8, 126.9, 69.3, 35.4. NMR matches literature reference.^[44] **HRMS**: calcd. for C₉H₉NO⁺, (M)⁺: 147.0679; found: 147.0685. **MF**: C₉H₉NO. **MW**: 147.18.



3-Phenyl-1-(p-tolyl)-4,5-dihydro-1H-pyrazole was prepared on 0.3 mmol scale using **2a** as starting material. **2a** from step 1 was dissolved in ethanol (3 mL) and tolylhydrazine hydrochloride (95 mg, 0.6 mmol, 2 equiv.) was added. The reaction was stirred for 24 hours at room temperature and afterwards concentrated *via* rotary evaporation, then purified by column chromatography yielding a white solid (34 mg, 0.14 mmol, 48% over 2 steps). **¹H NMR** (300 MHz, CDCl₃): δ 7.79-7.71 (m, 2H), 7.44-7.29 (m, 3H), 7.17-7.04 (m, 4H), 3.86 (t, *J* = 10.5 Hz, 2H), 3.23 (t, *J* = 10.5 Hz, 2H), 2.36-2.27 (m, 6H). **¹³C NMR** (75 MHz, CDCl₃): δ 148.7, 144.0, 133.2, 129.7, 128.6, 128.5, 128.5, 125.7, 113.2, 48.8, 32.1, 20.7. NMR matches literature reference.^[45] **HRMS**: calcd. for C₁₆H₁₇N₂⁺, (M+H)⁺: 237.1386; found: 237.1391. **MF**: C₁₆H₁₆N₂. **MW**: 236.32.



(3-Oxo-3-phenylpropyl)triphenylphosphonium chloride was prepared on 0.3 mmol scale using **2a** as starting material. **2a** from step 1 was dissolved in benzene (3 mL) and triphenylphosphine (81,1 mg, 0.3 mmol, 1 equiv.) was added. The reaction was refluxed for 3 hours and the formed, white precipitate was filtered, washed with 5 mL benzene twice and dried to give a white solid (88 mg, 0.2 mmol, 69% over 2 steps). **¹H NMR** (400 MHz, DMSO-d₆) δ 7.96-7.84 (m, 11H), 7.82-7.73 (m, 6H), 7.68-7.61 (m, 1H), 7.50 (t, *J* = 7.7 Hz, 2H), 3.97-3.85 (m, 2H), 3.54-3.43 (m, 2H). **¹³C NMR** (101 MHz, DMSO-d₆) δ 195.7 (d, *J* = 14.2 Hz), 135.5 (d, *J* = 1 Hz), 134.9 (d, *J* = 2.8 Hz), 133.8 (d, *J* = 10.3 Hz), 130.2 (d, *J* = 12.5 Hz), 128.7, 128.1, 118.4 (d, *J* = 86.4 Hz), 31.1 (d, *J* = 1.4 Hz), 16.0 (d, *J* = 55.0 Hz). **³¹P NMR** (162 MHz, DMSO-d₆) δ 26.53 **HRMS**: calcd. for C₂₄H₂₇NOP⁺, (M+H)⁺: 395.1559; found: 395.1605. **MF**: C₂₄H₂₇CINOP. **MW**: 430.91.

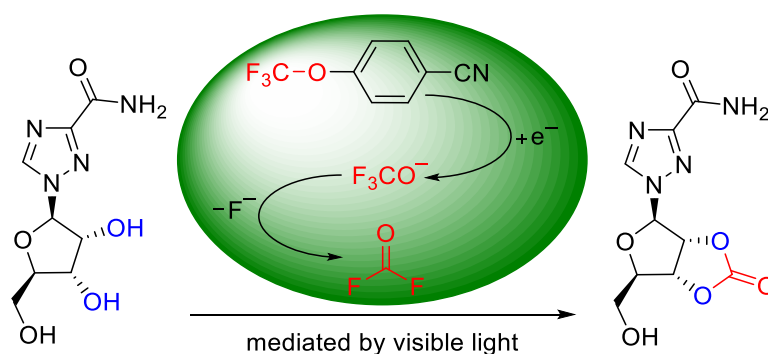
3.5 References

- [1] a) H. N. C. Wong, M. Y. Hon, C. W. Tse, Y. C. Yip, J. Tanko, T. Hudlicky, *Chem. Rev.* **1989**, *89*, 165-198; b) C. Ebner, E. M. Carreira, *Chem. Rev.* **2017**, *117*, 11651-11679; c) J. Salaun, *Chem. Rev.* **1989**, *89*, 1247-1270; d) O. G. Kulinkovich, *Chem. Rev.* **2003**, *103*, 2597-2632.
- [2] a) H.-U. Reissig, R. Zimmer, *Chem. Rev.* **2003**, *103*, 1151-1196; b) L. K. Sydnes, *Chem. Rev.* **2003**, *103*, 1133-1150.
- [3] a) K. L. Skubi, T. R. Blum, T. P. Yoon, *Chem. Rev.* **2016**, *116*, 10035-10074; b) L. Marzo, S. K. Pagire, O. Reiser, B. König, *Angew. Chem.* **2018**, *130*, 10188-10228.
- [4] a) V. R. Rao, S. S. Hixson, *J. Am. Chem. Soc.* **1979**, *101*, 6458-6459; b) S. S. Hixson, D. W. Garrett, *J. Am. Chem. Soc.* **1974**, *96*, 4872-4879.
- [5] a) A. V. Trukhin, E. V. Eliseenkov, A. S. Dneprovskii, *J. Phys. Org. Chem.* **2003**, *16*, 189-193; b) J. P. Dinnocenzo, T. R. Simpson, H. Zuilhof, W. P. Todd, T. Heinrich, *J. Am. Chem. Soc.* **1997**, *119*, 987-993; c) J. P. Dinnocenzo, H. Zuilhof, D. R. Lieberman, T. R. Simpson, M. W. McKechney, *J. Am. Chem. Soc.* **1997**, *119*, 994-1004.
- [6] a) K. Kaur, V. Kumar, A. K. Sharma, G. K. Gupta, *Eur. J. Med. Chem.* **2014**, *77*, 121-133; b) B. Varghese, S. N. Al-Busafi, F. O. Suliman, S. M. Z. Al-Kindy, *RSC Ad.* **2017**, *7*, 46999-47016; c) Z.-L. Shen, K. K. Goh, C. H. A. Wong, Y.-S. Yang, Y.-C. Lai, H.-L. Cheong, T.-P. Loh, *Chem. Commun.* **2011**, *47*, 4778-4780; d) Y. Zhu, K. Lin, D. Ye, W. Zhou, *Tetrahedron Lett.* **2015**, *56*, 5039-5042; e) D. Weichert, P. Gmeiner, *ACS Chem. Biol.* **2015**, *10*, 1376-1386.
- [7] W. J. Close, *J. Am. Chem. Soc.* **1957**, *79*, 1455-1458.
- [8] X. Fan, H. Zhao, J. Yu, X. Bao, C. Zhu, *Org. Chem. Front.* **2016**, *3*, 227-232.
- [9] D. Petzold, B. König, *Adv. Syn. Catal.* **2018**, *360*, 626-630.
- [10] a) J. A. D. Good, M. Kulén, J. Silver, K. S. Krishnan, W. Bahnan, C. Núñez-Otero, I. Nilsson, E. Wede, E. de Groot, Å. Gylfe, S. Bergström, F. Almqvist, *J. Med. Chem.* **2017**, *60*, 9393-9399; b) M. Kulén, M. Lindgren, S. Hansen, A. G. Cairns, C. Grundström, A. Begum, I. van der Lingen, K. Brännström, M. Hall, U. H. Sauer, J. Johansson, A. E. Sauer-Eriksson, F. Almqvist, *J. Med. Chem.* **2018**, *61*, 4165-4175; c) J. S. Pinkner; H. Remaut; F. Buelens; E. Miller; V. Åberg; N. Pemberton; M. Hedenström; A. Larsson; P. Seed; G. Waksman; S. J. Hultgren; F. Almqvist *Proc. Natl. Acad. Sci. USA* **2006**, *103*, 17897-17902; d) L. Cegelski; J. S. Pinkner; N. D. Hammer; C. K. Cusumano; C. S. Hung; E. Chorell; V. Åberg; J. N. Walker; P. C. Seed; F. Almqvist; M. R. Chapman; S. J. Hultgren *Nat. Chem. Biol.* **2009**, *5*, 913-919.
- [11] S. Callaghan, M. A. Filatov, E. Sitte, H. Savoie, R. W. Boyle, K. J. Flanagan, M. O. Senge, *Photochem. Photobiol. Sci.* **2017**, *16*, 1371-1374.
- [12] a) B. E. Maryanoff, A. B. Reitz, *Chem. Rev.* **1989**, *89*, 863-927; b) P. A. Byrne, D. G. Gilheany, *Chem. Soc. Rev.* **2013**, *42*, 6670-6696.
- [13] a) A. Beck, L. Goetsch, C. Dumontet, N. Corvaia, *Nat. Rev. Drug Discov.* **2017**, *16*, 315; b) K. Tsuchikama, Z. An, *Protein Cell* **2018**, *9*, 33-46; c) M. L. J. Doornbos, X. Wang, S. C. Vermond, L. Peeters, L. Pérez-Benito, A. A. Trabanco, H. Lavreysen, J. M. Cid, L. H. Heitman, G. Tresadern, A. P. Ijzerman, *J. Med. Chem.* **2018** (DOI: 10.1021/acs.jmedchem.8b00051); d) P. M. Kulkarni, A. R. Kulkarni, A. Korde, R. B. Tichkule, R. B. Laprairie, E. M. Denovan-Wright, H. Zhou, D. R.

- Janero, N. Zvonok, A. Makriyannis, M. G. Cascio, R. G. Pertwee, G. A. Thakur, *J. Med. Chem.* **2016**, *59*, 44-60.
- [14] D. A. Armstrong, R. E. Huie, S. Lyman, W. H. Koppenol, G. Merényi, P. Neta, D. M. Stanbury, S. Steenken, P. Wardman, *Biolnorg. React. Mech.*, **9**, **2013**, 59-61.
- [15] a) Y. Wang, L. Li, H. Ji, W. Ma, C. Chen, J. Zhao, *Chem. Commun.* **2014**, *50*, 2344-2346; b) C. Walling, B. Miller, *J. Am. Chem. Soc.* **1957**, *79*, 4181-4187.
- [16] W. C. Moore, *J. Am. Chem. Soc.* **1911**, *33*, 1091-1099.
- [17] B. H. J. Bielski, D. E. Cabelli, R. L. Arudi, A. B. Ross, *J. Phys. Chem. Rev. Data* **1985**, *14*, 1041-1100.
- [18] a) T. J. Fisher, P. H. Dussault, *Tetrahedron Lett.* **2010**, *51*, 5615-5617; b) H. Hock, H. Kropf, *Angew. Chem.* **1957**, *69*, 313-321.
- [19] F. A. Cotton, G. Wilkinson in *Advanced Inorganic Chemistry (4th ed.)*, Wiley-Interscience, New York, **1980** pp. 556-558.
- [20] a) G. R. Fulmer, A. J. M. Miller, N. H. Sherden, H. E. Gottlieb, A. Nudelman, B. M. Stoltz, J. E. Bercaw, K. I. Goldberg, *Organometallics* **2010**, *29*, 2176-2179; b) H. E. Gottlieb, V. Kotlyar, A. Nudelman, *J. Org. Chem.* **1997**, *62*, 7512-7515.
- [21] D. J. Wallace, C.-Y. Chen, *Tetrahedron Lett.* **2002**, *43*, 6987-6990.
- [22] J. C. Lorenz, J. Long, Z. Yang, S. Xue, Y. Xie, Y. Shi, *J. Org. Chem.* **2004**, *69*, 327-334.
- [23] Y.-Y. Zhou, C. Uyeda, *Angew. Chem. Int. Ed.* **2016**, *55*, 3171-3175.
- [24] B. Morandi, E. M. Carreira, *Science* **2012**, *335*, 1471-1474.
- [25] Y. Zhang, M. D. Tortorella, Y. Wang, J. Liu, Z. Tu, X. Liu, Y. Bai, D. Wen, X. Lu, Y. Lu, J. J. Talley, *ACS Med. Chem. Lett.* **2014**, *5*, 1162-1166.
- [26] G. Capocasa, G. Olivo, A. Barbieri, O. Lanzalunga, S. Di Stefano, *Catal. Sci. Technol.* **2017**, *7*, 5677-5686.
- [27] M. H. Gieuw, Z. Ke, Y.-Y. Yeung, *Angew. Chem. Int. Ed.* **2018**, *57*, 3782-3786.
- [28] G. A. Molander, P. E. Gormisky, *J. Org. Chem.* **2008**, *73*, 7481-7485.
- [29] M. Zhang, X. Cui, X. Chen, L. Wang, J. Li, Y. Wu, L. Hou, Y. Wu, *Tetrahedron* **2012**, *68*, 900-905.
- [30] M. H. Gieuw, Z. Ke, Y. Y. Yeung, *Angew. Chem. Int. Ed.* **2018**, *57*, 3782-3786.
- [31] M. Arndt, G. Hilt, A. F. Khlebnikov, S. I. Kozhushkov, A. de Meijere, *Eur. J. Org. Chem.* **2012**, 3112-3121.
- [32] M. Lemhadri, H. Doucet, M. Santelli, *Synth. Commun.* **2006**, *36*, 121-128.
- [33] C. Li, G. Xiao, Q. Zhao, H. Liu, T. Wang, W. Tang, *Org. Chem. Front.* **2014**, *1*, 225-229.
- [34] G. A. Molander, F. Beaumard, T. K. Niethamer, *J. Org. Chem.* **2011**, *76*, 8126-8130.
- [35] D. Petzold, B. König, *Adv. Syn. Catal.* **2018**, *360*, 626-630.
- [36] G. James A. D., J. Silver, C. Núñez-Otero, W. Bahnan, K. S. Krishnan, O. Sakin, P. Engström, R. Svensson, P. Artursson, Å. Gylfe, S. Bergström, F. Almqvist, *J. Med. Chem.* **2016**, *59*, 2094-2108.
- [37] H. S. G. Geiepl, G. Bernhart, P. Comba, G. Rajaraman, U. Hahn, F. Vögtle, *Eur. J. Inorg. Chem.* **2005**, 4501-4508.
- [38] S. Pérez-Silanes, J. Martínez-Esparza, A. M. Oficialdegui, H. Villanueva, L. Orúas, A. Monge, *J. Heterocyclic Chem.* **2001**, *38*, 1025-1030.
- [39] A. S.-Y. Lee, S.-H. Wang, Y.-T. Chang, *J. Chin. Chem. Soc.* **2014**, *61*, 364-368.

- [40] F.-Q. Huang, J. Xie, J.-G. Sun, Y.-W. Wang, X. Dong, L.-W. Qi, B. Zhang, *Org. Lett.* **2016**, *18*, 684-687.
- [41] S. An, D. Y. Moon, B. S. Park, *Tetrahedron* **2018**, *74*, 6922-6928.
- [42] J.-J. Yun, X.-Y. Liu, W. Deng, X.-Q. Chu, Z.-L. Shen, T.-P. Loh, *J. Org. Chem.* **2018**, *83*, 10898-10907.
- [43] S.-H. Guo, S.-Z. Xing, S. Mao, Y.-R. Gao, W.-L. Chen, Y.-Q. Wang, *Tetrahedron Lett.* **2014**, *55*, 6718-6720.
- [44] H. Huang, F. Li, Z. Xu, J. Cai, X. Ji, G.-J. Deng, *Adv. Syn. Catal.* **2017**, *359*, 3102-3107.
- [45] E. M. Afsah, E. M. Keshk, A.-R. H. Abdel-Rahman, N. F. Jomah, *J. Heterocyclic Chem.* **2018**, *55*, 326-334.

4. Visible Light Mediated Liberation and *in situ* Conversion of Fluorophosgene



Fluorophosgene was liberated by the photocatalytic reduction of a simple aryltrifluoromethoxyether. This highly reactive species was used for the synthesis of cyclic carbonates, carbamates and urea derivatives. The reaction mechanism was investigated by an in-depth NMR study as well as cyclovoltammetry and transient spectroscopy which suggests a charge-transfer complex dimer as the catalytic active species.

This chapter has been published in:

D. Petzold, P. Nitschke, F. Brandl, V. Scheidler, B. Dick, R. M. Gschwind, B. König, *Chem. Eur. J.* **2019**, 25, 361–366. (Communication) – Reproduced with permission from John Wiley and Sons.

Author Contributions:

DP and PN contributed equally to this work. DP carried out all photo reactions and wrote the manuscript, PN performed all the NMR mechanistic investigations and wrote the NMR chapter of the manuscript and the Supporting Information, FB performed the transient spectroscopic measurements and wrote the transient spectroscopy chapter of the Supporting Information, VS contributed to the NMR investigations. BD, RMG and BK supervised the project. BK is the corresponding author.

4.1 Introduction

Carbonates, carbamates and urea derivatives are privileged structures in organic synthesis and common motifs in pharmaceuticals, pesticides and plastics (Fig. 4-1 A).^[1] Many methods for the synthesis of these compounds have been described.^[2] The direct and most hazardous way is the use of gaseous phosgene or its less reactive derivatives diphosgene and triphosgene.^[3] However, handling of those compounds in the lab or in industry plants requires special safety precautions due to their severe toxicity.^[4] Alternative procedures utilize activated or non-activated carbonates or ureas, which are either prepared by reaction with phosgene or less efficiently from CO₂ (Fig. 4-1 B).^[2, 5] Some of these procedures require harsh reaction conditions or suffer from low reactivity and poor atom economy.^[2] Therefore, there is still a significant demand for a less hazardous, practical and easily controllable generation of reactive C1 building blocks.

Photoredox catalysis with organic photosensitizers has received tremendous attention in the past years.^[6] Many useful transformations without the need of metal catalysts were discovered, exploiting the versatile reduction and oxidation potentials of organic photocatalysts.^[7] The common requirement for a typical photocatalytic reaction is the generation of a radical species which can either react with another radical, a sp²/sp center, a nucleophile or a metal complex.^[8] However, the photocatalytic generation of intermediates with pure ionic reactivity remains elusive because energy and single electron transfer are the predominant reaction paths of all common photocatalysts.^[9] But especially under photo-reductive conditions most leaving groups are ionic species, e.g. halides, pseudo halides or cyanide, which are neglected in the course of the reaction because they possess only limited reactivity and/or were already exploited in thermal and photochemical reactions (Fig. 4-1 C).^[10] On the other hand, the C-OCF₃ bond could only be activated electrochemically or under harsh reaction conditions so far.^[11] However, the photocatalytic N-OCF₃ cleavage of complex starting materials was reported very recently.^[12] To address the need of a hazard- and metal-free access to highly reactive C1 building blocks, we envisioned to cleave the C-OCF₃ bond of a simple, commercially available aryl trifluoromethoxy ether by photoredox catalysis. We identified 4-(trifluoromethoxy)-benzonitrile as a suitable starting material, which can be cleaved quantitatively into benzonitrile and fluorophosgene by an organic photosensitizer (Fig. 4-1 D). Furthermore, we investigated the reaction mechanism by NMR kinetic and structural analyses and propose a photo-reductive mechanism based on the results of radical trapping experiments and excited state quenching experiments monitored by transient spectroscopy.

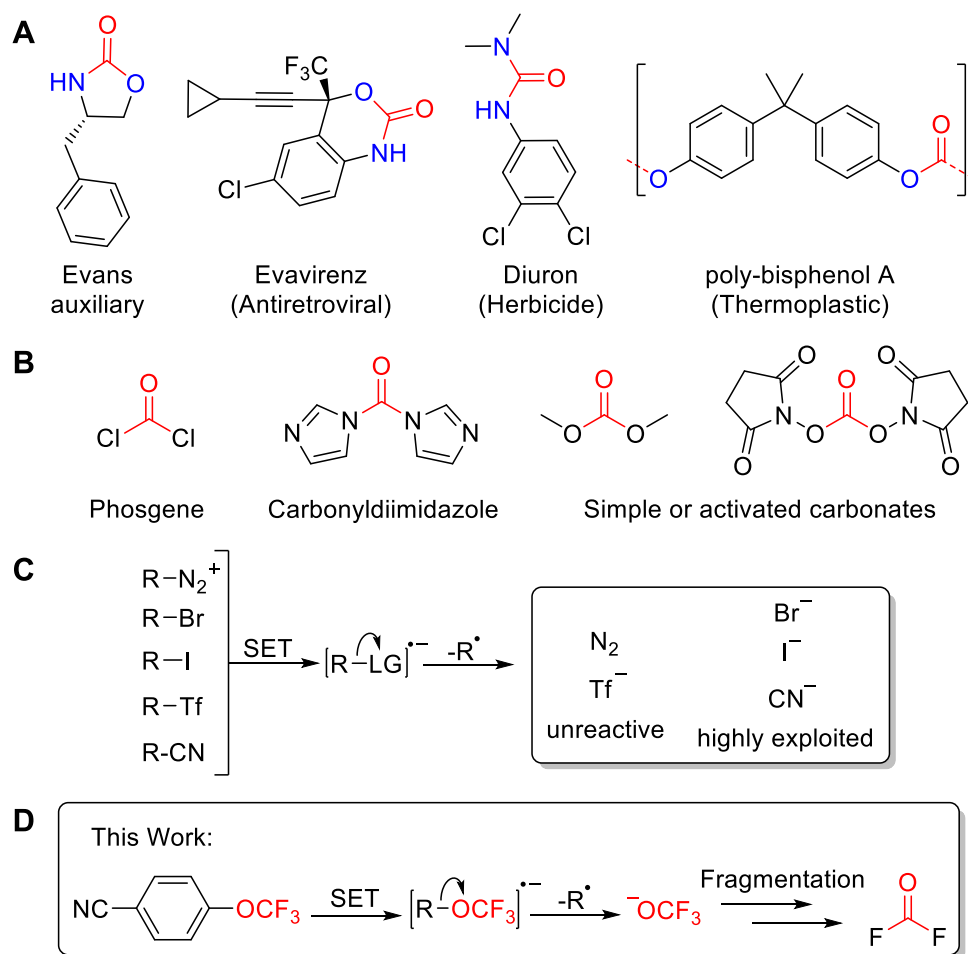
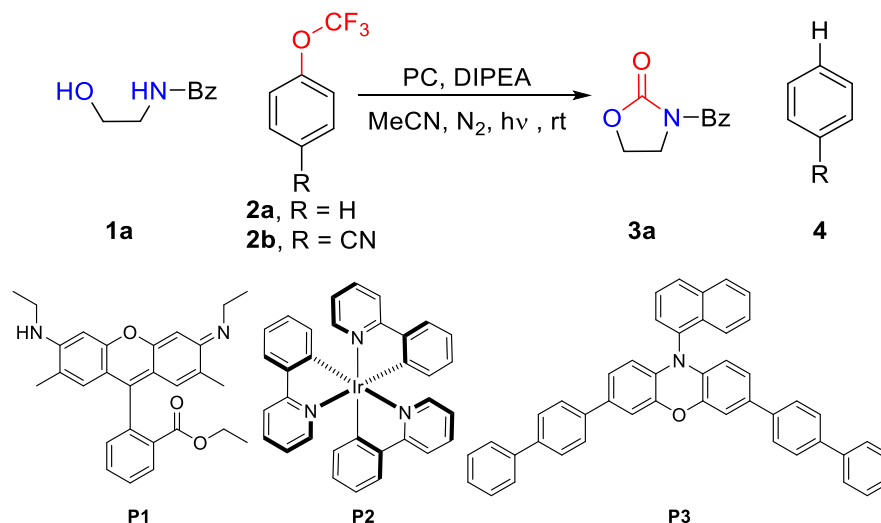


Figure 4-1. **A:** Structures of prominent carbamate or urea containing molecules used in synthesis, pharmacy, agriculture and daily life. **B:** Structures of phosgene and commonly employed alternatives. **C:** Typical leaving groups and their reactivity profile in photoredox catalysis. **D:** Overview of the photocatalytic fluorophosgene generation; Tf = trifluoromethanesulfonate, R = benzonitrile.

4.2 Results and Discussion

4.2.1 Synthesis

We began our investigation using 2-benzylaminoethanol (**1a**) as a model substrate, Rhodamine 6G (**P1**) as a strongly reducing photosensitizer, diisopropylethylamine (DIPEA) as electron donor and trifluoromethoxybenzene (**2a**) as fluorophosgene precursor in neat acetonitrile.^[7b, c] However, no conversion of **2a** was observed (Table 4-1 entry 1). Switching to commonly employed Ir(ppy)₃ (**P2**) or to the recently reported, phenoxazine based photosensitizer **P3** did also not lead to fragmentation of **2a** (entries 2-3).^[13] Therefore, trifluoromethoxybenzene derivative **2b** bearing an electron withdrawing nitrile group was employed. Hence, the redox potential of **2b** was much more accessible ($E_{red}(\mathbf{2a}) = -3.0$ V vs. SCE compared with $E_{red}(\mathbf{2b}) = -2.1$ V vs. SCE, see Chapter 4.4 for details) and **2b** showed slow conversion in the presence of photosensitizer **P2** (entry 4). The reaction was significantly improved by switching to **P3** giving full conversion of **2b** and **1** (entry 5). Further optimization of the reaction lead to conditions giving **3a** in an excellent isolated yield (entry 6). Control experiments revealed that without catalyst, light or DIPEA no or only trace amounts of product could be obtained (entries 7-9). Finally, we observed that the cleavage of **2b** was independent of the presence of **1** (entry 10).

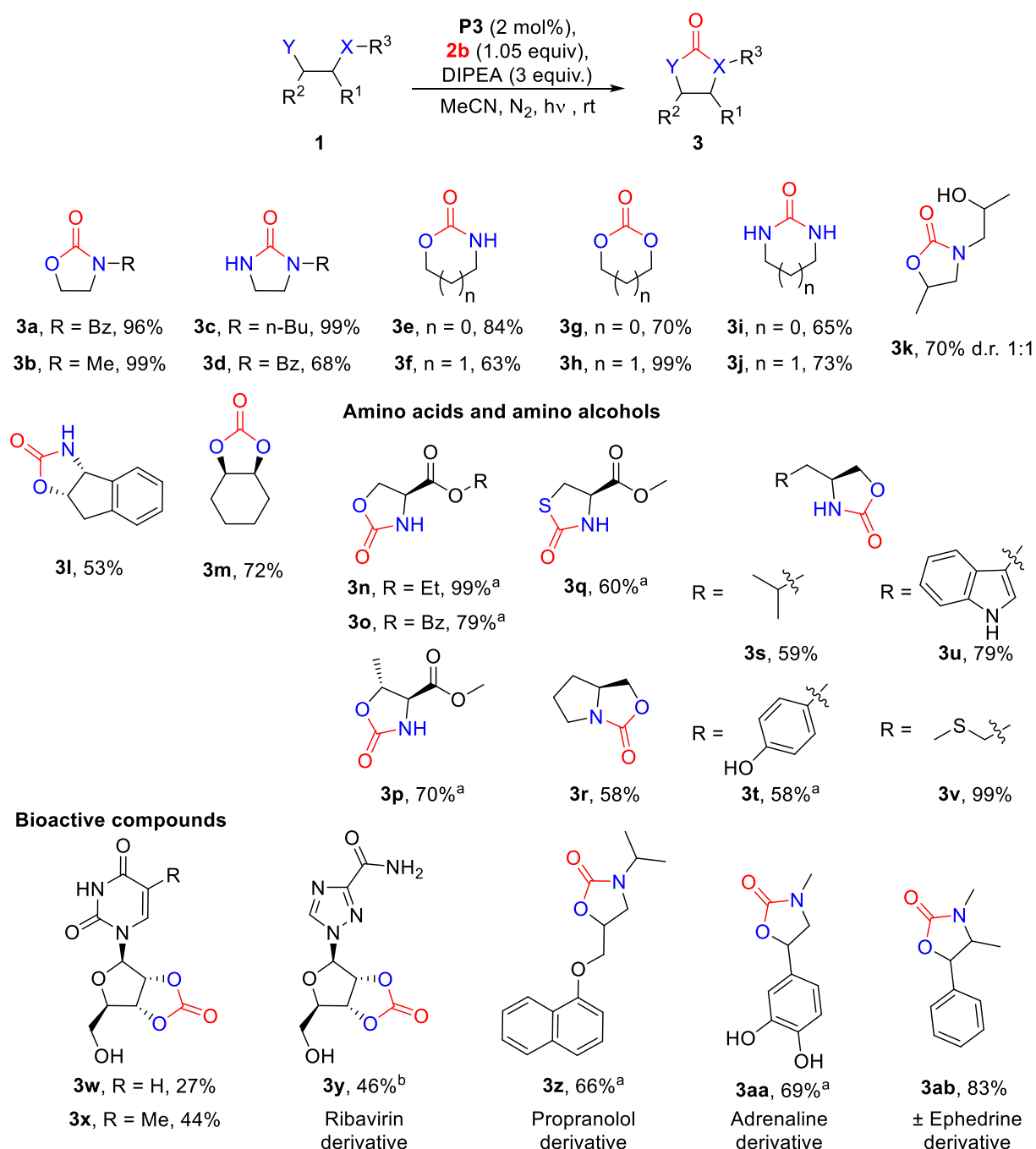
Table 4-1. Optimization of the reaction conditions

Entry	PC (mol%) / λ	Conversion of 2a/2b ^[a]	Conversion of 1a ^[a]
1	P1 (10) / 455 nm	2a 0%	0%
2	P2 (2) / 455 nm	2a 0%	0%
3	P3 (5) / 400 nm	2a 0%	0%
4	P2 (2) / 455 nm	2b 51%	40%
5	P3 (5) / 400 nm	2b 100%	100%
6 ^[b]	P3 (2) / 400 nm	2b 100%	100% [96%]
7 ^[b]	400 nm	2b 0%	0%
8 ^[b, c]	P3 (2)	2b 0%	0%
9 ^[b, d]	P3 (2) / 400 nm	2b traces	traces
10 ^[b, e]	P3 (2) / 400 nm	2b 100%	0%

General conditions: A mixture of 0.1 mmol of **1a**, 2 equiv. of **2b**, the indicated amount of PC, 4 equiv. of DIPEA in neat MeCN (0.1 M) under N₂ atmosphere were irradiated for 24 h with 400 nm light (or 455 nm for **P1** and **P2**). [a] Conversion determined by GC-FID, isolated yield of **3a** in brackets. [b] A mixture of 0.1 mmol of **1a**, 1.05 equiv. of **2b**, 2 mol% **P3**, 3 equiv. of DIPEA in dry MeCN (0.1 M) under N₂ atmosphere were irradiated for 24 h at 400 nm. [c] no light, 48 h. [d] no DIPEA. [e] no **1a**. Bz = benzyl.

In the next step, the synthetic scope of the method was investigated. *N*-substituted, five membered cyclic carbamates and ureas were prepared in good to excellent yield (Scheme 4-1 **3b-3d**). Unsubstituted, five and six membered cyclic carbamates, carbonates and ureas also showed good to excellent conversion (**3e-3j**). More complex carbamate **3k** was isolated in good yield with a diastereomeric ratio of 1:1. 1,2-Cis-configured carbamate **3l** and carbonate **3m** were prepared in moderate to good yield without racemization. Subsequently, amino acids and amino alcohols were investigated. The ethyl and benzyl ester of serine (**3n** and **3o**), as well as the methyl ester of threonine (**3p**) gave good to excellent yields. Noteworthy, **3p** was obtained diastereomerically pure indicating that no racemization of the reactive α -position took place. The methyl ester of cysteine (**3q**) gave a moderate yield, but demonstrated that also thiocarbamates can be obtained by this method. The corresponding carbamates of the amino alcohols prolinol, valinol and tyrosinol were isolated in moderate yields (**3r-3t**), whereas tryptophanol and methioninol showed good to excellent conversion to **3u** and **3v**, respectively.

Finally, some bioactive compounds were subjected to this method. Uridine and ribothymidine as well as the antiviral drug ribavirin were converted to **3w**, **3x** and **3y** with low to moderate yields. Finally, the beta-blocker propranolol, the neurotransmitter adrenalin and the sympathomimetic ephedrine gave good yields of the cyclized products (**3z-3ab**). To demonstrate the synthetic utility of the reaction, a gram scale reaction, using **1a** as substrate, was performed. The corresponding product **3a** was isolated with 70% yield after a prolonged reaction time of 48 h.



Scheme 4-1. General conditions: a mixture of 0.1 mmol of substrate, 1.05 equiv. of **2b**, 2 mol% **P3**, 3 equiv. of DIPEA in neat MeCN (0.1 M) under N₂ atmosphere were irradiated for 24 h with 400 nm light. **a**: 70% isolated yield on a 7 mmol (gram)scale. **b**: 4 equiv. of DIPEA were used because the starting material was a hydrochloride salt. **c**: DMF (0.1 M) was used as the solvent. Bz = benzyl, Me = methyl, n-Bu = n-butyl, Et = ethyl.

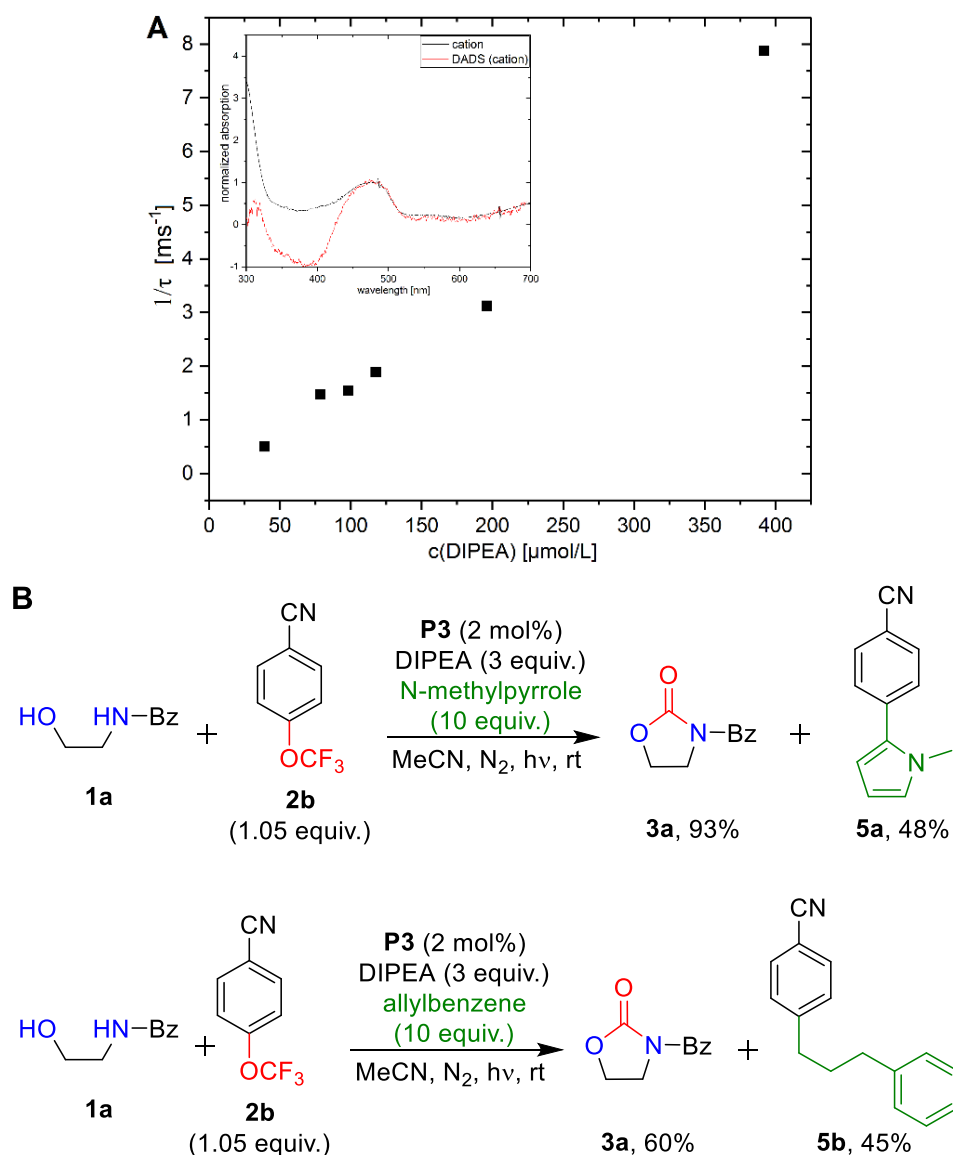
4.2.2 Mechanistic Investigations

To investigate the mechanism, transient spectroscopy, cyclovoltammetry as well as radical trapping experiments and *in-situ* and *ex-situ* NMR analyses were performed. To get insight into the photocatalytic mechanism, the quenching of the excited state of **P3** was investigated by transient spectroscopy. The measurements revealed that both, addition of DIPEA ($E_{\text{ox}} = +0.8$ V vs. SCE) and **2b** ($E_{\text{red}} = -2.1$ V vs. SCE) had no influence on the triplet lifetime of **P3** ($E_{\text{ox}} = +0.4$ V; $E_{\text{red}} = -1.7$ V, see Chapter 4.4.2 for details).^[14] However, during measurements at catalyst concentrations of 30 μM and above (compared to 2 mM under the reaction conditions), we observed a charge-transfer band originating from the radical cation part in the catalyst CT-complex dimer.^[15] The lifetime of this band decreases significantly by addition of DIPEA (Fig. 4-2 A). This indicates, that the charge recombination might be slowed down by interaction of the radical cation part of the CT-complex with DIPEA. As a consequence, the radical anion part can reduce **2b** to restore its uncharged ground state. This assumption is supported by cyclovoltammetry of **P3** revealing a ground state reduction potential of the **P3** radical anion of about -2.5 V vs. SCE in MeCN (see Chapter 4.4.2 for more data about the mechanistic investigation).

To find evidence for the presence of a benzonitrile radical originating from a photo-reductive mechanism, we performed radical trapping experiments in presence of **1a**. We observed 48% conversion of **2b** to the corresponding *N*-methylpyrrole adduct **5a** (Fig. 4-2 B). Moreover, the aryl radical could be trapped with the isolated double bond of allylbenzene giving adduct **5b** in 45% yield. The different radical trapping conditions did not influence the conversion of **1a** significantly, as **3a** was isolated in high yields. The formation of **5a** and **5b** is a good indication for the intermediacy of an aryl and the operation of a photo-reductive mechanism.^[16] *In-situ* ^1H and ^{19}F NMR profiles further corroborate this mechanistic step monitoring a clean transformation of **2b** into **4** upon illumination of **P3** in the presence of DIPEA (see Chapter 4.4.2 for details). Next, an *ex situ* NMR profile of the whole reaction with substrate **1a** was recorded (Fig. 4-2 C). Upon illumination, **2b** (black) and **1a** (violet) start to decrease, while the two main products **3a** (green) and **4** (red) can be readily detected. Furthermore, two more reaction intermediates could be identified (**F-I**, magenta and **OC-I**, cyan). Instead of the highly reactive free fluorophosgene itself, the formation of its next downstream more stable reaction intermediate (**F-I**) with **1a** was observed. Using advanced 1D and 2D NMR techniques for the ^1H , ^{19}F and ^{13}C assignment the intermediate was identified as a carbonyl fluoride adduct (**F-I**) of **1a**. The immediate formation of **F-I** combined with the lag-phase of **3a** in the illuminated *in situ* NMR profile (Fig. 4-2 D) suggested **F-I** as direct precursor of **3a**. This is further solidified by the fact that once the light is turned off, a distinct conversion of **F-I** into **3a** can be observed (for spectra see Chapter 4.4.2).

In addition, a second, off-cycle intermediate (**OC-I**, Fig. 4-2 C) could be assigned. The emergence of **OC-I** is the reason for the evidently faster decrease of **1a** with respect to **2b** (Fig. 4-2 C), as it stems from a side reaction of **1a** with acetaldehyde, which in turn is liberated after downstream reactions from DIPEA (see Chapter 4.4.2 for details). From the three hour mark on in Fig. 4-2 C, it is evident, that **1a** and **F-I** are already gone, whilst **OC-I** is slowly decreasing and **1a** is still slowly increasing. This suggests that **OC-I** and **1a** are in a slow off-cycle equilibrium. It could also be shown that this equilibrium is heavily water dependent (see Chapter 4.4.2 for details). This results in **3a** still being generated even after **1a** is

fully consumed as long as fluorophosgene is still liberated. Furthermore, addition of water can effectively reduce the formation of **OC-I** and increase the reaction rates significantly (see Chapter 4.4.2 for details). Therefore, we propose the following mechanism for the liberation of fluorophosgene from **2b** (Fig. 4-3). **P3** is excited by the light of 400 nm LEDs. The two excited photocatalyst molecules **P3*** form a CT-complex dimer which disproportionates to the corresponding **P3⁺** and **P3⁻**. The **P3⁻** reduces **2b** leading to its fragmentation into the aryl radical and trifluoromethanolate. Trifluoromethanolate decomposes into F⁻ and fluorophosgene, which readily reacts with amine- or alcohol- based nucleophiles resulting in a carbonyl fluoride intermediate (see **F-I**).^[17] Subsequent cyclization leads to the desired product. To regenerate **P3**, the **P3⁺** oxidizes DIPEA and the aryl radical abstracts a hydrogen atom from DIPEA⁺ or the solvent to give benzonitrile. Next to the main pathway, a second off-cycle pathway is in progress. Downstream reactions of DIPEA lead to the liberation of acetaldehyde, which can readily react with **1a** to yield the off-cycle intermediate **OC-I**. The resulting equilibrium of **OC-I** and **1** is heavily dependent on the water concentration. As long as fluorophosgene is provided, **OC-I** is slowly converted into **3a** through **1a**. Addition of extra water can virtually suppress the off-cycle equilibrium, which in turn accelerates the reaction.



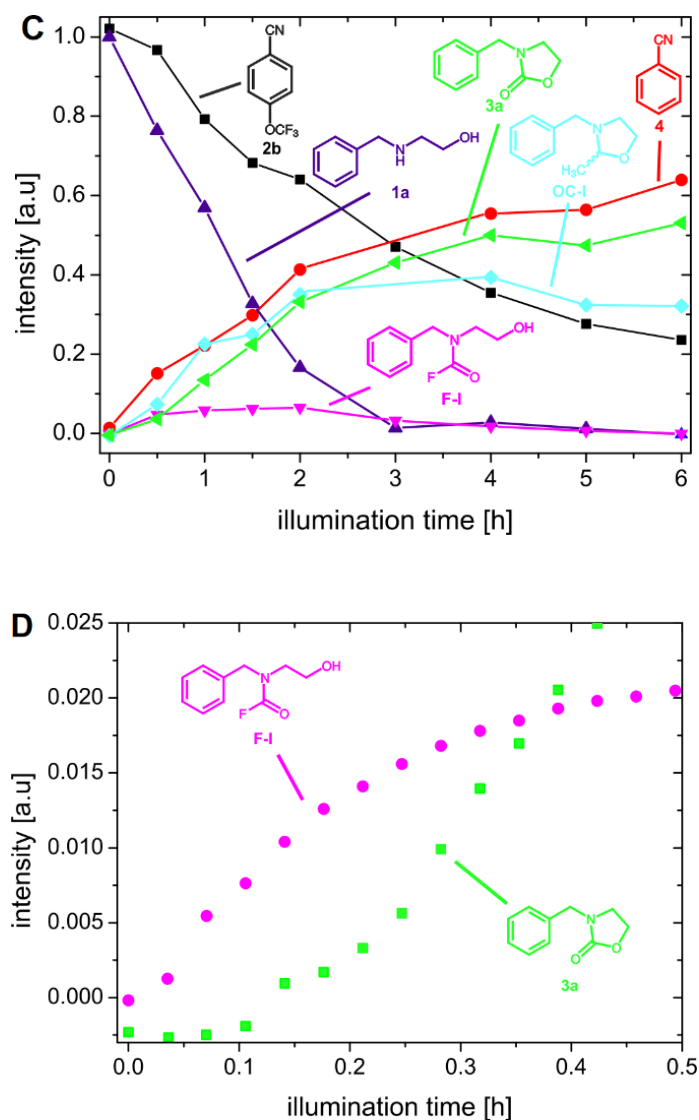


Figure 4-2. A: Stern-Volmer plot of quenching of the **P3** radical cation with DIPEA; inset: comparison of **P3** radical cation spectrum obtained *via* transient spectroscopy and spectro-electro chemistry (see Chapter 4.4.2 for details). **B:** Radical trapping experiments with *N*-methylpyrrole and allylbenzene. **C:** *Ex situ* reaction profile of **1a** (100 mM), **2b** (105 mM), **P3** (2 mM) and DIPEA (300 mM) in CD₃CN. Next to the major products **3a** (green) and **4** (red), two intermediates can be detected; **F-I** (magenta), which is the next downstream intermediate of fluorophosgene and the direct precursor of **3a** and **OC-I** (cyan). **OC-I** presents an off-cycle intermediate being in an ongoing water dependent equilibrium with **1a**. As long as fluorophosgene is generated, **OC-I** is slowly converted into **3a** through **1a**. **D:** Excerpt of the *in situ* reaction profile of **1a** (100 mM), **2b** (110 mM), **P3** (2 mM) and DIPEA (300 mM) in CD₃CN showing the initial trend of **3a** (green) and **F-I** (magenta). The formation of **3a** is preceded by an initial lag-phase whilst the intermediate **F-I** is generated immediately after the light is turned on as the direct precursor of **3a**.

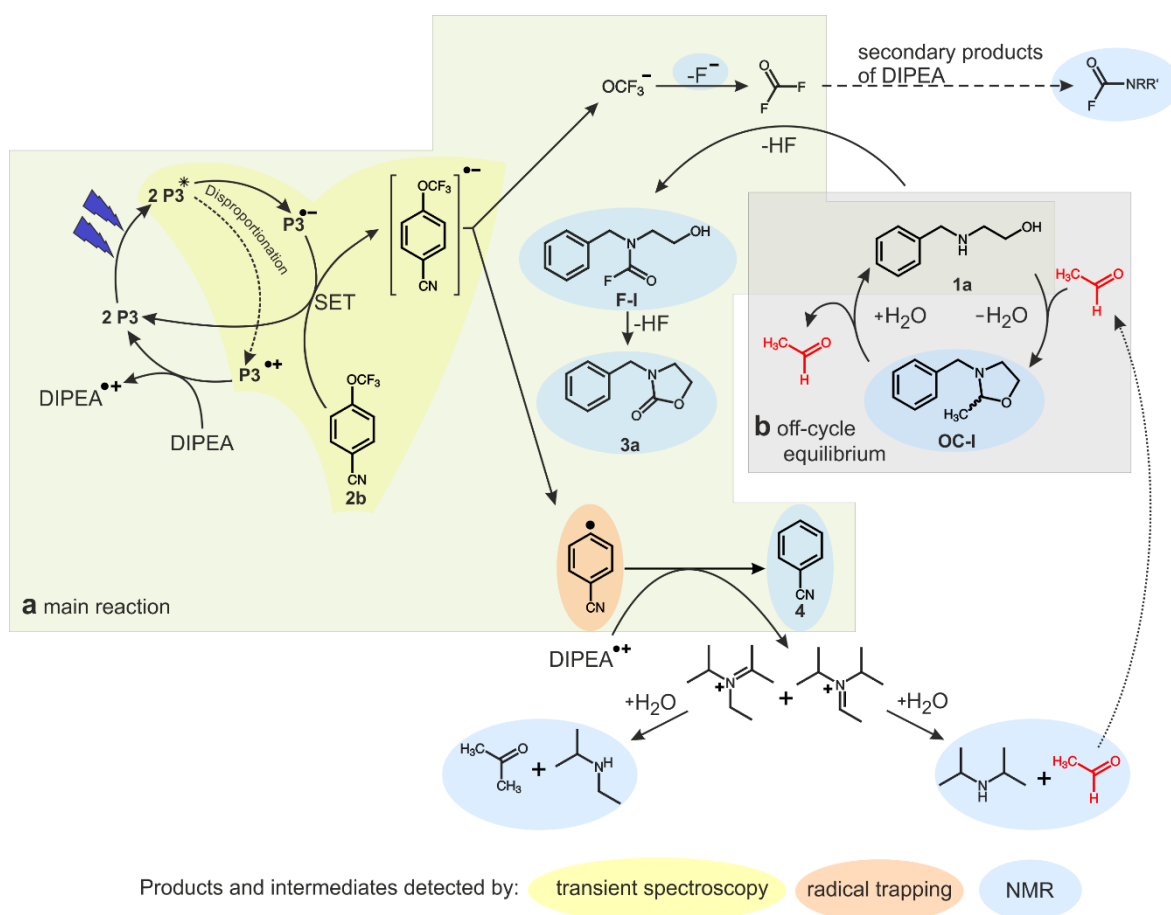


Figure 4-3. Proposed catalytic cycle for the photocatalytic liberation of fluorophosgene for substrate **1a**, based on the conducted mechanistic studies. The mechanism can be differentiated into two segments: **a**: The main reaction, which comprises the photocatalytic liberation of fluorophosgene by reducing **2b** and the subsequent reaction of fluorophosgene with **1a** over **F-I** to yield **3a**. **b**: The off-cycle equilibrium (gray background), which describes the water dependent equilibrium between **1a** and **OC-I** through addition and cleavage of acetaldehyde (secondary product of DIPEA). Detected products and intermediates are highlighted.

4.3 Conclusion

In summary, we have developed the first, visible light mediated procedure for the cleavage of an aryl trifluoromethoxy ether and the controlled liberation and *in-situ* conversion of fluorophosgene for the synthesis of carbamates, carbonates and urea derivatives. The method shows regio-selectivity for aliphatic amines and/or alcohols in presence of aromatic ones. No racemization of amino acid stereocenters was observed. Transient spectroscopy suggests the formation of a catalyst CT-complex dimer as the catalytic active species. NMR measurements identified key intermediates consolidating a stepwise fragmentation into fluorophosgene as the most likely mechanistic pathway; while also uncovering a water dependent off-cycle equilibrium, which can be effectively modulated to accelerate the reaction. Notably, this method expands the toolbox of photoredox catalysis by the generation of an extremely reactive species which is not based on radical reactivity under mild reaction conditions.

4.4 Experimental Part

4.4.1 General Information

See Chapter 2.4.1 for General Information.^[18]

Preparation of photocatalyst P3

P3 was prepared according to a reported literature procedure.^[19] All photoreactions and NMR investigations were performed with self-made catalyst. CV, online UV-VIS, spectro-electro chemistry and transient spectroscopic measurements were performed with a commercial catalyst (Sigma-Aldrich).

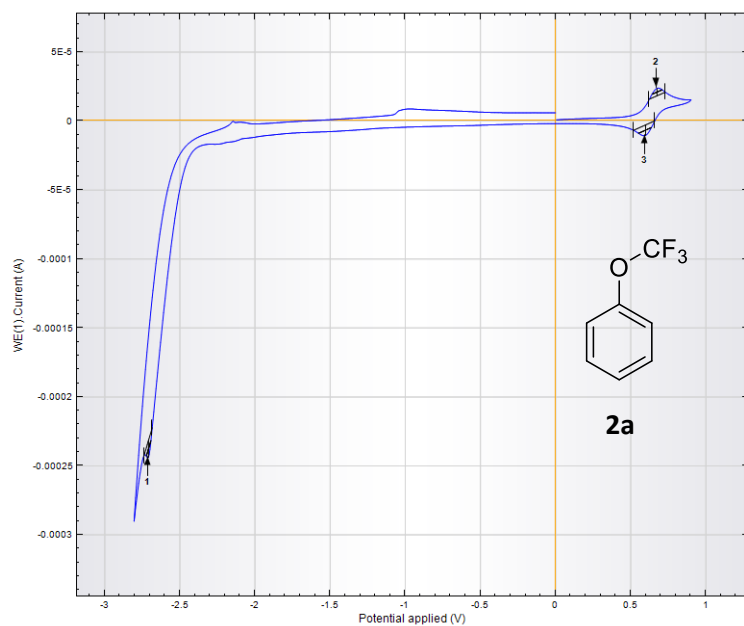
General Procedure for the preparation of carbonates, carbamates and urea derivatives

The photocatalyst (1.2 mg, 0.002 mmol, 0.02 equiv.) and the substrate (0.1 mmol) were weight into a 5 mL crimp cap vial. A stirring bar, 1 mL of dry MeCN, 15.6 μ L (0.105 mmol, 1.05 equiv.) 4-(trifluoromethoxy)benzonitrile and 51.0 μ L (0.3 mmol, 3 equiv.) DIPEA were added into the vial *via* syringe. The vial was sealed with a crimp cap with septum and set under nitrogen atmosphere by three consecutive freeze-pump-thaw cycles. The vial was placed approximately 1 cm above a 400 nm LED and stirred under continuous irradiation for 24 h. After completion, two equal reaction mixtures were combined and quenched by addition of 0.5 mL of H₂O. Silica was added, the solvent was evaporated from the suspension and the residue was used as dry load for column chromatography on a Biotage[®] Isolera[™] Spektra One using a petrol ether and ethyl acetate or a dichloromethane/methanol mixture as the mobile phase. A 10 g column was employed with silica gel of type 60 M (40-63 μ m, 230-440 mesh) by Merck as stationary phase.

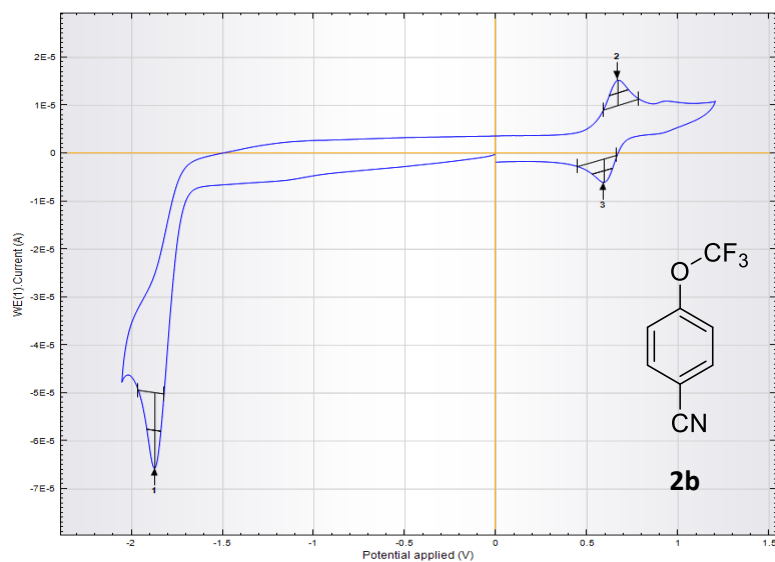
For the gram scale reaction, the photocatalyst (86 mg, 0.14 mmol, 0.02 equiv.) and **1a** (1.1 g, 7.0 mmol, 1.0 mL) were weight into a 250 mL Schlenk flask. A stirring bar, 70 mL of dry MeCN, 1.1 mL (7.4 mmol, 1.05 equiv.) 4-(trifluoromethoxy)benzonitrile and 3.6 mL (21 mmol, 3 equiv.) DIPEA were added into the flask *via* syringe. The flask was set under nitrogen atmosphere by three consecutive freeze-pump-thaw cycles. The vial was placed approximately 1 cm above two 400 nm LEDs and stirred under continuous irradiation for 48 h. The reaction was quenched by addition of 5 mL water and concentrated *in vacuo*. Purification was done as described above but a 25 g column was used instead of a 10 g column.

4.4.2 Mechanistic Investigations

Cyclovoltammetric data of 2a and 2b (in MeCN)

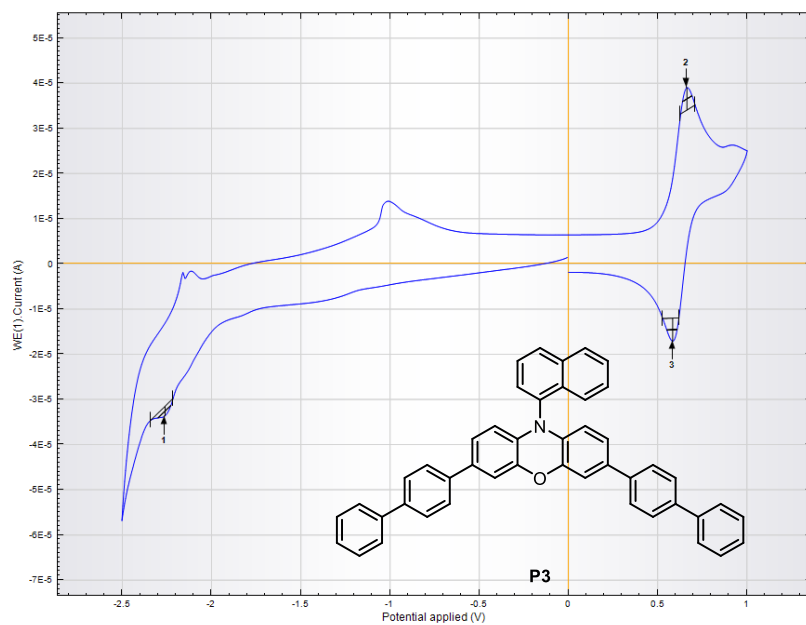


Index	Peak position
1	-2.709 V 2a
2	0.675 V Ferrocene
3	0.599 V Ferrocene



Index	Peak position
1	-1.873 V 2b
2	0.670 V Ferrocene
3	0.594 V Ferrocene

Cyclovoltammetric data of P3 (in MeCN)



Index	Peak position
1	-2.261 V P3
2	0.665 V Ferrocene
3	0.584 V Ferrocene

Transient Spectroscopy and further mechanistic discussion

2D Transient Absorption Setup:

The measurements were performed with a Pump-Probe Setup. The Pump source is the third Harmonic of a Nd:YAG laser (Surelite II, Continuum). The wavelength of 355 nm, with a pulse width of about 5 nm. The typical pulse duration is 8 ns. The repetition rate is 10 Hz and pulses are selected by a shutter (LS055, nmLaser). The white probe light is generated by a pulsed xenon flash lamp (MSP-05, Müller Elektronik-Optik) and passes the sample orthogonal to the Pump beam. Toroidal mirrors (aluminum-coated blanks of eyeglass lenses, Rodenstock) are used to focus and guide the probe light without chromatic aberrations. A shutter (LS6ZM, Uniblitz) is used to block the continuous light of the xenon lamp. A spectrograph (Bruker 200is) disperses the probe light after it passed the sample. The probe light is then passed on to a streak camera (C7799, Hamamatsu Photonics), a spectral and temporal resolved picture is projected on a phosphor screen and recorded by a CCD camera (ORCA-CR, Hamamatsu Photonics). The temporal window of the streak camera can be set between 0.5 ns and 10 ms. The time resolution in each window is about 0.5% of the temporal window width. All components are controlled by a home-built delay controller (DC).

A 2D transient absorption data matrix ($\Delta\mathbf{A}$) is generated from 4 separate images (I) recorded by the CCD camera.

$$\Delta\mathbf{A} = -\frac{(I_{L,P} - I_L)}{(I_P - I_D)}$$

$I_{L,P}$ is an image where both the pump (**L**) and probe (**P**) light is used.

I_L records only the emission and scattered light caused by a laser pulse.

I_P records the probe light passing through the sample without a pump pulse.

I_D is a dark picture and records only the sensor noise without any pump or probe light.

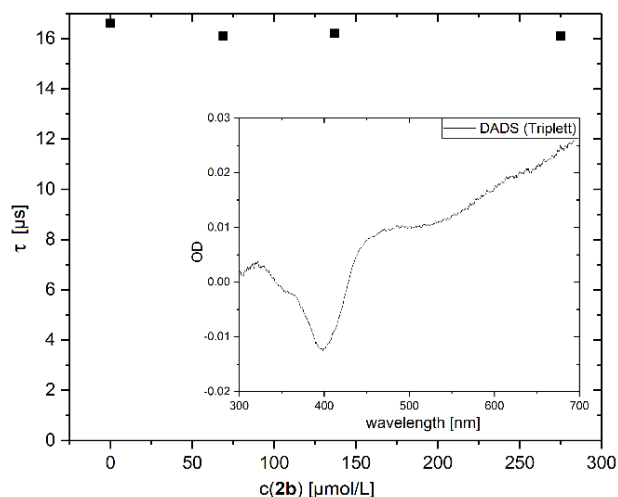
Data analysis

Data were analyzed with homemade software to obtain decay associated difference spectra (DADS). This analysis corresponds to the least-squares fit:

$$\left| \Delta OD(t, \lambda) - \sum_k^N f_k(t) DADS_k(\lambda) \right|^2 = \min,$$

where $\Delta OD(t, \lambda)$ is the measured data matrix and the $f_k(t)$ are exponential (or more complex) decay functions convoluted with a Gaussian function as the apparatus response function.

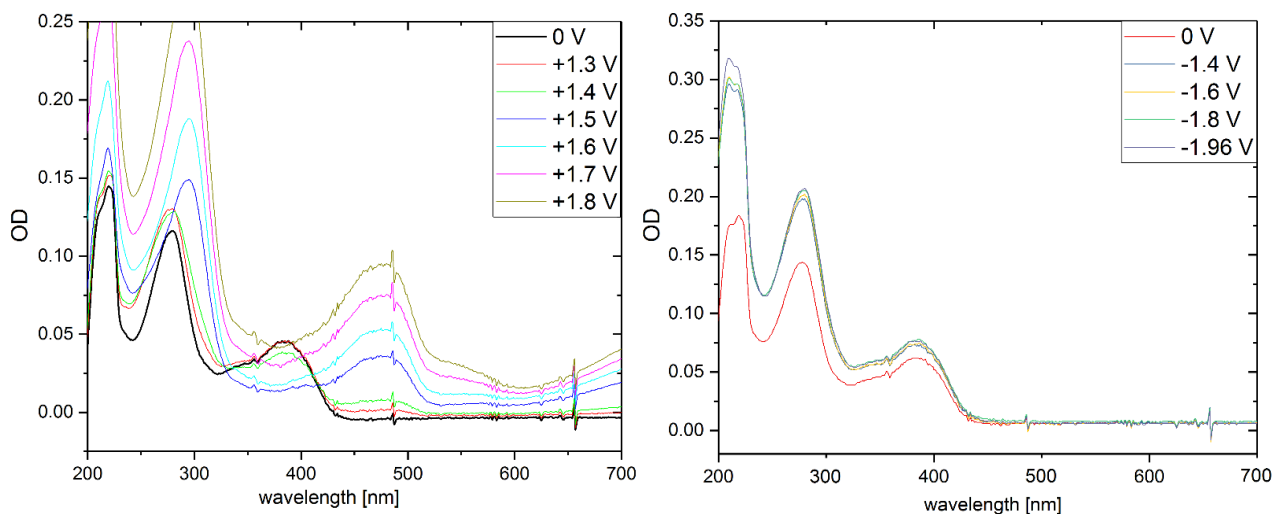
For each manifold $\{f_k$ the DADS display the spectral changes associated with particular decay times. The DADS are in turn linear combinations of the species spectra where increasing species have negative coefficients and decreasing species have positive coefficients.



Quenching of the **P3** triplet state with **2b** in a 30 μM solution of **P3** in MeCN. Inset: Transient spectrum of the triplet state of a 30 μM solution of **P3** in MeCN.

The lifetime of the triplet state remains unchanged upon addition of **2b** indicating that the reduction of **2b** does not proceed *via* direct SET the triplet state.

Verification of the radical cation and radical anion spectra via spectro-electro chemistry



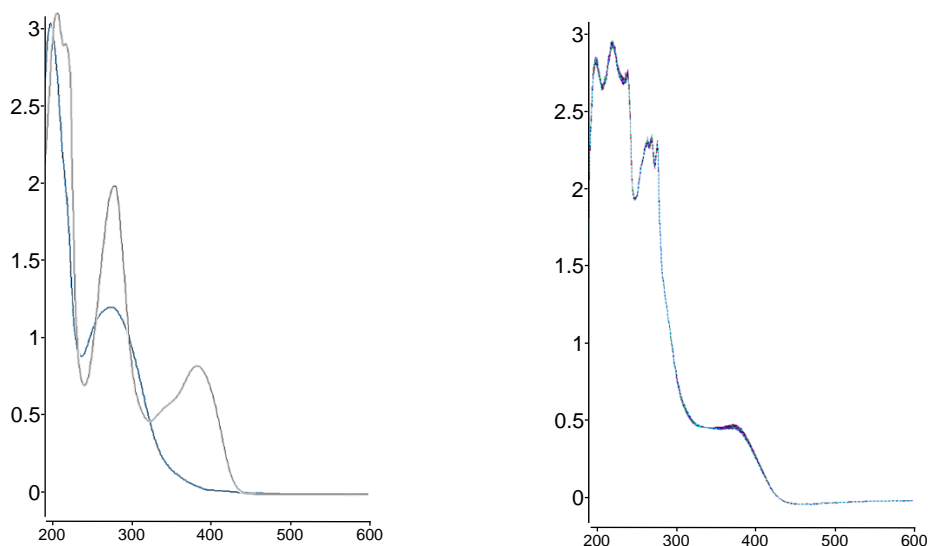
Left: Absorption spectra of **P3** at various positive potentials in MeCN. **Right:** Absorption spectra of **P3** at various negative potentials in MeCN.

At positive potentials a strong absorption at 475 nm occurs, while the absorption peak at 380 nm fades, indicating the formation of the **P3** radical cation. The same band was observed during the transient spectroscopic measurements of **P3** at concentrations around 30 μM (compared to 2 mM in the reaction mixture) which lead to the assumption of the formation of a charge-transfer complex dimer as catalytic active species. However, the direct observation and/or quenching of the **P3** radical anion could not be observed due to the very minuscule shift of the absorption peak at 280 nm compared to the ground state absorption spectrum.

Investigation of the catalytic active species via online irradiation

Online irradiation setup:

A traditional photometric setup was modified by adding a single high-power LED in 3 cm distance to the cuvette holder. The LED was mounted in a 90° angle with respect to the photometer lamp irradiation. The photometer sample was continuously irradiated by the LED while being stirred magnetically. Every 10 seconds a photometric scan of the absorption of the sample was performed.



Left: Absorption spectrum of **P3** in MeCN under argon atmosphere before (black) and after (blue) 30 min. irradiation with 400 nm light. **Right:** Absorption spectra of the diluted reaction mixture (**P3**, **2b** and DIPEA) in MeCN under argon atmosphere taken every 10 sec. for a total of 30 min. irradiation with 400 nm light.

If only **P3** is irradiated, it degrades rapidly into an unknown species indicated by a strong change of the absorption spectrum. However, in the reaction mixture the catalyst is much more stable resembled by the insignificant change of the catalyst absorption peak at 380 nm. As we assume the formation of a charge transfer complex between two catalyst molecules and subsequent disproportionation into **P3⁺** and **P3⁻**, further irradiation of these species might lead to catalyst degradation. Whereas, if these transient species can react with DIPEA and **2b** to restore the stable ground state, the catalyst can survive several turnovers.

NMR spectroscopic investigations

Materials:

The solvent CD₃CN was purchased from Deutero GmbH. The solvent was dried over 4 Å molecular sieves and deoxygenated by Freeze-Pump-Thaw cycling prior to use. Starting materials (2-benzylaminoethanol (**1a**) and 4-(trifluoromethyl)benzotrile (**2b**)) and reagents (DIPEA) were purchased from commercial suppliers (Sigma Aldrich, Alfa Aesar, Acros or Fluka) and were used without further purification.

Sample preparation: In situ measurements

For the measurements in CD₃CN 450 µL solutions of 100 mM starting material **1a**, 110 mM **2b**, 2 mM photocatalyst **P3** and 300 mM DIPEA were directly prepared in amberized NMR tubes to minimize the influence of ambient light in the reaction solution. The solvent was deoxygenated either by Freeze-Pump-Thaw cycling and then transferred to the NMR tube under argon atmosphere or purged with argon (10 min) directly inside the NMR tube. Then a transparent glass insert containing the glass fiber, was inserted and everything was sealed airtight.

Sample preparation: Ex situ measurements

1 mL or 2 mL reaction solutions in CD₃CN were prepared in a 5 mL crimp cap vial with a stirring bar. Under standard conditions these solutions contained 2 mM of the photocatalyst **P3**, 100 mM of substrate **1a**, 105 mM of **2b** and 300 mM DIPEA. Deviating conditions are directly mentioned in the text. The vial was sealed with a crimp cap with septum and deoxygenated by three consecutive Freeze-Pump-Thaw cycles or bubbled with argon for 10 minutes. The vial was placed approximately 1 cm above a 400 nm LED inside a cooling block and stirred under irradiation. An aliquot (50 µL or 100 µL) was taken from the solution and diluted with 350 µL DMSO-d₆ or 300 µL CD₃CN to give a total volume of 400 µL for the NMR measurements

NMR Measurements:

All measurements were conducted on a Bruker Avance III HD 600 (600.13 MHz for ¹H; 564.59 MHz for ¹⁹F) spectrometer with a fluorine selective TBIF probe or on a Bruker Avance 500 (500.13 MHz) spectrometer with a 5 mm QXI probe. Temperature control was ensured by a Bruker BVTE 3000 unit (298 K). The spectra were processed, evaluated and plotted with Bruker TopSpin 3.2. The *in situ* samples were illuminated by a NCSU279AT high power LED (Nichia, 405 nm; 950 mW).

In situ measurements

For the *in situ* reaction profiles an *in situ* illumination device previously reported by our working group was employed.^[20] The reaction profiles were generated by either alternately recording non-illuminated and illuminated ¹H NMR spectra (and/or ¹⁹F NMR spectra) or continuous illumination throughout the measurement. In some cases, the ¹H NMR spectra were recorded with a T2 spin echo filter (300 μs echo time, looped 128 times) to suppress broad, shifting signals like the water signal, which can significantly distort the integrals of other signals. After the first spectra without illumination a row of ¹H and/or ¹H and ¹⁹F spectra were collected either illuminating continuously or alternating between illuminated and non-illuminated spectra.

Ex situ measurements

The *ex situ* reaction profiles were recorded in a straightforward manner by putting the sample into the NMR spectrometer. The down time from taking an aliquot from the batch reaction to the NMR measurement was approximately 5 minutes. In some cases, the ¹H NMR spectra were recorded with a T2 spin echo (300 μs echo time, looped 64-128 times) filter to suppress broad, shifting signals like the water signal, which can significantly distort the integrals of other signals

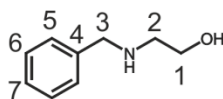
Processing and Evaluation

The NMR kinetics are derived from signal C3-H for **2b** and **4**, C3-H for **1a**, **3a** and the two conformations of the fluorointermediate (**F-I1** and **F-I2**) and C2-H for **OC-I** in the ¹H proton spectra and C6-F₃ for **2b** in the ¹⁹F spectra and referenced to the respective signal in the first spectrum without illumination (Fig. S-4-1). Inversion recovery experiments (for ¹H and ¹⁹F) were performed prior to illumination to ensure full relaxation of the reaction components of interest for correct quantification. Assignments were made by evaluation of full sets of 1D and 2D NMR spectra (Fig. S-4-2). For ¹H NMR spectra chemical shifts were referenced to the solvent signals of CD₃CN. For ¹⁹F NMR spectra trifluoro acetic acid (-76.55 δ (ppm) vs CFC₃ = 0.00 ppm) was added after the reaction was finished/ illumination was stopped.

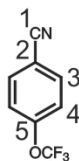
Pulse sequences and important parameters (O, transmitter frequency offset [ppm]; TD, size of FID; SW, spectral width [ppm]; D1, recycling delay [s]; NS, number of scans; DS; number of dummy scans) for the ¹H¹⁹F-HMBCs and the ¹⁹F¹³C-edHSQC are listed below the corresponding spectrum.

Numeration for integration and further assignments

starting materials:

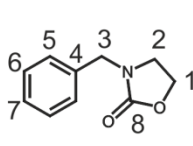


1a

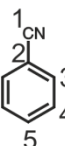


2b

products:

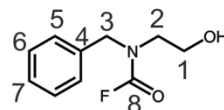


3a



4

off-cycle intermediate (OC-I)



fluorointermediate (F-I)

detectable as two conformations (F-I1 and F-I2)

Figure S-4-1. Numeration of starting materials and relevant reaction products as used for the assignments and further characterization.

Assignments:

Assignments were made by sets of 1D NMR spectra consisting of ^1H , ^{13}C , ^{19}F , and 2D NMR spectra consisting of $^1\text{H}^1\text{H}$ -COSY, $^1\text{H}^1\text{H}$ -TOCSY, $^1\text{H}^1\text{H}$ -NOESY, $^1\text{H}^{13}\text{C}$ -HSQC, $^1\text{H}^{13}\text{C}$ -HMBC, and in specific cases selective 1D $^1\text{H}^1\text{H}$ -TOCSY, selective 1D $^1\text{H},^1\text{H}$ -NOESY, $^1\text{H}^{19}\text{F}$ -HMBC and $^{19}\text{F}^{13}\text{C}$ -HSQC spectra were recorded.

The ^{13}C chemical shifts of **1a** weren't assigned because all 1D ^{13}C and 2D spectra were usually recorded after illumination when 2-benzylaminoethanol (**1a**) was already fully consumed. It was forgone to assign the ^{13}C chemical shifts in an additional measurement, as **1a** is commercially available and literature known. The chemical shift of the hydroxyl functionality of **1a** is heavily dependent on the water content of the reaction and is in some instances not detectable at all due to exchange. If detectable, it can be witnessed as either a triplet or broad singlet, again dependent on the water content. After illumination starts, it rapidly broadens and usually vanishes after a couple of minutes due to further interactions/exchange. Hence, its chemical shift was put in parentheses in Figure S-4-2.

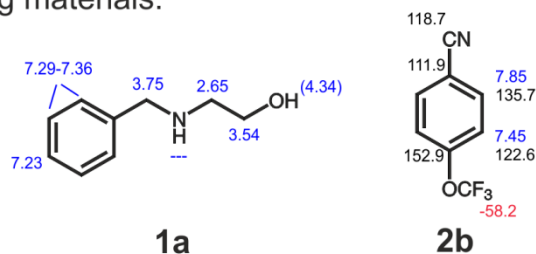
The ^1H and ^{13}C chemical shifts of position 6 and 7 for the off-cycle intermediate (**OC-I**) and the two conformations of the fluorointermediate (**F-I1** and **F-I2**) couldn't be assigned unambiguously, owing to heavy overlap with other signals from the starting material **1a** and the main product **3a**. Hence, only a chemical shift region is given for **OC-I**, **F-I1** and **F-I2** for signals 6 and 7 in Figure S-4-2.

Fluoride can be detected as a broad singlet at \sim -125 ppm as the reaction progresses. Its chemical shift is heavily dependent on the initial water content and progress of the reaction and shifts from high to low field during the reaction. Only small amounts of fluoride are detectable since most of the fluoride precipitates as insoluble salts.

The off-cycle intermediate OC-I is cyclized for substrate **1a**, but for other substrates it can also appear in its open form, which can also have at least two conformations probably similar the fluorointermediate conformations (**F-I1** and **F-I2**) detected for **1a** (data not shown).

CD₃CN (298 K)

starting materials:



reaction products:

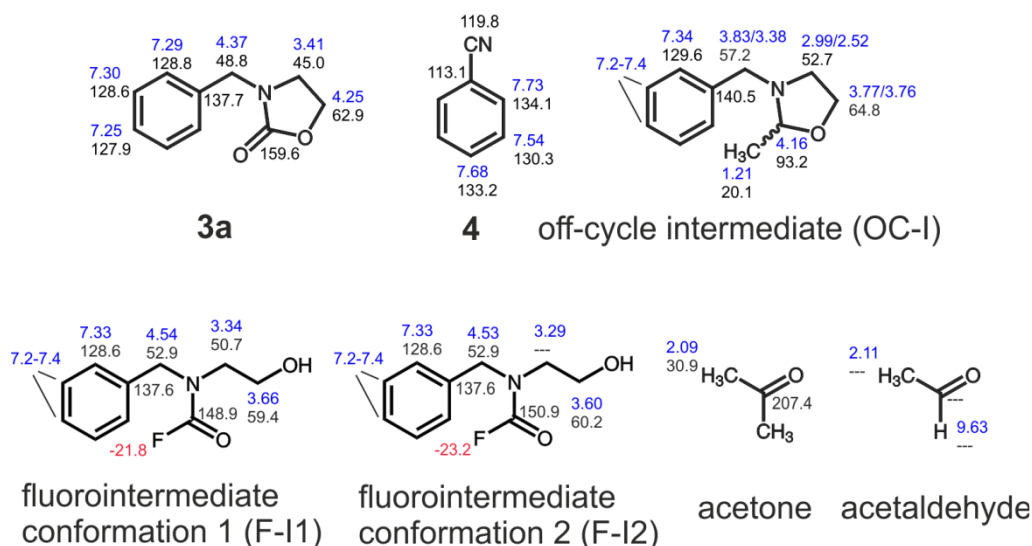


Figure S-4-2. Assignment of starting materials and relevant reaction products in CD₃CN at 298 K. ¹H chemical shifts are highlighted blue and ¹³C chemical shifts are highlighted black and referenced to CD₃CN (1.94 ppm ¹H; 1.32 ppm ¹³C). ¹⁹F chemical shifts are highlighted red and are referenced to trifluoro acetic acid (-76.55 ppm).

Relevant spectra for the assignments of the two conformations of the central fluorointermediate (F-I1 and F-I2)

The fluorointermediate **F-I** was completely assigned during the reaction, mostly under continuous illumination. In the case of substrate **1a**, **F-I** can be detected as two stable conformers (**F-I1** and **F-I2**) in solution. Figures S-4-3 to S-4-9 show excerpts of relevant spectra and important correlations, which were used to deduce the structure of **F-I** and its role as an intermediate.

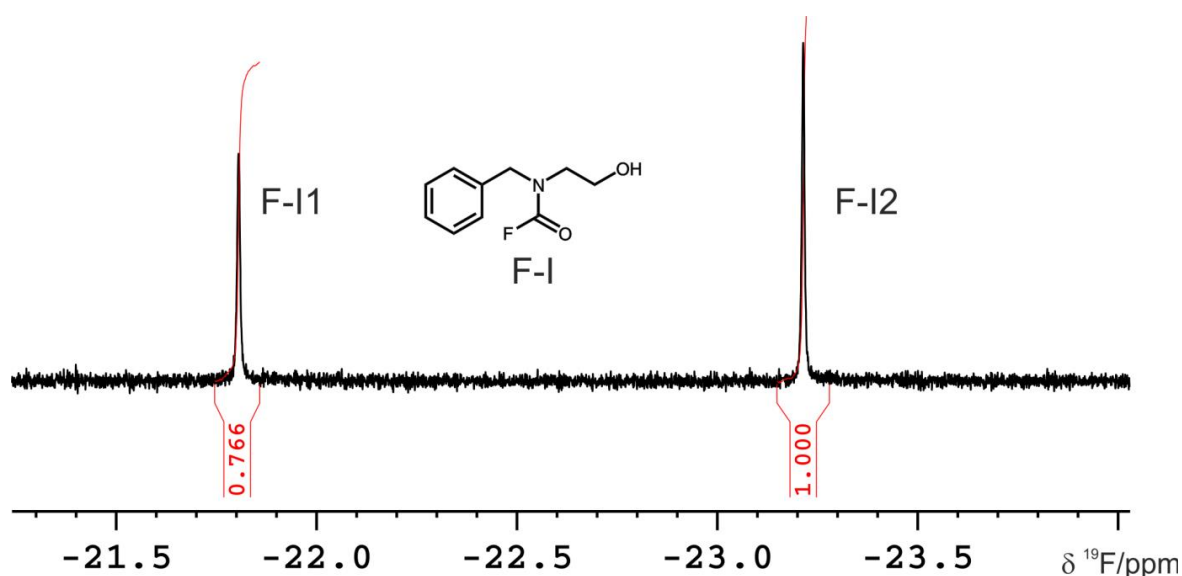


Figure S-4-3. Excerpt of the ^{19}F proton spectrum after 50 minutes of continuous illumination. The two conformations of the fluorointermediate **F-I** (**F-I1** and **F-I2**) both yield one singlet in the ^{19}F spectrum.

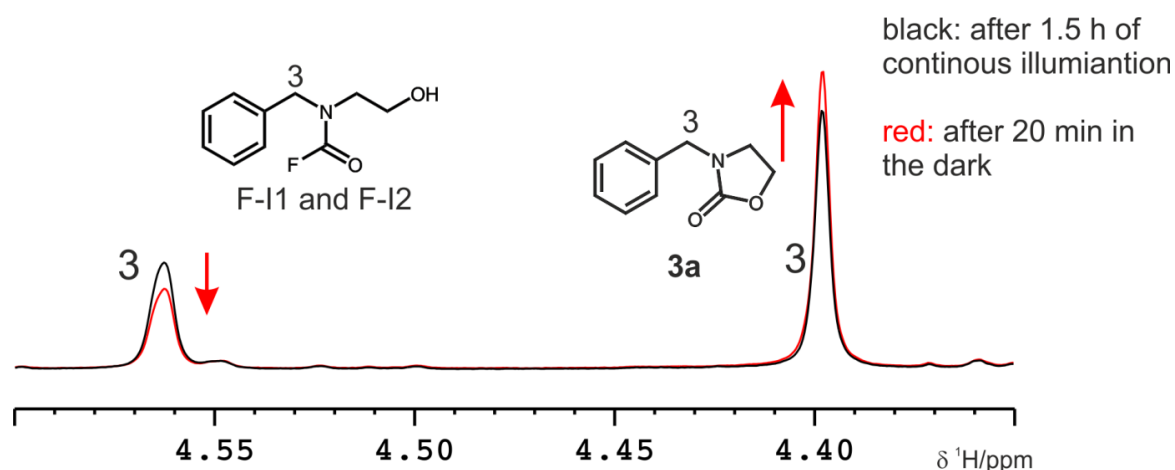


Figure S-4-4. Excerpt of the ^1H proton spectrum after 1.5 hours of continuous illumination (black) and the reaction mixture in the dark after 20 minutes (red). **F-I1** and **F-I2** convert into the desired product **3a** by a dark reaction. The position C3-H of **F-I1** and **F-I2** usually overlap, hence it appears as one singlet in the NMR spectrum. All other signal sets in the NMR spectrum stay constant within the observed time frame.

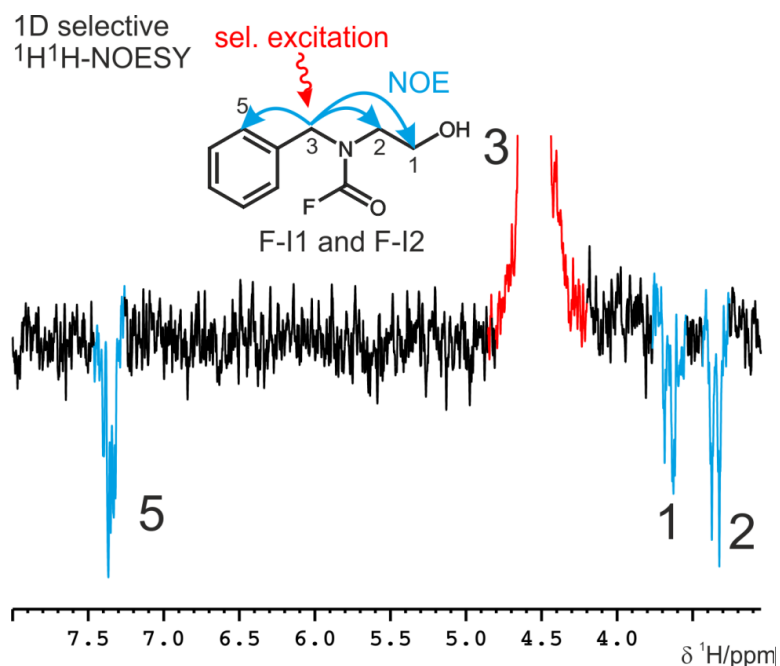


Figure S-4-5. 1D $^1\text{H}^1\text{H}$ -NOESY spectrum with selective excitation of the C3-H position at 4.54 ppm of F-I1 and F-I2 (red). The selective NOESY yields three distinctive NOE sets (blue) to the signals C1-H, C2-H and C5-H of both conformations **F-I1** and **F-I2**, due to spectral overlap at the C3-H position. $t_m = 600$ ms.

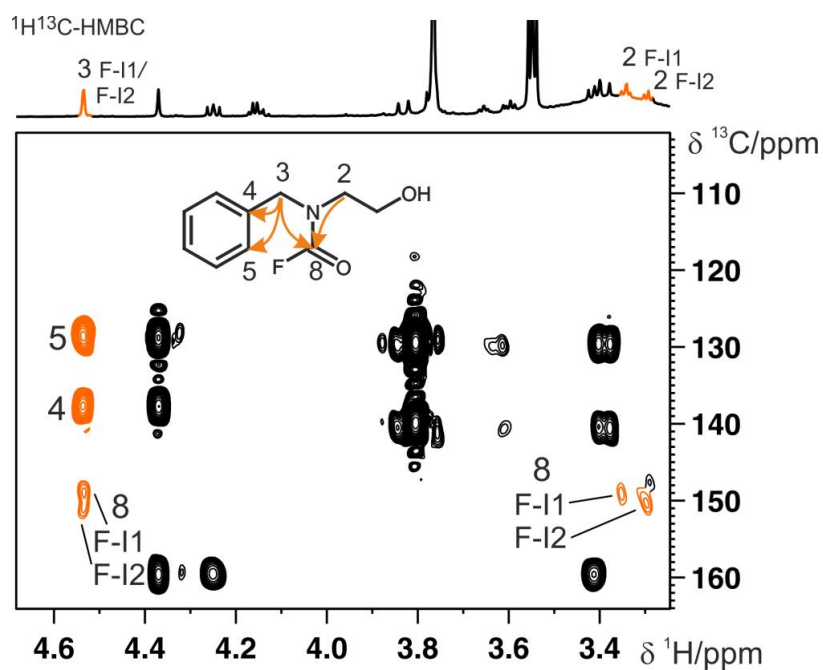


Figure S-4-6. $^1\text{H}^{13}\text{C}$ HMBC highlighting the relevant cross correlations (orange) for both conformations of the fluorointermediate (**F-I1** and **F-I2**).

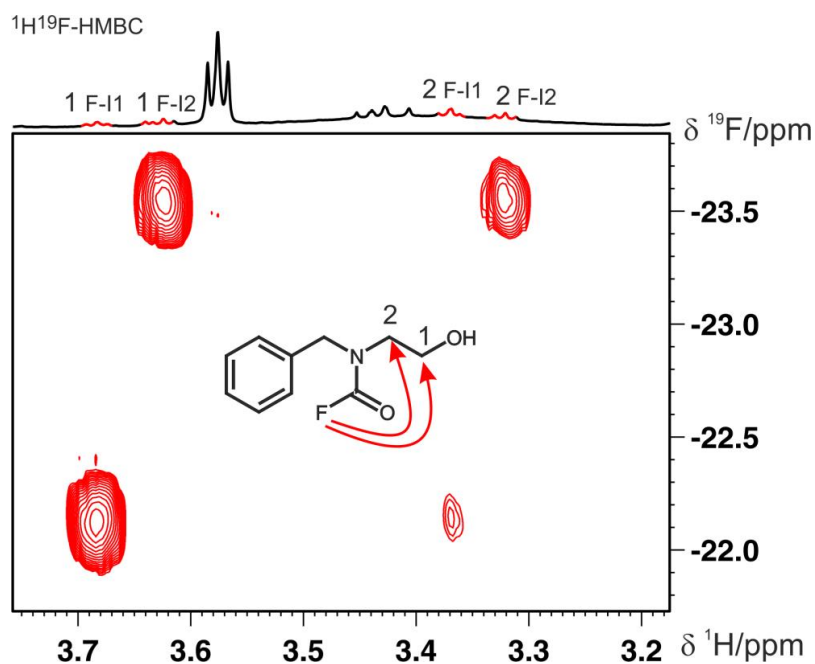


Figure S-4-7. ¹H¹⁹F-HMBC highlighting the relevant cross correlations (red) for both conformations of the fluorointermediate (**F-I1** and **F-I2**). Parameters: PP = *hmbcgpndqf*; NS = 64; DS = 16; TD-F1 = 16; TD-F2 = 2048; D1 = 1; SW-F1 = 5; SW-F2 = 12; O-F1 = -23; O-F2 = 5; evolution long range coupling = 71.4 ms.

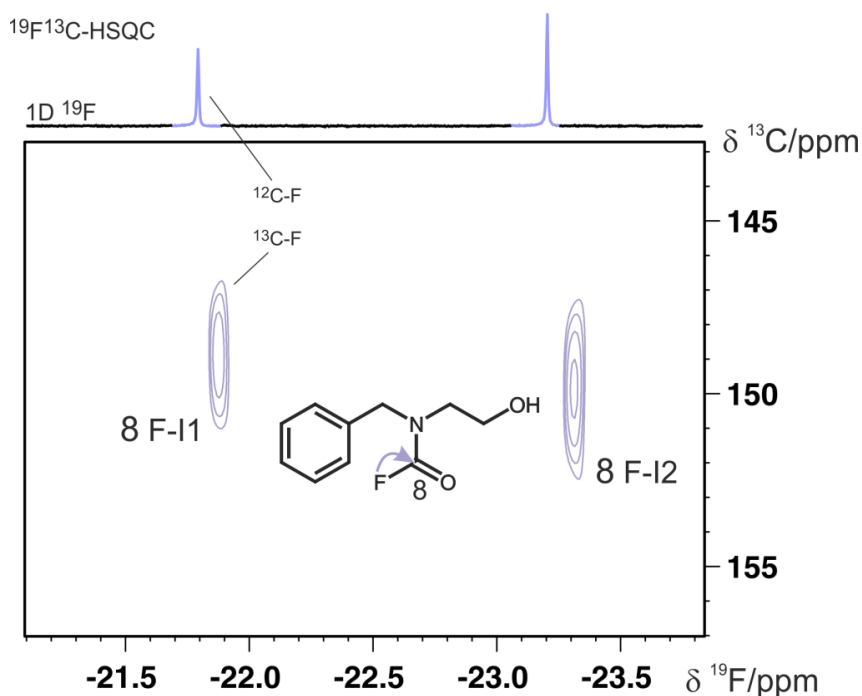


Figure S-4-8. Edited ¹⁹F¹³C-HSQC highlighting the relevant cross correlations (purple) for both conformations of the fluorointermediate (**F-I1** and **F-I2**). The cross signals in the HSQC are high field shifted in F2 with respect to the 1D ¹⁹F projection because of the strong isotope effect of ¹⁹F (¹²C-F in regular 1D ¹⁹F vs ¹³C-F in the HSQC). Parameters: PP = *hsqcedhpph*; NS = 1024; DS = 16; TD-F1 = 16; TD-F2 = 512; D1 = 1; SW-F1 = 50; SW-F2 = 10; O-F1 = 140; O-F2 = -23; adjusted for ¹J_{CF} = 283 Hz.

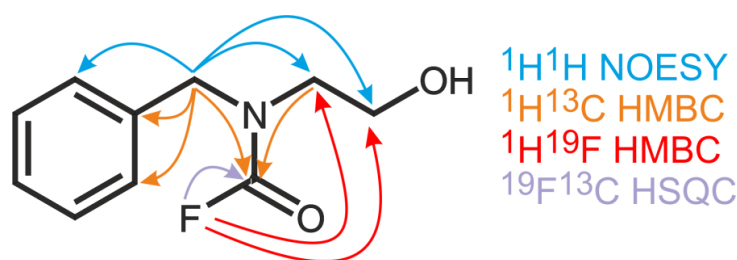


Figure S-4-9. Summary of important cross correlations for the assignment of both conformations of the fluorointermediate (**F-I1** and **F-I2**) consisting of $^1\text{H}^1\text{H}$ -NOESY (blue), $^1\text{H}^{13}\text{C}$ -HMBC (orange), $^1\text{H}^{19}\text{F}$ -HMBC (red) and $^{19}\text{F}^{13}\text{C}$ -HSQC (purple).

Conformations of **F-I1** and **F-I2**

Figure S-4-10 depicts two conceivable options for the conformational nature of **F-I1** and **F-I2**. Option 1 shows the (*s-cis*)- and (*s-trans*)-conformers of **F-I**. These could be possible due a hindered rotation around the NC(O) amide bond. But an inversion around the amide bond would also lead to an inversion of coupling constants e.g. the $^4J_{\text{HF}}$ couplings from position 8 to 3 and 8 to 2. The $^1\text{H}^{19}\text{F}$ -HMBC spectrum in Figure S-4-7 clearly shows that both conformations have clear cross signals to position 2 (and 1), but signals to position 3 have never been observed greatly diminishing the likelihood of option 1. Option 2 suggests an intramolecular hydrogen bond leading to a seven membered ring within the molecule. This option splits into two more possibilities as there could be either a slow equilibrium between the open form and the seven membered ring or the seven membered ring structure itself can engage two conformations. This would also be in line with the $^1\text{H}^{19}\text{F}$ -HMBC spectrum in Figure S-4-7 as the fluorine has cross signals to position 2 and 1 for both conformations, albeit slightly different in intensity. Option 2 is further supported when investigating other substrates (e.g. *N*-benzylethylenediamine leading to product **3d**) where only one conformation could be detected (data not shown). In summary, option 2 seems the more likely option, although it could never be proven unambiguously

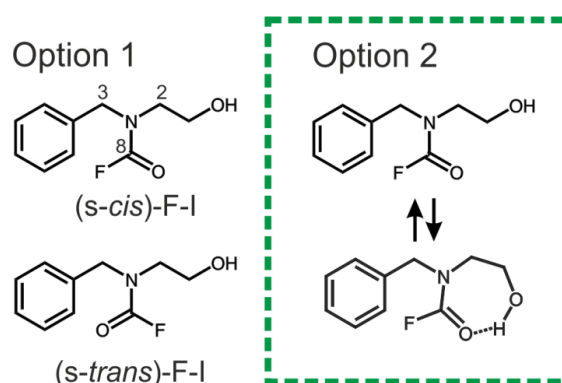


Figure S-4-10. Conceivable options for the two detectable conformers of **F-I**. Option 1, **F-I1** and **F-I2** are the (*s-cis*)- and (*s-trans*)-conformers of **F-I** due to a hindered rotation around the NC(O) amide bond. Option 2, **F-I** can form a stable intramolecular hydrogen bond between the hydroxyl group and the NC(O) carbonyl group leading to a seven membered structure. Exchange between the open form and the seven membered structure can lead to two conformers. The seven membered structure could also have two stable conformations of the seven membered ring. Option 2 is the more likely option as option 1 doesn't fit the experimental NMR data ($^1\text{H}^{19}\text{F}$ -HMBC) and is hence, highlighted. (for details see text above)

Illuminated NMR reaction profiles

In situ NMR reaction profiles

Figure S-4-11 illustrates the full *in situ* ^1H NMR reaction profile of the photoreaction of **1a** (100 mM), **2b** (110 mM), DIPEA (300 mM) and **P3** (2 mM) in CD_3CN at 298 K with illumination at 405 nm. Immediately after turning on the light, both starting materials (**1a** violet and **2b** black) start to decrease. Next to the starting materials the formation of two main products can be observed. First the fragmentation product of **2b**, benzonitrile **4** (red) can be assigned, whose formation is directly correlated with the decrease of **2b** (see also Fig. S-4-13). Secondly the desired product **3a** (green) can be designated, whose formation is also strongly correlated with the decrease of **2b** and the increase of **4**. Furthermore, a third major species could be assigned as the chiral off-cycle intermediate **OC-I** (cyan), resulting from a side reaction of **1a** with acetaldehyde, which in turn is a fragmentation product of DIPEA (see also Chapter 4.2.2 Fig. 4-2). Next to those three products one other significant intermediate species (**F-I**, magenta) could be readily assigned. This intermediate is a result from the reaction of the starting material **1a** with *in situ* generated fluorophosgene (COF_2) and thus presents a key intermediate supporting the proposed mechanism. **F-I** can be detected as two conformers (**F-I1** and **F-I2**) in solution albeit the unambiguous nature of both conformers could not be determined (see relevant spectra for the assignments of **F-I1** and **F-I2**). Owing to the heavy signal overlap and the overall small intensity of both conformers they are treated as one species (**F-I**) in the reaction profiles. Figure S-4-12 shows the initial combined build-up of **F-I1** and **F-I2** (**F-I**, magenta), and product **3a** (green). The formation of product **3a** is slightly delayed, whereas the formation of **F-I** starts immediately. After around 6 minutes the signals of **3a** start to increase as the intermediates are converted into **3a** in a concurrent dark reaction. This was further confirmed by turning the light off in some instances, leading to a steady decrease of **F-I1** and **F-I2** while **3a** is constantly generated (see Fig. S-4-2) solidifying the role of **F-I1** and **F-I2** as a precursor of **3a**.¹

In Figure S-4-11 it can be observed that the starting material **1a** decreases faster than **2b** and is fully consumed after ~6 hours, which also halts product conversion of **3a** (and **OC-I** as well as **F-I**) at ~40 %. This big difference compared to the batch reaction (96 % isolated yield, see Chapter 4.2.1 Table 4-1 entry **3a**) is due to heavy precipitation of a yellow solid. It could be demonstrated that this precipitate contains a significant amount of product **3a** next to DIPEA and probably fluoride salts (see Fig. S-4-14). It can also be assumed that parts of this solid could still participate in the reaction as it also contains photocatalyst **P3**. Next to the main products presented in Figure S-4-11 several other fragmentation products originating from DIPEA could be assigned (data not shown). These are diisopropylamine, *N*-ethylisopropylamine, acetaldehyde and acetone. These fragmentation products support the function of DIPEA as a hydrogen source for the formation of **4**. But it is to be noted that several other, unknown side products, originating from DIPEA are also present in solution in low amounts.

¹ It is to be noted that besides the signal sets of **3a**, **F-I1** and **F-I2**, all remaining signal sets stay constant within the observed time frame without illumination (10-20 minutes)

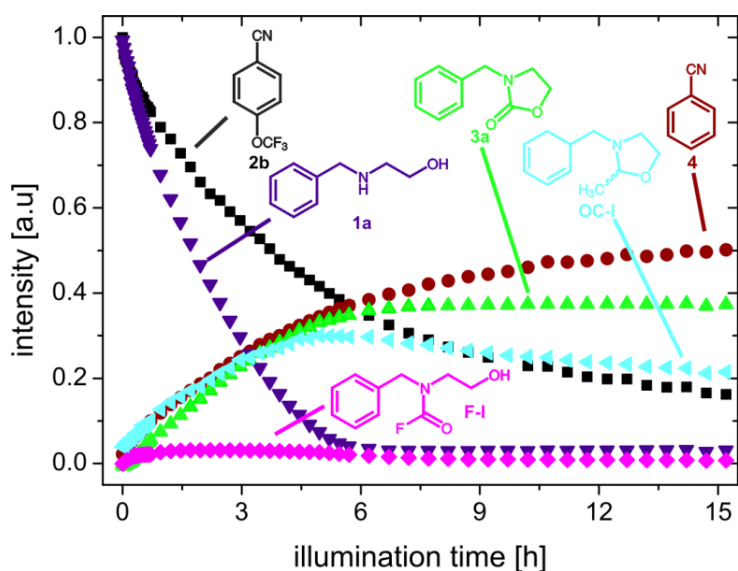


Figure S-4-11. ^1H NMR reaction profile recording the photoreaction of **1a** (100 mM), **2b** (110 mM), DIPEA (300 mM) and **P3** (2 mM) in CD_3CN at 298 K with illumination at 405 nm. The build-up of the desired product **3a** (green) correlates with the formation of the fragmentation product **4** (red) of **2b** (black). Moreover, two intermediates (**F-I**, magenta and **OC-I**, cyan) could be readily assigned. **F-I** is the direct precursor of **3a** stemming from the reaction of **1a** with *in situ* generated fluorophosgene whereas **OC-I** is the result from the reaction of **1a** with acetaldehyde, which in turn is a fragmentation product of DIPEA.

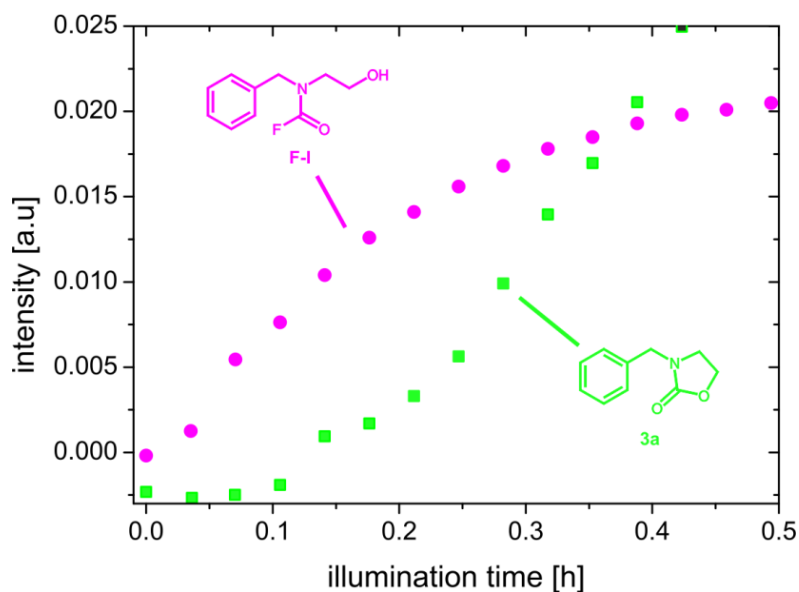


Figure S-4-12. ^1H NMR reaction profile showing the initial trend of **3a** (green) and **F-I** (**F-I1** + **F-I2**, magenta). The formation of **3a** is preceded by an initial lag-phase whilst the intermediate **F-I** is generated immediately after the light is turned on as the direct precursor of **3a** solidifying its role as a direct precursor to **3a**.

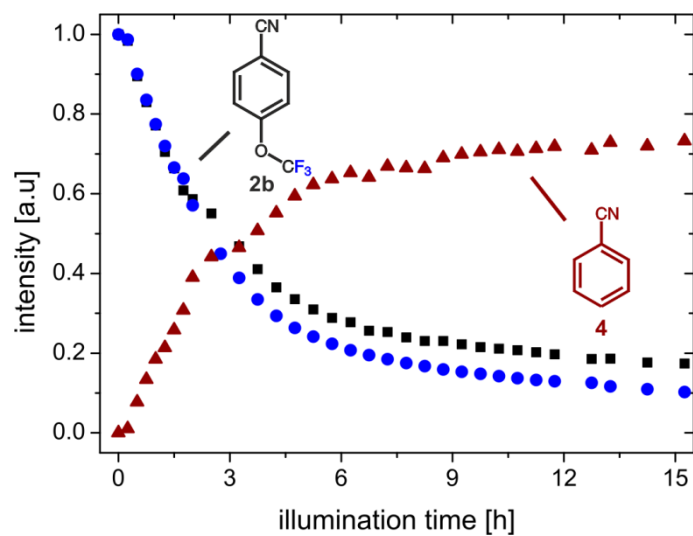


Figure S-4-13. ¹H and ¹⁹F NMR reaction profile. Increase and decrease in signal intensity of the starting material **2b** (¹H black; ¹⁹F blue) and the corresponding reaction product **4** (red). The profile shows a clean conversion of **2b** into **4**. The deviation of the ¹H and ¹⁹F intensities for **2b** comes from overlapping signals in the ¹H NMR spectrum

Figure S-4-14 shows the ^{19}F NMR reaction profile of the photoreaction of **1a** (100 mM), **2b** (110 mM), DIPEA (300 mM) and **P3** (2 mol %) in CD_3CN at 298 K with illumination at 405 nm. Although **2b** (blue) decreases continuously, there is only a slight increase of other fluorine species over time (green). At the end of illumination all other fluorine species only amount to ~12% of the total signal intensity (compared to **2b** in the beginning). As the proposed mechanism (Chapter 4.2.2 Fig. 4.3) suggest that fluoride (F^-) gets liberated not only from the OCF_3^- fragment from **2b** but also from the reaction of fluorophosgene with **1a** and the subsequent intramolecular cyclization to yield **3a**, it can be assumed that most of the fluorine in the reaction is F^- , which then mostly precipitates as some sort of insoluble salt, that can be witnessed as a yellowish solid at the bottom of the NMR tube after illumination. Only small amounts of free F^- can be observed in solution (broad singlet at ~-125 ppm).

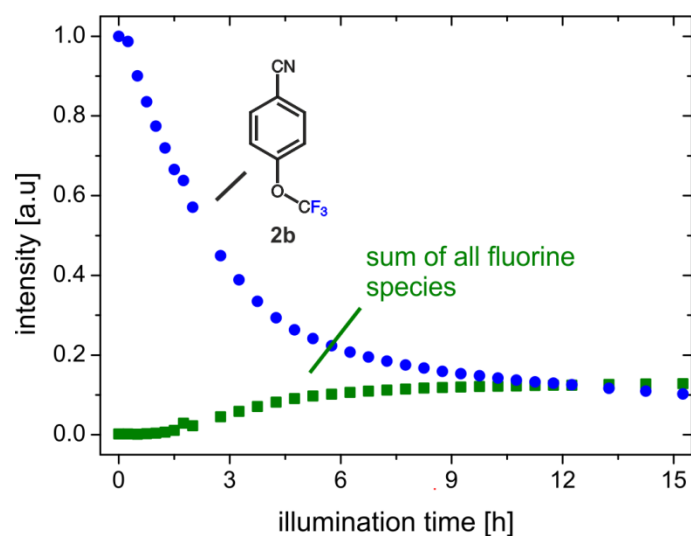


Figure S-4-14. ^{19}F NMR reaction profile showing the decrease of the starting material **2b** (blue) and the increase of all detectable fluorine species (green). The combined observable fluorine species only amount to ~12 % because the bulk of fluorine probably precipitates as various fluoride salts, as F^- is the main fluorine species generated in the reaction.

Ex situ NMR reaction profiles

Ex situ NMR reaction profiles were also recorded, besides the *in situ* reaction profiles. Figure S-4-15 shows the reaction profile of diluted 100 μ L aliquots (final volume 400 μ L; backfilled with CD_3CN) from the photoreaction of **P3** (2 mM), **2b** (110 mM), **1a** (100 mM) and DIPEA (300 mM) in 2 mL CD_3CN at 298 K under continuous illumination with 400 nm. Similar to the *in situ* reaction profile two main products (**3a**, green and **4**, red) and two significant intermediates (**F-I**, magenta and **OC-I**, cyan) can be assigned next to the two starting materials **2b** (black) and **1a** (blue). The decrease of **2b** and the increase of its fragmentation product **4** (red) directly correlate to one another, similar to *in situ* approach. Furthermore, the increase of the main product **3a** (green) also correlates with the decrease of **2b** and the increase of **4**. But it is evident that the conversion rate of **1a** to **3a** is significantly higher compared to the *in situ* reaction owing to the higher light intensity. The two conformations of the important fluorointermediate (**F-I1** and **F-I2**) can also be assigned. Analogous to the *in situ* reaction profile **F-I1** and **F-I2** are treated as one entity (**F-I**) in the reaction profile. Like in the *in situ* reaction, one can detect the chiral side product **OC-I** originating from a side reaction of **1a** with *in situ* generated acetaldehyde. Furthermore, large amounts of precipitate can be again witnessed. The precipitate contains product **3a**, photocatalyst **P3** and fluoride salts, similar to the *in situ* reaction. To sum up, the overall trend of the *ex situ* approach is very much comparable to the *in situ* approach, albeit the *ex situ* approach lead to significantly increased product conversion and shows increased reaction rates. However, there is still a noteworthy, observable difference between the results of the *ex situ* reaction kinetic and the *in situ* reaction kinetics. At the 3 hour mark it is evident that substrate **1a** and **F-I** are fully consumed. Nevertheless, product **3a** is still generated, whereas **OC-I** is decreasing steadily. This is due to a water off-cycle equilibrium between **1a** and **OC-I**. As a result, **OC-I** gets slowly converted back to **1a**, which can then react further on to yield **3a** (and **F-I**) as long as fluorophosgene is still liberated.

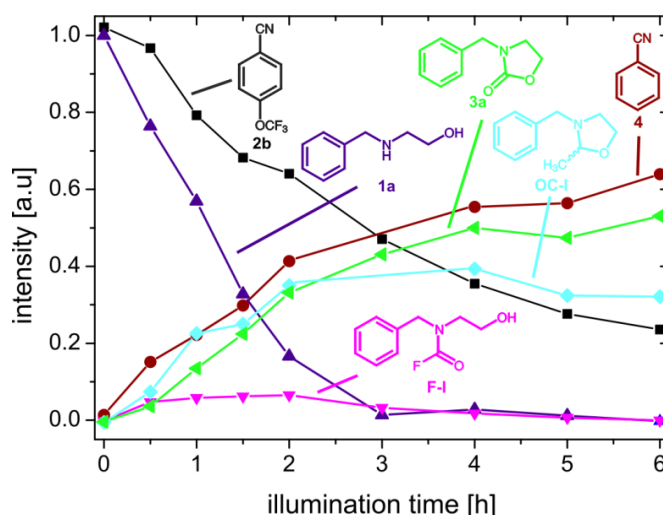


Figure S-4-15. *Ex situ* ^1H NMR reaction profile showing the photoreaction of **1a** (100 mM), **2b** (105 mM), DIPEA (300 mM) and **P3** (2 mM) in 2 mL CD_3CN at 298 K with illumination at 405 nm. The build-up of the desired product **3a** (green) correlates with the formation of the fragmentation product **4** (red) of **2b** (black). Furthermore, two intermediates (F-I, magenta and OC-I, cyan) can be detected. F-I is the direct precursor of **3a** stemming from the reaction of **1a** with *in situ* generated fluorophosgene whereas OC-I is the result from the reaction of **1a** with acetaldehyde, which in turn is a fragmentation product of DIPEA. OC-I and **1a** are in a water dependent off-cycle equilibrium leading to an ongoing generation of **3a** even after **1a** and F-I are consumed as long as fluorophosgene is still liberated.

In situ NMR reaction profiles without **1a**

Next to reaction profiles of the full photoreaction, NMR reaction profiles without the starting material **1a** were recorded as well.

Figure S-4-16 illustrates the full ^1H and ^{19}F NMR reaction profile of the photoreaction of **2b** (110 mM), DIPEA (300 mM) and **P3** (2 mM) in CD_3CN at 300 K with illumination at 405 nm. Immediately after turning on the light all signals of **2b** (^1H ; black and ^{19}F ; blue) start to decrease. Simultaneously a new signal set belonging to **4** (red) appears in the ^1H NMR spectra. The decrease of **2b** and the increase of **4** show that both are directly correlated, as **4** presents the fragmentation product of **2b**. Similar to the full reaction mixture only low amounts of other fluorine signals can be observed in the ^{19}F NMR spectra. Next to a ^{19}F signal of fluoride, several carbonylfluoride signals could be detected. Most of the fluorine again reacts to F^- (broad singlet at ~ 125 ppm) and precipitates as an insoluble salt at the bottom of the NMR tube (see *in situ* NMR reaction profiles with **1a**).

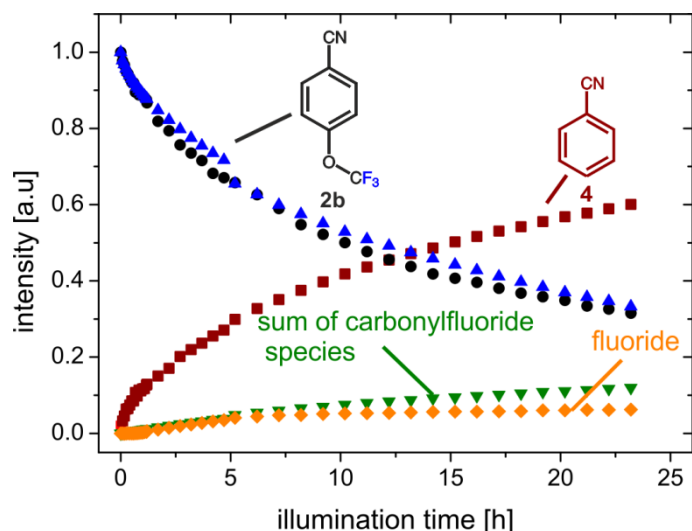


Figure S-4-16. ^1H and ^{19}F NMR reaction profile recording the photoreaction of **2b** (110 mM), DIPEA (300 mM) and **P3** (2 mM) in CD_3CN at 300 K with illumination at 405 nm. The decrease of **2b** (^1H black; ^{19}F blue) directly correlates with the formation of the fragmentation product **4** (red). The combined observable fluorine species only amount to ~13 % because the bulk of fluorine probably precipitates as various fluorides.

Figure S-4-17 shows an excerpt of the reaction mixture of **2b** (110 mM), DIPEA (300 mM) and **P3** (2 mM) in CD_3CN at 300 K after illumination with 405 nm. Overall three ^{19}F signals can be detected (F1-F3; all singlets) next to the starting material **2b** and fluoride², $^1\text{H}^{19}\text{F}$ -HMBC spectra show clear cross signals in the HMBC spectrum for all three signals (Fig. S-4-18). Hence, concerning the proton chemical shifts (3.2 to 1.2 ppm), it can be concluded that F1 to F3 are side products from the reaction with DIPEA and/or its fragmentation products (diisopropylamin, *N*-ethylisopropylamine, etc).

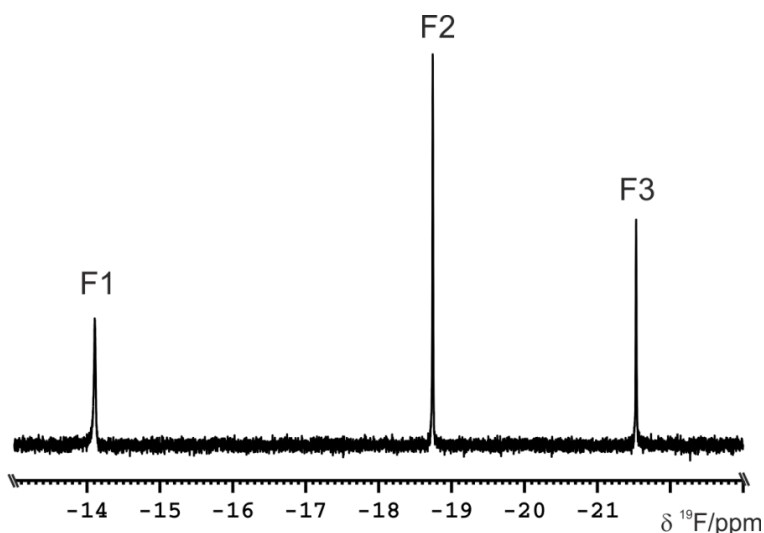


Figure S-4-17. Excerpt of the ^{19}F fluorine spectrum region of the signals in the chemical shift range of carbonylfluorides. Up to three ^{19}F signals (F1-F3) can be clearly identified. Reaction conditions: **2b** (100 mM), DIPEA (300 mM) and **P3** (2 mM) in CD_3CN at 300 K after illumination with 405 nm.

² Fluoride usually appears as a broad singlet at around ~-125 ppm, but the chemical shift heavily depends on the reaction conditions and the progress of the reaction.

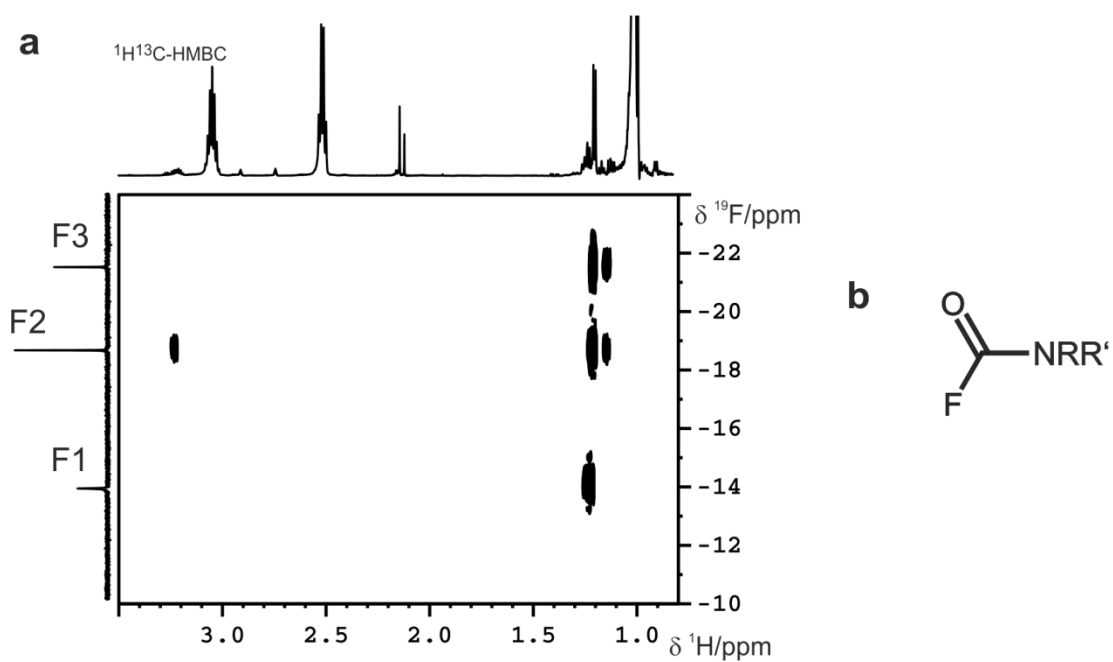


Figure S-4-18. a, ${}^1\text{H}^{19}\text{F}$ -HMBC. All fluorine signals (F1-F3) in the carbonylfluoride region show clear HMBC cross signals to protons of secondary DIPEA products. Parameters: PP = *hmbcgpndqf*; NS = 16; DS = 16; TD-F1 = 128; TD-F2 = 4096; D1 = 1; SW-F1 = 120; SW-F2 = 12; O-F1 = -10; O-F2 = 5; evolution long range coupling = 71.4 ms. b, Likely framework of the secondary products from the reaction of COF_2 with fragmentation products of DIPEA.

Off-cycle equilibrium and role of water

Next to the NMR reaction profiles, further NMR studies were conducted to corroborate the proposed mechanism (see Chapter 4.2.2 Fig. 4.3). Figure S-4-19 depicts a proposal for the water dependent off-cycle equilibrium between **1a** and **OC-I**. Acetaldehyde is released through fragmentation after secondary reactions of DIPEA (see also Chapter 4.2.2 Fig. 4.3), which hereupon can react with starting material **1a** under dehydration to yield the off-cycle intermediate **OC-I**. In turn, addition of water to **OC-I** yields **1a** and acetaldehyde again. The proposed water dependent off-cycle equilibrium leads to two conclusions. First, as long as fluorophosgene is liberated from **2b**, the reaction towards **3a** should continue if **OC-I** is in solution, independent of **1a** and/or **F-I** still being present in detectable amounts. Second, addition of water should shift the equilibrium presented in Figure S-4-19 towards **1a**, eventually suppressing **OC-I**.

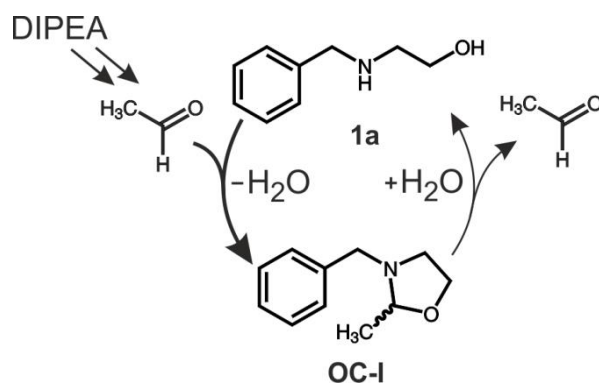


Figure S-4-19. Proposed water dependent off-cycle equilibrium between **1a** and **OC-I**. Secondary reactions of DIPEA lead to the liberation of acetaldehyde, which readily reacts with starting material **1a** to yield **OC-I**. Afterwards **OC-I** and **1a** are in a slow water dependent equilibrium, which can be shifted towards **1a** by the addition of extra water.

Figure S-4-20 shows excerpts of the 1H NMR spectra of the aliphatic region for position 3 of **F-I**, position 3 and 1 of **3a** and position 8 for **OC-I**. Spectrum **a** at the bottom depicts the reaction mixture under standard conditions after 24 hours of illumination. Both starting materials (**2b** and **1a**) and **F-I** are fully consumed. Hence, no reaction is running anymore and only **3a** and **OC-I** are present in solution as relevant reaction products. Spectrum **b** at the top shows the same reaction mixture from spectrum **a** after addition of 5 μ L of **2b** and 1 hour of continuous illumination (total illumination 25 h). It can be clearly witnessed that the intermediate **F-I** is again present in solution, while **OC-I** has decreased in intensity, despite the absence of **1a** and **2b** (product **3a** also increased but concerning the big intensity difference of **3a** and **OC-I** it is hardly presentable). This experiment demonstrates that there has to be an equilibrium between **1a** and **OC-I**, as **OC-I** presents the only conceivable source to provide **1a**.

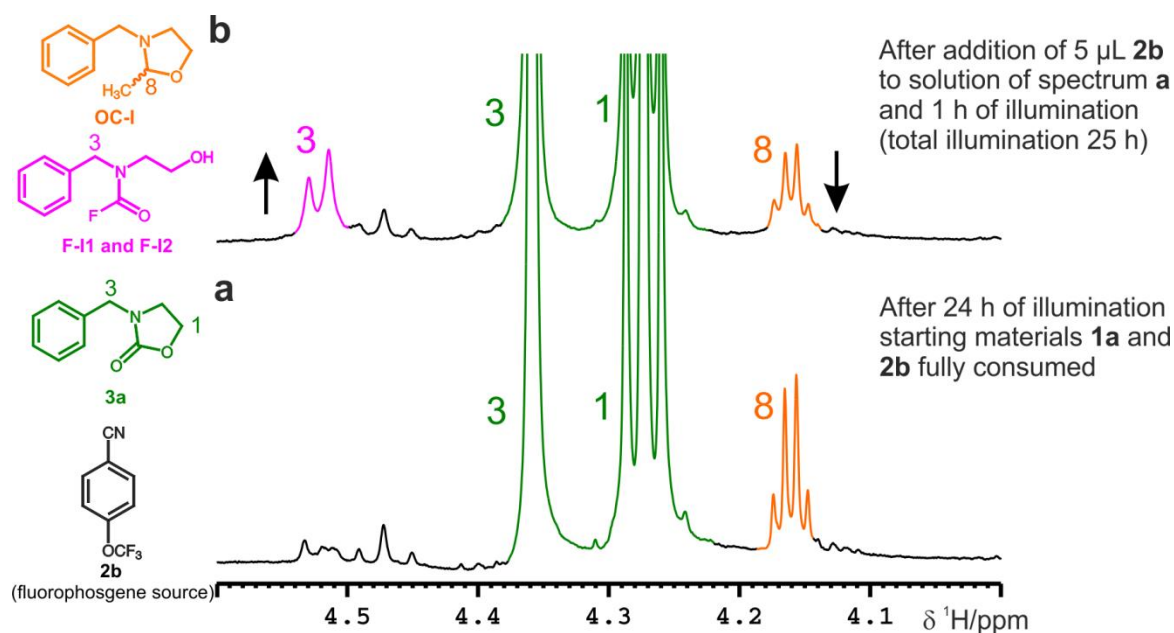


Figure S-4-20. Excerpts of the ¹H NMR spectra of the aliphatic region for position 3 of **F-I**, position 3 and 1 of **3a** and position 8 for **OC-I** of the reaction mixture under standard conditions. **Spectrum a**, reaction solution after 24 hours of illumination. **1a**, **2b** and **F-I** are fully consumed, hence no reaction is progressing. **Spectrum b**, reaction solution after addition of 5 μL **2b** to the mixture of spectrum **a** and 1 hour of further illumination (total illumination time 24 h). **F-I** and **3a** start to be generated again, while **OC-I** is decreasing affirming the proposed off-cycle equilibrium.

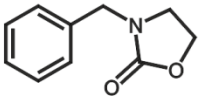
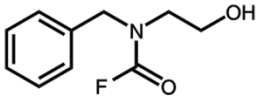
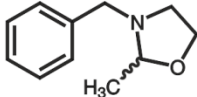
To further investigate on how to influence the off-cycle equilibrium *ex situ* NMR measurements were performed testing different reaction conditions with respect to the general conditions (general conditions: **1a** 100 mM, **2b** 105 mM, **P3** 2 mM, DIPEA 300 mM, in CD₃CN). Next to the general conditions, three modified reaction conditions were tested which were derived from the off-cycle proposal (Fig. S-4-19).³ Samples were taken after two hours of continuous illumination comparing the amount of **3a**, **F-I** (comprising of **F-I1** and **F-I2**) and **OC-I**. The results are summarized in Table S1. First the general conditions yield the same result as the regular *ex situ* NMR reaction kinetics with a comparable amount of **3a** and **OC-I** and low amounts of **F-I**. For the first modified condition, the concentration of **2b** was doubled from 105 mM (1.05 eq) to 210 mM (2.10 equiv.) with the idea that more **2b** should lead to a longer and increased supply of fluorophosgene. The result shows a heavily increased amount of generated **F-I**, while **OC-I** is already suppressed by around 50 % with respect to the general conditions whereas the amount of **3a** stays rather constant. For the second modified reaction condition, the influence of water on the off-cycle equilibrium between **1a** and **3a** was investigated. Here, the solvent mixture was changed to CD₃CN/H₂O (9:1) instead of pure CD₃CN. The results in Table S-4-1 indicate a distinct shift in the off-cycle equilibrium towards **1a** as well as a much faster reaction. After two hours the sum of **3a** and **F-I** already reaches above 90 % and **OC-I** is almost fully suppressed. This shows that the water amount influences the off-cycle equilibrium considerably and can be used to effectively accelerate the reaction. The last modification of reaction conditions is basically a combination of the two

³ All reactions within the *ex situ* NMR measurements including the general conditions also contained 12 equiv. of 1,4-cyclohexadiene, which leads to a partial recovery of DIPEA. But it didn't notably affect any kinetics or yields.

modifications already described. The concentration of **2b** is increased from 105 mM (1.05 equiv.) to 210 mM (2.1 equiv.) and the solvent was changed from pure CD₃CN to CD₃CN/H₂O (9:1). Under these conditions, generation of **OC-I** can be completely suppressed, while conserving the high amount of **3a** + **F-I**.

The results presented in Table S-4-1 allow the conclusion that the reaction can be very much optimized substrate specific by tuning the amount of **2b** and the water content.

Table S-4-1. Influence of **2b** and water on product and intermediate formation investigated by *ex situ* NMR measurements.

Conditions	amount after two hours of continuous illumination		
	 3a	 F-I	 OC-I
General conditions	38 %	5 %	32 %
2.1 eq. of 2b instead of 1.05 eq.	34 %	33 %	15 %
Solvent CD ₃ CN/H ₂ O(9:1) instead of pure CD ₃ CN	70 %	21 %	6 %
Solvent CD ₃ CN/H ₂ O (9:1) and 2.1 eq. of 2b	57 %	31 %	>1 %

The amount of **3a** + **F-I** can be viewed as 'potential' amount of product **3a**, because **F-I** converts into **3a** by a self-propagating dark reaction and serves as better comparison between the different reaction conditions (red bracket).

The appearing precipitate during the reaction was also investigated, because a considerable amount was observed in both the *ex situ* and *in situ* reaction approaches. Figure S-4-21 shows an excerpt of the ¹H NMR spectrum of the precipitate dissolved in DMSO. It is evident that the reaction product **3a** is one of the main constituents within the precipitate apart from fluoride which isn't observable in the proton NMR spectrum. The presence of **3a** in the precipitate is one likely reason that the conversion of **1a** to **3a** is never fully completed in the *in situ* ¹H NMR reaction profiles (and sometimes also *ex situ* ¹H NMR measurements). Next to **3a**, DIPEA and secondary products of DIPEA were also found in small amounts within the precipitate. Furthermore, the photocatalyst **P3** could be identified probably owing to its poor solubility in CD₃CN even at low concentrations. Due to the precipitate being dissolved in non-deuterated DMSO, a double solvent suppression comprising of presaturation and excitation sculpting was employed to get rid of the DMSO and water signals.

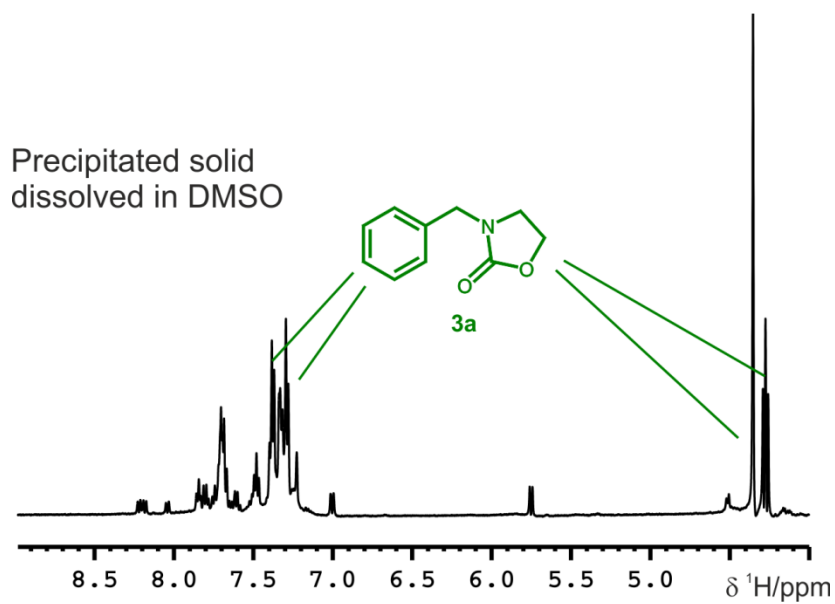
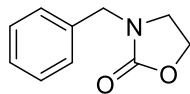


Figure S-4-21. Excerpt of the ¹H proton spectrum of the precipitated solid during the reaction dissolved in DMSO. The signals clearly show product **3a** as one of the prominent components besides the photocatalyst **P3**, DIPEA and secondary products of DIPEA. The DMSO and water peaks were suppressed *via* a combination of excitation sculpting and presaturation.

4.5 Product Characterizations

3-Benzylloxazolidin-2-one^[21]

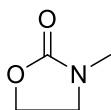


3a

Yield: 96%, 0,096 mmol, 17.0 mg, yellowish oil; (70%, 4.9 mmol, 865 mg for the gram scale reaction).

¹H NMR (400 MHz, CDCl₃); δ [ppm]: 7.39-7.27 (m, 5H); 4.43 (s, 2H); 4.33-4.27 (t, *J* = 8.0 Hz, 2H); 3.45-3.39 (t, *J* = 8.0 Hz, 2H). **¹³C NMR** (101 MHz, CDCl₃); δ [ppm]: 158.7; 135.9; 129.0; 128.3; 128.1; 61.9; 48.6; 44.1. **HR-MS (ESI):** (M+H)⁺: calc.: 178.0863, found: 178.0867. **MF:** C₁₀H₁₁NO₂. **MW:** 177.20 g/mol.

3-Methyloxazolidin-2-one^[22]

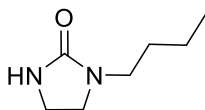


3b

Yield: 99%, 0,199 mmol, 20.1 mg, yellowish oil.

¹H NMR (400 MHz, CDCl₃); δ [ppm]: 4.32-4.26 (t, *J* = 8.0 Hz 2H); 3.58-3.52 (t, *J* = 8.0 Hz 2H); 2.87 (s, 3H). **¹³C NMR** (101 MHz, CDCl₃); δ [ppm]: 158.9; 61.6; 46.9; 31.2. **HR-MS (ESI):** (M+H)⁺: calc.: 102.0550, found: 102.0550. **MF:** C₄H₇NO₂. **MW:** 101.11 g/mol.

1-Butylimidazolidin-2-one

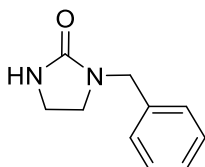


3c

Yield: 99%, 0,198 mmol, 28.2 mg, yellowish oil.

¹H NMR (400 MHz, CDCl₃); δ [ppm]: 4.73 (brs, 1H); 3.42-3.68 (m, 4H); 3.19-3.13 (t, *J* = 7.3 Hz, 2H); 1.51-1.43 (m, 2H); 1.36-1.29 (m, 2H); 0.94-0.89 (t, *J* = 7.3 Hz, 3H). **¹³C NMR** (101 MHz, CDCl₃); δ [ppm]: 163.1; 45.1; 43.4; 38.4; 29.9; 20.1; 13.9. **HR-MS (ESI):** (M+H)⁺: calc.: 143.1179, found: 143.1182. **MF:** C₇H₁₄N₂O. **MW:** 142.20 g/mol.

1-Benzylimidazolidin-2-one^[23]

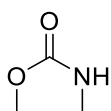


3d

Yield: 68%, 0,136 mmol, 25.6 mg, yellowish solid.

¹H NMR (400 MHz, CDCl₃); δ [ppm]: 7.36-7.24 (m, 5H); 4.85 (brs, 1H); 4.37 (s, 2H); 3.43-3.37 (m, 2H); 3.33-3.27 (m, 2H). **¹³C NMR** (101 MHz, CDCl₃); δ [ppm]: 162.8; 137.2; 128.7; 128.2; 127.6; 47.8; 44.7; 38.2. **HR-MS (ESI):** (M+H)⁺: calc.: 177.1022, found: 177.1025. **MF:** C₁₀H₁₂N₂O. **MW:** 176.22 g/mol.

Oxazolidin-2-one^[24]

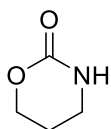


3e

Yield: 84%, 0,146 mmol, 14.6 mg, yellowish solid.

¹H NMR (400 MHz, CDCl₃); δ [ppm]: 5.98 (brs, 1H); 4.49-4.39 (t, *J* = 8.0 Hz 2H); 3.66-3.60 (t, *J* = 8.0 Hz 2H). **¹³C NMR** (101 MHz, CDCl₃); δ [ppm]: 160.8; 65.1; 40.8. **HR-MS (EI):** (M)⁺: calc.: 87.0315, found: 87.0330. **MF:** C₃H₅NO₂. **MW:** 87.08 g/mol.

1,3-Oxazinan-2-one^[25]

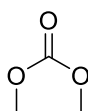


3f

Yield: 63%, 0,126 mmol, 12.8 mg, yellowish solid.

¹H NMR (400 MHz, DMSO-d₆); δ [ppm]: 7.11 (brs, 1H); 4.17-4.11 (t, *J* = 5.3 Hz 2H); 3.18-3.12 (m, 2H); 1.85-1.77 (quint., *J* = 5.0 Hz, 6.0 Hz, 2H). **¹³C NMR** (101 MHz, DMSO-d₆); δ [ppm]: 152.8; 66.1; 38.9; 20.9. **HR-MS (ESI):** (M+H)⁺: calc.: 102.0550, found: 102.0552. **MF:** C₄H₇NO₂. **MW:** 101.11 g/mol.

1,3-Dioxolan-2-one^[26]

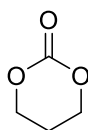


3g

Yield: 70%, 0,139 mmol, 12.3 mg, yellowish oil.

¹H NMR (400 MHz, CDCl₃); δ [ppm]: 4.52 (s, 1H). **¹³C NMR** (101 MHz, CDCl₃); δ [ppm]: 155.5; 64.7. **HR-MS (EI):** (M)⁺: calc.: 88.0160, found: 88.0168. **MF:** C₃H₄O₃. **MW:** 88.06 g/mol.

1,3-Dioxan-2-one^[27]

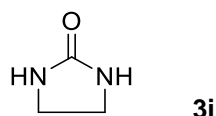


3h

Yield: 99%, 0,198 mmol, 20.2 mg, yellowish oil.

¹H NMR (400 MHz, CDCl₃); δ [ppm]: 4.47-4.41 (t, *J* = 5.7 Hz, 4H); 2.17-2.10 (quint, *J* = 5.7 Hz, *J* = 5.7 Hz, 2H). **¹³C NMR** (101 MHz, CDCl₃); δ [ppm]: 148.6; 68.0; 21.9. **HR-MS (EI):** (M)⁺: calc.: 102.0317, found: 102.0320. **MF:** C₄H₆O₃. **MW:** 102.09 g/mol.

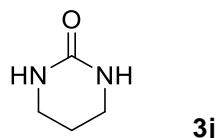
Imidazolin-2-one^[28]



Yield: 65%, 0,130 mmol, 11.2 mg, yellowish solid.

¹H NMR (400 MHz, Acetone-d₆); δ [ppm]: 5.61 (brs, 2H); 3.42 (s, 4H). **¹³C NMR** (101 MHz, Acetone-d₆); δ [ppm]: 165.4; 41.4. **HR-MS (ESI):** (M+H)⁺: calc.: 87.0553, found: 87.0551. **MF:** C₃H₆N₂O. **MW:** 86.09 g/mol.

Tetrahydropyrimidin-2-(1H)-one^[29]

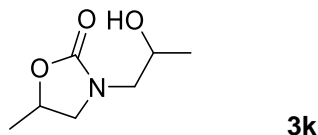


Yield: 73%, 0,146 mmol, 14.7 mg, yellowish solid.

¹H NMR (400 MHz, DMSO-d₆); δ [ppm]: 6.05 (s, 2H); 3.10-3.04 (m, 4H); 1.71-1.63 (quint, *J* = 5.8 Hz, 5.8 Hz, 2H). **¹³C NMR** (101 MHz, DMSO-d₆); δ [ppm]: 155.8; 39.4; 21.5. **HR-MS (ESI):** (M+H)⁺: calc.: 101.0709, found: 101.0710.

MF: C₄H₈N₂O. **MW:** 100.12 g/mol.

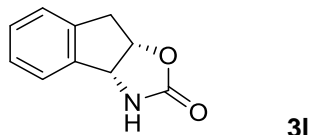
3-(2-Hydroxypropyl)-5-methyloxolidin-2-one



Yield: 70%, 0,140 mmol, 22.4 mg, yellowish oil.

¹H NMR (400 MHz, CDCl₃); δ [ppm]: 4.71-4.56 (m, 1H); 4.07-3.97 (m, 1H); 3.83-3.74 (m, 1H); 3.30-3.12 (m, 3H); 2.65 (brs, 1H); 1.44-1.40 (d, *J* = 6.3 Hz, 3H); 1.22-1.19 (d, *J* = 6.3 Hz, 3H). **¹³C NMR** (101 MHz, CDCl₃); δ [ppm]: 159.1; 70.6; 66.7; 53.2; 51.8; 21.1; 20.7. **HR-MS (ESI):** (M+H)⁺: calc.: 160.0968, found: 160.0968. **MF:** C₇H₁₃NO₃. **MW:** 159.19 g/mol.

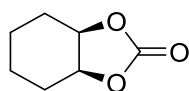
(3aR,8aS)-decahydro-2H-indeno[1,2-d]oxazol-2-one



Yield: 53%, 0,106 mmol, 18.3 mg, yellowish solid.

¹H NMR (400 MHz, CDCl₃); δ [ppm]: 7.34-7.23 (m, 4H); 6.37 (brs, 1H); 5.44-5.38 (m, 1H); 5.20-5.15 (d, *J* = 7.3 Hz, 1H); 3.45-3.30 (m, 2H). **¹³C NMR** (101 MHz, CDCl₃); δ [ppm]: 159.5; 140.3; 140.0; 129.6; 128.1; 125.8; 124.8; 80.7; 61.3; 39.0. **HR-MS (ESI):** (M+H)⁺: calc.: 176.0706, found: 176.0707. **MF:** C₁₀H₉NO₂. **MW:** 175.19 g/mol.

(3aR,7aS)-Hexahydrobenzo[d][1,3]dioxol-2-one

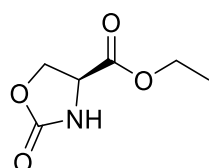


3m

Yield: 72%, 0,144 mmol, 20.6 mg, yellowish oil.

¹H NMR (400 MHz, CDCl₃); δ [ppm]: 4.71-4.64 (m, 2H); 1.94-1.85 (m, 4H); 1.68-1.56 (m, 2H); 1.47-1.37 (m, 2H). **¹³C NMR** (101 MHz, CDCl₃); δ [ppm]: 155.5; 75.9; 26.9; 19.3. **HR-MS (EI):** (M-HCO₂)⁺: calc.: 97.0653, found: 97.0655. **MF:** C₇H₁₀O₃. **MW:** 142.15 g/mol.

Ethyl (S)-2-oxooxazolidinine-4-carboxylate^[30]



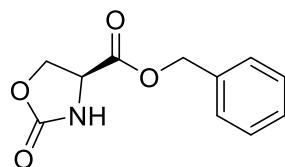
3n

Yield: 99%, 0,198 mmol, 31.6 mg, yellowish oil.

¹H NMR (400 MHz, CD₃CN); δ [ppm]: 6.23 (brs, 1H); 4.56-4.49 (m, 1H); 4.40-4.34 (m, 2H); 4.23-4.16 (q, *J* = 7.2 Hz, 7.0 Hz, 2H); 1.28-1.23 (t, *J* = 7.1 Hz, 3H). **¹³C NMR** (101 MHz, CD₃CN); δ [ppm]: 171.8; 159.6; 67.7; 62.7; 54.6; 14.4. **HR-MS (ESI):** (M+H)⁺: calc.: 160.0604, found: 160.0610. **MF:** C₆H₉NO₄. **MW:** 159.14 g/mol.

Reaction conditions: The compound was prepared according to general procedure A but 4 equiv. of DIPEA were used because the starting material was a hydrochloride salt.

Benzyl (S)-2-oxooxazolidinine-4-carboxylate



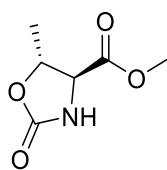
3o

Yield: 79%, 0,158 mmol, 35.1 mg, yellowish oil.

¹H NMR (400 MHz, CD₃CN); δ [ppm]: 7.38-7.32 (m, 5H); 6.28 (brs, 1H); 4.62-4.55 (m, 1H); 4.52-4.46 (m, 1H); 4.45-4.39 (m, 1H). **¹³C NMR** (101 MHz, CD₃CN); δ [ppm]: 170.0; 158.9; 134.6; 129.0; 128.9; 128.7; 68.1; 66.7; 53.9. **HR-MS (ESI):** (M+H)⁺: calc.: 222.0761, found: 222.0764. **MF:** C₁₁H₁₁NO₄. **MW:** 221.21 g/mol.

Reaction conditions: The compound was prepared according to general procedure A but 4 equiv. of DIPEA were used because the starting material was a hydrochloride salt.

Methyl (4*S*,5*R*)-5-methyl-2-oxooxazolidine-4-carboxylate^[31]



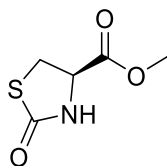
3p

Yield: 70%, 0,140 mmol, 22.4 mg, yellowish oil.

¹H NMR (400 MHz, CDCl₃); δ [ppm]: 6.25 (brs, 1H); 4.77-4.68 (quint, *J* = 6.3 Hz, 5.9 Hz, 1H); 4.01-3.97 (d, *J* = 5.4 Hz, 1H); 3.80 (s, 3H); 1.56-1.53 (d, *J* = 6.4 Hz, 3H). **¹³C NMR** (101 MHz, CDCl₃); δ [ppm]: 170.3; 158.3; 75.7; 60.4; 53.1; 21.2. **HR-MS (ESI):** (M+H)⁺: calc.: 160.0604, found: 160.0612. **MF:** C₆H₉NO₄. **MW:** 159.14 g/mol.

Reaction conditions: The compound was prepared according to general procedure A but 4 equiv. of DIPEA were used because the starting material was a hydrochloride salt.

Methyl (R)-2-oxothiazolidine-4-carboxylate^[30]



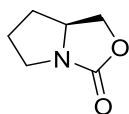
3q

Yield: 60%, 0,120 mmol, 19.4 mg, yellowish oil.

¹H NMR (400 MHz, CDCl₃); δ [ppm]: 6.14 (brs, 1H); 4.47-4.39 (m, 1H); 3.82 (s, 3H); 3.71-3.67 (d, *J* = 8.2 Hz, 1H); 3.66-3.62 (d, *J* = 5.2 Hz, 1H). **¹³C NMR** (101 MHz, CDCl₃); δ [ppm]: 174.4; 170.5; 55.9; 53.3; 31.9. **HR-MS (ESI):** (M+H)⁺: calc.: 162.0219, found: 162.0219. **MF:** C₅H₇NO₃S. **MW:** 161.18 g/mol.

Reaction conditions: The compound was prepared according to general procedure A but 4 equiv. of DIPEA were used because the starting material was a hydrochloride salt.

(S)-Tetrahydro-1*H*,3*H*-pyrrolo[1,2-*c*]oxazol-3-one^[32]

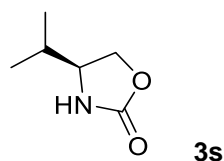


3r

Yield: 58%, 0,116 mmol, 14.8 mg, yellowish oil.

¹H NMR (400 MHz, CDCl₃); δ [ppm]: 4.54-4.47 (t, *J* = 8.3 Hz, 1H); 4.19-4.13 (dd, *J* = 8.9 Hz, 3.7 Hz, 1H); 3.90-3.84 (m, 1H); 3.69-3.60 (m, 1H); 3.22-3.13 (m, 1H); 2.11-2.01 (m, 2H); 1.97-1.87 (m, 1H); 1.53-1.41 (m, 1H). **¹³C NMR** (101 MHz, CDCl₃); δ [ppm]: 161.8; 67.9; 59.6; 45.9; 30.9; 25.8. **HR-MS (ESI):** (M+H)⁺: calc.: 128.0706, found: 128.0709. **MF:** C₆H₉NO₂. **MW:** 127.14 g/mol.

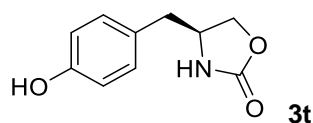
(S)-4-Isopropylloxazolidin-2-one^[32]



Yield: 59%, 0,118 mmol, 15.1 mg, yellowish oil.

¹H NMR (400 MHz, CDCl₃); δ [ppm]: 6.39 (brs, 1H); 4.47-4.40 (t, *J* = 8.6 Hz, 3.7 Hz, 1H); 4.13-4.06 (dd, *J* = 6.3 Hz, 2.4 Hz, 1H); 3.64-3.56 (q, *J* = 6.8 Hz, 8.4 Hz, 1H); 1.76-1.69 (m, 1H); 0.97-0.94 (d, *J* = 6.7 Hz, 2H); 0.91-0.88 (d, *J* = 6.8 Hz, 2H). **¹³C NMR** (101 MHz, CDCl₃); δ [ppm]: 160.4; 68.7; 58.5; 32.8; 18.1; 17.8. **HR-MS (ESI):** (M+H)⁺: calc.: 130.0863, found: 130.0866. **MF:** C₆H₁₁NO₂. **MW:** 129.16 g/mol.

(S)-4-(4-Hydroxybenzyl)oxazolidin-2-one^[33]

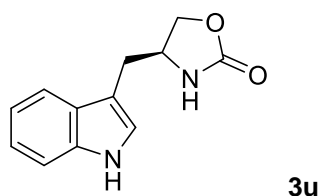


Yield: 58%, 0,116 mmol, 22.5 mg, white solid.

¹H NMR (400 MHz, DMSO-d₆); δ [ppm]: 9.24 (s, 1H); 7.72 (s, 1H); 7.04-7.00 (d, *J* = 8.5 Hz, 2H); 6.70-6.66 (d, *J* = 8.5 Hz, 2H); 4.27-4.18 (m, 1H); 4.00-3.91 (m, 2H); 2.73-2.67 (m, 1H); 2.64-2.57 (m, 1H). **¹³C NMR** (101 MHz, DMSO-d₆); δ [ppm]: 158.6; 156.0; 130.3; 126.5; 115.2; 68.0; 52.7; 39.4. **HR-MS (ESI):** (M+H)⁺: calc.: 194.0821, found: 194.0816. **MF:** C₁₀H₁₁NO₃. **MW:** 193.20 g/mol.

Reaction conditions: The compound was prepared according to general procedure A but 4 equiv. of DIPEA were used because the starting material was a hydrochloride salt.

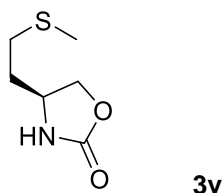
(S)-4-((1H-Indol-3-yl)methyl)oxazolidin-2-one^[30]



Yield: 79%, 0,158 mmol, 34.0 mg, yellowish oil.

¹H NMR (400 MHz, Acetone-d₆); δ [ppm]: 10.14 (brs, 1H); 7.63-7.57 (d, *J* = 7.8 Hz, 1H); 7.43-7.37 (d, *J* = 8.1 Hz, 1H); 7.27 (s, 1H); 7.14-6.99 (dt, *J* = 33.5 Hz, 7.6 Hz, 2H); 6.69 (brs, 1H); 4.41-4.33 (t, *J* = 8.4 Hz, 1H); 4.28-4.19 (quint, *J* = 6.6 Hz, 1H); 4.14-4.07 (m, 1H); 3.13-2.94 (m, 2H). **¹³C NMR** (101 MHz, Acetone-d₆); δ [ppm]: 159.6; 137.7; 128.6; 124.3; 122.3; 119.7; 119.1; 112.3; 110.6; 70.0; 53.4; 31.7. **HR-MS (ESI):** (M+H)⁺: calc.: 217.0972, found: 217.0970. **MF:** C₁₂H₁₂N₂O₂. **MW:** 216.24 g/mol.

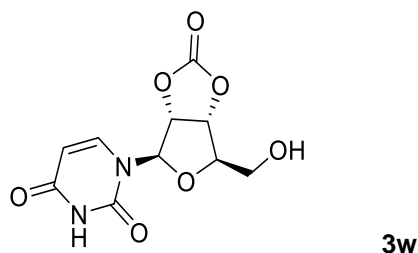
(S)-4-(2-(Methylthio)ethyl)oxazolidin-2-one^[34]



Yield: 99%, 0,198 mmol, 32.0 mg, yellowish oil.

¹H NMR (400 MHz, CDCl₃); δ [ppm]: 6.19 (brs, 1H); 4.56-4.48 (m, 1H); 4.07-3.98 (m, 2H); 2.59-2.54 (t, *J* = 7.1 Hz, 2H); 2.11 (s, 3H); 1.93-1.84 (m, 2H). **¹³C NMR** (101 MHz, CDCl₃); δ [ppm]: 159.7; 70.2; 52.1; 34.2; 30.5; 15.7. **HR-MS (EI):** (M)⁺: calc.: 161.0505, found: 161.0506. **MF:** C₆H₁₁NO₂S. **MW:** 161.22 g/mol.

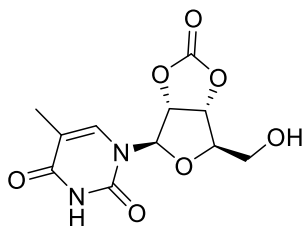
1-((3a*R*,4*R*,6*R*,6a*R*)-6-(Hydroxymethyl)-2-oxotetrahydrofuro[3,4-*d*][1,3]dioxol-4-yl)-pyrimidine-2,4(1*H*,3*H*)-dione



Yield: 27%, 0,054 mmol, 14.5 mg, colorless solid.

¹H NMR (400 MHz, DMSO-*d*₆); δ [ppm]: 11.48 (brs, 1H); 7.77-7.71 (d, *J* = 8.1 Hz, 1H); 6.00-5.95 (d, *J* = 2.2 Hz, 1H); 5.68-5.63 (dd, *J* = 8.0 Hz, 2.1 Hz, 1H); 5.59-5.52 (dd, *J* = 7.8 Hz, 2.2 Hz, 1H); 5.25-5.20 (dd, , *J* = 7.7 Hz, 3.8 Hz, 1H); 5.18-5.13 (t, *J* = 5.5 Hz, 1H); 4.29-4.24 (q, *J* = 5.5 Hz, 4.1 Hz, 1H); 3.63-3.58 (t, *J* = 5.5 Hz, 2H). **¹³C NMR** (101 MHz, DMSO-*d*₆); δ [ppm]: 163.3; 153.7; 150.3; 142.8; 101.8; 92.0; 86.2; 82.8; 80.2; 60.7. **HR-MS (ESI):** (M-H)⁻: calc.: 269.0415, found: 269.0420. **MF:** C₁₀H₁₀N₂O₇. **MW:** 270.20 g/mol.

1-((3aR,4R,6R,6aR)-6-(Hydroxymethyl)-2-oxotetrahydrofuro[3,4-d][1,3]dioxol-4-yl)-5-methylpyrimidine-2,4(1H,3H)-dione

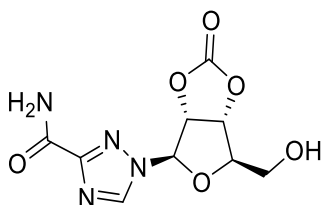


3x

Yield: 44%, 0,088 mmol, 25.0 mg, colorless solid.

¹H NMR (400 MHz, Acetone-d₆); δ [ppm]: 10.21 (brs, 1H); 7.63-7.58 (m, 1H); 5.97-5.93 (m, 1H); 5.68-5.63 (dd, *J* = 2.3 Hz, 5.4 Hz, 1H); 5.44-5.37 (m, 1H); 4.42-4.35 (q, *J* = 4.8 Hz, 4.2 Hz, 1H); 4.34-4.27 (t, *J* = 5.7 Hz, 1H); 3.89-3.80 (m, 2H); 1.84-1.81 (m, 3H). **¹³C NMR** (101 MHz, Acetone-d₆); δ [ppm]: 164.3; 154.4; 151.4; 139.3; 111.2; 94.2; 87.7; 83.9; 81.0; 62.3; 12.3. **HR-MS (ESI):** (M-H)⁻: calc.: 283.0572, found: 283.0580. **MF:** C₁₁H₁₂N₂O₇. **MW:** 284.22 g/mol.

1-((3aR,4R,6R,6aR)-6-(Hydroxymethyl)-2-oxotetrahydrofuro[3,4-d][1,3]dioxol-4-yl)-1H-1,2,4-triazole-3-carboxamide



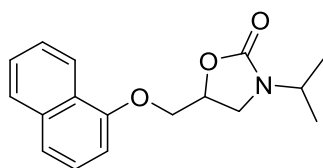
3y

Yield: 45%, 0,090 mmol, 24.1 mg, colorless solid.

¹H NMR (400 MHz, DMSO-d₆); δ [ppm]: 8.85 (s, 1H); 7.90 (brs, 1H); 7.70 (brs, 1H); 6.58 (s, 1H); 5.80-5.76 (d, *J* = 7.2 Hz, 1H); 5.49-5.45 (m, 1H); 5.14-5.09 (t, *J* = 5.5 Hz, 1H); 4.48-4.42 (t, *J* = 6.5 Hz, 1H); 3.53-3.38 (m, 2H). **¹³C NMR** (101 MHz, DMSO-d₆); δ [ppm]: 160.5; 158.0; 153.9; 146.3; 110.0; 91.2; 88.0; 83.7; 81.6; 60.8. **HR-MS (ESI):** (M+H)⁺: calc.: 271.0673, found: 271.0677. **MF:** C₉H₁₀N₄O₆. **MW:** 270.20 g/mol.

Reaction conditions: The compound was prepared according to general procedure A but DMF was used as a solvent instead of MeCN.

3-Isopropyl-5-((naphthalen-1-yloxy)methyl)oxazolidine-2-one



3z

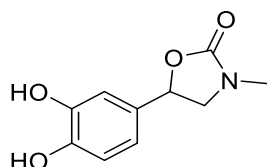
Yield: 66%, 0,132 mmol, 37.6 mg, yellowish oil.

¹H NMR (300 MHz, CDCl₃); δ [ppm]: 8.22-8.14 (m, 1H); 7.83-7.77 (m, 1H); 7.51-7.43 (m, 3H); 7.40-7.33 (m, 1H); 6.83-6.77 (d, *J* = 7.4 Hz, 1H); 5.01-4.90 (m, 1H); 4.32-4.25 (d, *J* = 4.6 Hz, 2H); 4.25-4.14 (quint, *J* = 6.8 Hz, 6.8 Hz, 1H); 3.76-3.69 (t, *J* = 8.8 Hz, 2H); 3.63-3.56 (m, 1H); 1.25-1.20 (d, *J* = 6.8 Hz, 6H).

¹³C NMR (75 MHz, CDCl₃); δ [ppm]: 156.9; 153.9; 134.6; 127.6; 126.7; 125.7; 125.6; 121.8; 121.3; 104.9; 71.0; 68.4; 45.0; 42.0; 19.9. **HR-MS (ESI):** (M+H)⁺: calc.: 286.1438, found: 286.1452. **MF:** C₁₇H₁₉NO₃. **MW:** 285.34 g/mol.

Reaction conditions: The compound was prepared according to general procedure A but 4 equiv. of DIPEA were used because the starting material was a hydrochloride salt.

5-(3,4-Dihydroxyphenyl)-3,4-dimethyloxazolidin-2-one



3aa

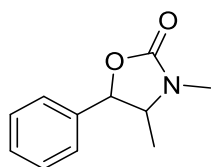
Yield: 67%, 0,134 mmol, 28.0 mg yellowish solid.

¹H NMR (400 MHz, Acetone d₆); δ [ppm]: 8.05 (brs, 2H); 6.92-6.88 (m, 1H); 6.86-6.81 (m, 1H); 6.78-6.74 (m, 1H); 5.38-5.30 (t, *J* = 7.9 Hz, 1H); 3.94-3.88 (t, *J* = 8.6 Hz, 1H); 3.47-3.41 (m, 1H); 2.85 (s, 3H).

¹³C NMR (101 MHz, Acetone d₆); δ [ppm]: 158.7; 146.4; 146.2; 132.0; 118.8; 116.1; 114.1; 75.0; 54.8; 31.2. **HR-MS (ESI):** (M+H)⁺: calc.: 210.0761, found: 210.0765. **MF:** C₁₀H₁₁NO₄. **MW:** 209.20 g/mol.

Reaction conditions: The compound was prepared according to general procedure A but 4 equiv. of DIPEA were used because the starting material was a hydrochloride salt.

3,4-Dimethyl-5-phenyloxazolidin-2-one^[30]



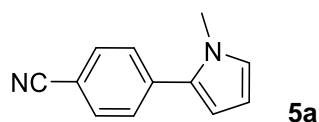
3ab

Yield: 83%, 0,166 mmol, 31.8 mg, yellowish solid.

¹H NMR (400 MHz, CDCl₃); δ [ppm]: 7.41-7.24 (m, 5H); 5.60-5.55 (d, *J* = 8.2 Hz, 1H); 4.05-3.97 (m, 1H); 2.88 (s, 3H); 0.80-0.76 (d, *J* = 6.6 Hz, 3H). **¹³C NMR** (101 MHz, CDCl₃); δ [ppm]: 158.2; 135.3; 128.61;

128.59; 126.3; 78.5; 57.2; 29.1; 14.4. **HR-MS (ESI):** (M+H)⁺: calc.: 192.1019, found: 192.1024. **MF:** C₁₁H₁₃NO₂. **MW:** 191.23 g/mol.

4-(1-Methyl-1H-pyrrol-2-yl)benzonitrile^[35]

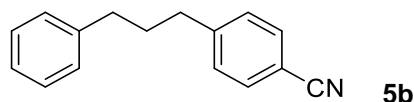


Yield: 48%, 0,096 mmol, 17.5 mg, yellowish oil.

¹H NMR (400 MHz, CDCl₃); δ [ppm]: 7.69-7.65 (m, 2H); 7.83-7.77 (m, 1H); 7.53-7.48 (m, 2H); 6.80-6.77 (m, 1H); 6.37-6.34 (m, 1H); 6.26-6.22 (m, 1H); 3.72 (s, 3H). **¹³C NMR** (101 MHz, CDCl₃); δ [ppm]: 137.8; 132.7; 132.4; 128.4; 126.0; 119.2; 110.9; 109.8; 108.7; 35.6. **HR-MS (EI):** (M)⁺: calc.: 182.0838, found: 182.0839. **MF:** C₁₂H₁₀N₂. **MW:** 182.23 g/mol.

Reaction conditions: The compound was prepared according to general procedure A but an additional 10 equiv. of *N*-methylpyrrole were added to trap the aryl radical.

4-(3-Phenylpropyl)benzonitrile^[36]



Yield: 45%, 0,090 mmol, 20.0 mg, colorless oil.

¹H NMR (400 MHz, CDCl₃); δ [ppm]: 7.60-7.54 (d, *J* = 8.3 Hz, 2H); 7.32-7.26 (m, 4H); 7.25-7.18 (m, 3H); 2.75-2.61 (m, 4H); 2.02-1.92 (m, 2H). **¹³C NMR** (101 MHz, CDCl₃); δ [ppm]: 148.1; 141.7; 132.3; 129.4; 128.6; 128.5; 126.1; 119.3; 109.8; 35.6; 35.4; 32.6. **HR-MS (EI):** (M)⁺: calc.: 221.1199, found: 221.1194. **MF:** C₁₆H₁₅N. **MW:** 221.30 g/mol.

Reaction conditions: The compound was prepared according to general procedure A but an additional 10 equiv. of allylbenzene were added to trap the aryl radical.

4.6 References

- [1] a) M. M. Heravi, V. Zadsirjan, B. Farajpour, *RSC Adv.* **2016**, *6*, 30498-30551; b) M. A. Rodrigo, N. Oturan, M. A. Oturan, *Chem. Rev.* **2014**, *114*, 8720-8745; c) J. Magano, J. R. Dunetz, *Chem. Rev.* **2011**, *111*, 2177-2250; (d) Y. Zhou, J. Wang, Z. Gu, S. Wang, W. Zhu, J. L. Aceña, V. A. Soloshonok, K. Izawa, H. Liu, H. Chem. Rev. **2016**, *116*, 422-518.
- [2] a) A. K. Ghosh, M. Brindisi, *J. Med. Chem.* **2015**, *58*, 2895-2940; b) J. P. Parrish, R. N. Salvatore, K. W. Jung, *Tetrahedron* **2000**, *56*, 8207-8237; c) D. J. Díaz, A. K. Darko, L. McElwee-White, *Eur. J. Org. Chem.* **2007**, 4453-4465.
- [3] L. Pasquato, G. Modena, L. Cotarca, P. Delogu, S. Mantovani, *J. Org. Chem.* **2000**, *65*, 8224-8228.
- [4] a) W. Schneider, W. Diller in *Ullmann's Encyclopedia of Industrial Chemistry*, Vol. 26, Wiley-VCH: Weinheim, **2000**, pp 623-632; b) L. Cotarca, T. Geller, J. Répási, *Org. Process Res. Dev.* **2017**, *21*, 1439-1446.
- [5] T. Sakakura, K. Kohnoa, *Chem. Commun.* **2009**, 1312-1330.
- [6] N. A. Romero, D. A. Nicewicz, *Chem. Rev.* **2016**, *116*, 10075-10166.
- [7] a) D. Petzold, B. König, *Adv. Synth. Catal.* **2018**, *360*, 626-630; b) I. Ghosh, T. Ghosh, J. I. Bardagi, B. König, *Science* **2014**, *346*, 725-728; c) I. Ghosh, B. König, *Angew. Chem. Int. Ed.* **2016**, *55*, 7676-7679; d) S. J. S. Düsel, B. König, *J. Org. Chem.* **2018**, *83*, 7676; e) N. A. Romero, K. A. Margrey, N. E. Tay, D. A. Nicewicz, *Science* **2015**, *349*, 1326-1330.
- [8] a) J. Twilton, C. Le, P. Zhang, M. H. Shaw, R. W. Evans, D. W. C. MacMillan, *Nat. Rev. Chem.* **2017**, *1*, 0052; b) H. Seo, M. H. Katcher, T. F. Jamison, *Nat. Chem.* **2017**, *9*, 453-456; c) A. Studer, D. P. Curran, *Nat. Chem.* **2014**, *6*, 765-773; d) M. N. Hopkinson, A. Tlahuext-Aca, F. Glorius, *Acc. Chem. Res.* **2016**, *49*, 2261-2272.
- [9] a) A. Neubauer, G. Grell, A. Friedrich, S. I. Bokarev, P. Schwarzbach, F. Gärtner, A.-E. Surkus, H. Junge, M. Beller, O. Kühn, S. Lochbrunner, *J. Phys. Chem. Lett.* **2014**, *5*, 1355-1360; b) A. Singh, C. J. Fennell, J. D. Weaver, *Chem. Sci.* **2016**, *7*, 6796-6802; c) Z. Lu, T. P. Yoon, *Angew. Chem. Int. Ed.* **2012**, *51*, 10329-10332.
- [10] a) M. H. Shaw, J. Twilton, D. W. C. MacMillan, *J. Org. Chem.* **2016**, *81*, 6898-6926; b) M. Majek, A. Jacobi von Wangelin, *Acc. Chem. Res.* **2016**, *49*, 2316-2327; c) D. A. Petrone, J. Ye, M. Lautens, *Chem. Rev.* **2016**, *116*, 8003-8104.
- [11] (a) A. Iijima, H. Amii, *Tetrahedron Lett.* **2008**, *49*, 6013-6015; b) K. K. K. Goh, A. Sinha, C. Fraser, R. D. Young, *RSC Adv.* **2016**, *6*, 42708-42712; c) C. Combellas, F. Kanoufi, A. Thiébault, *J. Electroanal. Chem.* **1997**, *432*, 181-192.
- [12] a) B. Sahoo, M. N. Hopkinson, *Angew. Chem. Int. Ed.* **2018**, *57*, 7942-7944; b) B. J. Jelier, P. F. Tripet, E. Pietrasiak, I. Franzoni, G. Jeschke, A. Togni, *Angew. Chem. Int. Ed.*, **2018**, *57*, 13784-13789
- [13] a) R. M. Pearson, C. Hooi-Lim, B. G. McCarthy, C. B. Musgrave, *J. Am. Chem. Soc.* **2016**, *138*, 11399-11407; b) Y. Du, R. M. Pearson, C. Hooi-Lim, S. M. Sartor, M. Ryan, H. Yang, N. H. Damrauer, G. M. Miyake, *Chem. Eur. J.*, **2017**, *23*, 10962-10968.

- [14] B. G. McCarthy, R. M. Pearson, C. Hooi-Lim, S. M. Sartor, N. H. Damrauer, G. M. Miyake, *J. Am. Chem. Soc.* **2018**, *140*, 5088-5101.
- [15] S. M. Sartor, B. G. McCarthy, R. M. Pearson, G. M. Miyake, N. H. Damrauer, *J. Am. Chem. Soc.* **2018**, *140*, 4778-4781.
- [16] D. P. Hari, P. Schroll, B. König, *J. Am. Chem. Soc.* **2012**, *134*, 2958-2961.
- [17] M. Nguyen, M. H. Matus, V. Ngan, R. Haiges, K. O. Christe, D. A. Dixon, *J. Phys. Chem. A* **2008**, *112*, 1298-1312.
- [18] a) G. R. Fulmer, A. J. M. Miller, N. H. Sherden, H. E. Gottlieb, A. Nudelman, B. M. Stoltz, J. E. Bercaw, K. I. Goldberg, *Organometallics* **2010**, *29*, 2176-2179; b) H. E. Gottlieb, V. Kotlyar, A. Nudelman, *J. Org. Chem.* **1997**, *62*, 7512-7515.
- [19] R. M. Pearson, R. M.; Lim, C.-H.; McCarthy, B. G.; Musgrave, C. B.; Miyake, G. M. *J. Am. Chem. Soc.* **2016**, *138*, 11399-11407.
- [20] A. Seegerer, P. Nitschke, R. M. Gschwind, *Angew. Chem. In. Ed.* **2018**, *57*, 7493-7497.
- [21] X. D. Li, Q. W. Song, X. D. Lang, Y. Chang, L. N. He, *ChemPhysChem* **2017**, *18*, 3182-3188.
- [22] J. W. Lown, S. M. S. Chauhan, *J. Org. Chem.* **1983**, *48*, 3901-3908.
- [23] a) P. Thanigaimalai, K. C. Lee, S. C. Bang, J. H. Lee, C. Y. Yun, E. Roh, B. Y. Hwang, Y. Kim, S. H. Jung, *Bioorg. Med. Chem.* **2010**, *18*, 1135-1142; b) R. C. F. Jones, J. N. Iley, P. M. J. Lory, *ARKIVOC* **2002**, *VI*, 152-163.
- [24] S. Zheng, F. Li, J. Liu, C. Xia, *Tetrahedron Lett.* **2007**, *48*, 5883-5886.
- [25] S. Picard, M. L. Roch, J. Renault, P. Uriac, *Org. Lett.* **2004**, *6*, 4711-4714.
- [26] J. Wang, L. He, X. Dou, F. Wu, *Aust. J. Chem.* **2009**, *62*, 917-920.
- [27] D. J. Darensbourg, A. Horn. Jr., A. I. Moncada, *Green Chem.* **2010**, *12*, 1376-1379.
- [28] D. L. Kong, L. N. He, J. Q. Wang, *Synlett* **2010**, *8*, 1276-1280.
- [29] V. Krishnakumar, B. Chatterjee, C. Gunanathan, *Inorg. Chem.* **2017**, *56*, 7278-7284.
- [30] J. Paz, C. Pérez-Balado, B. Iglesias, L. Munos, *J. Org. Chem.* **2010**, *75*, 3037-3046.
- [31] G. S. Lemen, J. P. Wolfe, *Org. Lett* **2010**, *12*, 2322-2325.
- [32] N. Caldwell, P. S. Campbell, C. Jamieson, F. Potjewyd, I. Simpson, A. J. B. Watson, *J. Org. Chem.* **2014**, *79*, 9347-9354.
- [33] R. Green, J. Peed, J. E. Taylor, R. A. R. Blackburn, S. D. Bull, *Nat. Protoc.* **2013**, *8*, 1890-1906.
- [34] P. Li, X. Yuan, S. Wang, S. Lu, *Tetrahedron* **2007**, *63*, 12419-12423.
- [35] I. Ghosh, B. König, *Angew. Chem. Int. Ed.* **2016**, *55*, 7676-7679.
- [36] M. Amatore, C. Gosmini, *Chem. Eur. J.* **2010**, *16*, 5848-5852.

5. Summary

This thesis presents photochemical and photocatalytic oxidative halogenations of arenes and aryl cyclopropanes as well as the reductive generation of fluorophosgene. The common aspect of the different projects is the presence of halides which are an often-encountered functional group in organic molecules (**Chapter 1**). Therefore, both innovative ways for the introduction of halides into organic molecules (**Chapter 2-3**) as well as new methods for their use as leaving group (**Chapter 4**) were investigated.

Chapter 1 gives a summary of visible light mediated halogenation strategies involving fluorinations, chlorinations, brominations and iodinations of aliphatic and aromatic molecules.

Aryl bromides are a versatile class of organic reagents and although many traditional, thermal methods for their preparation have been developed, **Chapter 2** describes a visible light mediated procedure for this important transformation. The regio-selective bromination of electron rich arenes and heteroarenes can be realized with commercially available sodium-2-anthraquinone sulfate (SAS) as a “green” photocatalyst. SAS was characterized by determination of its excited state oxidation potential by UV-VIS spectroscopy and cyclovoltammetry. Further mechanistic investigations and control reactions suggest the direct single electron oxidation of the arene to the corresponding aryl radical cation intermediate as the catalytic key-step.

Chapter 3 deals with the photochemical oxochlorination of aryl cyclopropanes to form β chloro ketones. These versatile building blocks can act as precursors for several follow-up reactions especially the synthesis of heterocycles and could potentially serve as starting materials for bioconjugation e.g. to form antibody drug conjugates. To achieve this transformation, only common lab chemicals (HCl, HNO₃ and O₂) as well as 395 nm light are necessary. The reaction mechanism was elucidated by ¹⁸O labelling experiments, cyclovoltammetry, UV-VIS spectroscopy and several control reactions suggesting a chlorine radical based chain reaction as operative pathway.

In **Chapter 4** the photocatalytic generation of fluorophosgene is presented. This hazardous and highly toxic reagent can be liberated safely from a commercially available and bench stable aryl trifluoromethoxyether *via* single electron reduction and subsequent fragmentation. The fluorophosgene can react *in situ* with diol, diamines and 2-aminoalcohols to give the corresponding carbonates, urea derivatives and carbamates. A key part of the project was the investigation of the reaction mechanism by in-depth NMR studies as well as transient spectroscopy, cyclovoltammetry and control reactions leading to a complex, but well supported mechanistic proposal.

6. Zusammenfassung

In dieser Arbeit werden photochemische und photokatalytische oxidative Halogenierungen von Arenen und Arylcyclopropanen, sowie die reduktive Erzeugung von Fluorphosgen vorgestellt. Die Gemeinsamkeit der Projekte ist das Strukturmotiv der Halogene, die eine wichtige funktionelle Gruppe in der organischen Synthese darstellen (**Kapitel 1**). Sowohl das Einführen von Halogenen in organische Moleküle (**Kapitel 2-3**), als auch ihre Nutzung als Abgangsgruppe (**Kapitel 4**) wurde intensiv erforscht.

Kapitel 1 gibt einen Überblick über verschiedene durch sichtbares Licht vermittelte Halogenierungsstrategien und beinhaltet sowohl die neusten Forschungsergebnisse über photokatalytische Fluorierungen als auch Chlorierungen, Bromierungen und Iodierungen.

Arylbromide sind eine vielseitige Klasse organischer Reagenzien und obwohl viele thermische Verfahren zu ihrer Herstellung entwickelt wurden, beschreibt **Kapitel 2** ein durch sichtbares Licht vermitteltes neues Verfahren für diese wichtige synthetische Umwandlung. Die regioselektive Bromierung elektronenreicher Aromaten und Heteroaromaten kann mit handelsüblichem Natrium-2-Anthrachinonsulfat (SAS) als "grünem" Photokatalysator realisiert werden. SAS wurde durch Bestimmung seines Oxidationspotentials im angeregten Zustand, durch UV-VIS-Spektroskopie und Cyclovoltammetrie charakterisiert. Weitere mechanistische Untersuchungen und Kontrollreaktionen legen die direkte Eielektronenoxidation des Aromaten zu dem entsprechenden Arylradikalkationen-Intermediat als katalytischen Schlüsselschritt nahe.

Kapitel 3 befasst sich mit der photochemischen Oxochlorierung von Arylcyclopropanen zu β -Chlorketonen. Diese vielseitigen Bausteine können als Vorläufer für mehrere Folgereaktionen, insbesondere für die Synthese von Heterocyclen, dienen und könnten möglicherweise als Ausgangsmaterialien für die Konjugation von Wirkstoffen an Biomoleküle verwendet werden (Antikörper-Wirkstoff-Konjugate). Um diese synthetische Umwandlung zu erreichen, sind nur gewöhnliche Laborchemikalien (HCl, HNO₃ und O₂) sowie Licht mit einer Wellenlänge von 395 nm erforderlich. Der Reaktionsmechanismus wurde durch ¹⁸O-Markierungsexperimente, Cyclovoltammetrie, UV-VIS-Spektroskopie und verschiedene Kontrollreaktionen aufgeklärt und läuft wahrscheinlich über eine Chlorradikal-Kettenreaktion ab.

In **Kapitel 4** wird die photokatalytische Erzeugung von Fluorphosgen vorgestellt. Dieses gefährliche und hochtoxische Reagens kann aus einem stabilen, im Handel erhältlichen Trifluormethoxybenzol-Derivat durch Eielektronenreduktion mit anschließender Fragmentierung freigesetzt werden. Das Fluorphosgen kann *in situ* mit Diolen, Diaminen und 2-Aminoalkoholen zu den entsprechenden Carbonaten, Harnstoffderivaten und Carbamaten reagieren. Ein wesentlicher Teil des Projekts war die Untersuchung des Reaktionsmechanismus durch umfassende NMR-Studien sowie transiente Spektroskopie, Cyclovoltammetrie und Kontrollreaktionen, die zu einem komplexen, aber experimentell gut belegten, mechanistischen Vorschlag führten.

7. Curriculum Vitae

Daniel Petzold



- Nationality: German
- Date of birth: 05 November 1989
- Daniel.Petzold1@gmx.de

PERSONAL PROFILE Creative and proactive team player and independent worker with excellent communication skills and problem-solving abilities

AREA OF RESEARCH Organic Synthesis, Photoredox Catalysis, Late-Stage Functionalization

PROFESSIONAL EXPERIENCE

Research Associate, 01/2016 – 03/2019 (University of Regensburg)

- Successful completion of multiple research projects in the field of organic synthesis utilizing visible light photoredox catalysis
- Supervision of practical lab courses (organic chemistry) and Master students (4)

Research Assistant, 04/2018 – 07/2018 (Umeå University, Sweden)

- Contribution to the synthesis of novel ring fused 2-pyridones as novel antibacterial agents

Chemical laboratory technician / student trainee, 07/2011 – 06/2014 (Grünenthal GmbH)

- LC-MS analysis of building blocks and APIs with Waters™ and Agilent™ UPLC-MS systems (Single-Quad, TOF, Q-TOF)
 - Purification of APIs with preparative HPLC systems
 - API library management, preparation of final compounds for biological testing
-

EDUCATION

PhD in Chemistry (Dr. rer. nat.), 11/2017 – 03/2019 (University of Regensburg)

- Fast-Track PhD program within the DFG Research Training Group GRK1626 “Chemical Photocatalysis“
 - *“Visible Light Mediated Oxidative Halogenation Reactions and Reductive Liberation of Fluorophosgene”*,
Supervisor: Prof. Dr. Burkhard König
-

M.Sc. in Medicinal Chemistry, 09/2014 – 08/2016 (University of Regensburg)

- Medicinal Chemistry, Organic Chemistry, Bioanalytics (“very good”, average: 1.2)
- “*Photocatalysis in the Micro-Flow Reactor*” (“very good”, 1.0),
Supervisor: Prof. Dr. Burkhard König

B.Sc. in Pharmaceutical Chemistry, 09/2010 – 08/2014 (Technical University of Cologne)

- Integrated dual course study, major: Bio-Pharmaceutical Chemistry (“very good”, average: 1.4)
- “*Liposomes as versatile drug delivery system*” (“good”, 1.7),
Supervisors: Prof. Dr. Nicole Teusch and Prof. Dr. Dirk Burdinski

Teaching Post, 04/2013 – 04/2014 (Technical University of Cologne)

- Tutor for organic chemistry, mentor for freshmen

Apprenticeship as Chemical Laboratory Technician, 07/2011 – 01/2013 (Grünenthal GmbH)

- Practical part of the integrated dual course study in Pharmaceutical Chemistry
- Major: Instrumental Analytics (“good”, average: 85%),
Instructor: Roland Glowaki

Apprenticeship as Chemical Production Technician, 08/2009 – 07/2011 (Grünenthal GmbH)

- Operation and maintenance of multi-kilogram scale reactors (“good”, average: 91%),
Instructors: Siegfried Peeters and Roland Glowaki

High School, 09/2000 – 06/2009 (Stiftisches Gymnasium, Düren)

- Graduation with **Allgemeine Hochschulreife** (A-Levels, average 2.0)

ADDITIONAL ACHIEVEMENTS AND QUALIFICATIONS

- Participant of a two-day leadership seminar (leadership styles, feedback, motivation, conflict management)
- “Deutschlandstipendium” at the University of Regensburg (04/2015 – 03/2016)
- First graduate of the “Rheinländisches Verbundzertifikat für Tutorinnen und Tutoren” (a certificate program for tutoring and teaching skills)

MEMBERSHIPS AND GRANTS

- Member of the **DFG Research Training Group GRK 1626 “Chemical Photocatalysis”** (2016 – 2019)
- Travel grant for the research internship at Umeå University
- Member of the **GDCh** (Gesellschaft Deutscher Chemiker e.V., 2018 – present)

RESEARCH PUBLICATIONS

- D. Petzold, B. König, *Adv. Synth. Catal.* **2018**, *360*, 626-630, DOI:10.1002/adsc.201701276 (Communication). Cover Picture: DOI:10.1002/adsc.201701420.
- D. Petzold, P. Nitschke, F. Brandl, V. Scheidler, B. Dick, R. M. Gschwind, B. König, *Chem. Eur. J.* **2019**, *25*, 361-366, DOI:10.1002/chem.201804603 (Full Paper)
- D. Petzold, P. Singh, F. Almqvist, B. König, *manuscript submitted* (Communication)
- D. Petzold, M. Giedyk, A. Chatterjee, B. König, *manuscript in preparation* (Review)

CONFERENCE CONTRIBUTIONS

- **TOCUS Stuttgart 2018**, oral contribution
- **26. Lecture Conference on Photochemistry**, Munich, poster presentation (09/2018)
- **24th - 35th Seminar Days of the GRK 1626**, oral contributions (2016 – 2019)

SKILLS

Instrumental Techniques

- Analytical methods: NMR, IR, GC, LCMS, HPLC, CV, TLC, UV-VIS spectroscopy
- Purification: Prep. HPLC, column chromatography, (re-)crystallization, ...
- Working under inert conditions (Schlenk-techniques, glovebox)

Languages

- German (native)
- English (business fluent, TOEFL IBT, 102 points)
- Spanish (basics, 3 years school education)

HOBBIES

Rock Climbing (Bouldering), (Beach-)Volleyball

REFERENCES

Prof. Dr. Burkhard König,

Institut für Organische Chemie

Universität Regensburg, 93040 Regensburg

E-Mail: Burkhard.Koenig@chemie.uni-regensburg.de

Phone: (+49)-941-943-4575

Prof. Dr. Nicole Teusch,

Fakultät für Angewandte Naturwissenschaften

Technische Hochschule Köln – Campus Leverkusen,

Kaiser-Wilhelm-Allee 51368 Leverkusen

E-Mail: nicole.teusch@th-koeln.de

Phone: +49 214-32831-4623

Hans Hoenig,

Grünenthal GmbH, 52099 Aachen

E-Mail: Hans.Hoenig@grunenthal.com

Regensburg,

Daniel Petzold

8. Abbreviations

A	A	ampere	
	Å	Ångström	
	AcOH	acetic acid	
	Ar	aryl	
	ATRA	atom transfer radical addition	
B	BDE	bond dissociation energy	
	bpy	2,2'-bipyridine	
	Bu	butyl	
	Bz	benzyl	
C	°C	degree Celsius	
	calc.	calculated	
	CBr ₄	tetrabromomethane	
	CDCl ₃	deuterated chloroform	
	CH ₂ I ₂	diiodomethane	
	CT	charge transfer	
	CV	cyclic voltammetry	
D	<i>d_x</i>	deuterated (x times)	
	DADS	decay associated difference spectrum	
	DCE	1,2-dichloroethane	
	DCM	dichloromethane	
	DIPEA	<i>N,N</i> -diisopropylethylamine	
	DMF	<i>N,N</i> -dimethylformamide	
	DMF- <i>d</i> ₇	deuterated <i>N,N</i> -dimethylformamide	
	DMSO	dimethyl sulfoxide	
	DMSO- <i>d</i> ₆	deuterated dimethyl sulfoxide	
	dr	diastereomeric ratio	
	dtbbpy	4,4'-di- <i>tert</i> -butyl-2,2'-dipyridyl	
	E	E _{Ox/Red}	oxidation or reduction potential
		EDG	electron donating group
EI		electron ionization	
equiv.		equivalent	
ESI		electrospray ionization	
ET		electron transfer	
Et		ethyl	
EtOAc		ethyl acetate	
EtOH		ethanol	
Et ₂ Zn		diethyl zinc	
eV		electron volt	
EWG	electron withdrawing group		
EY	Eosin Y		

F	Fc	ferrocene	
	Fc ⁺	ferrocenium	
	FID	flame ionization detector	
	Fukuzumi Cat.	9-mesityl-10-methylacridinium tetrafluoroborate	
G	GC	gas chromatography	
H	h	hour(s)	
	HBF ₄	tetrafluoroboric acid	
	H ₂ SO ₄	sulfuric acid	
	HAT	hydrogen atom transfer	
	HPLC	high-performance/pressure liquid chromatography	
	HRMS	high resolution mass spectrometry	
	I	1-ITMH	1-iodo-3,5,5-trimethylhydantoin
		IS	internal standard
ISC		intersystem crossing	
J	<i>J</i>	coupling constant	
K	K	Kelvin	
	K ₂ S ₂ O ₈	potassium persulfate	
	K ₃ PO ₄	potassium phosphate	
	KBr	potassium bromide	
	KHSO ₄	potassium bisulfate	
L	LC	liquid chromatography	
	LCMS	liquid chromatography coupled with mass spectrometry	
	LED	light emitting diode	
	LUMO	lowest unoccupied molecular orbital	
	λ	wavelength	
M	M	molarity = mol/L	
	Me	methyl	
	MeCN	acetonitrile (= ACN)	
	MeOD	deuterated methanol	
	MeOH	methanol	
	MF	molecular formula	
	MgSO ₄	magnesium sulfate	
	MHz	mega hertz	
	min	minute(s)	
	mL	milli liter	
	μL	micro liter	
	mm	milli meter	
	mol%	mol percent	
	MS	mass spectrometry	
	MW	molecular weight	
	N	NaBr	sodium bromide
		Na ₂ HPO ₄	disodium phosphate
Na ₂ SO ₄		sodium sulphate	
NaHCO ₃		sodium bicarbonate	
NaNO ₂		sodium nitrite	
NBS		<i>N</i> -bromosuccinimide	
NCS		<i>N</i> -chlorosuccinimide	
NFSI		<i>N</i> -fluorobenzenesulfonimide	

	NHE	normal hydrogen electrode
	NIS	<i>N</i> -iodosuccinimide
	nm	nano meter
	NMR	nuclear magnetic resonance
	ns	nanosecond(s)
	Nu	nucleophile
O	OD	optical density
P	p.a.	pro analysis
	PC	photocatalyst
	P(Cy) ₃	tricyclohexyl phosphine
	Pd(II)Ac ₂	palladium(II) acetate
	PE	petroleum ether (hexanes)
	PET	positron emission tomography
	Ph	phenyl
	PhCl	chlorobenzene
	phen	phenanthroline
	PIDA	phenyliodine(III) diacetate
	ppm	parts per million
	ppy	2-phenylpyridine
	Py	pyridine
R	R	alkyl or aryl and functional group(s), respectively
	rt	room temperature
S	s	second(s)
	SCE	saturated calomel electrode
	SET	single electron transfer
	SF ₆	sulfur hexafluoride
T	t	time
	TBADT	tetrabutylammonium decatungstate
	TBATFB	tetrabutylammonium tetrafluoroborate
	TEA	triethylamine
	Tf	trifluoromethanesulfonate
	TFA	trifluoroacetic acid
	THF	tetrahydrofuran
	TLC	thin-layer chromatography
U	UV	ultraviolet
V	V	volt
	VIS	visible
	vs	versus
W	W	watt

9. Danksagung

Zu aller erst gilt mein Dank Prof. Dr. Burkhard König für die Möglichkeit, meine Master- und Doktorarbeit in seiner Gruppe anzufertigen. Ich bedanke mich für seine Unterstützung während der gesamten Zeit, die hilfreichen Diskussionen und das Vertrauen in mich, meine Projekte selbst zu entwickeln.

Prof. Dr. Martin Breugst danke ich für die Übernahme des Zweitgutachtens und Prof. Dr. Antje Bäumner, für die Übernahme der Rolle als Drittprüferin. Außerdem danke ich Prof. Julia Rehbein für den Vorsitz in meinem Promotionskolloquium.

Für die Finanzierung meiner Promotion danke ich dem GRK 1626 „Chemische Photokatalyse“.

Ich danke all meinen Kooperationspartnern: Prof. Dr. Burkhard König, Philipp Nitschke, Fabian Brandl, Veronica Scheidler, Dr. Pardeep Singh, Prof. Dr. Ruth M. Gschwind, Prof. B. Dick und Prof. F. Almqvist.

Ein besonderer Dank gebührt Prof. Fredrik Almqvist dafür, dass er mir die Gelegenheit gegeben hat, einen Auslandsforschungsaufenthalt in seiner Gruppe an der Umeå University in Schweden zu absolvieren. Außerdem möchte ich mich bei Pardeep Singh, Martina Kulén und Souvik Sakar für ihre Unterstützung im Labor, sowie für die gemeinsamen außeruniversitären Aktivitäten bedanken.

Des Weiteren möchte ich mich bei Viola Rappenegger, Katharina Nickl, Britta Badziura, Simone Strauss, Dr. Petra Hilgers, Julia Zach und Ernst Lautenschlager für die Hilfe bei Problemen aller Art, ob nun organisatorischer, bürokratischer oder technischer Natur, bedanken. Mein besonderer Dank gilt Regina Hoheisel für die CV-Messungen sowie Dr. Rudolf Vasold für die GC/MS-Messungen.

Meinen Forschungspraktikanten Nikolai Wurzer, Janis Musso, Felix Seeberger und Katarzyna-Anna Glowacz danke ich für ihre fleißige und tatkräftige Unterstützung im Labor und Mithilfe bei meinen Forschungsprojekten.

Mein Dank gilt natürlich auch allen ehemaligen und aktuellen Kollegen des AK König für die Unterstützung, die Zusammenarbeit, die Gespräche, ob nun fachlicher oder fachfremder Natur und die gemeinsamen sportlichen Aktivitäten und insbesondere Simon Düsel für eine großartige, gemeinsame Zeit im Superlabor 24.

Zu guter Letzt möchte ich mich bei meiner Familie bedanken. Insbesondere der stetige Rückhalt durch meine Mutter Andrea und ihre bedingungslose Unterstützung waren und sind mir heute noch sehr wichtig. Am wichtigsten jedoch bist du mir, Katharina. Wir sind diesen Weg gemeinsam gegangen und ich bin unendlich dankbar dich auch in Zukunft an meiner Seite zu wissen.